Biomodification of Abiotic Surfaces for the Prevention of Hospital-Associated Infection

Hathaway, Hollie

Award date:
2017

Awarding institution:
University of Bath

Biomodification of Abiotic Surfaces for the Prevention of Hospital–Associated Infection

Hollie Jane Hathaway

A thesis submitted for the degree of Doctor of Philosophy

University of Bath

Department of Chemistry

September 2017

Table of Contents

Acknowledgements

First and foremost, I would like to thank my supervisors, Professor Toby Jenkins and Dr. Mark Sutton. The support and guidance you have given me over the past 4 years has been exceptional. Toby, your "motivational" one-liners have been, dare I say it, actually motivational at times. You have always given me a fair amount of freedom to pursue my own ideas, which could be described as 'high risk, high reward'. Nonetheless, I am very grateful to you for putting your faith in my research. Mark, thank you for always being available, not only for scientific guidance but also just for a coffee and a chat, your advice in all matters has been invaluable.

To the Biophysical Chemistry Group, both past and present, it has been a pleasure working (and socialising) with you, I am especially grateful to Thet, Jess, Diana, Patricia, Liam, George and Laura who have made my time as a PhD student so enjoyable. I would also like to thank Scarlet Milo, it is hard to put into words how truly grateful I am for your loyalty, support and friendship. I am indebted to you for so many reasons, not least for the continuous proof-reading, troubleshooting and help in the lab, but also for your consistency; you have always been there, both to celebrate the good and to commiserate the bad. I count myself very lucky to call you my friend. The memories we have shared (the sock incident being one of my personal favourites), will stay with me forever and I am certain we will make many more.

To my friends and family, your unwavering support has encouraged me to achieve far more than I ever believed possible. I would especially like to thank my wonderful grandparents, you are my inspiration and I am forever grateful for your seemingly endless supply of love and encouragement. To Dad and Julia, thank you for being there to offer support and guidance, you never fail to provide perspective when I lose sight of the horizon.

Finally, I would like to thank my Mum. It is impossible to describe how grateful I am to have you as a role model, your continuous support and encouragement has formed the basis of everything I am today. From the day you bought me my first microscope (and helped me to find some questionable specimens to put under it), I didn't expect to be thanking you in my PhD thesis over 20 years later. I can never repay you for everything you have done for me, for always providing and for playing all roles so well. However, I hope that in some small way, this dedication can express a tiny fragment of my gratitude. So this is for you, not only for being a mother, but for being so much more.

Publication List

Publications included in this thesis:

- Hathaway, H. J.; Sutton, J. M.; Jenkins, A. T., Study into the kinetic properties and surface attachment of a thermostable adenylate kinase. *Biochemistry and Biophysics Reports* **1**, 1-7 (2015).

- Hathaway, H.; Alves, D. R.; Bean, J.; Esteban, P. P.; Ouadi, K.; Sutton, J. M.; Jenkins, A. T., Poly(*N*-isopropylacrylamide-*co*-allylamine) (PNIPAM-*co*-ALA) nanospheres for the thermally triggered release of Bacteriophage K. *European Journal of Pharmaceutics and Biopharmaceutics* **96**, 437-41 (2015).

- Hathaway, H.; Ajuebor, J.; Stephens, L.; Coffey, A.; Potter, U.; Sutton, J. M.; Jenkins, A. T., Thermally triggered release of the bacteriophage endolysin $CHAP_K$ and the bacteriocin lysostaphin for the control of methicillin resistant *Staphylococcus aureus* (MRSA). *Journal of Controlled Release* **245**, 108-115 (2017).

- Hathaway, H., Milo, S., Sutton, J. M. & Jenkins, T. A. Recent advances in therapeutic delivery systems of bacteriophage and bacteriophage-encoded endolysins. *Therapeutic Delivery* **8**, 543-556 (2017).

Additional Publications:

- Milo, S.; Hathaway, H.; Nzakizwanayo, J.; Alves, D.; Perez Esteban, P.; Jones, B. V.; Jenkins, A. T. A., Prevention of Encrustation and Blockage of Urinary Catheters by *Proteus mirabilis* via pH-Triggered Release of Bacteriophage. *Journal of Materials Chemistry B* **5**, 5403-5411 (2017).

- Milo, S.; Acosta, F. B.; Hathaway, H.; Wallace, L.; Thet, N. T.; Jenkins, A. T. A., A Simple *In Situ* Fluorescent Sensor for the Early Detection of Urinary Catheter Blockage. *Journal of Biomedical Materials Research Part B: Applied Biomaterials*, Submitted.

Abstract

This research aims to investigate the application of medical biotechnology with regard to the detection and treatment of hospital-associated infection. Various strategies focused on the implementation of biological detection agents and biotherapeutics are discussed, with particular emphasis placed on surface-anchoring technologies. This thesis is presented in the alternative format, consisting of published research papers embedded within the text. An extended introduction precedes each publication and a reflective commentary accompanies each research paper. For the purpose of continuity, all figure captions and references are in keeping with the body of the text.

Part A concerns the detection of residual sources of transmissible infection, via the utilisation of an enzymatic detection agent, capable of modelling clinical surface contamination post sterilisation. *Chapter 1* details the development of a current clinical biosensor, focused on modification of polymeric substrates via plasma activation. Covalent immobilisation facilitated enhanced proteinaceous surface retention, alongside retention of biological activity, potentially providing a more stringent assessment of hospital sterilisation measures. *Chapter 2* (unpublished) investigates the possibility of protein engineering for further development of the aforementioned biosensor. This research focuses on genetic modification of the detection agent and subsequent covalent conjugation to a fluorescent reporting system, with the intention of quantifying surface contamination in the clinical setting.

Part B focuses on the development of potential biological therapeutics for the treatment of infection. *Chapter 3* aims to provide the theoretical background to the proceeding research in the form of a review paper. *Chapter 4* concerns the utilisation of surface-anchored, polymeric nanoparticles as delivery vectors for bacteriophage, facilitating the controlled delivery of the antimicrobial cargo at an elevated temperature associated with chronic wound infection. *Chapter 5* is presented as an extension of the preceding research, detailing the use of a synergistic enzybiotic cocktail as oppose to bacteriophage, in an attempt to alleviate certain regulatory concerns.

Acronyms and Abbreviations

CDC	Centers for Disease Control and Prevention
CJD	Creutzfeldt-Jacob Disease
[E]	Enzyme
[S]	Substrate
[ES]	Enzyme Substrate complex
[P]	Product
AK	Adenylate Kinase
AMP	Adenosine Monophosphate
ADP	Adenosine Diphosphate
ATP	Adenosine Triphosphate
D-LH_2	Luciferin
S. acidocaldarius	*Sulfolobus acidocaldarius*
tAK	Thermostable Adenylate Kinase
PHE	Public Health England
PBS	Phosphate Buffered Saline
FT-IR	Fourier Transform Infrared Spectroscopy
RLU	Relative Light Units
AA	Allylamine
PP	Polypropylene
PCR	Polymerase Chain Reaction
E. coli	*Escherichia coli*
PTM	Post-translational Modification
PEG	Poly(ethylene glycol)
MA	Maleic Anhydride
tAK_{WT}	Thermostable Adenylate Kinase (Wild Type)
tAK_{M}	Thermostable Adenylate Kinase (Mutant)
tAK_{MC}	Thermostable Adenylate Kinase (Mutant) - conjugated to fluorophore
tAK_{M*}	Thermostable Adenylate Kinase (Mutant) - exposed to conjugation conditions
LB	Luria Bertani broth
SDS	Sodium Dodecyl Sulfate

DTT	Dithiothreitol
DMSO	Dimethyl Sulfoxide
dNTP	Deoxynucleotide Triphosphate
MWCO	Molecular Weight Cut off
RFU	Relative Fluorescence Units
AK_e	Adenylate Kinase from *Escherichia coli*
BRET	Bioluminescence Resonance Energy Transfer
FRET	Fluorescence Resonance Energy Transfer
RLuc	*Renilla* Luciferase
GFP^2	Green Fluorescent Protein^2
MOA	Mechanism of Action
MOR	Mechanism of Resistance
HGT	Horizontal Gene Transfer
MIC	Minimum Inhibitory Concentration
WHO	World Health Organisation
FDA	Food and Drug Administration
NPV	Net Present Value
MDR	Multi-drug Resistance
EPI	Efflux Pump Inhibitors
agr	Accessory gene regulation
S. aureus	*Staphylococcus aureus*
P. aeruginosa	*Pseudomonas aeruginosa*
QSI	Quorum Sensing Inhibitor
ADMET	Adsorption, Distribution, Metabolism, Excretion and Toxicity
PK	Pharmacokinetics
PD	Pharmacodynamics
CRISPR	Clustered Regularly Interspaced Short Palindromic Repeats
K. pneumoniae	*Klebsiella pneumoniae*
GI	Gastrointestinal
MOI	Multiplicity of Infection
BCC	*Burkholderia cepacia* Complex
DPI	Dry Powder Inhaler
PNIPAM	Poly(*N*-isopropylacrylamide)

ALA	Allylamine
PNIPAM-*co*-ALA	Poly(*N*-isopropylacrylamide) copolymerised with Allylamine
LCST	Lower Critical Solution Temperature
HA	Hyaluronic Acid
HAse	Hyaluronidase
HAMA	Hyaluronic Acid Methacrylate
VLP	Virus-like Particle
C. perfringens	*Clostridium perfringens*
SSTI	Skin and Soft Tissue Infection
ABSSSI	Acute Bacterial Skin and Skin Structure Infection
MRSA	Methicillin Resistant *Staphylococcus aureus*
MSSA	Methicillin Susceptible *Staphylococcus aureus*
OD	Optical Density
CFU	Colony Forming Unit
PFU	Plaque Forming Unit
DLS	Dynamic Light Scattering
TSA	Tryptic Soy Agar
TSB	Tryptic Soy Broth
TEM	Transmission Electron Microscopy
EPS	Exopolysaccharide
NW	Non-woven
S. epidermidis	*Staphylococcus epidermidis*
HA-MRSA	Hospital-Acquired Methicillin Resistant *Staphylococcus aureus*
CA-MRSA	Community-Acquired Methicillin Resistant *Staphylococcus aureus*
DI	Deionised
BSA	Bovine Serum Albumin
CLSI	Clinical and Laboratory Standards Institute
HMDS	Hexamethyldisilazane
FESEM	Field Emission Scanning Electron Microscope
LE	Loading Efficiency
FIC	Fractional Inhibitory Concentration

List of Figures

Part A: Detection of Infection

Chapter 1: Study into the Kinetic Properties and Surface Attachment of a Thermostable Adenylate Kinase

Chapter 2: Site-Directed Mutagenesis of a Thermostable Adenylate Kinase for Biosensor Development

Part B: Treatment of Infection

Chapter 3: Recent Advances in Therapeutic Delivery Systems of Bacteriophage and Bacteriophage-Encoded Endolysins

Chapter 4: Poly(*N*-isopropylacrylamide-*co*-allylamine) (PNIPAM-*co*-ALA) Nanospheres for the Thermally Triggered Release of Bacteriophage K

Chapter 5: Thermally Triggered Release of the Bacteriophage Endolysin $CHAP_K$ and the Bacteriocin Lysostaphin for the Control of Methicillin Resistant Staphylococcus aureus (MRSA)

List of Tables

Part A: Detection of Infection

Chapter 1: Study into the Kinetic Properties and Surface Attachment of a Thermostable Adenylate Kinase

Chapter 2: Site-Directed Mutagenesis of a Thermostable Adenylate Kinase for Biosensor Development

Part B: Treatment of Infection

Chapter 3: Recent Advances in Therapeutic Delivery Systems of Bacteriophage and Bacteriophage-Encoded Endolysins

Chapter 5: Thermally Triggered Release of the Bacteriophage Endolysin $CHAP_K$ and the Bacteriocin Lysostaphin for the Control of Methicillin Resistant *Staphylococcus aureus* (MRSA)

Part A: Detection of Infection

"Problems are the price of progress. Don't bring me anything but trouble. Good news weakens me".

Charles F. Kettering – Engineer, inventor of the electrical starting motor.

Chapter 1: Study into the Kinetic Properties and Surface Attachment of a Thermostable Adenylate Kinase

1.1 Introduction

The aim of this research concerns the effective modelling of surface contamination within the clinical setting, focused on eliminating cross contamination through improperly sterilised surgical equipment. Despite the best efforts of clinicians and technical staff worldwide, the complete eradication of surface contamination, specifically proteinaceous contamination, can prove challenging owing to the resilient nature of certain hospital-associated infectious agents. This research aims to model particularly surface adherent species through utilisation of a thermostable enzyme, the activity of which can be monitored in order to quantify simulated protein contamination as a function of surface anchoring strategies. The overall intention being the provision of a more stringent assessment of hospital sterilisation measures through the development of a current clinical biosensor.

1.1.1 Hospital Sterilisation Efficacy

The importance of rigorous and efficient cleaning of reusable surgical equipment cannot be underestimated. The Centers for Disease Control and Prevention (CDC) has published a set of guidelines for the disinfection and sterilization of healthcare equipment, detailing the mandatory cleaning procedures required for a variety of tools and equipment [1]. However, there are certain pathogens which are resistant to common sterilization techniques; the most relevant in this case being prions.

Prions are exceptionally stable, extracellular misfolded proteins formed by the post-translational modification of a normal host encoded glycoprotein into an abnormal isoform. Prions replicate by converting cellular proteins into the corresponding infectious conformers. A recent study has utilised cryomicroscopy in order to deduce the structure of the infective prion protein, which has eluded scientists for decades as a result of its poor solubility and tendency towards aggregation [2]. Whilst the exact mechanism of prion replication remains unknown, it is believed that it is solely a conformational change in the protein that brings about the infectious nature of the newly formed isoform, rather than covalent modification [3].

Prions are associated with a range of fatal, neurodegenerative diseases including Creutzfeldt-Jacob disease (CJD), Gerstmann-Sträussler-Scheinker syndrome, fatal familial insomnia and kuru. Prion diseases can be inherited or sporadic, whilst the most concerning in terms of transmission through accidental exposure is termed acquired or iatrogenic. The iatrogenic form of prion disease can be contracted through contact with infected tissue. From 1970 to 2015, 85 such cases have been reported in the UK following procedures such as dura mater implants, corneal transplants and administration of human-derived growth hormone and human gonadotrophin [4]. There have also been six cases worldwide of iatrogenic CJD transmission as a result of insufficient cleaning of surgical tools (neurosurgical instruments and depth electrodes) [5]. Whilst this may seem like a low incidence rate, evaluation of clinical disinfection measures has demonstrated inadequacy in preventing the transmission of prion agents, meaning the potential threat of exposure remains a cause for concern [6]. Furthermore, there have been a number of incidents whereby the transmission of CJD via surgical equipment was suspected. Whilst there have been no confirmed reports of iatrogenic transmission as a result of these incidents, the associated repercussions were significant. Entire operating theatres were shut down, patients were sent elsewhere for emergency surgery, ambulances were diverted and hundreds of neurosurgical patients were contacted and informed of the risk (albeit very low) of having contracted prion disease [7]. As a result, the UK Department of Health published a set of guidelines in 2012 detailing the appropriate measures required in order to prevent the spread of CJD within the healthcare setting, largely owing to the fact that conventional decontamination methods (treatment with formalin or ethylene oxide, autoclaving and irradiation) are ineffective [8]. To date, the characteristic presentation of human prion disease can only be definitively confirmed post mortem via the identification of plaques within the brain tissue of those affected. Thus, the need to eliminate the risk of transmission both in terms of the unnecessary spread of infectious disease, and the economic and social implications associated with any potential or suspected risk of infection must be addressed and ultimately eliminated.

1.1.2 Enzymes

Enzymes are proteins found in abundance in living cells, capable of catalysing biochemical reactions. They consist of a sequence of amino acids joined in a specific order, dictated by the genetic code responsible for cellular enzyme synthesis, resulting in a complex protein structure. The nature of this amino acid sequence gives rise to unique enzymatic properties characteristic of the class and activity of each individual enzyme. Enzymes are classified according to the type of reaction they catalyse, for example transferase, cyclase, reductase,

oxidase etc. [9]. Owing to their complex structure, enzymes are capable of exhibiting innate specificity for certain substrate molecules both in terms of chemo/ stereoselectively as well as enantiomeric and regioselective properties. The way in which this is achieved is typically accounted for by either; the lock and key model (first described by Fisher in 1894, detailing how a certain enzyme is specific for a certain substrate, which fits exactly in the enzyme's active site), or by the induced fit model (stating that protein geometry changes during substrate binding in order to accommodate the substrate molecule) [10]. As biological catalysts, enzymes have a complex 3D structure which results in small clefts or pockets specific for a certain substrate, known as the enzyme's active site. Like all catalysts, enzymes are capable of increasing the rate of a reaction without being consumed in the process. This is achieved by the ability of the enzyme to lower the activation energy required for the formation of the intermediate transition state, allowing more molecules to successfully react. An enzyme does not affect the thermodynamics of a reaction, nor does it affect the position of equilibrium, that is to say the rate of reaction is enhanced in both directions. This is in agreement with the second law of thermodynamics as the difference in the Gibbs free energy between the reactants and the products is unchanged; it is solely the transition state which is affected.

1.1.3 Enzyme Kinetics

One of the most effective ways to investigate the mechanism of an enzyme-catalysed reaction is to establish the rate of reaction as a function of enzyme activity. This is known as enzyme kinetics. It concerns the rate of product formation over time as a function of enzyme and substrate concentration under specific, predefined conditions. By deducing how and why the rate of product turnover is limited by the system, it is possible to calculate key parameters allowing quantifiable determination of enzyme activity.

1.1.3.1 The Michaelis - Menten Model

In 1903 Victor Henri highlighted the importance of the formation of an enzyme substrate complex as a key step in catalysis. This idea was taken forward in 1913 by German biochemist Leonor Michaelis, and Canadian pathologist Maud Menten. They postulated that the enzyme [E] and substrate [S] combine in a reversible manner to form the enzyme substrate [ES] complex, which is subsequently converted into product [P]. This gave a generalised reaction scheme for enzyme-catalysed product formation:

$$E + S \underset{k_{-1}}{\overset{k_1}{\rightleftharpoons}} ES \xrightarrow{k_2} E + P$$

Scheme 1 - The enzyme-catalysed conversion of substrate into product via an intermediate enzyme-substrate complex. k_1, k_{-1}, k_2 represent rate constants for each step.

Note that there is no k_{-2} value; this results from the fact that the model takes into account the initial rate of reaction, therefore in the absence of any significant amount of product, it can be assumed that there is no reversal from product to the enzyme substrate complex. In order to mathematically describe the changes occurring in an enzyme-catalysed reaction it is necessary to consider four differential equations relating to Scheme 1.

$$\frac{d[E]}{dt} = - k_1 [E][S] + k_{-1}[ES] + k_2[ES] \quad (1)$$

$$\frac{d[S]}{dt} = - k_1 [E][S] + k_{-1}[ES] \quad (2)$$

$$\frac{d[ES]}{dt} = k_1 [E][S] - k_{-1}[ES] - k_2[ES] \quad (3)$$

$$\frac{d[P]}{dt} = k_2[ES] \quad (4)$$

The law of conservation must then be applied, relating enzyme activity to general catalysis, implying that the overall enzyme concentration does not change (i.e. the catalyst is not used up during the reaction). Rather, it exists in two forms; as free enzyme and enzyme bound to substrate in the intermediate complex:

$$[E_0] = [E] + [ES] \quad (5)$$

Michaelis and Menten applied the assumption that the enzyme substrate complex exists in rapid equilibrium with the free enzyme and substrate [11]. This holds true provided that k_2 is

much smaller than k_{-1}, such that a thermodynamic equilibrium exists whereby the concentration of the enzyme substrate complex is not perturbed to a significant extent via breakdown (through k_2) to release product.

$$k_1 [E][S] = k_{-1} [ES] \quad (6)$$

Hence, equation (3) then simplifies to:

$$\frac{d[ES]}{dt} = k_1 [E][S] - k_{-1}[ES] \quad (7)$$

Combining the law of conservation (5) with the equilibrium approximation (6) provides a new differential equation describing the change in concentration of the enzyme substrate complex:

$$\frac{d[ES]}{dt} = k_1 [(E_0) - (ES)][S] - k_{-1}[ES] \quad (8)$$

Solving for [ES]:

$$[ES] = \frac{k_1[E_0]\,[S]}{k_{-1} + k_1[S]} \quad (9)$$

The rate of product formation is reliant upon k_2 as shown in equation (4), thus combining (4) and (9):

$$v = \frac{k_1[E_0]\,[S]k_2}{k_{-1} + k_1[S]} \quad (10)$$

$$v = \frac{k_2[E_0]\,[S]}{\frac{k_{-1}}{k_1} + [S]} \quad (11)$$

Simplifying:

$$v = \frac{k_2[\mathrm{E}_0]\,[\mathrm{S}]}{K_M + [\mathrm{S}]} \tag{12}$$

Where:

$$K_M = \frac{k_{-1}}{k_1}$$

This is commonly referred to as the Michaelis constant and is effectively an equilibrium constant for the enzyme substrate complex. Often, it is used as a measure of the affinity an enzyme has for its substrate as it describes the dissociation of substrate from enzyme. A higher K_M value indicates a lower affinity for substrate (weak binding), whereas a low K_M value indicates tight binding.

Simplifying further:

$$v = \frac{V_{max}[\mathrm{S}]}{K_M + [\mathrm{S}]} \tag{13}$$

Where:

$$V_{max} = k_2\,[E_0]$$

V_{max} refers to the point at which all enzyme molecules are bound as enzyme substrate complex. This correlates to the maximum velocity possible under any given set of conditions. It is a theoretical value rarely seen in experimental data but can be found via various graphing and software techniques. Equation 13 is a fundamental equation, derived according to a specific set of assumptions outlined by scientists at the turn of the 20th century (which is still very much in use today), in order to calculate key parameters relating enzyme activity to a wide range of reaction conditions.

1.1.3.2 The Briggs - Haldane Model

One of the major limitations of the Michaelis-Menten model is the assumption that $k_2 << k_{-1}$. This is not the case for a number of enzymes. Indeed, there are cases where $k_2 > k_{-1}$ and where k_2 and k_{-1} are comparable. In cases such as these it is impossible to omit k_2 from the differential, thereby changing the meaning of K_M. This is not to say that the model is rendered invalid, rather it just prevents K_M being considered dissociation constant or a measure of substrate affinity. However in 1925 George Edward Briggs and John Burdon Sanderson

Haldane provided an alteration to the standard Michaelis-Menten model in a publication entitled 'A Note on the Kinetics of Enzyme Action' [12]. Rather than making assumptions based on the nature of the rate constants, they derived a complementary model in which they describe the enzyme substrate complex as being in a 'steady state'. This term assumes that the concentration of the enzyme substrate complex does not change; the rate of formation is equal to the rate of breakdown [13]. This can be expressed as:

$$k_1 [E][S] = k_{-1} [ES]+k_2[ES] \tag{14}$$

Combining the law of conservation (5) with the new steady state assumption (14) gives rise to a new differential equation for the change in concentration of the enzyme substrate complex:

$$\frac{d[ES]}{dt} = k_1 [(E_0) - (ES)][S]- k_{-1}[ES] - k_2[ES] \tag{15}$$

$$= k_1 [(E_0) - (ES)][S]- (k_{-1} + k_2)[ES] \tag{16}$$

$$= k_1 (E_0) - (k_1[S] + k_{-1} + k_2)[ES] \tag{17}$$

Solving for [ES]:

$$[ES] = \frac{k_1[E_0] [S]}{k_{-1} + k_1[S] + k_2} \tag{18}$$

The rate of product formation remains reliant upon k_2 as shown in equation (4), thus combining (4) and (18):

$$v = \frac{k_1[E_0] [S] k_2}{k_{-1} + k_1[S] + k_2} \tag{19}$$

$$v = \frac{k_2[E_0] [S]}{\frac{k_{-1} + k_2}{k_1} + [S]} \tag{20}$$

Simplifying:

$$v = \frac{k_2[\mathrm{E}_0]\,[\mathrm{S}]}{K_M + [\mathrm{S}]} \qquad (21)$$

Where:

$$\mathrm{K_M} = \frac{k_{-1} + k_2}{k_1}$$

This combination of rate laws is often still referred to as the Michaelis-Menten constant despite the fact that it is actually a deviation from the model first put forward by Michaelis and Menten in 1913. It can be seen from this equation that K_M can only be considered equal to the dissociation constant of the enzyme substrate complex when $k_2 << k_{-1}$ (i.e. only when the equilibrium approximation becomes the limiting case of the steady state assumption). Despite the change in derivation, the overall rate equation looks exactly the same with the sole exception of a change in meaning of K_M:

$$v = \frac{V_{max}[\mathrm{S}]}{K_M + [\mathrm{S}]} \qquad (13)$$

Where:

$$V_{max} = k_2\,[E_0]$$

The Briggs-Haldane model is now widely accepted as a general rate law for simple one substrate enzyme kinetics, whilst the Michaelis-Menten model is associated with cases where there are clear measureable differences in rate constants (k_{-1} and k_2). An additional case has been put forward by Van Slyke and Cullen which invokes the converse assumption that $k_1 << k_2$. Following the previous derivations, this produces a K_M value equal to k_2/k_1, however this is only applicable in certain cases [14].

1.1.3.3 Multisubstrate Reactions

Both the Michaelis-Menten and the Briggs-Haldane models accounts for simple, uninhibited, one substrate binding enzyme kinetics. However, many enzymes bind more than one

substrate often resulting in the release of more than one product. There are three key models that describe the kinetic behaviour of such enzymes; random sequential, ordered sequential and the ping pong mechanism (the former being of particular importance to this research) [15]. The process whereby an enzyme binds to more than one substrate without any organised sequence is referred to as a random binding mechanism. This is shown in Figure 1 [16].

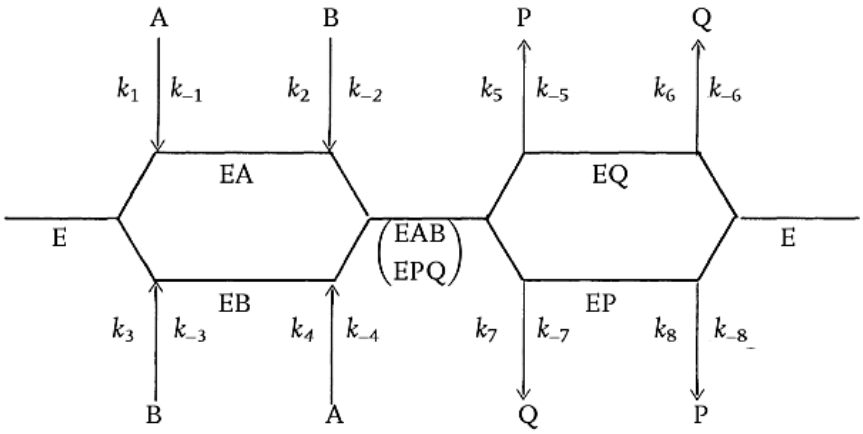

Figure 1 Reaction scheme for a random *bi bi* sequential enzyme binding mechanism.

When considering the rate equation for a random *bi bi* sequential mechanism, the system becomes much more complex. Alongside the maximum velocities (V_{max}) for the overall forward and reverse reactions, each reversible step has its own Michaelis-Menten constant associated with it (K_{MA}, K_{MB}, K_{MC}, K_{MP}, K_{MQ}). Unlike single substrate reactions, a reaction involving two substrates will proceed via an intermediate transitory complex prior to formation of the enzyme substrate complex. Therefore the initial binding of substrate A can be characterised by a pure dissociation constant. This differs from the Michaelis-Menten constant for substrate A and so is referred to as K_D. The entire rate equation is shown in equation 22, where K*e* is the equilibrium constant for the overall reaction.

$$v = \frac{V_1 V_2 \left([A][B] - \frac{[P][Q]}{Ke} \right)}{K_{DA}K_{MB}V_2 + K_{MB}V_2[A] + K_{MA}V_2[B] + \frac{K_{MQ}V_1[P]}{K_e} + \frac{K_{MP}V_1[Q]}{K_e} + V_2[A][B] + \frac{V_1[P][Q]}{K_e}} \quad (22)$$

Whilst a rate equation such as the one above may initially appear complex and extensive, it may be simplified by applying certain assumptions and limitations to the system. If the rapid equilibrium assumption is made, so that the breakdown of the ternary complex (EAB.EPQ) is slower than the return to the reactants, the V_2 and product terms may be omitted from the equation. Secondly, if the rate of formation of the ternary complex is not limited by substrate concentration and only initial velocities are considered, the overall rate equation simplifies to simple one substrate Michaelis-Menten kinetics.

1.1.3.4 Sigmoidal Kinetics

In some cases a typical rate vs. substrate concentration graph for an enzyme-catalysed reaction will display a sigmoidal curve (as opposed to the predicted hyperbolic curve). A possible explanation for this type of behaviour relates to cooperativity. True cooperativity is defined as a reflection of the equilibrium binding of substrates to both the free enzyme and the enzyme substrate complex. It is characterised by a change in binding affinity of one substrate as a direct consequence of the binding of another [17]. This can be a positive effect (the binding of one substrate increasing the affinity for the second substrate), or a negative effect (the affinity for the second substrate is decreased as a result of the binding of the first substrate). An extension of the Michaelis-Menten model aimed at expressing the concept of cooperativity was presented by Archibald Hill in 1910 [18]; his modification to the standard model is presented in equation (23), where *n* is the Hill constant:

$$v = \frac{V_{max}[\mathrm{S}]^n}{K + [\mathrm{S}]^n} \qquad (23)$$

It should be noted that the Hill constant does not directly correspond to the number of substrate binding sites within an enzyme; rather, it is a measure of the degree of cooperativity, often calculated as a non-integer value [19]. Whilst the Hill equation has been widely used in order to model cooperativity in enzymatic systems (its use has been reviewed elsewhere [20]), there are certain limitations associated with its use. Owing to its derivation, the Hill equation does not provide a physically realistic reaction scheme, as it is limited predominantly to modelling positive cooperativity and hence is only linear over a restricted range of substrate concentrations [21,22]. Nonetheless, sigmoidal response curves are often successfully fitted to the Hill equation (provided no further information is required regarding reaction mechanism).

A second possible explanation for the appearance of sigmoidal kinetics arises as a result of a multisubstrate reaction involving two or more of the same substrate. A two substrate, enzyme-catalysed reaction, following a random binding sequence can display sigmoidal kinetics without exhibiting true cooperativity. This occurs when the formation of the intermediate containing both substrates (EAB) is formed faster than the individual binding of the second substrate (EB). Meaning the affinity of the initial enzyme substrate complex (EA) for the second substrate (B) is greater than the affinity of the free enzyme (E). This results in a 'switching on' of the sigmoidal part of the graph; initially the reaction proceeds via the standard binding mechanism, until the concentration of (EA) builds up to such an extent that the velocity of the reaction increases, owing to an increase in affinity for the second substrate (B) [23].

1.1.4 Enzyme Inhibition

The activity of an enzyme may be inhibited by a number of factors owing to the sensitivity of enzymes to external reaction conditions, such as temperature, ionic strength and pH, alongside specific molecules capable of interrupting enzyme activity. There are two distinct classes of enzyme inhibitor: reversible and irreversible [24]. Irreversible inhibitors covalently and irreversibly modify part of the enzyme (usually the active site) via the formation of adducts, rendering the enzyme permanently inactive. This is not to be confused with enzyme inactivation, which involves the destruction of protein structure as a result of changes in temperature or pH. Reversible inhibition may include competitive, non-competitive and uncompetitive inhibition, all of which have been discussed extensively elsewhere [25]. However, a noteworthy form of inhibition surrounds the ability of a participating substrate (or an enzyme-catalysed product) to affect the overall rate of reaction.

Substrate inhibition is often considered a strange phenomenon. However, there appears to be some highly significant biological reasoning behind its existence. Enzymes are often found to be inhibited by their own substrate, although it is a common misconception that this arises from "using artificially high substrate concentration in a laboratory setting" as pointed out by Reed *et al* [26]. In fact, the ability of substrate molecules to regulate enzyme activity may arise as a result of specially evolved biochemical behaviour, tailored toward metabolic/ signalling control mechanisms. In terms of kinetic analysis, substrate inhibition is characterised by a sudden decline in the rate of reaction after a certain substrate concentration has been reached.

Another important biochemical control mechanism is the ability of an enzyme-catalysed product to inhibit further enzyme activity via a negative feedback loop. This kind of inhibition can also play a crucial role in metabolic and signalling pathways, an example of which is exhibited by the enzyme aspartate kinase [27]. Kinetically, this type of inhibition also presents itself as a decrease in the rate of reaction at a specific substrate concentration. However, unlike substrate inhibition, product inhibition can be overcome by a drastic increase in substrate concentration. This occurs as the substrate can eventually out-compete the inhibitor (the product) at high concentrations.

1.1.5 Enzymes as Biosensors

Immobilisation is an effective way to exploit the catalytic properties of certain enzymes, not only does it allow the recovery of the enzyme, it also allows separation from the products and/or reactants. Enzymes may be immobilised according to a number of different strategies including covalent attachment, bio-affinity binding, crosslinking and encapsulation. The pros and cons of each method have been discussed elsewhere [28]. The potential to exploit the specificity of biological catalysts has driven the development of enzyme-based biosensors for a range of applications from health care to agriculture [29].

1.1.5.1 Adenylate Kinase

The enzyme adenylate kinase (AK) is a phosphotransferase enzyme which catalyses the reversible formation of adenosine diphosphate (ADP) from adenosine triphosphate (ATP) and adenosine monophosphate (AMP) as shown in Scheme 2.

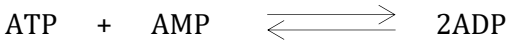

Scheme 2 – Adenylate kinase catalysed ADP formation.

ATP is considered the main form of cellular energy, therefore this interconversion of nucleoside phosphates is essential for sustaining life. By exploiting the necessity for all forms of life to carry this enzyme, AK has been widely used in the detection and monitoring of surface contamination. An interesting development in the utilisation of AK as a biomarker for surface contamination involves evaluating bacterial presence in the hygiene industry [30]. ATP

production can be monitored via a coupled system using a secondary enzyme, luciferase and its substrate luciferin (D-LH_2). The mechanism of which is shown in Scheme 3 [31].

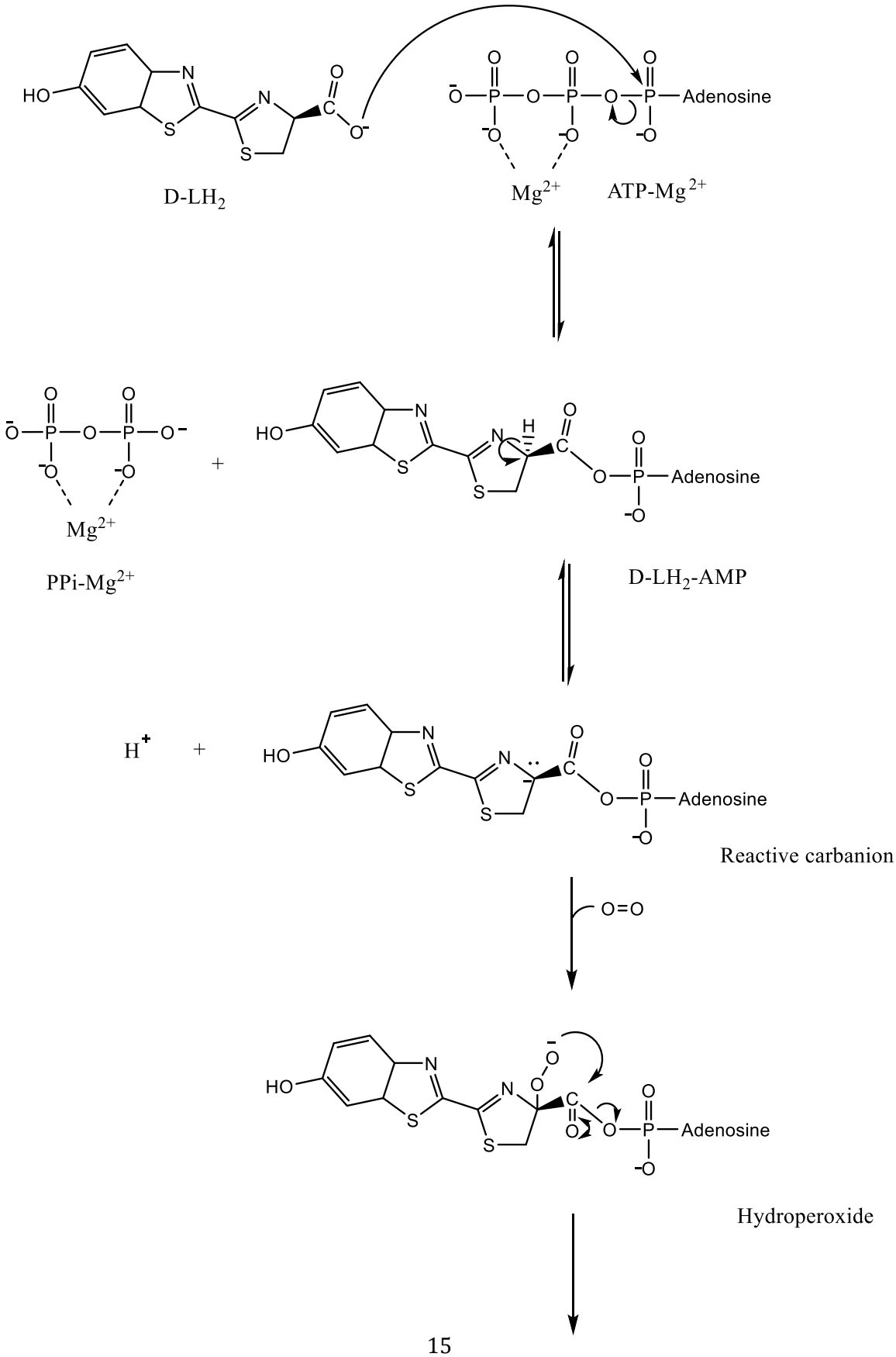

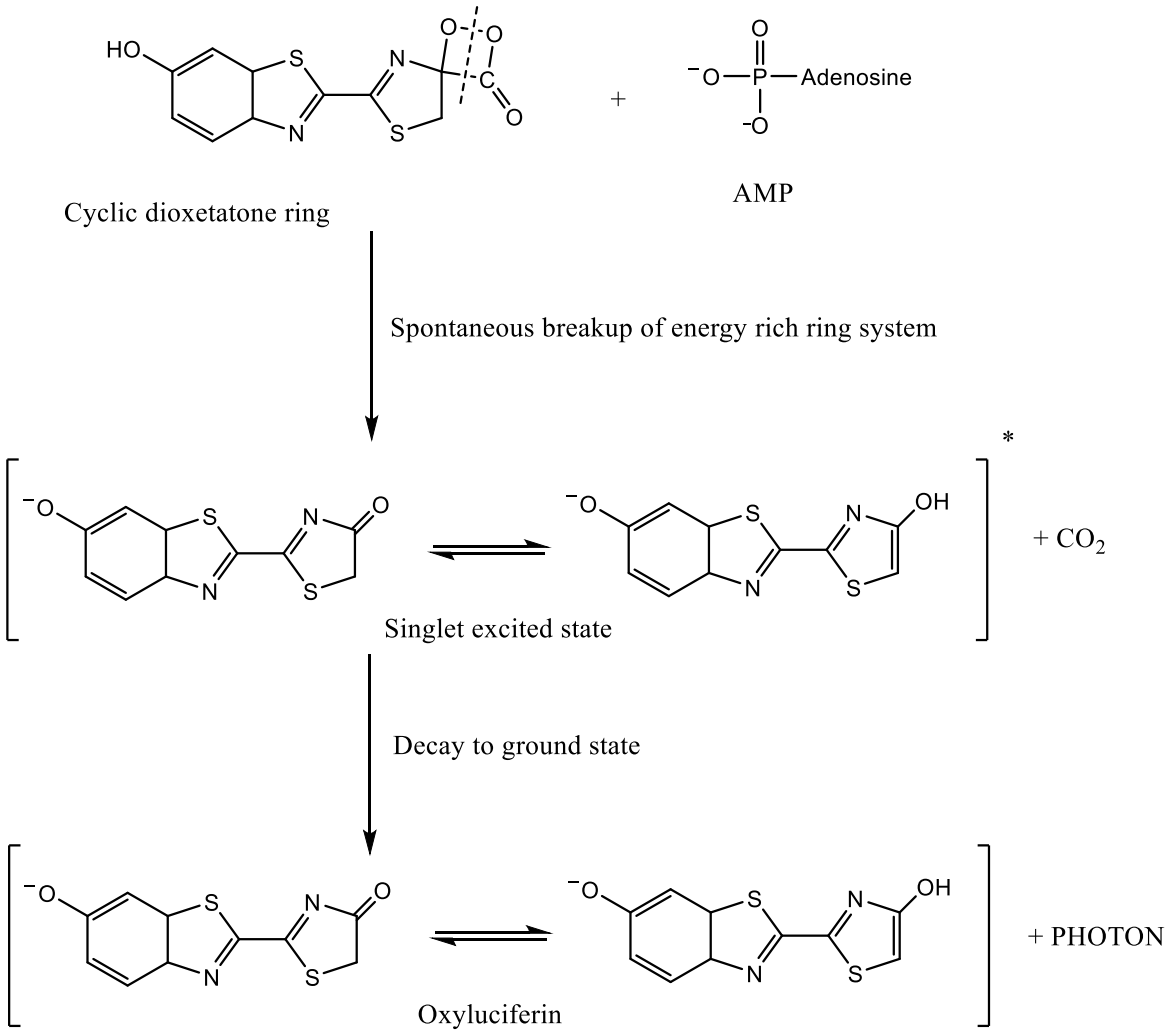

Scheme 3 – Luciferase-catalysed bioluminescent formation of oxyluciferin from luciferin (D-LH_2) and ATP, resulting in the emission of a photon from the singlet excited state.

The decay from the singlet excited state of oxyluciferin back to the ground state is responsible for the observed emission of light in the form of bioluminescence, although there has been a number of conflicting theories regarding which tautomer (keto or enol) is responsible [32]. However, a theoretical study conducted by Song *et al* [33], using molecular dynamics and quantum-mechanics/molecular-mechanics methods, under conditions mimicking the physiological excited state (oxyluciferin bound to luciferase), has shown that the keto to enol isomerisation is unlikely to occur within the lifetime of the excited species. They also suggested that the acquisition of a proton from a neighbouring lysine side chain (in order to facilitate tautomerisation) is unlikely owing to the potential charge stabilization offered by surrounding water and/or protein groups. Thus, they argue that the keto tautomer

is likely the emitting species. Regardless of the exact reaction pathway, as a result of this process it is possible to quantitatively correlate light output to ATP concentration. This has been exploited in the food processing industry by the chemically driven lysis of potential microbial contaminants. This results in the release of microbial AK, which is then exposed to its substrate (ADP) and coupled to the luciferase/ luciferin system. It is then possible to quantify the number of microbial cells present via evaluation of ATP turnover [30].

1.1.5.2 Thermostable Adenylate Kinase

Thermostable enzymes have been employed in a number of new and novel technologies, largely owing to the fact that many other enzymes will denature (lose their structural integrity rendering them inactive), at relatively low temperatures. The isolation and purification of a thermostable AK (tAK) from the archaebacterium *Sulfolobus acidocaldarius* (*S. acidocaldarius*) in 1993, paved the way for the significant development of surface contamination detection within the healthcare setting [34]. The archaebacterium from which tAK is isolated is an extremophile found growing in volcanic springs at temperatures between 75 – 80 °C. The corresponding tAK isolated from this thermophile exhibits a temperature optimum of around 90 °C and is stable to very low pH [35]. It exists as a 69 kDa trimer with highly conserved nucleotide binding sites. Figure 2 shows the crystal structure of tAK (PDB ID 1NKS [36]).

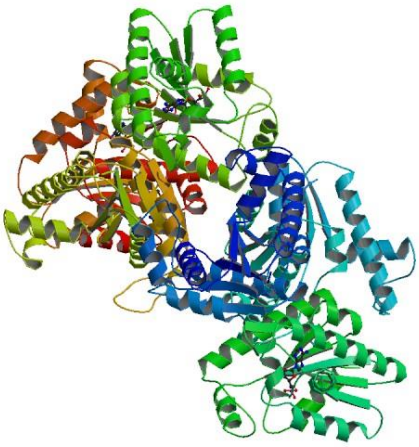

Figure 2 Crystallographic ribbon plot of two AK trimers isolated from *S. acidocaldarius.*

tAK catalyses a multisubstrate, multiproduct reaction in a random *bi bi* sequential fashion, as previously described in Section 1.1.2.3 [37]. The reaction scheme specific to AK can be seen in Figure 3 [38].

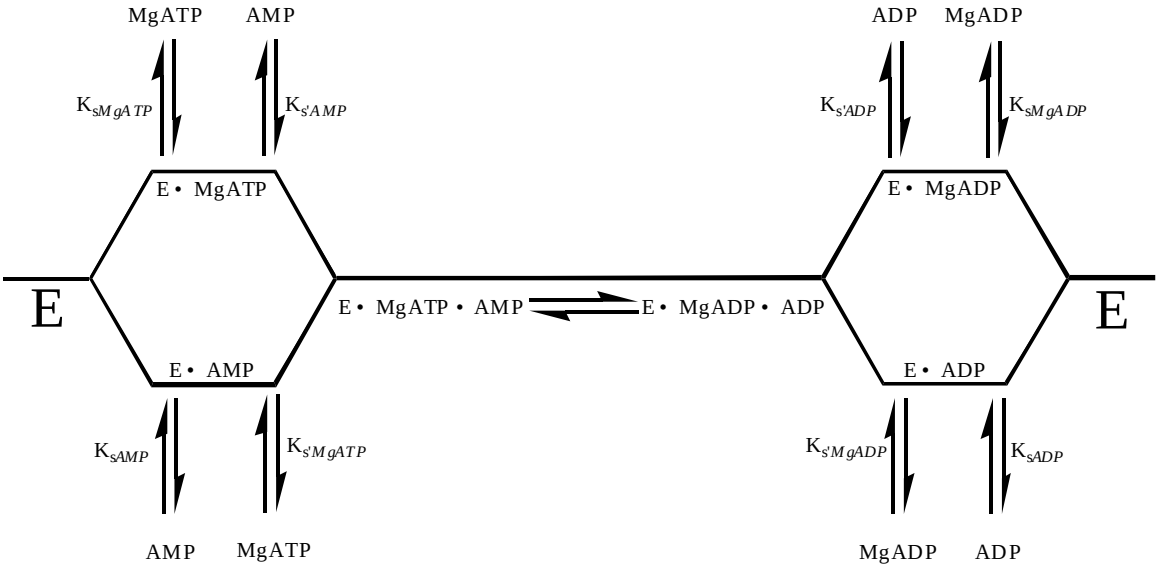

Figure 3 Random *bi bi* sequential reaction scheme for AK.

However, as previously mentioned when looking at the kinetics of such a system, they can simplify to the one substrate, Michaelis-Menten model provided that certain limitations are established.

1.1.5.3 WASHtAK

The novelty of tAK surrounds its ability to withstand extreme conditions, rather than the specific reaction it catalyses. tAK is currently used in the clinical setting as a model for highly surface adherent species commonly associated with surface contamination. Owing to the highly resilient nature of tAK, it can be used to model the cleaning efficacy of reusable surgical equipment post disinfection. Alongside tAK, there are other protein-based structures which are also resistant to high temperatures and low pH (two common methods of disinfection within hospitals) [39]. An example of which are prions; protease resistant, transmissible glycoproteins responsible for a range of transmissible spongiform encephalopathies (as discussed in Section 1.1.1) [40]. tAK is employed in the clinical setting as WASHtAK, patented by BIOtAK® [41]. The technology behind this device is detailed in a paper entitled "Quantitative measurement of the efficacy of protein removal by cleaning formulations; comparative evaluation of prion-directed cleaning chemistries", which highlights how protein removal is modelled by tAK as an indicator of cleaning efficiency [42]. WASHtAK can be seen in Figure 4.

Figure 4 WASHtAK. Copyright ©2017 BIOtAK Ltd.

WASHtAK comprises of a polymer based support with tAK physisorbed to its surface. It is placed into the clinical disinfection washer alongside any surgical equipment to be sterilised. Post washing, it is removed and exposed to its substrate, ADP. Any ATP produced is detected using the luciferase based coupling system. Light emitted post wash cycle correlates directly to the amount of tAK remaining on the stick, indicating the efficacy of sterilisation of the surrounding surgical equipment [43].

1.2 Extended Methodology

1.2.1 Plasma Polymerisation

The use of plasma technology for the modification of surfaces has been extensively reviewed and employed in recent years [44-46]. Plasma technology including etching, deposition and polymerisation are currently utilised for a variety of applications including within the medical, automotive, aeronautical and environmental sectors [47-50]. Plasma is capable of both removing and depositing material onto a surface, which offers the possibility of custom surface design suited to specific requirements, including sterilised platforms for use in medical devices, functionalised surfaces for biomolecule immobilisation (e.g. for use in biosensors), activated surfaces for electrochemical applications (such as supercapacitors) and plasma polymerised thin films for use as coatings (protective, anti-reflective, drug release etc.) [51-58].

Plasma discharge polymerisation involves the generation of high energy chemical species (ions, electrons and radicals), both in the solid and the gas phase via application of an external electric field, which combine to form stable covalent linkages. Polymerisation occurs as a result of chemical reactions within the energetic plasma species; between the plasma and the surface and between the surface active groups to form large, complex polymeric units.

Poly-recombination of the previously generated excited species may occur in the solid or the gas phase. Whilst low pressure plasma systems favour polymerisation in the solid phase (i.e. at the surface, owing to the low collision rate in the gas phase), increasing the pressure encourages polymer formation in the gas phase [59]. The difference in properties of the resultant polymer films can be substantial, a detailed study of which has been carried out by Saboohi *et al* [60]. Regardless of their difference in physical and chemical characteristics, these newly generated polymeric architectures should not be confused with conventional polymers (consisting of repeat monomer units). Plasma polymerised structures often consist of fragmented and rearranged monomers with a high degree of branching and crosslinking (Figure 5 [61]), the structure of which can often take some time to establish and optimise [62].

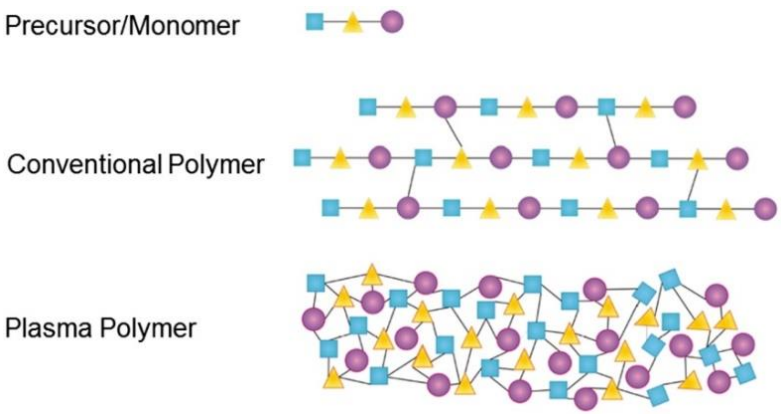

Figure 5 Schematic showing the difference between a conventional polymer and a plasma polymer comprised of the same starting material. Reprinted from [61] with permission from Elsevier, Copyright ©2016.

Plasma polymerisation offers a number of advantages over conventional surface modification methods: it can be achieved at ambient temperature (cold plasma – not in thermal equilibrium), it is a solvent free process (which has the advantage of facilitating subsequent biomolecule immobilisation) and the deposition is largely a controllable process. Parameters associated with the generation of plasma, such as pressure, excitation method, excitation source, flow rate and reactor geometry can be tailored in order to achieve the desired properties of the polymer [63].

1.2.2 Bioluminescence

Luminescence concerns the emission of light in the absence of thermal radiation, i.e. as a consequence of anything other than heat (as oppose to incandescence). This term encompasses phenomenon including photoluminescence, chemiluminescence, radioluminescence and bioluminescence. Bioluminescence, first formally observed by Aristotle *ca.* 300 BC, occurs within a living organism, resulting in the emission of light from an electronically or vibrationally excited species [64,65]. Biocatalysis of a chemical reaction is often an exothermic process, whereby the excess energy is retained within the system and converted from chemical potential energy into electronic excitation energy, rather than being released as heat (as with exergonic reactions). This gives rise to the transition of a reaction intermediate into the excited state. The subsequent relaxation to the ground state proceeds in the same manner as fluorescence and other forms of photoluminescence (excluding phosphorescence) [66]. Bioluminescent emission of light is very efficient, often exhibiting high quantum yields and therefore high emission intensities. The firefly luciferase/ luciferin system is one of the most efficient (relative to other forms of bioluminescence), with a quantum yield of 41 ± 7.4% at pH 8.5 [67]. The process of bioluminescence can be monitored using a luminometer which has several advantages over other analytical techniques. Luminometry is far more sensitive than both adsorption and fluorescence spectroscopy, and is capable in many cases of measuring femtomole quantities. Luminescent light from chemi- or bioluminescence is monochromatic, it is emitted as a result of a single reaction, therefore wavelength selectors/ filters are not required. There is also a much smaller background light contribution in luminometry and samples can be measured over a vast concentration range without dilution or modification of the sample in question [68].

1.3 Publication

1.3.1 Declaration of Authorship

<table>
<tr><td colspan="10">This declaration concerns the article entitled:</td></tr>
<tr><td colspan="10">Study into the Kinetic Properties and Surface Attachment of a Thermostable Adenylate Kinase</td></tr>
<tr><td colspan="10">Publication status (tick one)</td></tr>
<tr><td>Draft manuscript</td><td></td><td>Submitted</td><td></td><td>In review</td><td></td><td>Accepted</td><td></td><td>Published</td><td>✓</td></tr>
<tr><td>Publication details (reference)</td><td colspan="9">Hathaway, H. J., Sutton, J. M. & Jenkins, A. T. A. Study into the kinetic properties and surface attachment of a thermostable adenylate kinase. Biochemistry and Biophysics Reports 1, 1-7, doi:10.1016/j.bbrep.2015.03.011 (2015).</td></tr>
<tr><td>Candidate's contribution to the paper (detailed, and also given as a percentage).</td><td colspan="9">The candidate predominantly executed the…

Formulation of ideas:
Candidate decided on the direction of the research and the way in which to obtain results, based on previous research into the described technology (90%).
Design of methodology:
Candidate designed the experiments including troubleshooting, implementation of equipment and associated training as required (100%).
Experimental work:
All experiments for the research paper were carried out by the candidate (100%)
Presentation of data in journal format:
All data work up was performed by the candidate. Publication was written by the candidate with minor corrections and suggestions offered by the co-authors (90%)</td></tr>
<tr><td>Statement from Candidate</td><td colspan="9">This paper reports on original research I conducted during the period of my Higher Degree by Research candidature.</td></tr>
<tr><td>Signed</td><td colspan="5">  </td><td>Date</td><td colspan="3">29.09.17</td></tr>
</table>

1.3.2 Copyright Agreement

1.3.3 Data Access Statement

All data created during this research is openly available from the University of Bath data archive at https://doi.org/10.15125/BATH-00334.

1.3.4 Published Article

Study into the Kinetic Properties and Surface Attachment of a Thermostable Adenylate Kinase

H. J. Hathaway[1], J.M Sutton[2], A.T.A. Jenkins[1*]

[1] Department of Chemistry, University of Bath, Bath and North East Somerset, UK

[2] Technology Development Group, Public Health England, Porton Down, Salisbury, Wiltshire, UK

*Correspondence: Dr. Toby Jenkins , Department of Chemistry, University of Bath, Claverton Down, Bath and North East Somerset, BA2 7AY, Tel: +44 (0) 1225 386118, Email: a.t.a.jenkins@bath.ac.uk

Abstract

A thermostable adenylate kinase (tAK) has been used as model protein contaminant on surfaces, so used because residual protein after high temperature wash steps can be detected at extremely low concentrations. This gives the potential for accurate, quantitative measurement of the effectiveness of different wash processes in removing protein contamination. Current methods utilise non-covalent (physisorption) of tAK to surfaces, but this can be relatively easily removed. In this study, the covalent binding of tAK to surfaces was studied to provide an alternative model for surface contamination. Kinetic analysis showed that the efficiency of the enzyme expressed as the catalytic rate over the Michaelis constant (k_{cat}/K_M) increased from **8.45** ± 3.04 mM^{-1} s^{-1} in solution to **32.23** ± 3.20 or **24.46** ± 4.41 mM^{-1} s^{-1} when the enzyme was immobilised onto polypropylene or plasma activated polypropylene respectively. Maleic anhydride plasma activated polypropylene showed potential to provide a more robust challenge for washing processes as it retained significantly higher amounts of tAK enzyme than polypropylene in simple washing experiments. Inhibition of the coupled enzyme (luciferase/luciferin) system used for the detection of adenylate kinase activity was observed for a secondary product of the reaction. This needs to be taken into consideration when using the assay to estimate cleaning efficacy.

Keywords: Thermostable Adenylate Kinase, Kinetic Parameters, Plasma Deposition, Cleaning Efficacy, Enzyme Inhibition.

Introduction

Efficient modelling of protein attachment to surfaces has generated wide interest within the scientific community over the years, largely owed to the significant number of implications this phenomenon is responsible for. Perhaps one of the most clinically relevant implications is the residual protein contamination of surgical equipment post cleaning and disinfection. Equipment such as endoscopes and other reusable tools are subject to vigorous disinfection cycles within the clinic; however, there are certain biological species which are resistant to such cleaning processes. An example of which are prions, protease resistant, transmissible glycoproteins responsible for a range of transmissible spongiform encephalopathies including Creutzfeldt-Jacob disease (CJD) [40]. Therefore evaluation of proteinaceous surface contamination has become paramount in preventing the spread of disease within the healthcare setting. This has led to specific review and revision of processes for cleaning surgical instruments in the health service in England [69]. A current clinical model aimed at quantifying residual protein presence post disinfection utilises a thermostable adenylate kinase (tAK) enzyme, so used due to the resilient nature of the enzyme drawing potential comparison to equally resilient species such as prions.

The enzyme adenylate kinase (AK) is a phosphotransferase enzyme which catalyses the reversible formation of adenosine triphosphate (ATP) and adenosine monophosphate (AMP) from adenosine diphosphate (ADP), as shown in Scheme 4.

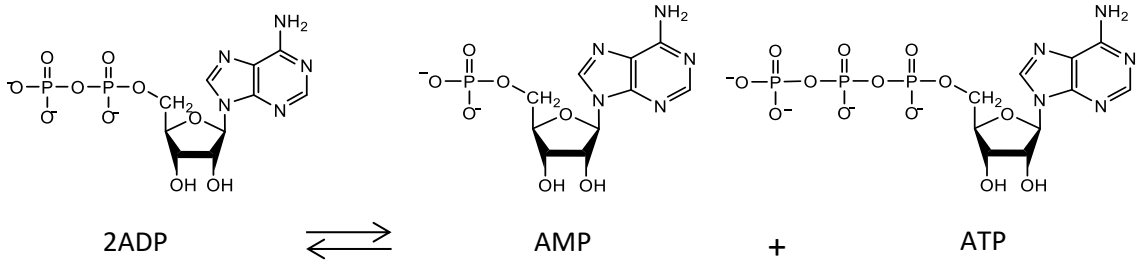

Scheme 4 tAK catalysed ATP formation.

The isolation and purification of a thermostable AK (tAK) from the archaebacterium *Sulfolobus acidocaldarius* in 1993, paved the way for the significant development of proteinaceous surface contamination detection within the healthcare setting [34]. The

archaebacterium from which tAK is isolated is an extremophile found growing in volcanic springs in temperatures between 75 – 80 °C. The corresponding tAK isolated from this thermophile demonstrates a temperature optimum of around 90 °C and is stable to very low pH [35]. The novelty of tAK lies with its ability to withstand extreme conditions, tAK is currently in use in the clinical setting (WASHtAK [41]) as a model for highly surface adherent species commonly associated with residual surface contamination. The technology behind this device is detailed in a previous paper, which highlights that protein removal is modelled by tAK as an indicator of cleaning efficiency [42]. Briefly, in this system tAK is physisorbed to a polypropylene strip and is placed into a surgical equipment washer to undergo the standard disinfection cycle that reusable surgical equipment is subject to. Post wash cycle the polypropylene strip is removed and the residual tAK is exposed to its substrate (ADP) which is then converted to ATP. Subsequently the ATP concentration is measured via a well-known coupled enzymatic reaction involving a standard preparation of luciferase and its substrate luciferin. This assay has been extensively optimised over the years in order to accurately determine ATP concentration as a function of light output [70]. Ultimately the system relies on the excitation of luciferin to a higher energy level using ATP, the decay from this excited state to the ground state then leads to the generation of light in the form of bioluminescence. The full mechanism of bioluminescence emission from the luciferase/ luciferin assay has been published elsewhere [31].

Previous studies on AK isolated from *Sulfolobus acidocaldarius* (in conjunction with the luciferase method of quantification) have been largely studied at high temperatures close to the optimum. One such study conducted at 70 °C reported a K_M value of 0.7 mM with ADP as the substrate in the presence of 5 mM MgCl [34]. The study also reported a k_{cat}/K_M (catalytic capacity) value of 2.8 $x10^5$ M^{-1} s^{-1} based on a calculated theoretical V_{max} value. The kinetic properties of this specific AK at 25 °C, which would be the case where it used for daily monitoring of cleaning efficacy, are absent in the literature both in solution and bound to surfaces. As such there is no direct comparison or evaluation of the effect on activity when the enzyme is restricted to a solid support, such as it is in its current clinical application.

There are a number of ways in which proteins can bind to surfaces, both the prevention and promotion of such a phenomenon has been vastly studied highlighting the effects of protein conformation/ orientation, hydrophobicity/hydrophilicity, electrostatic nature of the support, binding temperature/ pH and the structural stability of the protein in question [71,72]. The prevention of protein attachment to surfaces is of particular importance when considering the anti-fouling properties of a range of materials including, but not limited to

biosensors, surgical equipment/ medical devices, food containment and industrial equipment, the significance of which has been reviewed elsewhere [73].

Plasma activated materials have generated considerable interest in terms of functionalising solid supports to promote protein attachment to surfaces, and this may be useful if one wishes to accurately model the removal of tightly adhered proteins, including prions. The highly energized state of plasma has the potential to modify the outermost layer of a polymer surface by deposition of various functional groups. The successfully deposited functional groups (which can vary from amines to carboxyl groups depending on the monomer used), can then go on to react with a variety of species which would otherwise remain unreactive towards the inert polymer support. Not only does plasma deposition provide a predominantly solvent free alternative to wet chemistry, which in turn reduces the amount of chemical waste, it is also a largely 'controllable' process, meaning surface modification can be achieved homogeneously with the final composition tailored towards the intended application [74]. Numerous biomolecules have been successfully anchored onto polymer supports following plasma activation of the surface, many of which have been reviewed elsewhere [63]. Plasma activation of surfaces to improve coating has been used on a large scale in the automotive industry, and this suggests that such processes should be scaleable if required for high volume applications.

One of the main concerns when considering the possibility of utilising surface bound proteins is the apparent loss of activity when restricting biologically active species to a solid support. Random attachment (disregarding the orientation of the protein) can often result in the modification of critical resides within the protein structure, which can directly affect the overall stability of the complex. This in turn can have repercussions in terms of accessibility of the protein in question, often as a result of steric hindrance affecting access to particular biologically active sites within the protein structure. One must also consider the impact of utilising potentially charged functional groups (such as those commonly found in lysine and aspartic acid residues), the masking or complete removal of such a charge can have detrimental effects in terms of protein stability [75]. An advantage of using a thermostable adenylate kinase which is largely resistant to extreme pH, is the resilient nature of the protein itself, tAK is essentially a stable protein, reducing its capacity to denature when anchored to a solid support, thus increasing the ways in which immobilisation can be carried out.

To date, there have been no studies carried out evaluating the kinetic behaviour of tAK and the subsequent coupled luciferase system when considering surface binding. This report aims to detail the catalytic activity and surface binding properties of tAK when immobilised onto a solid support, with the intention of potentially providing a more robust challenge for use in cleaning process validation and modelling. .

Materials and Methods

Materials

tAK was obtained from the Technology Development Group, Public Heath England (PHE - Salisbury UK). Its isolation, expression in *Escherichia coli* and purification has been detailed previously [42,43]. Mucin from porcine stomach was purchased from Sigma-Aldrich (Poole, Dorset, UK). ATP Reagent (luciferase/ luciferin/ divalent metal ions and stabilisers), Diluent C (reconstitution solution for ATP Reagent), tris-EDTA buffer, ADP and ATP standard solutions were all purchased from BioThema (Sweden).

AMP, ethanol, maleic anhydride and preformed phosphate buffered saline (PBS) tablets (pH 7.4) were purchased from Sigma-Aldrich (Poole, Dorset, UK).

Methods

Generation of an ATP Standard Curve

ATP standard solutions were prepared via serial dilution from stock (0.01 mM) to give a range of concentrations from 1 x10^{-3} mM to 1 x10^{-8} mM, diluted in tris-EDTA buffer. 100 µl of ATP standard was added to each well of a white 96 well polystyrene microtitre plate. Luminescence output was recorded for 3 s using the bioluminescence module on a BMG Labtech Spectrastar plate reader. ATP Reagent (standard preparation of luciferase, luciferin, magnesium ions and stabilisers) was prepared via reconstitution with Diluent C at room temperature, 30 µl was injected after 3 s using the inbuilt injector system. Luminescence output was recorded for a further 27 s at 25 °C. 5 replicates were performed for each ATP concentration.

tAK in Solution

ADP standard solutions were prepared via serial dilution from stock (0.2 mM) to give a range of concentrations from 0.1 mM to 0.0016 mM, diluted in tris-EDTA buffer. An 8 ng/µl tAK standard solution was serial diluted from stock (2.32 µg/µl) using a solvent system consisting of 80% water, 20% ethanol and 0.1% hog mucin to give a range of tAK concentrations – 4, 2, 1, 0.5 ng/µl [43,76]. 100 µl of ADP standard was added to each well of a white 96 well polystyrene microtitre plate. ATP Reagent was prepared as before and a 2 component injection system was used; 10 µl tAK and 30 µl ATP Reagent were mixed and luminescence output was monitored for 5 s prior to injection and continued for a further 55 s at 25 °C post injection. This was performed in triplicate for each enzyme concentration.

Adsorption of tAK to Polypropylene Surface

A 0.8 ng/µl tAK standard solution was serial diluted from stock as before to give the same range of tAK concentrations. 50 µl of tAK was added to each well of a white 96 well polypropylene microtitre plate. This was allowed to dry down at 37°C for 2 h with agitation. 30 µl ATP Reagent was then added to each well. ADP standard solutions were prepared via serial dilution from stock to give the same range of concentrations diluted in tris-EDTA buffer. Luminescence output was recorded for 5 s prior to the injection of 100 µl ADP and continued for a further 55 s post injection at 25 °C. This was repeated in triplicate for each concentration of enzyme with each concentration of ADP.

Plasma Activation of Polypropylene Surface

Plasma deposition was carried out using a plasma reactor unique to the research group as previously detailed [77]. White 96 well polypropylene microtitre plates were placed inside the plasma reactor chamber; 0.1 g maleic anhydride was added to the Young's flask, before being reduced to 10^{-3} mbar pressure. The flask then underwent three freeze thaw cycles using liquid nitrogen in order to remove any water. The plasma was ignited and pulsed at a duty cycle of 1 s (on) / 40 ms (off) with a peak power of 40 W input for 10 min. tAK was added to the plasma deposited maleic anhydride microtitre plates immediately after deposition (at 37 °C with agitation for 2 h). Successful deposition was confirmed with Fourier-Transform Infrared Spectroscopy (FT-IR) (Figure 1 Supplementary Information). A peak at 1788 cm^{-1} represents the carbonyl stretching frequency of the newly deposited anhydride moieties. It is likely that the primary amines found in a number of amino acid residues within tAK can go on

to react with the anhydride ring retained within the deposited maleic anhydride present on the modified polymer surface [77]. A potential mechanism for the reaction of tAK with plasma deposited maleic anhydride is shown in Figure 6.

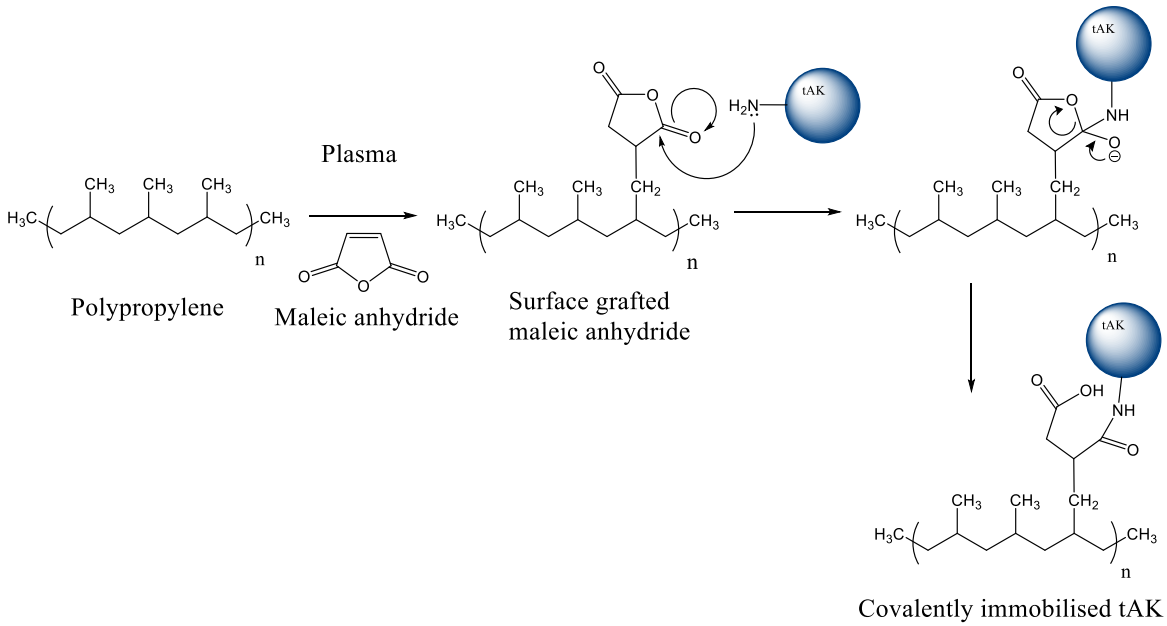

Figure 6 Putative reaction scheme showing the reaction between plasma deposited maleic anhydride on polypropylene with tAK.

Luciferase Inhibition

Inhibition experiments were undertaken using AMP and luciferase. A concentration of 1 x10^{-5} mM ATP was chosen based on previous experiments as this concentration of ATP produces light output in the mid-range of the experimental setup. The AMP concentration was varied from 1 mM to 1 x 10^{-4} mM. 100 µl of each ATP/AMP solution was added to each well of a white 96 well polypropylene microtitre plate, luminescence output was monitored for 5 s prior to the injection of 30 µl of ATP Reagent. The reaction was further monitored for 55 s at 25 °C, and again performed in triplicate.

Washing Experiments

Washing experiments were performed after immobilisation of tAK by pipetting 100 µl of either water or PBS buffer into each well followed by manual swirling of the plate before removal via pipette. This was repeated three times for each well.

Results and Discussion

Standard Curve

A standard curve was produced in order to quantify the initial rate of reaction of subsequent tAK experiments to ATP concentration for use in kinetic parameter calculations. The standard curve is shown in Figure 7 demonstrating a linear correlation between light output and ATP concentration. From this graph it was possible to relate ATP concentration to the rate of light production when considering the enzyme-catalysed formation of ATP.

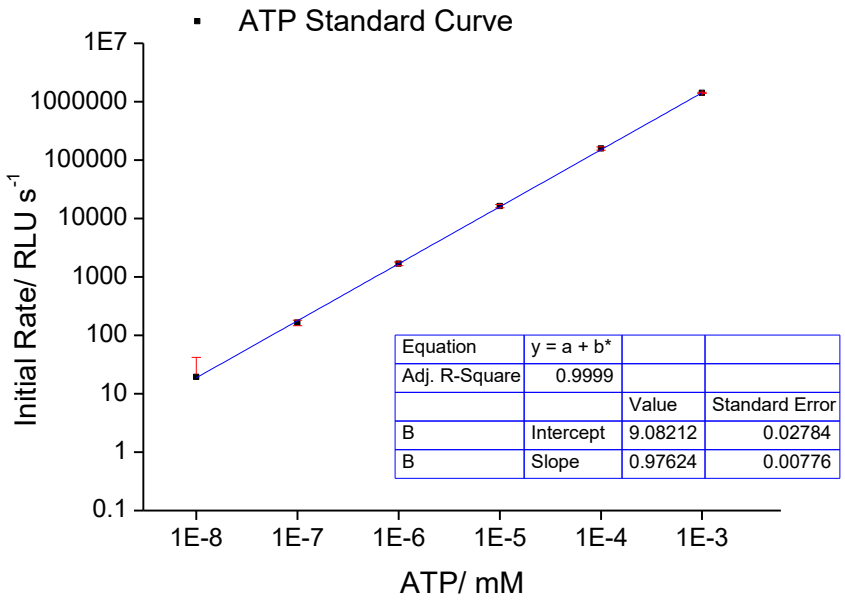

Figure 7 ATP standard curve used to correlate light output to ATP concentration in tAK experiments.

The kinetic properties of the tAK enzyme as evaluated following physical adsorption onto polypropylene

Different concentrations of tAK were immobilised under standard conditions (80% water, 20% ethanol, 0.1% mucin, reacted for 2 h at 37 °C with agitation) Data is shown as relative light units (Figure 8). The initial rate of reaction was calculated between 5 and 15 s by means of tangents and plotted as a function of ADP concentration, as shown in Figure 9.

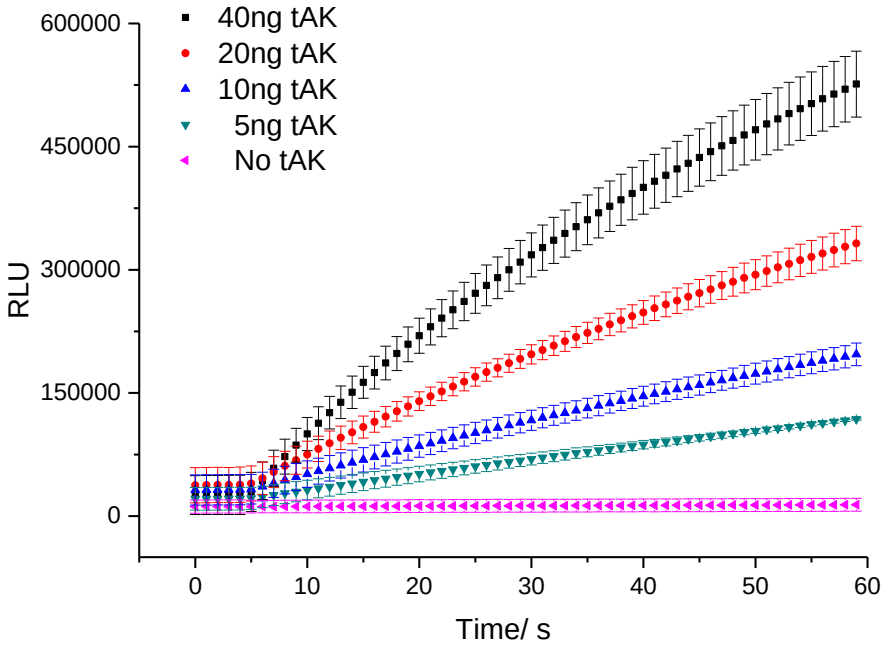

Figure 8 Luminescence output (RLU) plotted as a function of tAK concentration over time. This figure shows the reaction of tAK adsorbed to polypropylene using a substrate concentration of 0.1 mM ADP. Data is shown as Relative Light Units (RLU) with error bars representing standard deviation. The data is an average of at least three independent repeats.

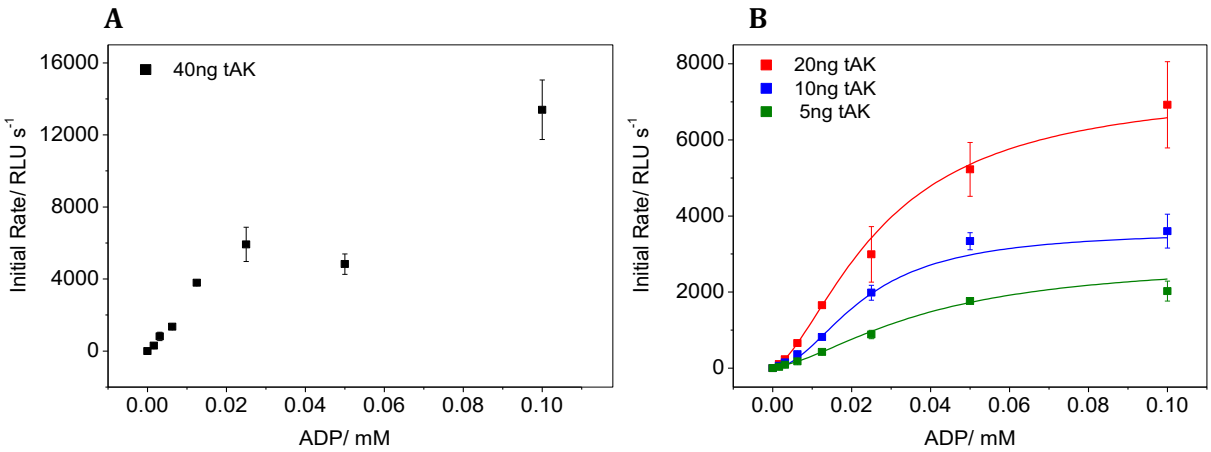

Figure 9 Comparison of initial rate of reaction (RLU s^{-1}) when using a high tAK concentration (**A**) and for lower tAK concentrations (**B**) adsorbed to polypropylene. Tangents were fitted according to a linear fit function within Origin graphing software between 5 and 15 s.

Table 1 Summary of the fitting values and the standard error for 20, 10 and 5 ng of tAK from Figure 4B according to the Hill Equation.

tAK (ng)	Adjusted R-Squared Value	V_{max} (RLU s^{-1})	K_M (mM)	*n* value
20	0.942	7420.79 ± 4355.85	0.028 ± 0.020	1.60 ± 0.63
10	0.939	3619.22 ± 1371.42	0.023 ± 0.011	1.97 ± 0.94
5	0.998	2024.45 ± 147.18	0.027 ± 0.003	1.73 ± 0.21

A curious observation is the apparent drop in initial rate at a concentration of 0.05 mM ADP when using the highest concentration of tAK (40 ng). A possible explanation for this could be product inhibition, which is outcompeted at high substrate concentrations. This trend was not seen when lowering the concentration of tAK. The curves were fitted to the Hill equation (1), using a non-linear curve fit function generated within Origin graphing software, the fitting values for Figure 9B are shown in Table 1. The Hill equation is a slight modification of the traditional Michaelis-Menten equation, allowing for a certain degree of cooperativity (represented by the *n* value) in a multi-substrate reaction. tAK binds two molecules of ADP in a random *bi bi* sequential fashion [37], meaning there is an increased likelihood of cooperativity. This phenomenon is also predicted due to the sigmoidal nature of curve.

$$v = \frac{V_{max}\,[\mathrm{S}]^n}{K + [\mathrm{S}]^n} \quad (1)$$

The Michaelis-Menten equation (2) was employed in order to quantify enzyme activity, which normally accounts for simple one substrate binding kinetics, however random sequential kinetics will simplify to the Michealis-Menten model provided that $k_2 << k_{-1}$, which has been confirmed as being the case for AK [78], whereby the dissociation of bound nucleotides has been shown to be the rate limiting step. V_{max} values were obtained via extrapolation and again produced using Origin graphing software, they were then compared with the standard curve in order to quantify maximum rate of reaction in terms of moles per litre per second of ATP produced. k_{cat} values were then calculated based on the molecular weight of tAK (69 kDa).

$$v = \frac{V_{max}[S]}{K_M + [S]} \quad (2)$$

tAK Bound to Plasma Deposited Maleic Anhydride on Polypropylene

In an attempt to increase the binding and retention of tAK to polypropylene, maleic anhydride was coated using a plasma deposition method. Deposition was carried out under conditions previously optimised for maximum surface retention of functional groups [79]. Initial rate data for 40 ng and 5 ng tAK is shown in Figure 10, and again the reduction in rate of reaction is present at mid-range ADP concentrations. This was mirrored for all tAK concentrations.

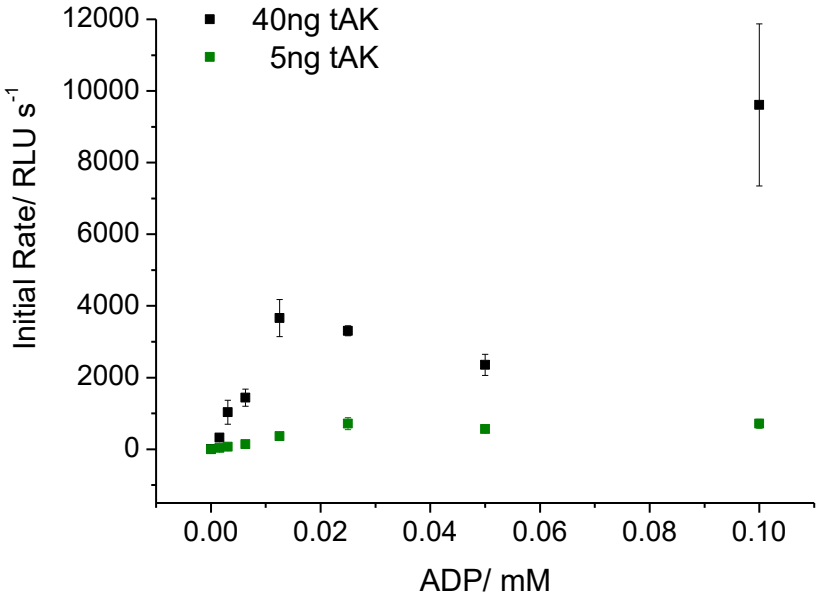

Figure 10 Initial rate of reaction (RLU s^{-1}) plotted as a function of ADP concentration for two tAK concentrations covalently bound to maleic anhydride deposited onto polypropylene.

The decrease in rate of reaction in the mid-range of ADP concentrations presented when tAK was covalently bound to the surface of the polymer was not seen when considering tAK in solution and was only observed at high tAK concentration when adsorbed to the polymer surface. This may suggest some form of inhibition caused by the restriction of the anchored enzyme, possibly as a result of a decrease in the rate of diffusion due to obstructed access to

the enzyme's active site, or as a result of steric hindrance. However the difficulty in assessing this hypothesis lies with the use of a coupled system. Whilst the apparent decrease in rate of reaction may be as a result of the anchoring of the enzyme to a surface, it may equally be due to interference from the luciferase system. It has long been known that luciferase can be inhibited by AMP if the concentration of AMP reaches a concentration whereby it outcompetes ATP, a decrease in luminescence will be observed due to inhibition [70]. Whilst this is not seen in solution when using the same concentration of reactant, it could be possible that due to a change in the rate of diffusion of nucleotides away from tAK in its anchored state (AMP being smaller and thus potentially diffusing away faster than the larger ATP molecules), the inhibition effect is enhanced.

Inhibition Studies

The inhibition of luciferase by various AMP concentrations was investigated in order to assess whether the coupled system can indeed be inhibited by a secondary product of the primary reaction in question. Figure 11 shows the initial rate of light production when utilising luciferase to turn over ATP whilst increasing the concentration of AMP. From the standard curve a concentration of 1 x10^{-5} mM ATP should give an initial rate of reaction of around 16000 RLU s^{-1}. Therefore it has been shown that even a very small amount of AMP can inhibit the coupled system involved in monitoring tAK activity.

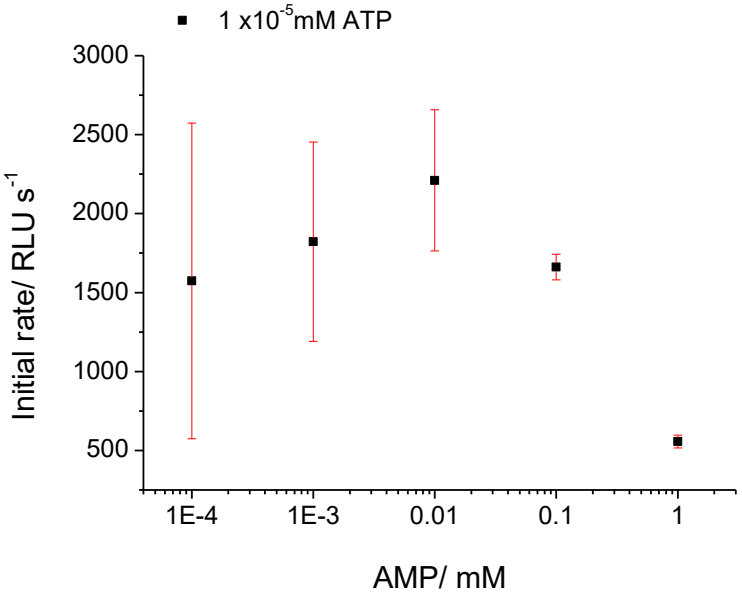

Figure 11 Effect of AMP concentration on initial rate of reaction in the luciferase catalysed turnover of ATP.

To avoid this effect impacting on the measurement of tAK activity during assessment of wash processes it is important that a large excess of ADP is used to ensure that it outcompetes any AMP for binding to the enzyme. This approach has been used in previous studies looking at the use of tAK to monitor wash efficacy in different settings [41,43,76]. In addition, the reaction that luciferase catalyses can also be self-inhibiting, that is to say that two of the primary products formed in the production of light from ATP (oxyluciferin and dehydroluciferyl-adenylate) are both competitive inhibitors of luciferase [80]. Table 2 shows a summary of the calculated kinetic parameters.

Table 2 Summary of calculated kinetic parameters for tAK in solution and bound to activated and non-activated surfaces. The previously highlighted deviations from the hyperbola in the initial rate data (e.g. when using 0.05 mM ADP) were omitted from the calculations.

	k_{cat} (s^{-1})	K_M (mM)	k_{cat}/K_M (mM^{-1} s^{-1})
Solution	0.138 ± 0.040	0.017 ± 0.003	8.45 ± 3.04
Adsorbed to Polypropylene	0.855 ± 0.029	0.027 ± 0.003	32.23 ± 3.20
Plasma Activation of Polypropylene	0.558 ± 0.182	0.024 ± 0.011	24.46 ± 4.41

The results presented here show that in terms of activity and catalytic efficiency tAK performs best when adsorbed to polypropylene. The data shows a large increase in the k_{cat} with six and four-fold increase for tAK immobilised to polypropylene and maleic anhydride derivatised polypropylene respectively. A small increase in the K_M is also observed for the immobilised enzyme. This is consistent with an increase in the turnover number observed in other enzymes immobilised onto surfaces [81,82].

Removal of tAK during simple wash experiment

Simple wash experiments were conducted to evaluate whether the maleic anhydride treatment of the polypropylene altered the retention of the enzyme. For tAK absorbed onto polypropylene, even simple washing removed significant amounts of bound enzyme, between 97.4 and 97.5% of the surface bound protein was removed with water or PBS. This is consistent with previous studies using the tAK enzyme as a model for assessing washing

performance. In these studies, tAK removal is biphasic with the majority of the enzyme being rapidly (<5 min) removed by water or cleaning formulations and subsequent protein removal being very slow (>2 h). The ability of the assay system to measure protein removal over a greater than 5-log dynamic range means that it is possible to model such removal with formulations that affect the slow-phase of tAK removal [41]. With tAK covalently bound to maleic anhydride modified polypropylene which had been plasma deposited onto the polymer support, only 16.5 and 68% of the surface bound protein was removed when washed with water and PBS respectively, thus demonstrating a higher degree of surface binding. This is shown in Figure 12.

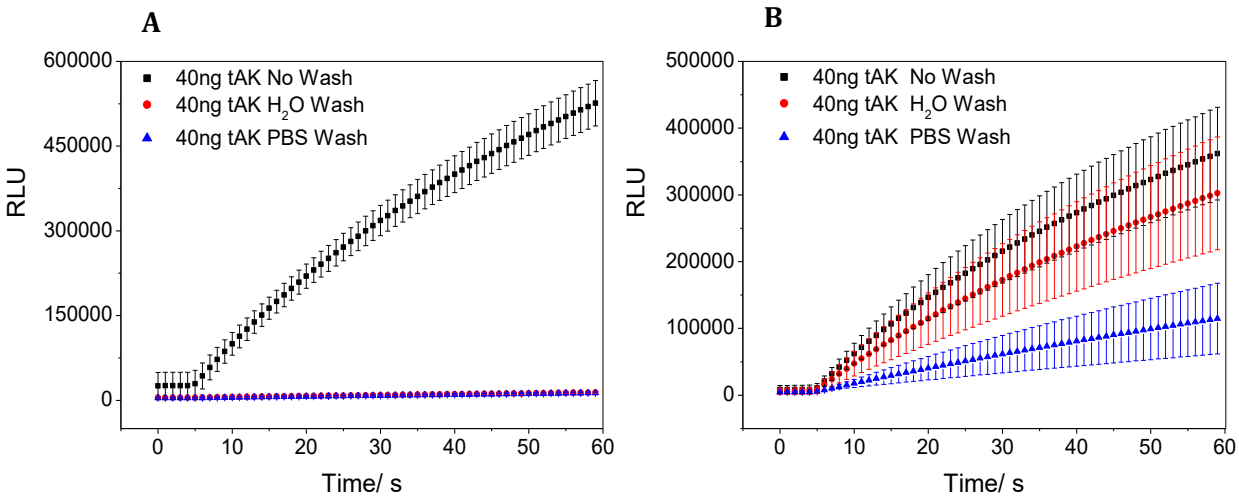

Figure 12 Effect of different washing strategies on the surface removal of tAK physisorbed to a polypropylene surface (**A**) and covalently bound to a polypropylene surface (**B**).

Enhancing the binding capacity of the surface for retention of the tAK enzyme provides a more challenging comparison for evaluating cleaning products or approaches which have improved protein removal.

Conclusions

In conclusion this study has highlighted the importance of methods for the evaluation of hospital cleaning procedures related to reusable surgical equipment. Whilst the current system in use (WASHtAK) provides a reasonable method of assessing washing efficacy, it has been shown that modification of the surface contamination model with tAK may provide a model with greater ability to differentiate between effective cleaning and decontamination processes such as those required to remove exceptionally adherent molecules such as prions.

There may be scope to develop this system based on optimising the immobilisation of tAK through the use of plasma activation of surfaces, or by improving the detection reagents in order to remove any inhibition of signal output. The use of maleic anhydride plasma modification of polypropylene to improve the binding of proteins and to reduce desorption form materials, may have additional value in the study of biofilm communities which adhere to surfaces and for a variety of biotechnology processes that depend on immobilised enzymes for biocatalysis or other applications.

Acknowledgements

The authors wish to acknowledge the BBSRC and Public Health England for funding an iCASE studentship.

Supplementary Information

The authors A.T.A. Jenkins and H.J. Hathaway have no conflict of interest in submitting this paper for publication. For the record, Dr M. Sutton contributed to the development of a spin-off company which uses tAK technology: BiotAK.

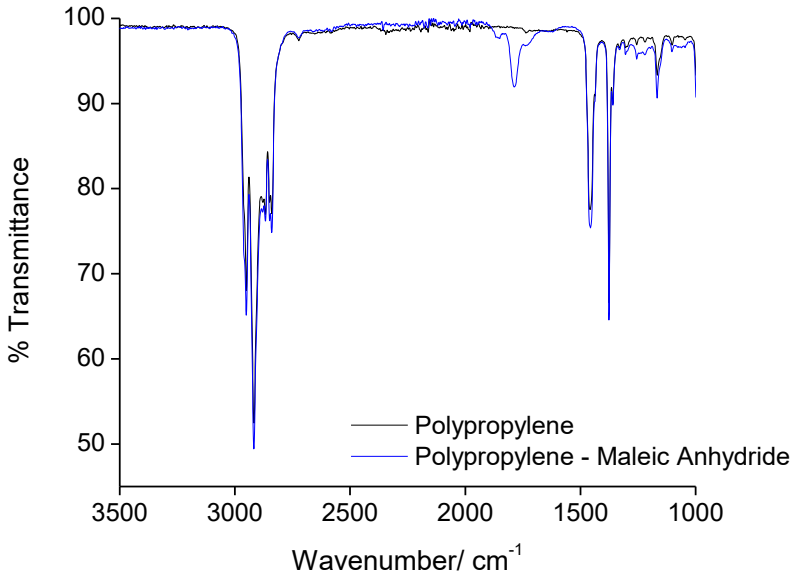

Supplementary Figure 1 FT-IR spectra showing retention of the anhydride functionality, demonstrated by the presence of a carbonyl peak at 1780 cm^{-1}, confirming successful plasma deposition of maleic anhydride.

1.4 Additional Research

Additional research was carried out following the publication of the research article in order to evaluate other methods of covalent surface attachment of the tAK enzyme. Experiments were undertaken in order to establish the effect of a spacer arm when investigating protein immobilisation. This was achieved via plasma deposition of allylamine and subsequent reaction with glutaraldehyde.

1.4.1 Materials and Methods

1.4.1.1 Plasma Deposition of Allylamine

Plasma deposition of allylamine was carried out according to the protocol detailed in Section 1.3.4, conditions were optimised according to a study by Chen *et al* [83] and deposition was characterised by FT-IR. Briefly, 1 ml allylamine was added to the Young's flask, before being reduced to 0.5 mbar pressure. The plasma was ignited and set to continuous wave of 10 W input and adjusted for zero reflected energy for 30 min. A needle valve was used to restrict the entry of allylamine vapour into the reaction chamber. A clear colour change was observed upon ionisation of allylamine as shown in Figure 13.

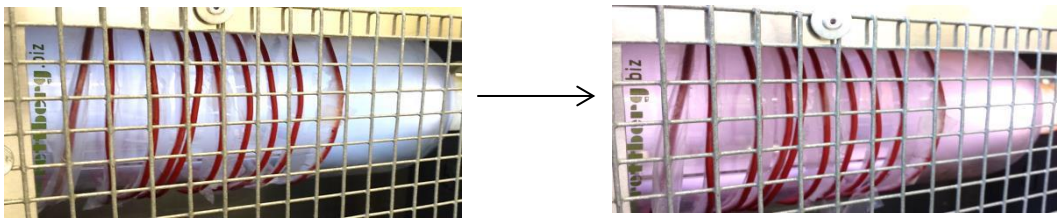

Figure 13 Colour change from blue to pink following plasma polymerisation of allylamine.

1.4.1.2 Activation of Plasma Deposited Allylamine

Prior to addition of tAK to the plasma deposited allylamine microtitre plates, 100 µl of 2.5% glutaraldehyde solution in H_2O was added to each well and allowed to react for 1 h at 37 °C, (according to the protocol laid out by Vartiainen *et al* [84]). Each well was washed thrice with 100 µl of H_2O to remove any unreacted glutaraldehyde. tAK was then added to the activated plates and activity was monitored according to Section 1.3.4, with a slight modification in the

buffer, which was changed from tris-EDTA to PBS in all of the stock preparation in order to remove any amine-containing components.

1.4.2 Results and Discussion

1.4.2.1 Plasma Deposition of Allylamine

Successful deposition was confirmed via FT-IR (Figure 14) with the primary amine N-H stretching frequency observed at 3205 cm^{-1} and the N-H bending frequency at 1638 cm^{-1}. The peak at 1715 cm^{-1} could indicate the presence of an amide. The bands observed between 2100 cm^{-1} and 2260 cm^{-1} may be attributed to species such as C≡N and C≡C, present as a result of fragmentation of the monomer structure [85]. These peaks can be used as a reference when undertaking plasma deposition. The harsher the deposition conditions, the higher the degree of fragmentation.

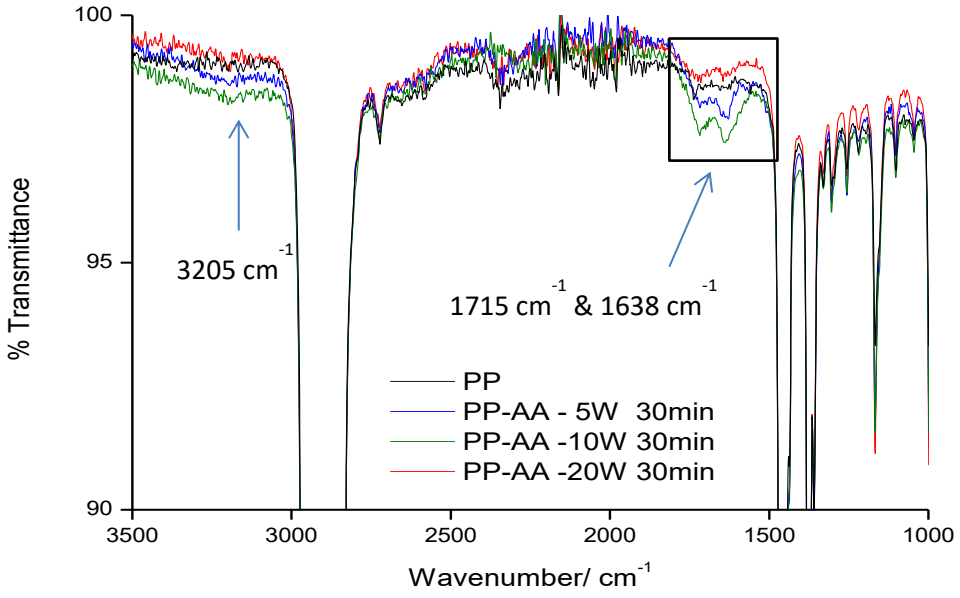

Figure 14 FT-IR spectra of allylamine (AA) plasma deposited onto polypropylene (PP) as a function of power input.

1.4.2.2 Activation of Plasma Deposited Allylamine

Following plasma deposition, the surface amine groups were reacted with glutaraldehyde in order to provide anchor sites for the subsequent immobilisation of tAK, both of which rely on

the formation of a Schiff base or imine in order to achieve covalent attachment. Figure 15 shows a possible reaction pathway for glutaraldehyde activation and subsequent tAK immobilisation; however it is difficult to determine the exact mechanism in this case, as glutaraldehyde can exist as a variety of structures in aqueous solution [86].

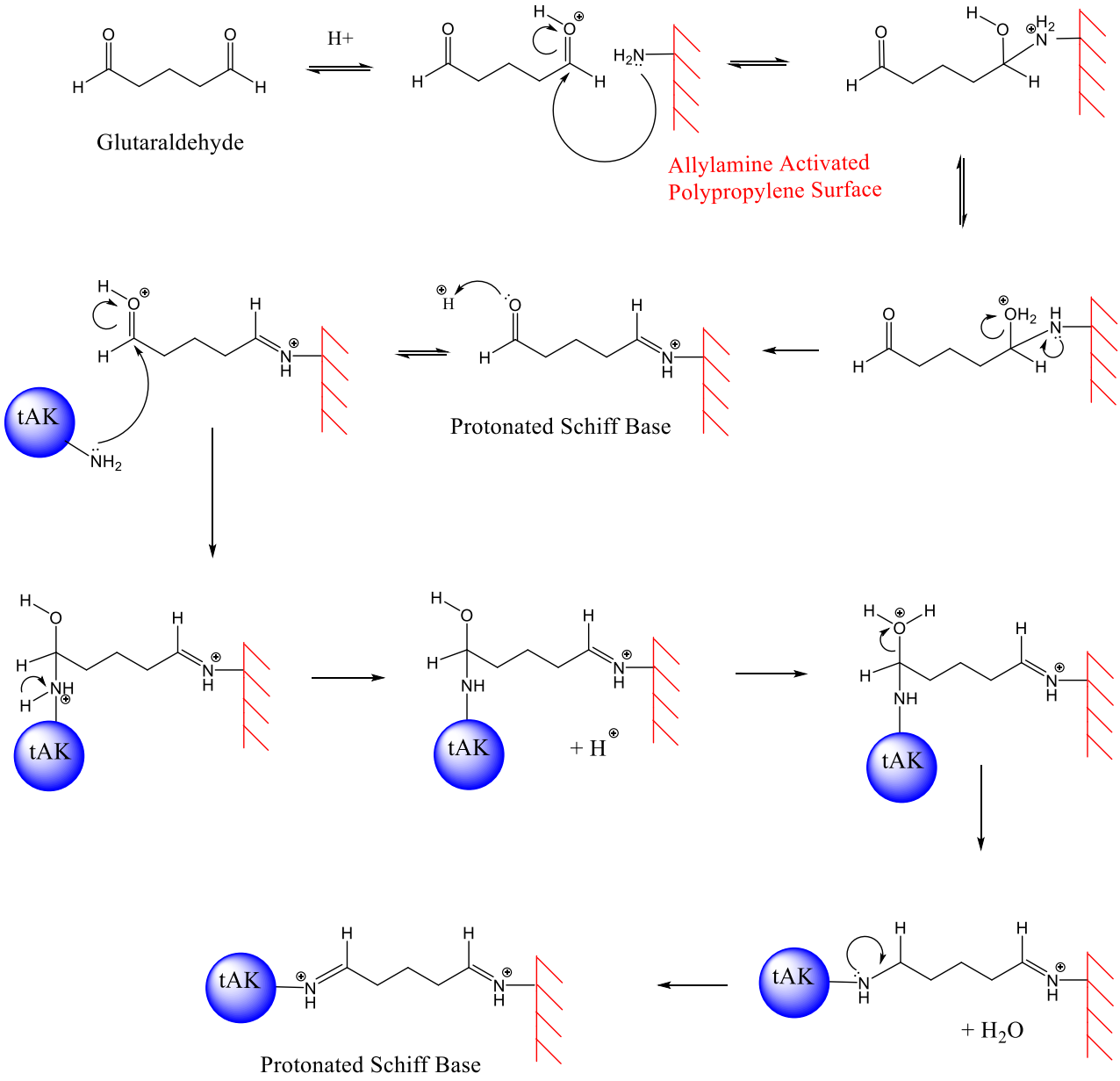

Figure 15 Reaction of plasma deposited allylamine with glutaraldehyde and subsequent tAK immobilisation.

The stability of the Schiff base has been called into question on numerous occasions owing to the possibility that it will break down in solution to reform the amine and aldehyde. The stability of the imine may be enhanced at elevated pH or by subjection to reductive amination

using sodium cyanoborohydride. However experiments were undertaken without further modification to the imine in order to establish whether successful immobilisation had taken place. The reaction of glutaraldehyde with the allylamine deposited support was again monitored by FT-IR (Figure 16).

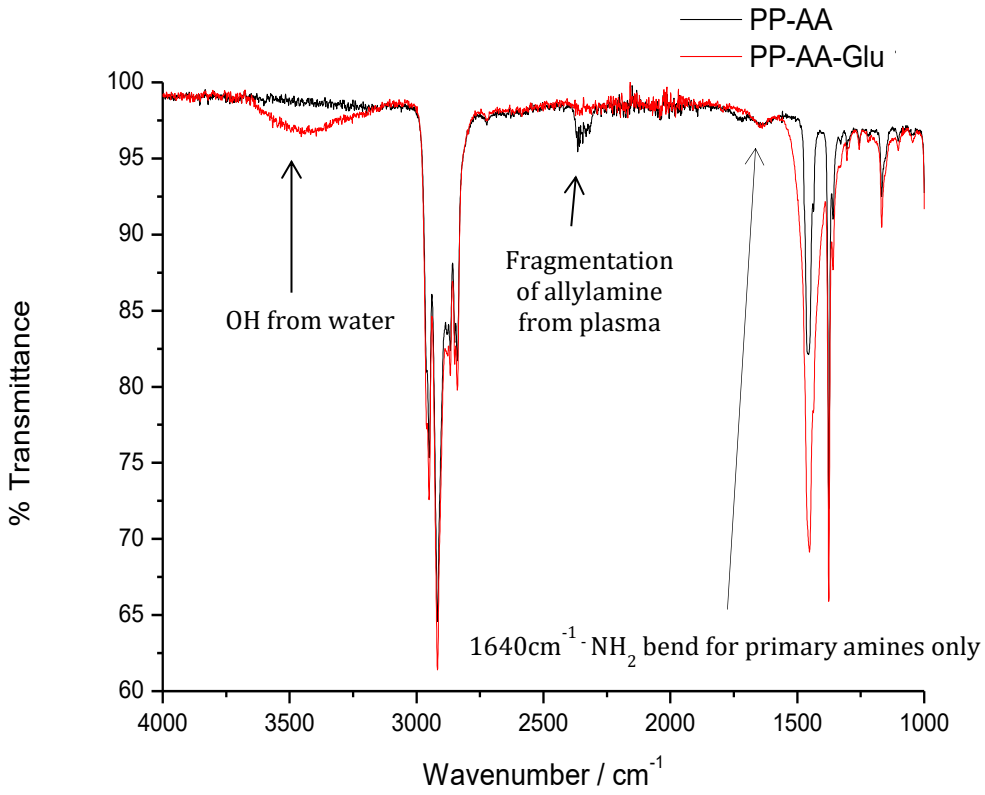

Figure 16 FT-IR spectra of plasma deposited allylamine on polypropylene (PP-AA) and plasma deposited allylamine reacted with glutaraldehyde (PP-AA-Glu).

The peak at approximately 3400 cm^{-1} can be attributed to the O-H stretching frequency from residual water (used to wash off unreacted glutaraldehyde). As previously mentioned, there appears to be a certain degree of fragmentation of the allylamine, producing a range of peaks at around 2300 cm^{-1}. The spectrum for allylamine activated polypropylene and glutaraldehyde (AA-PP-Glu) shows a missing peak at 1723 cm^{-1} (previously attributed to the possibility of an amide). The peak at 1640 cm^{-1} could indicate the presence of remaining primary amines. However, the C=N stretching frequency for an imine is normally found at 1628 cm^{-1} so it is possible that a new imine peak is overlaid with any residual amine presence. Noteworthy also is that the shift in wavenumber for a protonated imine has been reported to exist at around 1738 cm^{-1} where there are a distinct lack of peaks in the

glutaraldehyde spectrum [87]. Therefore, it may be that the imine deprotonates in solution (provided that Schiff base formation is indeed the mechanism of glutaraldehyde conjugation).

1.4.2.3 tAK Immobilisation

Preliminary experiments were carried out evaluating the strength of the immobilisation of tAK onto the modified polymer support (Figure 17).

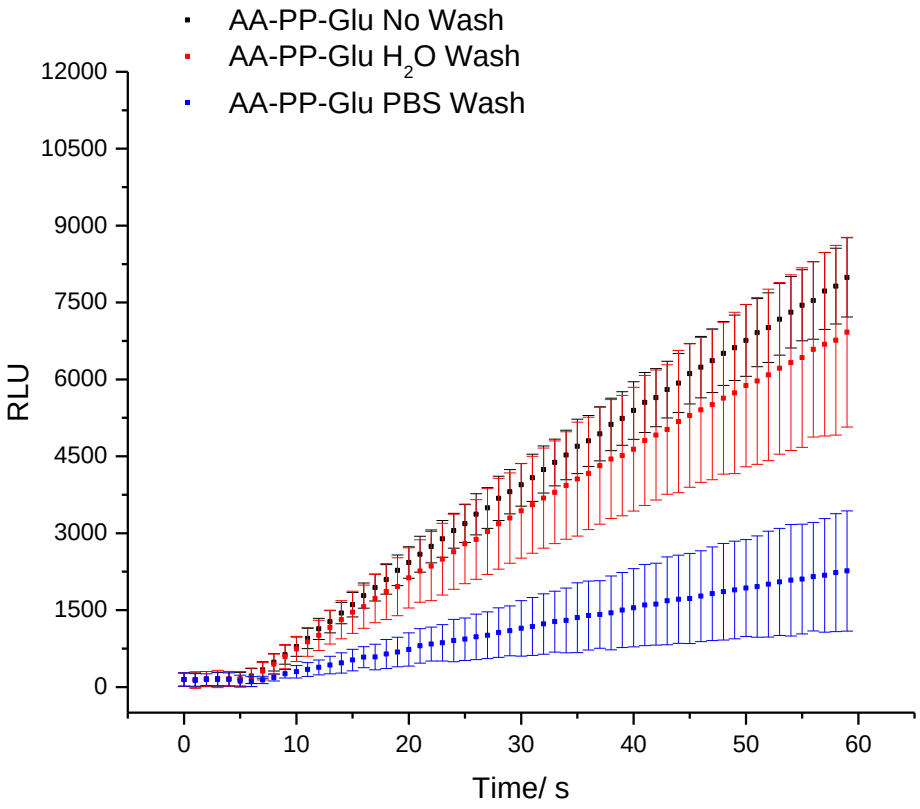

Figure 17 Effect of different washing strategies on the surface removal of tAK covalently bound to a polypropylene surface, plasma deposited with allylamine and activated with glutaraldehyde.

From the graph it can be seen that using a H_2O wash results in minimal surface removal of tAK with just 13.4% removed, the lowest of all washing experiments. However, when looking at the endpoint value of 7990 RLU for the glutaraldehyde activation without washing, this is significantly lower than the parallel experiment using tAK adsorbed to a polypropylene plate with an endpoint of 171457 RLU. This generates a difference in initial rate of 152 RLU s^{-1} for glutaraldehyde activation compared to 3795 RLU s^{-1} for the parallel adsorption experiments. As such, it could be argued that the degree of surface protein removal as a result of washing is

merely a function of initial surface protein concentration. Although a smaller proportion of protein is removed from the surface using a glutaraldehyde spacer linkage, less protein was successfully bound to the surface initially. Owing to the poor retention of tAK onto the plasma activated polymer, this system was not taken forward for full kinetic analysis.

1.5 Conclusion and Future Work

The research presented in this chapter demonstrates the possibility of covalent surface attachment of a thermostable protein with increased surface retention post washing. This offers the benefit of potentially providing a more challenging assessment of current clinical sterilisation protocols. Arguably, one of the key findings of this research surrounds the possibility of covalent anchoring of the tAK enzyme onto a solid support without the loss of activity. Entropic confinement of a protein can often result in a change in protein structure, and in many cases, resulting in complete loss of function. The utilisation of plasma as a means of activating surfaces may assist in preventing protein denaturation as discussed in section 1.2.1. However, there is a fundamental consideration which, if addressed, would enhance the capacity of this technology to effectively model residual surface contamination. The surface binding of tAK (either through adsorption or covalent attachment) should be directly correlated to the surface binding of the relevant infectious agents. It would be more accurate to draw conclusions regarding sterilisation efficacy based on residual tAK presence (or lack thereof), if protein concentration could be directly correlated to the pathogens associated with the spread of infectious disease. Whilst it is commonly accepted that species such as prions are exceptionally surface adherent and resistant to almost all forms of sterilisation, there has been little research into the exact extent of their resilience in terms of comparison to alternative proteinaceous species (such as tAK), which can safely be used for modelling purposes.

In terms of future development of this technology, alongside correlating the model system to the reality, there are a number of considerations which could potentially improve the current biosensor. Firstly, a change in polymer support may offer enhanced surface adhesion. For example, changing to a more hydrophobic polymer may facilitate hydrophobic interactions between the surface and specific amino acid residues within the protein (such as tyrosine or phenylalanine). Secondly, it would be of interest to investigate the use of a spacer arm further. In terms of the allylamine/ glutaraldehyde system it may be possible to reduce the imine in order to stabilise the system in aqueous solution, as previously mentioned. Removal of the luciferase/ luciferin coupled system would avoid any inhibitory effects which have

shown to affect the observed tAK activity. This concept was taken further as part of this research and is discussed in Chapter 2. Finally, the utilisation of plasma for direct inactivation of prions has received considerable attention in recent years. Studies conducted by von Keudell *et al* demonstrated complete prion inactivation *in vitro* using low pressure Ar/O_2 plasma [88]. Similarly, Baxter *et al* conducted *in vivo* experiments which showed complete elimination of prion infectivity through radio frequency gas plasma treatment of contaminated surgical instruments [89]. The development of plasma induced inactivation of prions as an alternative to the current and often ineffective sterilisation strategies, could offer a more efficient method of surface decontamination. As such, it may be possible to use tAK as a real time sensor in order to analyse the efficacy of plasma decontamination within the clinic, provided that the similarity in protein effects can be proven.

1.6 References

1 Rutala, W., Weber, D. & the Healthcare Infection Control Practices Advisory Committee (HICPAC), Guideline for Disinfection and Sterilization in Healthcare Facilities, (CDC) (2008).

2 Vazquez-Fernandez, E., Vos, M. R., Afanasyev, P., Cebey, L., Sevillano, A. M., Vidal, E., Rosa, I., Renault, L., Ramos, A., Peters, P. J., Fernandez, J. J., van Heel, M., Young, H. S., Requena, J. R. & Wille, H. The Structural Architecture of an Infectious Mammalian Prion Using Electron Cryomicroscopy. *PLoS Pathogens* **12** (2016).

3 Prusiner, S. B. Genetic and infectious prion diseases. *Archives of Neurology* **50**, 1129-1153 (1993).

4 Creutzfeldt-Jakob Disease Surveillance in the UK, 24th Annual Report 2015. The National CJD Research & Surveillance Unit) (2015).

5 Will, R. G. Acquired prion disease: iatrogenic CJD, variant CJD, kuru. *British Medical Bulletin* **66**, 255-265 (2003).

6 Sutton, J. M., Dickinson, J., Walker, J. T. & Raven, N. D. H. Methods to minimize the risks of Creutzfeldt-Jakob disease transmission by surgical procedures: Where to set the standard? *Clinical Infectious Diseases* **43**, 757-764 (2006).

7 Thomas, J. G., Chenoweth, C. E. & Sullivan, S. E. Iatrogenic Creutzfeldt-Jakob disease via surgical instruments. *Journal of Clinical Neuroscience* **20**, 1207-1212 (2013).

8 Department of Health. Prevention of CJD and vCJD by Advisory Committee on Dangerous Pathogens' Transmissible Spongiform Encephalopathy (ACDP TSE) Risk Management Subgroup. Creutzfeldt-Jakob disease (CJD): guidance, data and analysis reports (GOV.UK, England, 2015).

9 Palmer, T. & Bonner, P. *Enzymes: Biochemistry, Biotechnology, Clinical Chemistry*. Second edn, 3-5 (Woodhead Publishing Limited, 2007).

10 Pandey, A. *Enzyme Technology*. 12-13 (Springer Science & Business Media, Inc. and Asiatech Publishers, Inc. 2006).

11 Michaelis, L., Menten, M. L., Johnson, K. A. & Goody, R. S. The original Michaelis constant: translation of the 1913 Michaelis-Menten paper. *Biochemistry* **50**, 8264-8269 (2011).

12 Briggs, G. E. & Haldane, J. B. A Note on the Kinetics of Enzyme Action. *The Biochemical journal* **19**, 338-339 (1925).

13 Price, N. & Stevens, L. *Fundamentals of Enzymology*. Second edn, 142 (Oxford University Press, 1989).

14 Tze-Fei Wong, J. *Kinetics of Enzyme Mechanisms*. 2-4 (Academic Press Inc., 1977).

15 Marangoni, A. *Enzyme Kinetics: A Modern Approach*. (John Wiley & Sons, 2003).

16 Bisswanger, H. *Enzyme Kinetics: Principles and Methods*. Second edn, (John Wiley & Sons, 2008).

17 Di Biasio, A., Agliari, E., Barra, A. & Burioni, R. Mean-field cooperativity in chemical kinetics. *Theoretical Chemistry Accounts* **131** (2012).

18 Hill, A. The possible effects of the aggregation of the molecules of haemoglobin on its dissociation curves. *The Journal of Physiology* **40** (1910).

19 Tracey, T. *Drug Metabolism in Drug Design and Development*. 94-99 (John Wiley & Sons, 2007).

20 Goutelle, S., Maurin, M., Rougier, F., Barbaut, X., Bourguignon, L., Ducher, M. & Maire, P. The Hill equation: a review of its capabilities in pharmacological modelling. *Fundamental & Clinical Pharmacology* **22**, 633-648 (2008).

21 Tipton, K. *Enzyme Assays A Practical Approach*. (Oxford University Press, 1992).

22 Weiss, J. N. The Hill equation revisited: uses and misuses. *Faseb Journal* **11**, 835-841 (1997).

23 Copeland, R. *Enzymes: A Practical Introduction to Structure, Mechanism, and Data Analysis*. Second edn, (Wiley-Blackwell, 2000).

24 Walsh, R., Martin, E. & Darvesh, S. Limitations of conventional inhibitor classifications. *Integrative Biology* **3**, 1197-1201 (2011).

25 Flynn, K. *Handbook of Enzyme Inhibition*. (Callisto Reference, 2015).

26 Reed, M. C., Lieb, A. & Nijhout, H. F. The biological significance of substrate inhibition: A mechanism with diverse functions. *Bioessays* **32**, 422-429 (2010).

27 Cao, W. & De La Cruz, E. M. Quantitative full time course analysis of nonlinear enzyme cycling kinetics. *Scientific Reports* **3** (2013).

28 Tischer, W. W., F. *Biocatalysis - From Discovery to Application, Immobilized Enzymes: Methods and Applications*. Vol. 200 95 - 126 (Springer Berlin Heidelberg, 1999).

29 Yoo, Y. J., Feng, Y., Kim, Y. H. & Yagonia, C. F. J. in *Fundamentals of Enzyme Engineering*181-188 (Springer Netherlands, 2017).

30 Corbitt, A. J., Bennion, N. & Forsythe, S. J. Adenylate kinase amplification of ATP bioluminescence for hygiene monitoring in the food and beverage industry. *Letters in Applied Microbiology* **30**, 443-447 (2000).

31 Marques, S. M. & da Silva, J. C. G. E. Firefly Bioluminescence: A Mechanistic Approach of Luciferase Catalyzed Reactions. *IUBMB Life* **61**, 6-17 (2009).

32 da Silva, L. P. & Esteves da Silva, J. C. G. Computational Studies of the Luciferase Light-Emitting Product: Oxyluciferin. *Journal of Chemical Theory and Computation* **7**, 809-817 (2011).

33 Song, C.-i. & Rhee, Y. M. Dynamics on the Electronically Excited State Surface of the Bioluminescent Firefly Luciferase–Oxyluciferin System. *Journal of the American Chemical Society* **133**, 12040-12049 (2011).

34 Lacher, K. & Schafer, G. Archaebacterial Adenylate Kinase from the Thermoacidophile Sulfolobus-acidocaldarius – Purification, Characteristation, and Partial Sequence. *Archives of Biochemistry and Biophysics* **302**, 391-397 (1993).

35 Kath, T., Schmid, R. & Schafer, G. Identification, Cloning and Expression of the Gene for Adenylate Kinase from the Thermoacidophilic Archaebacterium Sulfolobus-acidocaldarius. *Archives of Biochemistry and Biophysics* **307**, 405-410 (1993).

36 Vonrhein, C., Bonisch, H., Shafer, G. & Schulz, G. E. The structure of a trimeric archaeal adenylate kinase. *Journal of Molecular Biology* **282**, 167-179 (1998).

37 Sheng, X. R., Li, X. & Pan, X. M. An iso-random BiBi mechanism for adenylate kinase. *Journal of Biological Chemistry* **274**, 22238-22242 (1999).

38 Awasthi, S. Bisubstrate Kinetics, University of Texas at Arlington, http://www.uta.edu/faculty/sawasthi/Enzymology-4351-5324

39 Taylor, D. M. Resistance of transmissible spongiform encephalopathy agents to decontamination. *Contributions to microbiology* **11**, 136-145 (2004).

40 Clarke, A. R., Jackson, G. S. & Collinge, J. The molecular biology of prion propagation. *Philosophical Transactions of the Royal Society of London Series B-Biological Sciences* **356**, 185-194 (2001).

41 BIOtAK-LTD. WASHtAK, Manage, Monitor, Optimise, http://www.biotak.net/products/washtak#.VLPT9SusWk8

42 Ungurs, M., Hesp, J. R., Poolman, T., McLuckie, G., O'Brien, S., Murdoch, H., Wells, P., Raven, N. D. H., Walker, J. T. & Sutton, J. M. Quantitative measurement of the efficacy of protein removal by cleaning formulations; comparative evaluation of prion-directed cleaning chemistries. *Journal of Hospital Infection* **74**, 144-151 (2010).

43 Hesp, J. R., Poolman, T. M., Budge, C., Batten, L., Alexander, F., McLuckie, G., O'Brien, S., Wells, P., Raven, N. D. H. & Sutton, J. M. Thermostable adenylate kinase technology: a new process indicator and its use as a validation tool for the reprocessing of surgical instruments. *Journal of Hospital Infection* **74**, 137-143 (2010).

44 Michelmore, A., Steele, D. A., Whittle, J. D., Bradley, J. W. & Short, R. D. Nanoscale deposition of chemically functionalised films via plasma polymerisation. *RSC Advances* **3**, 13540-13557 (2013).

45 Tendero, C., Tixier, C., Tristant, P., Desmaison, J. & Leprince, P. Atmospheric pressure plasmas: A review. *Spectrochimica Acta Part B: Atomic Spectroscopy* **61**, 2-30 (2006).

46 Shenton, M. & Stevens, G. Surface modification of polymer surfaces: atmospheric plasma versus vacuum plasma treatments. *Journal of Physics D: Applied Physics* **34**, 2761 (2001).

47 Cools, P., Geyter, N. D. & Morent, R. Non-thermal plasma assisted lithography for biomedical applications: an overview. *International Journal of Nanotechnology* **13**, 695-715 (2016).

48 Kemp, M. Unlocking the potential of graphenes for the development of multi-scale composites – Functionalization via plasma. *Reinforced Plastics* **60**, 332-334 (2016).

49 Dallas, P., Kelarakis, A. & Giannelis, E. P. in *Sustainable Nanotechnology and the Environment: Advances and Achievements* Vol. 1124 ACS Symposium Series Ch. 4, 59-72 (American Chemical Society, 2013).

50 Zimcik, D. G., Wertheimer, M. R., Balmain, K. B. & Tennyson, R. C. Plasma-deposited protective coatings for spacecraft applications. *Journal of Spacecraft and Rockets* **28**, 652-657 (1991).

51 Moreira, A. J., Mansano, R. D., Andreoli Pinto, T. d. J., Ruas, R., Zambon, L. d. S., da Silva, M. V. & Verdonck, P. B. Sterilization by oxygen plasma. *Applied Surface Science* **235**, 151-155 (2004).

52 Cvelbar, U., Vujoševič, D., Vratnica, Z. & Mozetič, M. The influence of substrate material on bacteria sterilization in an oxygen plasma glow discharge. *Journal of Physics D: Applied Physics* **39**, 3487 (2006).

53 Meyer-Plath, A. A., Schröder, K., Finke, B. & Ohl, A. Current trends in biomaterial surface functionalization—nitrogen-containing plasma assisted processes with enhanced selectivity. *Vacuum* **71**, 391-406 (2003).

54 Grimaldi, I. A., Testa, G., Persichetti, G., Loffredo, F., Villani, F. & Bernini, R. Plasma functionalization procedure for antibody immobilization for SU-8 based sensor. *Biosensors and Bioelectronics* **86**, 827-833 (2016).

55 Hussain, S., Amade, R., Jover, E. & Bertran, E. Nitrogen plasma functionalization of carbon nanotubes for supercapacitor applications. *Journal of Materials Science* **48**, 7620-7628 (2013).

56 Dong, S., Zhao, Z. & Dauskardt, R. H. Dual Precursor Atmospheric Plasma Deposition of Transparent Bilayer Protective Coatings on Plastics. *ACS Applied Materials & Interfaces* **7**, 17929-17934 (2015).

57 Sainiemi, L., Jokinen, V., Shah, A., Shpak, M., Aura, S., Suvanto, P. & Franssila, S. Non-Reflecting Silicon and Polymer Surfaces by Plasma Etching and Replication. *Advanced Materials* **23**, 122-126 (2011).

58 Tanaka, K., Kogoma, M. & Ogawa, Y. Fluorinated polymer coatings on PLGA microcapsules for drug delivery system using atmospheric pressure glow plasma. *Thin Solid Films* **506**, 159-162 (2006).

59 Friedrich, J. Mechanisms of Plasma Polymerization – Reviewed from a Chemical Point of View. *Plasma Processes and Polymers* **8**, 783-802 (2011).

60 Saboohi, S., Jasieniak, M., Coad, B. R., Griesser, H. J., Short, R. D. & Michelmore, A. Comparison of Plasma Polymerization under Collisional and Collision-Less Pressure Regimes. *The Journal of Physical Chemistry B* **119**, 15359-15369 (2015).

61 Thiry, D., Konstantinidis, S., Cornil, J. & Snyders, R. Plasma diagnostics for the low-pressure plasma polymerization process: A critical review. *Thin Solid Films* **606**, 19-44 (2016).

62 Kylián, O., Choukourov, A. & Biederman, H. Nanostructured plasma polymers. *Thin Solid Films* **548**, 1-17 (2013).

63 Siow, K. S., Britcher, L., Kumar, S. & Griesser, H. J. Plasma Methods for the Generation of Chemically Reactive Surfaces for Biomolecule Immobilization and Cell Colonization - A Review. *Plasma Processes and Polymers* **3**, 392-418 (2006).

64 Fereja, T. H., Hymete, A. & Gunasekaran, T. A Recent Review on Chemiluminescence Reaction, Principle and Application on Pharmaceutical Analysis. *ISRN Spectroscopy* **2013**, 12 (2013).

65 Lee, J. Perspectives on Bioluminescence Mechanisms. *Photochemistry and Photobiology* **93**, 389-404 (2017).

66 Brovko, L. *Bioluminescence for Food and Environmental Microbiological Safety*. Vol. Volume 74 of Tutorial texts in optical engineering 1 - 6 (SPIE Press, 2007).

67 Ando, Y., Niwa, K., Yamada, N., Enomoto, T., Irie, T., Kubota, H., Ohmiya, Y. & Akiyama, H. Firefly bioluminescence quantum yield and colour change by pH-sensitive green emission. *Nature Photonics* **2**, 44-47 (2008).

68 Rana, S. V. S. *Biotechniques Theory & Practice*. 109-112 (Rastogi Publications, 2008).

69 Department of Health. Choice framework for local policy and procedures (CFPP) 01-01: guidance about the management and decontamination of reusable medical devices. *Decontamination and infection control and Health technical memoranda* (2013). https://www.gov.uk/government/publications/management-and-decontamination-of-surgical-instruments-used-in-acute-care.

70 Ford, S. R. & Leach, F. R. Improvements in the application of firefly luciferase assays. *Bioluminescence Methods and Protocols* **102**, 3-20 (1998).

71 Nakanishi, K., Sakiyama, T. & Imamura, K. On the adsorption of proteins on solid surfaces, a common but very complicated phenomenon. *Journal of Bioscience and Bioengineering* **91**, 233-244 (2001).

72 Rabe, M., Verdes, D. & Seeger, S. Understanding protein adsorption phenomena at solid surfaces. *Advances in Colloid and Interface Science* **162**, 87-106 (2011).

73 Banerjee, I., Pangule, R. C. & Kane, R. S. Antifouling Coatings: Recent Developments in the Design of Surfaces That Prevent Fouling by Proteins, Bacteria, and Marine Organisms. *Advanced Materials* **23**, 690-718 (2011).

74 Biazar, E., Heidari, M., Asefnezhad, A. & Montazeri, N. The relationship between cellular adhesion and surface roughness in polystyrene modified by microwave plasma radiation. *International Journal of Nanomedicine* **6**, 631-639 (2011).

75 Wong, L. S., Khan, F. & Micklefield, J. Selective Covalent Protein Immobilization: Strategies and Applications. *Chemical Reviews* **109**, 4025-4053 (2009).

76 Nugent, P. G., Modi, T., McLeod, N., Bock, L. J., Smith, C., Poolman, M., Warburton, R., Meighan, P., Wells, P. & Sutton, J. M. Application of rapid read-out cleaning indicators for improved process control in hospital sterile services departments. *Journal of Hospital Infection* **84**, 59-65 (2013).

77 Liu, S., Vareiro, M., Fraser, S. & Jenkins, A. T. A. Control of attachment of bovine serum albumin to pulse plasma-polymerized maleic anhydride by variation of pulse conditions. *Langmuir* **21**, 8572-8575 (2005).

78 Olsson, U. & Wolf-Watz, M. Overlap between folding and functional energy landscapes for adenylate kinase conformational change. *Nature Communications* **1** (2010).

79 Jenkins, A. T. A., Hu, J., Wang, Y. Z., Schiller, S., Foerch, R. & Knoll, W. Pulsed plasma deposited maleic anhydride thin films as supports for lipid bilayers. *Langmuir* **16**, 6381-6384 (2000).

80 Ribeiro, C. & Esteves da Silva, J. C. G. Kinetics of inhibition of firefly luciferase by oxyluciferin and dehydroluciferyl-adenylate. *Photochemical & Photobiological Sciences* **7**, 1085-1090 (2008).

81 Jia, H., Zhu, G. & Wang, P. Catalytic behaviors of enzymes attached to nanoparticles: the effect of particle mobility. *Biotechnology and Bioengineering* **84**, 406-414 (2003).

82 Kubitzki, T., Minor, D., Mackfeld, U., Oldiges, M., Noll, T. & Lutz, S. Application of immobilized bovine enterokinase in repetitive fusion protein cleavage for the production of mucin 1. *Biotechnology Journal* **4**, 1610-1618 (2009).

83 Chen, Q., Forch, R. & Knoll, W. Characterization of pulsed plasma polymerization allylamine as an adhesion layer for DNA adsorption/hybridization. *Chemistry of Materials* **16**, 614-620 (2004).

84 Vartiainen, J., Ratto, M. & Paulussen, S. Antimicrobial activity of glucose oxidase-immobilized plasma-activated polypropylene films. *Packaging Technology and Science* **18**, 243-251 (2005).

85 Chu, L.-Q., Knoll, W. & Förch, R. *Surface Design: Applications in Bioscience and Nanotechnology*. 271-283 (Wiley- VCH Publishing, 2009).

86 Migneault, I., Dartiguenave, C., Bertrand, M. J. & Waldron, K. C. Glutaraldehyde: behavior in aqueous solution, reaction with proteins, and application to enzyme crosslinking. *Biotechniques* **37**, 790 (2004).

87 Wang, Y. L. & Poirier, R. A. Factors that influence the C=N stretching frequency in imines. *Journal of Physical Chemistry A* **101**, 907-912 (1997).

88 von Keudell, A., Awakowicz, P., Benedikt, J., Raballand, V., Yanguas-Gil, A., Opretzka, J., Flötgen, C., Reuter, R., Byelykh, L., Halfmann, H., Stapelmann, K., Denis, B., Wunderlich, J., Muranyi, P., Rossi, F., Kylián, O., Hasiwa, N., Ruiz, A., Rauscher, H., Sirghi, L., Comoy, E., Dehen, C., Challier, L. & Deslys, J. P. Inactivation of Bacteria and Biomolecules by Low-Pressure Plasma Discharges. *Plasma Processes and Polymers* **7**, 327-352 (2010).

89 Baxter, H. C., Campbell, G. A., Whittaker, A. G., Jones, A. C., Aitken, A., Simpson, A. H., Casey, M., Bountiff, L., Gibbard, L. & Baxter, R. Elimination of transmissible spongiform encephalopathy infectivity and decontamination of surgical instruments by using radio-frequency gas-plasma treatment. *Journal of General Virology* **86**, 2393-2399 (2005).

Chapter 2: Site-Directed Mutagenesis of a Thermostable Adenylate Kinase for Biosensor Development

2.1 Introduction

The research presented in this Chapter encompasses the genetic modification of tAK and subsequent selective conjugation to a fluorescent reporter system. The overall aim is focused on the direct fluorescent detection of tAK activity in real time. As detailed in Chapter 1, the luciferase-catalysed turnover of ATP appears to be subject to product inhibition. This potentially arises from secondary products of the tAK-catalysed reaction and additional products from the luciferin/ ATP reaction. Theoretically, removing the coupled system would provide a singular enzymatic system, capable of quantifying ATP concentration as a function of fluorescence output. This has added benefits in enabling direct detection without the addition of substrates, for example for use in wound dressings. It also opens up the potential to develop new sensors for purine nucleotides (ADP, AMP and ATP) and their derivatives.

This concept relies on the functionalisation of tAK via introduction of site-specific cysteine residues located adjacent to the substrate binding positions. tAK, in its native form does not contain any cysteine residues, therefore subsequent thiol-mediated conjugation will facilitate specific binding, avoiding other conserved amino acids. *N*-(1-Pyrene)maleimide was chosen as the fluorophore pair for conjugation via Michael addition to two cysteine residues per protein. tAK comprises three major domains, two of which are involved in substrate binding (LID and NMP domains) and one relatively rigid domain which is not involved in catalysis (CORE). Exploiting the conformational change in the protein structure upon substrate binding (closure of the LID domain to form the closed structure), results in an increase in the proximity of the conjugated pyrene ligands which facilitates π - π stacking interactions. These interactions shift the fluorescence intensity from monomer to excimer emission, producing an observable change in the fluorescence spectrum. Hence, substrate binding (and indirectly, product formation) can be monitored according to the change in fluorescence at specific wavelengths. This is shown schematically in Figure 1.

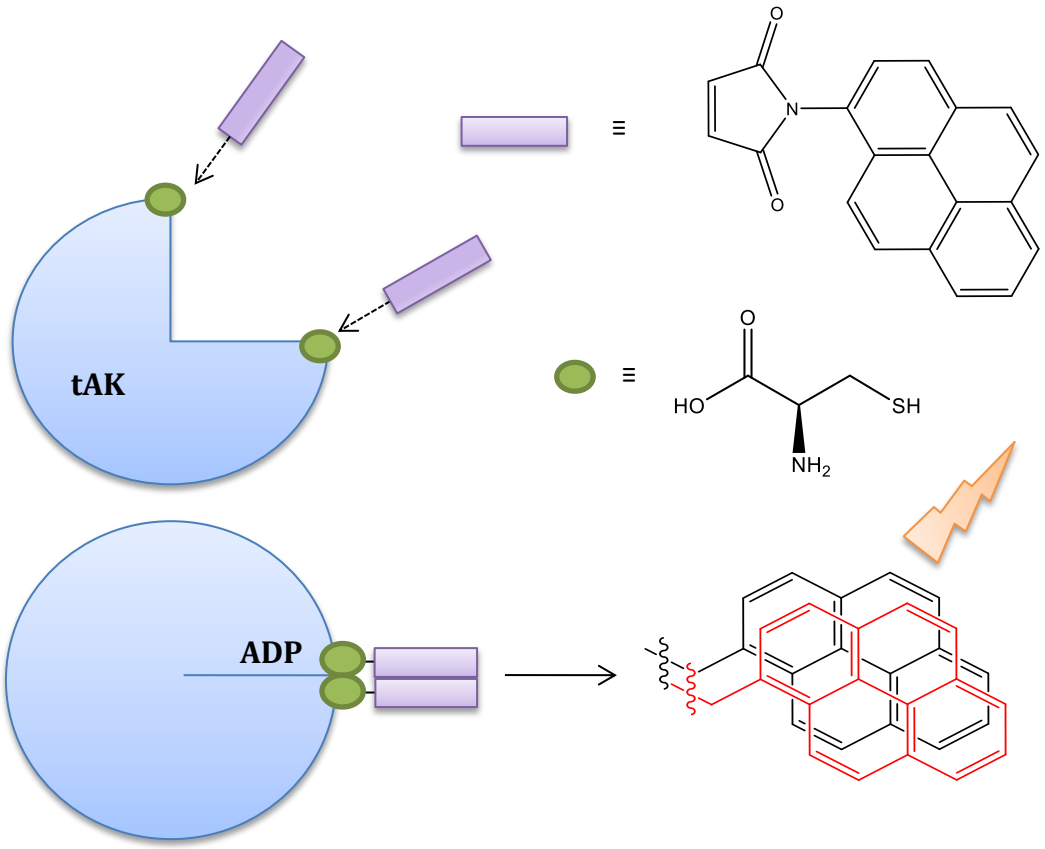

Figure 1 Schematic showing tAK conjugated to pyrene ligands via attachment to mutant cysteine residues (shown as –SH moieties). Substrate (ADP) binding results in a conformational change in the protein (LID closure), facilitating π- π stacking interactions resulting in a change in fluorescence output.

2.2 Protein Synthesis

Cellular protein synthesis controls and regulates the production of functional polypeptides, via the precise assembly of individual amino acids from their corresponding nucleotide sequence [a]. The genetic code responsible for the structure and function of a protein is transcribed from deoxyribonucleic acid (DNA), into messenger ribonucleic acid (mRNA) and translated into the fully formed protein by ribosomal subunits (Figure 2). The predefined amino acid sequence and the subsequent peptide folding give rise to unique proteins with specific functions and activities [1].

[a] Nucleotide base pairs consisting of cytosine (C), guanine (G), adenine (A) and thymine (T) make up the structure of DNA. 3 bases form a codon; each codon corresponds to a specific amino acid.

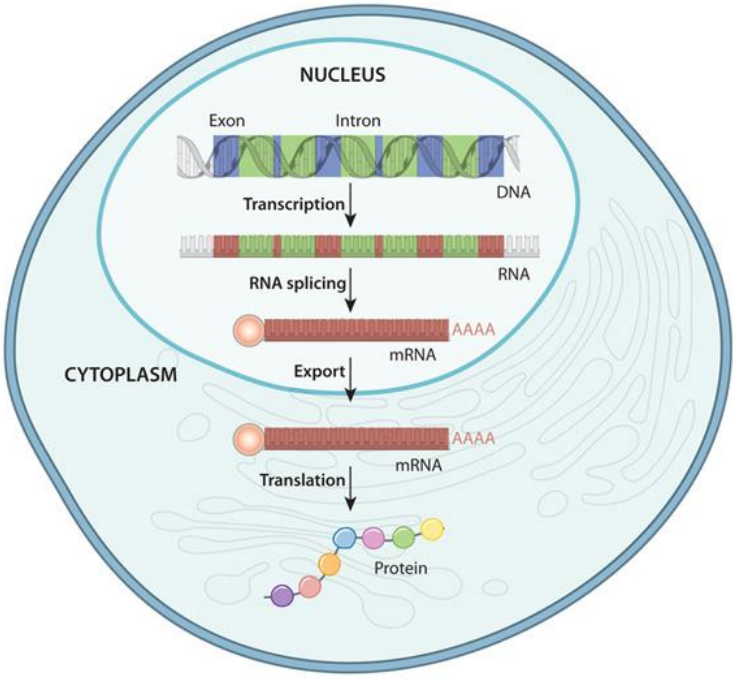

Figure 2 Schematic showing eukaryotic DNA transcription via splicing into mature mRNA in order to remove non-coding introns and ligate exons. The mature mRNA is then exported from the nucleus into the cytoplasm, where it is then translated into individual amino acids constituting the final protein structure. Copyright © 2010 Nature Education.

The process of gene expression, in terms of protein biosynthesis, is a highly regulated process which takes place in both eukaryotic and prokaryotic cells, although there are slight differences in the mechanism of polypeptide construction. In prokaryotic cells transcription and translation occur simultaneously, the ribosomes are smaller, mRNAs are relatively short lived and the initiation and termination sites (the point at which the ribosome attaches and detaches from the mRNA) are different [2]. The longer time scale and additional steps involved in eukaryotic biosynthesis (such as mRNA translocation from the cytoplasm), offers a greater degree of control in protein construction, including additional opportunities to modify the intended protein structure. Proteins can be modified either at the genetic level, via alteration of the DNA sequence, or post-translationally by covalent modification of amino acids.

2.2.1 Site-Directed Mutagenesis

The specific sequence of amino acids constituting a protein dictates the intrinsic properties of the protein itself, including stability, activity and versatility. Whilst nature has refined the process of protein biosynthesis through evolutionary development of the required molecular machinery, the intentional modification of proteins has been of interest to scientists for

decades. The alteration (via insertion, deletion or substitution) of base pairs in the DNA sequence, and the resultant modification of single, or multiple amino acids can provide valuable insight into gene/ protein function, protein-protein interactions and structure-function relationships [3]. Exploiting intentional genetic changes in the structure of a protein provides an effective strategy for the development of various investigative tools, including probing the genetic causes of disease, determining the process of cellular signalling and providing insights into the mechanisms involved in protein folding. Furthermore, modification of an otherwise specific amino acid sequence often results in a change in the properties of the resulting protein [4]. An early example of this is the substitution of a single amino acid (methionine) in subtilisin, for a non-oxidizable amino acid (such as serine, alanine or leucine). This substitution prevents subtilisin inactivation via oxidation, thus increasing its potential for commercial use (predominantly for use in detergents) [5]. Genetic engineering offers a vast array of benefits in terms of protein applications, for example, improved biosensor sensitivity, enhanced specificity and reduced immunogenicity of therapeutic proteins, and an extension in shelf life of protein-containing food products [6-8].

In order to intentionally modify the amino acid sequence of a protein at the genetic level, the DNA sequence must be altered so that it codes instead for an 'edited' version of the protein in question. Such events occur naturally in the form of alternative mRNA splicing [9,10], however synthetic gene alteration is referred to as mutagenesis, which can be random or directed. Early examples of mutagenesis involved the random insertion of mutations into the genome via exposure to chemical mutagens such as ethyl methanesulfonate [11]. However, the potential advantages offered by site-specific changes to the primary protein structure, drove the development of rational design and site-directed mutagenesis [12].

Site-directed mutagenesis, first reported in 1978 by Michael Smith [13] (who later received the Nobel Prize for his work in this area), involves the introduction of predefined changes to a section of DNA, corresponding to an alteration in the amino acid sequence. This method has been significantly adapted and improved in recent years, predominantly owing to the discovery and advancement of the polymerase chain reaction (PCR) [14-16]. PCR is a fundamental technique which has revolutionised molecular biology; illustrated by the fact the two key scientists responsible for its development (Kary Mullis and Har Gobind Khorana), both received Nobel Prizes in their respective fields. PCR involves the *in vitro* exponential amplification of DNA sequences via thermal cycling, in order to produce billions of copies of the target DNA strand [17]. There are a number of commercially available kits for introducing mutations into double stranded DNA (plasmid DNA), which are widely used. Mutagenesis in

the context of this report will refer to double stranded DNA modification from this point onwards, in order to remain relevant to the research presented in the Experimental Section. Additionally, the steps involved in mutagenesis (as detailed in the following Sections) largely refer to the QuickChange® Lightning Mutagenesis Kit (Stragene, La Jolla, CA, USA) which was used in this research.

2.2.1.1 Primer Design

Site-directed mutagenesis relies on the design and selection of synthetic oligonucleotide primers; short, synthetic sequences of nucleotides, complementary to opposite strands of the vector, containing the desired mutations. Primers anneal to the section of template DNA to be amplified and direct the replication process. In plasmid mutagenesis this results in the synthesis of copies of the *entire plasmid* rather than just the mutated DNA section. There are a number of considerations to take into account when designing primers, such as:

- Primers should be between 25 and 45 nucleotides long.
- They should have a high guanine/ cytosine content (at least 40%).
- Mutations must be contained within both primers.
- The mutation should be in the middle of the primer sequence.
- Primers should have melting temperature (defined as the temperature at which the primer dissociates from the template DNA [18]) of at least 78 °C, in order to prevent mismatches.

There are a number of primer design programmes currently available (many of which have been reviewed elsewhere [12,19]), capable of optimising primer characteristics such as melting temperature and the prevention of mispriming. An example of such software is Primer-BLAST, available from the National Center for Biotechnology Information (NCBI) [20], this software assists in the design of target specific primers. In addition to optimised primer design, the resulting nucleotide sequences are searched against BLAST (Basic Local Alignment Search Tool) which is coupled to a global alignment algorithm, in order to find any regions of similarity over the entire primer range, thereby reducing any cases of mismatching [21].

2.2.1.2 Mutant Strand Synthesis

Following successful primer design, the double stranded template DNA must be denatured in order to separate the DNA strands. The complementary primers containing the mutations (in the form of mismatched bases) are then annealed to the DNA. Extension of the primer sequence is achieved using a thermostable DNA polymerase, and a mix of deoxynucleotide triphosphates (dNTPs) as the monomeric substrates for DNA extension. The DNA polymerase continues to extend the DNA in a circular fashion, until it reaches the end of the primer sequence (the polymerase is non-strand displacing), and a single stranded copy of the entire mutated vector sequence is produced. This process occurs at varying temperatures during thermal cycling and is repeated in order to amplify the mutated DNA. Once multiple copies of the mutated template DNA have been generated, two complementary single strands anneal, resulting in double stranded, mutated plasmid DNA (Figure 3 [22]).

There are two points to note regarding the newly synthesised mutant plasmids. Firstly, they are not completely circular; they contain staggered nicks or strand breaks where the newly formed DNA meets the primer (i.e. they are not covalently bound together). This is rectified upon transformation of the plasmids into bacteria, where any nicks are sealed by bacterial ligases via formation of phosphodiester bonds [23]. Secondly, the parental DNA is methylated, whereas the newly formed DNA is not. This provides a helpful distinction, facilitating the eventual destruction of any non-mutated DNA.

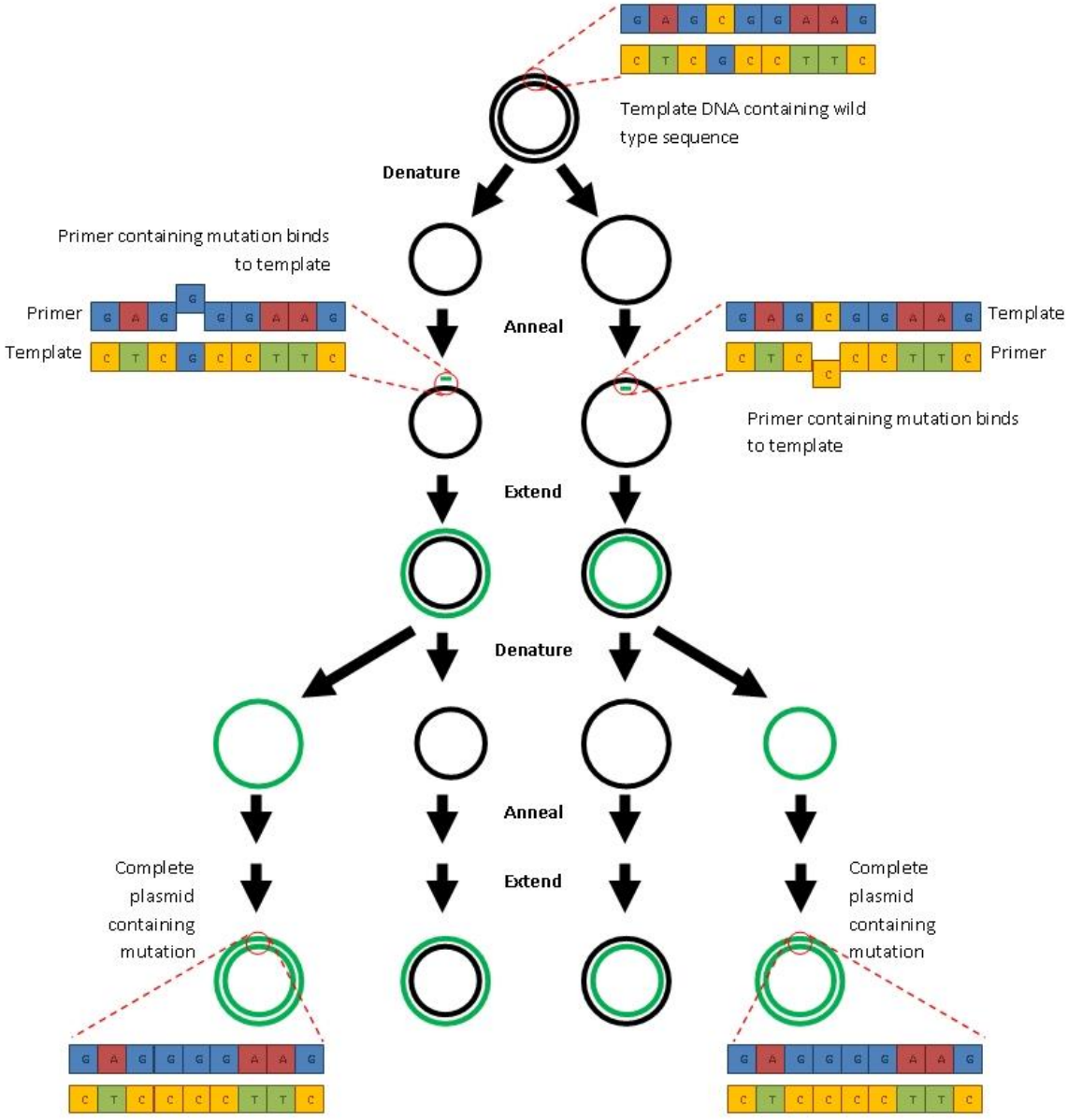

Figure 3 Schematic illustrating the generation of mutant DNA strands via thermal cycling.

2.2.1.3 Digestion of Template DNA

As depicted in Figure 3, following a number of rounds of thermal cycling, some template DNA remains which is devoid of the desired mutation(s). This wild type DNA is removed via restriction digest using endonucleases. Owing to the fact the parent DNA is frequently propagated in *Escherichia coli* (*E. coli*), often methylation occurs at the N6 position of an adenine residue within the GATC sequence, via a methyltransferase encoded by the *dam* gene [24,25]. Therefore, utilising *dam*$^+$ *E. coli* strains to propagate plasmid DNA for mutagenesis results in parental DNA which differs from the resulting mutated DNA (which is not

methylated). Therefore, selective digestion can be achieved using restriction endonucleases which only target methylated DNA. There are a number of endonucleases which can be employed for this purpose, however their precise cleavage site and recognition sequence can differ, thus careful selection of the appropriate enzyme must be undertaken [26].

2.2.1.4 Transformation

The final step in site-directed mutagenesis is the transformation of the newly formed DNA into competent cells. These cells are engineered to exhibit a higher degree of porosity in order to facilitate plasmid binding to the cell membrane. There are a range of commercially available competent cells for use in genetic cloning; commonly prepared by chemical treatment (calcium chloride) or via electroporation [27]. When selecting competent cells, there are a number of considerations to take into account, including: transformation efficiency, genetic markers (i.e. antibiotic resistance) and workflow requirements [28,29]. Transformation typically involves either heat shock of chemically competent cells, or electroporation of electrocompetent cells. Transformation efficacy can be evaluated via colony screening using antibiotic-containing media. When undertaking genetic cloning, the vector in which the mutations are inserted normally carries an antibiotic resistance marker. Hence, any cells that have successfully taken up the cloning vector will survive when plated onto antibiotic-containing agar plates, whereas bacteria without the vector will not [30]. Furthermore, in order to confirm whether the plasmid contained within the bacteria actually exhibits the desired mutation(s), blue/white screening is often employed. This technique can distinguish between plasmids containing the desired insert which present as white colonies, and plasmids which do not. There may be some failed products (i.e. no insert, unligated insert, modified insert etc.), which will result in blue colonies [31].

2.2.2 Post-Translational Modification

The genetic assembly of bioactive proteins with predefined functionality is achieved during transcription and later, translation. However, there are numerous cases throughout nature in which the fully translated protein is yet to be considered functional. The post-translational modification (PTM) of a protein is a covalent alteration in the protein structure, which occurs outside of the ribosome. Largely controlled by enzymes, PTMs may involve the addition or removal of a functional groups (i.e. phosphorylation, acetylation, glycosylation), the addition of complex molecules, or the formation of inter- or intramolecular bonds. This results in a

substantial increase in the diversity of the proteome, thus creating a plethora of proteins far exceeding the allowance dictated by gene transcripts. Both reversible and irreversible protein PTMs have been extensively reviewed elsewhere [32-34]. The ability to tune the functionality of a protein provides control over its activity state, cellular location and stability. This in turn can both initiate and terminate specific cellular events such as gene expression and signalling cascades [35-37]. Indeed, PTMs have been implicated in both the cause and prevention of a range of diseases including cardiovascular disease, chronic kidney disease and a range of neurodegenerative disorders [38,39].

Not surprisingly, the ability to chemically induce post-translational alterations in order to synthetically modify proteins has gained considerable attention in recent years. The applications of such engineered proteins are vast, including, but not limited to: use as tools in synthetic biology, industrial biocatalysis and biological therapeutics [40-42]. A principle example of the latter is Levemir® (Novo Nordisk), a long-acting insulin, engineered via acylation and currently on the market as a biotherapeutic. The addition of a fatty acid to a lysine residue in the insulin B chain acts as an anchor point for the binding to human serum albumin *in vivo*. This results in the prolonged release of free insulin, increasing the bioactivity three-fold [43].

2.2.3 Protein Conformational Changes

Functional conformational changes are commonplace in proteinaceous architectures; they can determine both function and activity. Many different techniques have been devised in recent years in order to study the nature and effect of such structural transitions, offering potential mechanistic insights into protein activity [44,45]. There are a number of factors involved in regulating the conformation of a protein, some of which include: protein-protein interactions, protein-ligand interactions, environmental conditions, transcriptional regulation and PTMs [46,47]. A change in the conformational state of a protein can be of critical importance, the consequences of which are often associated with essential cellular processes such as signal transduction, gene regulation and catalysis [48].

2.2.3.1 Adenylate Kinase

A change in conformation upon substrate binding is a well-documented phenomenon in a number of enzymes; a well-studied example of which is exhibited by AK during the catalysis of adenine nucleotide interconversion [49-53]. The structural dynamics accounting for this

process are extensive and complex (a detailed study has been presented by Li *et al* [54]). The binding of substrate molecules facilitates opening and closing of the LID and NMP domains, resulting in a conformational shift of the protein from open state (PDB ID 4AKE [55]), to the closed state (PDB ID 1AKE [56]), (Figure 4 [57]).

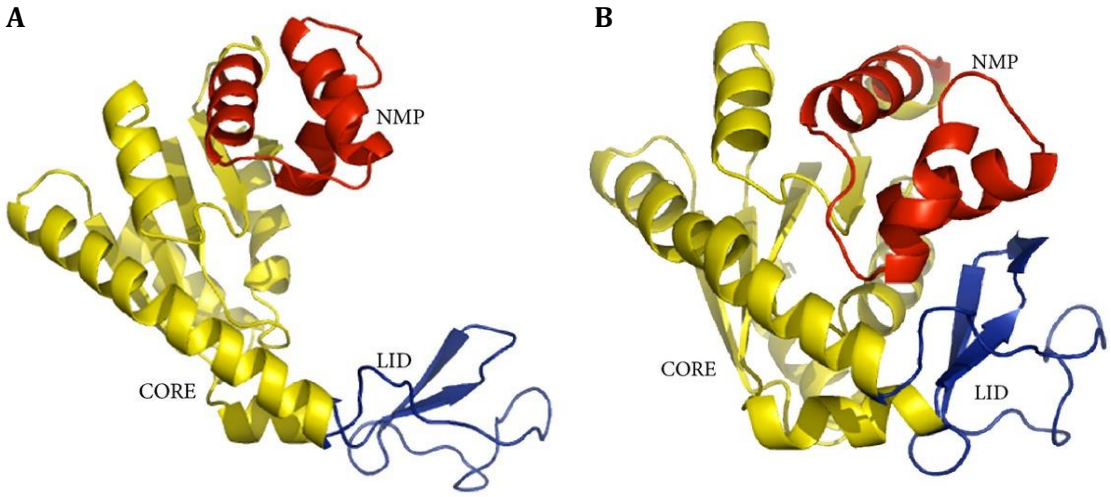

Figure 4 Crystallographic ribbon plot showing AK isolated from *E. coli*, (**A**) in the open form in the absence of substrate and (**B**) in the closed form. Adapted from [57] Copyright © 2013 Ping *et al.*

The transition between the open and closed states has been reported to occur on the microsecond-millisecond timescale and is a common feature of a number of AKs from a range of different organisms (including tAK) [58]. The difference in spatial arrangement arising from the transition from the open to closed form manifests as a change in distance between NMP and LID amino acids (Ala55 and Val169), of ~ 17Å upon LID closure in the case of *E. coli* AK [59]. As an alteration to the induced-fit theory of enzyme-substrate binding (stating that only the specific substrate can induce a protein conformational change), the conformational selection model (or pre-existing equilibrium model), suggests that an enzyme exists in a number of conformational substates and the ligand selectively binds to the active conformation. This is the current theory for AK-substrate binding based on a multitude of molecular dynamics simulations [57,60]. The proposed mechanism of which is shown in Figure 5 [61].

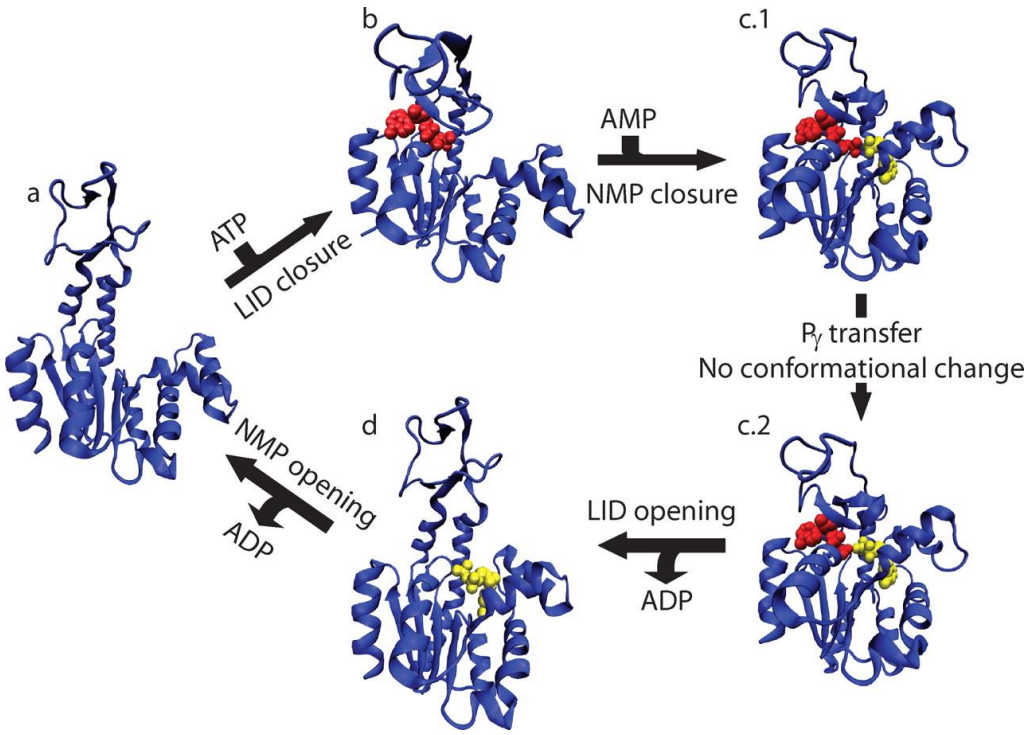

Figure 5 Proposed substrate binding scheme for AK, (**a**) initially in the open conformation, followed by ATP binding to the LID domain (**b**) resulting in LID closure, AMP binding to the NMP domain (**c.1**), phosphotransfer to form two molecules of ADP (**c.2**), LID opening resulting in release of the first molecule of ADP (**d**), and return to the open conformation following final ADP release via opening of NMP domain. Reproduced from [61]. Copyright © the American Society for Biochemistry and Molecular Biology.

The change in proximity of amino acids resulting from the conformational change of a protein upon substrate binding has been exploited in a number of studies [62-64]. Yuan *et al* prepared enzyme-based hybrid hydrogel structures containing a covalently crosslinked AK mutant. The triple mutant was engineered to contain cysteine functionality to serve as attachment points for subsequent crosslinking (via thiol-maleimide reaction), with either *N*-(2-hydroxypropyl)methacrylamide (HPMA), or poly(ethylene glycol) (PEG) hydrogels. The conformational change upon ATP binding resulted in macroscopic motion of the hydrogel network (manifesting as a decrease in polymer volume) [59]. Similarly, Fujii *et al* prepared a pyrene-conjugated AK mutant in order to create an "*in situ* chromic system" based on the switching of monomer/excimer emission [65]. This approach is the basis of the experimental work undertaken in this Chapter; in order to remove the luciferase/luciferin coupled system and instead, to develop a one component, thermostable biosensor.

2.3 Materials and Methods

2.3.1 Materials

Wildtype tAK (tAK_{WT}), plasmid pMTL 1015 and *E. coli* expression strain RV308 were all obtained from the Technology Development Group, Public Heath England (PHE – Salisbury, UK) [66]. Luria bertani (LB) broth, mucin from porcine stomach, tetracycline, isopropanol, ethanol, sodium dodecyl sulfate (SDS), phosphate buffered saline (PBS) tablets (pH 7.4), sodium chloride, magnesium sulfate, tris-hydrochloride (pH 7.5), sodium phosphate dibasic/monobasic, dithiothreitol (DTT), dimethyl sulfoxide (DMSO) were all purchased from Sigma-Aldrich.

QIAprep® Spin Miniprep Kit and HiSpeed® Plasmid Purification Midi-prep Kit were purchased from Qiagen Ltd. QuickChange® Lightning Site-Directed Mutagenesis Kit and XL10-Gold® Ultracompetent cells were purchased from Agilent Technologies. Super optimal broth (SOC), NuPAGE™ 4-12% Bis-Tris Protein Gels (1.0 mm, 12-well), SeeBlue™ Plus2 Pre-stained Protein Standard, NuPAGE™ MES SDS Running Buffer, SimplyBlue™ SafeStain, NuPAGE™ Sample Reducing Agent, One Shot™ TOP10 Chemically Competent *E. coli* cells and *N*-(1-Pyrene)maleimide were all purchased from Invitrogen™, ThermoFisher. BugBuster® 10X Protein Extraction Reagent was purchased from Merck Millipore. ATP Reagent, Diluent C, tris-EDTA buffer, ADP and ATP standard solutions were all purchased from BioThema (Sweden).

PCR primers were obtained from Sigma Genosys; sequences are shown in Table 1. Bases shown in red lower case correspond to the amino acid modified in each case.

Table 1 Oligonucleotide sequences of forward (for) and reverse (rev) PCR primers.

Name	Oligonucleotide sequence	Strand
Sac AK L60C.for	CGTGACGAAATGCGCAAAtgcAGCGTGGAAAAACAGAAGAAGCTGCAG	+
Sac AK L60C.rev	CTGCAGCTTCTTCTGTTTTTCCACGCTgcaTTTGCGCATTTCGTCACG	-
Sac AK S61C.for	CGTGACGAAATGCGCAAACTGtGCGTGGAAAAACAGAAGAAGCTGCAG	+

Sac AK S61C.rev	CTGCAGCTTCTTCTGTTTTTCCACGCaCAGTTTGCGCATTTCGTCACG	-
Sac AK V62C.for	CGTGACGAAATGCGCAAACTGAGCtgcGAAAAACAGAAGAAGCTGCAG	+
Sac AK V62C.rev	CTGCAGCTTCTTCTGTTTTTCgcaGCTCAGTTTGCGCATTTCGTCACG	-
Sac AK S148C.for	GCAACGATTATAGCGACGAAtGCGTTATCCTGGAGACCATCAACTTTGCG	+
Sac AK S148C.rev	CGCAAAGTTGATGGTCTCCAGGATAACGCaTTCGTCGCTATAATCGTTGC	-
Sac AK V149C.for	GCAACGATTATAGCGACGAAAGCtgcATCCTGGAGACCATCAACTTTGCG	+
Sac AK V149C.rev	CGCAAAGTTGATGGTCTCCAGGATgcaGCTTTCGTCGCTATAATCGTTGC	-
Sac AK I150C.for	GCAACGATTATAGCGACGAAAGCGTTtgcCTGGAGACCATCAACTTTGCG	+
Sac AK I150C.rev	CGCAAAGTTGATGGTCTCCAGgcaAACGCTTTCGTCGCTATAATCGTTGC	-

2.3.2 Methods

2.3.2.1 Bacterial Growth Conditions

Bacterial cultures were grown from frozen stocks via streaking an LB agar plate, incubation overnight at 37 °C, addition of a single colony to 10 ml LB broth and further overnight incubation with agitation. LB plates used for cloning were supplemented with 0.1% tetracycline.

2.3.2.2 Plasmid Isolation, Transformation and Purification

The plasmid (pMTL 1015) encoding tAK was isolated from an *E. coli* expression strain (RV308) using QIAprep® Spin Miniprep Kit according to the manufacturer's instructions [67]. Briefly, an overnight culture was pelleted via centrifugation, resuspended, lysed and neutralised in order to release the cellular DNA. The suspension was re-centrifuged and the

supernatant passed through a spin column to allow DNA binding to the silica membrane. The column was washed to remove any impurities and the DNA was eluted in buffer. Plasmid DNA was transformed into Top10 competent cells via heat shock treatment. The DNA was added to the competent cells on ice and left for 5 min, the solution was then heated for 30 s at 42 °C and returned to ice for a further 2 min. SOC was added and the solution was incubated with agitation at 37 °C for 30 min. Aliquots were spread onto tetracycline-supplemented LB agar plates and incubated overnight at 37 °C. Plasmid DNA was purified using HiSpeed® Plasmid Purification Midi-prep Kit according to the manufacturer's instructions [68]. Briefly, a single colony from a freshly streaked selective plate was cultured in tetracycline-supplemented LB broth overnight at 37 °C with agitation. The culture was pelleted via centrifugation and resuspended in buffer. The cells were lysed and any RNA digested with RNase A. The solution was neutralised, resulting in the precipitation of any remaining detergent (from the lysis step), cellular proteins and genomic DNA. This was removed via filtration, the plasmid DNA was bound to a resin-containing column, washed and eluted into buffer. The purified DNA was precipitated in isopropanol, filtered, washed with ethanol and eluted into buffer.

2.3.2.3 Design and Construction of Oligonucleotide Primers

Oligonucleotides were designed to introduce the desired amino acid change within the coding sequence of the tAK enzyme. Simple design rules were used to generate oligonucleotides with mismatched (mutagenic) sequences flanked by 20-24 bases. Pyrimidine bases were used at the 3' end of the oligonucleotide to ensure efficient base-pairing and sequences were checked for the formation of primer dimers and/or hairpin structures using primer design software (https://www.ncbi.nlm.nih.gov/tools/primer-blast/).

2.3.2.4 Mutagenesis and Transformation

Mutagenesis was carried out using QuickChange® Lightning Site-Directed Mutagenesis Kit according to the manufacturer's instructions [69]. Briefly, sample reaction solutions were prepared containing buffer, two oligonucleotide primers (containing the desired mutation(s)), dNTP mix, varying concentrations of the parental DNA template and QuickSolution reagent (to facilitate replication of large plasmids). Control solutions were prepared in parallel (in order to assess efficacy of mutagenesis protocol), containing a control template (pWhitescript 4.5kb) and control primers. QuickChange Lightning Enzyme (DNA

polymerase) was added and the solutions were subject to thermal cycling. *Dpn* I restriction endonuclease was then used to digest any parental DNA and the mutated DNA was transformed into XL10-Gold® Ultracompetent cells according to the manufacturer's instructions [70]. Control transformations were carried out in parallel using a control plasmid (pUC18). Mutant samples were plated on tetracycline-supplemented LB plates and incubated overnight at 37 °C. Samples were sequenced to evaluate mutation efficacy.

2.3.2.5 Expression

Small scale expression was undertaken in order to assess the viability of the newly synthesised mutant proteins. Cells containing the mutant plasmid with the desired insert(s) were grown overnight at 37 °C in tetracycline-supplemented LB broth. Cultures were pelleted via centrifugation and resuspended in BugBuster® Protein Extraction Reagent according to the manufacturer's instructions [71]. Briefly, after lysing the cells with BugBuster (detergent), the solution was centrifuged, forcing cellular debris into a pellet and retaining any proteins contained within the cytoplasm/ periplasm within the supernatant. Dependent on the success of the expression, tAK_M should be located in the supernatant. However, if there are any misfolded proteins or if the expression strain fails to produce the protein correctly, tAK_M may be located within an inclusion body (insoluble membrane casing) within the pellet. It is possible to recover a protein from within an inclusion body but it can be difficult to refold the protein into an active conformation. The supernatant was then heated to 80 °C for 20 min, centrifuged and recovered. If the tAK_M is heat stable it will remain in the supernatant, if not, it will precipitate to form a pellet. This process is shown in Figure 6. Samples were run on NuPAGE™ Protein Gels at 200 V for 30 min and successful mutations were chosen to take forward for large scale expression.

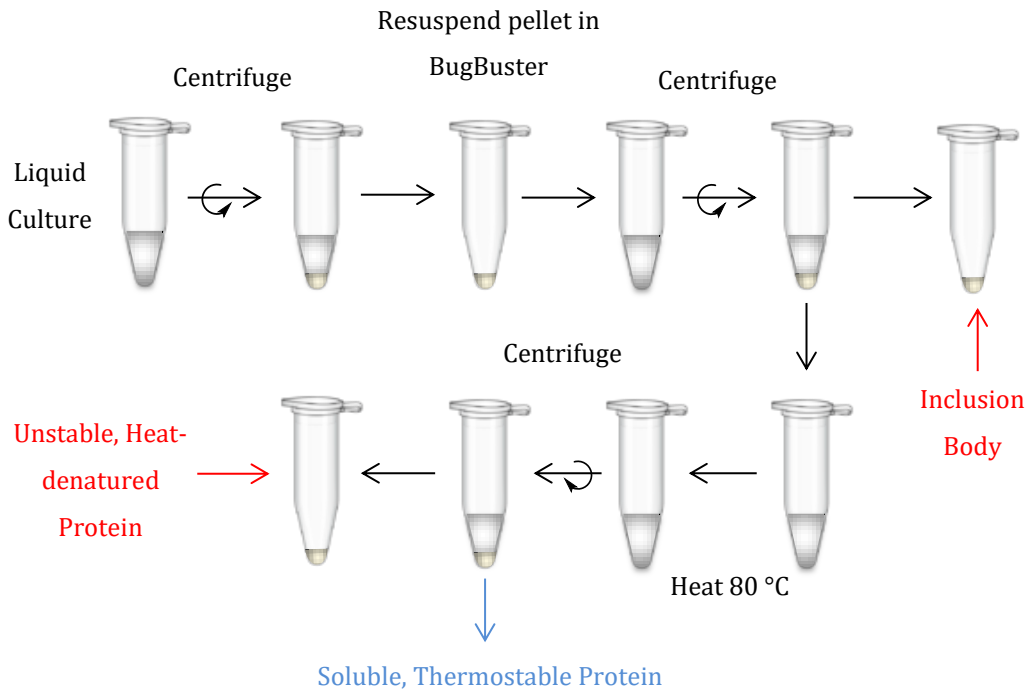

Figure 6 Protein extraction protocol showing recovery of the desired soluble, thermostable protein (blue) from liquid media, as oppose to misfolded or heat-denatured proteins (red).

For large scale preparation, 5 ml of overnight culture was added to 800 ml of tetracycline-supplemented LB broth and incubated overnight at 30 °C with agitation. Samples were harvested via centrifugation and resuspended in deionised (DI) H_2O (for freezing) or equilibration buffer (20 mM Tris, 0.9 mM NaCl, 10 mM $MgCl_2$, pH 8) for purification.

2.3.2.6 Purification

Protein purification was achieved via ion-exchange chromatography (ÄKTA Purifier, GE Healthcare Life Sciences), using HiScreen Capto™ Blue columns. Samples resuspended in equilibration buffer were sonicated (50 s on, 40 s off, 10 cycles), centrifuged, heated to 80 °C for 30 min and re-centrifuged to release cell contents. Samples were loaded onto the column following equilibration and eluted in 10 mM sodium phosphate, 2 M NaCl (pH 12) [72]. Approximately 10 fractions were collected and 100 µl of neutralisation buffer (0.2 M sodium phosphate, pH 6 [73]) was added to each fraction. Column eluents were run on NuPAGE™ Protein Gels in order to determine the fraction containing the modified tAK enzyme. NuPAGE™ Sample Reducing Agent was added prior to loading onto the gels in order to reduce aggregation.

2.3.2.7 Characterisation

Protein concentration was determined via the Bradford Assay [74]. Enzyme activity of the tAK mutant (tAK_M) was determined as previously detailed (Section 1.3.4, Published Article). Reducing experiments were undertaken in the same manner with the addition of 300, 200, 100, 50, 10 mM DTT.

2.3.2.8 Bioconjugation

Conjugation was carried out according to Invitrogen Molecular Probes [75] with some modifications. Briefly, tAK_M was dissolved in PBS buffer at a concentration of 50 μM. In order to reduce any disulfide bonds (inter- and intramolecular) within the tAK_M solution, 100-fold molar excess of DTT (in H_2O) was added, this was allowed to react for 10 min at room temperature with stirring. The solution was passed through a spin column (10 kDa MWCO, 10 min) in order to remove the DTT and the reduced enzyme was resuspended in sterile PBS. Control experiments were undertaken using the tAK_{WT} in parallel. 100-fold molar excess of *N*-(1-Pyrene)maleimide (in DMSO) was added to the resuspended enzymes dropwise and reacted for 24 h in the dark with stirring. Solutions were centrifuged and the supernatant dialysed for 2 days at 4 °C, firstly against tris-EDTA and then DI H_2O.

Enzyme-conjugate activity was determined as previously described (Section 1.3.4, Published Article). Control experiments were undertaken using the mutant enzyme exposed to the coupling conditions.

2.3.2.9 Fluorescence Analysis

Excitation and emission scanning was undertaken (CLARIOstar®, BMG Labtech), in order to establish the correct fluorescence parameters. Results are presented in triplicate, representing the excitation/emission spectra of the tAK mutant - conjugate (tAK_{MC}), baseline corrected against the substrate (ADP).

tAK_M and tAK_{MC} were exposed to 5 mM ADP (1:1 v/v tAK: ADP), supplemented with 10 mM $MgCl_2$ and the fluorescence output was measured immediately from 360 – 520 nm with an excitation wavelength of 340 nm ± 8 nm. The same experiments were undertaken replacing ADP with tris-EDTA buffer.

2.4 Results and Discussion

2.4.1 Evaluation of Mutagenesis

Samples containing the desired mutation(s) were sequenced and compared to the wildtype enzyme. Figure 7 shows the sequence alignment demonstrating successful mutagenesis of all cysteine substitutions. The double mutant (Sac AK 61 – 148) was chosen to take forward for large scale expression, this mutant contains 2 cysteine substitutions at serine 61 and serine 148 (Scheme 1). The observed success in formation of the double mutant ruled out the necessity to induce further mutations into the single mutants, (a concept explored as a potential alternative in the case of unsuccessful double mutation).

```
Sac WT             MKIGIVTGIPGVGKSTVLAKVKEILDNQGINNKIINYGDFMLATALKLGYAKDRDEMRKLSVEKQKKLQIDAAKGIAEEA
Sac AK 60-1.pro    MKIGIVTGIPGVGKSTVLAKVKEILDNQGINNKIINYGDFMLATALKLGYAKDRDEMRKCSVEKQKKLQIDAAKGIAEEA
Sac AK 61-1.pro    MKIGIVTGIPGVGKSTVLAKVKEILDNQGINNKIINYGDFMLATALKLGYAKDRDEMRKLCVEKQKKLQIDAAKGIAEEA
Sac AK 62-1.pro    MKIGIVTGIPGVGKSTVLAKVKEILDNQGINNKIINYGDFMLATALKLGYAKDRDEMRKLSCEKQKKLQIDAAKGIAEEA
Sac AK 61-148-1    MKIGIVTGIPGVGKSTVLAKVKEILDNQGINNKIINYGDFMLATALKLGYAKDRDEMRKLCVEKQKKLQIDAAKGIAEEA
Sac AK 148-1.pro   MKIGIVTGIPGVGKSTVLAKVKEILDNQGINNKIINYGDFMLATALKLGYAKDRDEMRKLSVEKQKKLQIDAAKGIAEEA
Sac AK 149-1.pro   MKIGIVTGIPGVGKSTVLAKVKEILDNQGINNKIINYGDFMLATALKLGYAKDRDEMRKLSVEKQKKLQIDAAKGIAEEA
Sac AK 150-1.pro   MKIGIVTGIPGVGKSTVLAKVKEILDNQGINNKIINYGDFMLATALKLGYAKDRDEMRKLSVEKQKKLQIDAAKGIAEEA

Sac WT             RAGGEGYLFIDTHAVIRTPSGYLPGLPSYVITEINPSVIFLLEADPKIILSRQKRDTTRNRNDYSDESVILETINFARYA
Sac AK 60-1.pro    RAGGEGYLFIDTHAVIRTPSGYLPGLPSYVITEINPSVIFLLEADPKIILSRQKRDTTRNRNDYSDESVILETINFARYA
Sac AK 61-1.pro    RAGGEGYLFIDTHAVIRTPSGYLPGLPSYVITEINPSVIFLLEADPKIILSRQKRDTTRNRNDYSDESVILETINFARYA
Sac AK 62-1.pro    RAGGEGYLFIDTHAVIRTPSGYLPGLPSYVITEINPSVIFLLEADPKIILSRQKRDTTRNRNDYSDESVILETINFARYA
Sac AK 61-148-1    RAGGEGYLFIDTHAVIRTPSGYLPGLPSYVITEINPSVIFLLEADPKIILSRQKRDTTRNRNDYSDECVILETINFARYA
Sac AK 148-1.pro   RAGGEGYLFIDTHAVIRTPSGYLPGLPSYVITEINPSVIFLLEADPKIILSRQKRDTTRNRNDYSDECVILETINFARYA
Sac AK 149-1.pro   RAGGEGYLFIDTHAVIRTPSGYLPGLPSYVITEINPSVIFLLEADPKIILSRQKRDTTRNRNDYSDESCILETINFARYA
Sac AK 150-1.pro   RAGGEGYLFIDTHAVIRTPSGYLPGLPSYVITEINPSVIFLLEADPKIILSRQKRDTTRNRNDYSDESVCLETINFARYA

Sac WT             ATASAVLAGSTVKVIVNVEGDPSIAANEIIRSMK
Sac AK 60-1.pro    ATASAVLAGSTVKVIVNVEGDPSIAANEIIRSMK
Sac AK 61-1.pro    ATASAVLAGSTVKVIVNVEGDPSIAANEIIRSMK
Sac AK 62-1.pro    ATASAVLAGSTVKVIVNVEGDPSIAANEIIRSMK
Sac AK 61-148-1    ATASAVLAGSTVKVIVNVEGDPSIAANEIIRSMK
Sac AK 148-1.pro   ATASAVLAGSTVKVIVNVEGDPSIAANEIIRSMK
Sac AK 149-1.pro   ATASAVLAGSTVKVIVNVEGDPSIAANEIIRSMK
Sac AK 150-1.pro   ATASAVLAGSTVKVIVNVEGDPSIAANEIIRSMK
```

Figure 7 Amino acid sequence alignment showing cysteine mutations (red) in 7 tAK mutants compared to the wildtype (Sac WT) enzyme.

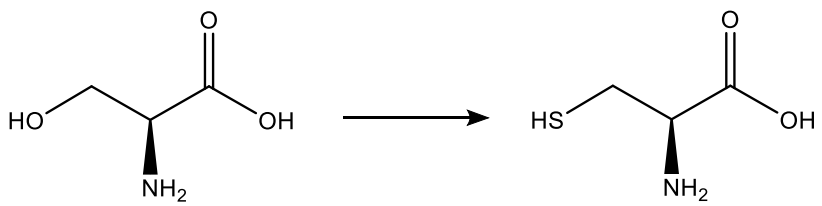

Scheme 1 - Conversion of serine to cysteine as demonstrated in the double tAK mutant.

Following expression and purification of tAK_M, column fractions were loaded onto SDS-Page gels for analysis. Fractions 3, 4 and 5 were found to contain tAK_M, exhibited by the band appearing at approximately (26 kDa) shown in Figure 8A. Whilst tAK (monomer) has a predicted molecular weight of ~23 kDa, the protein fragment runs slightly longer on the gels, hence the band at 26 kDa. However, the observed band appears as a doublet, possibly indicating the formation of an intramolecular disulfide bond. The bands above 26 kDa suggest the presence of intermolecular disulfide bonds resulting in the formation of dimers, trimers and tetramers, appearing at 56, 82, 108 kDa respectively. The fractions were reduced (50 mM DTT), resulting in removal of both the doublet at 26 kDa and the majority of the larger aggregates (Figure 8B).

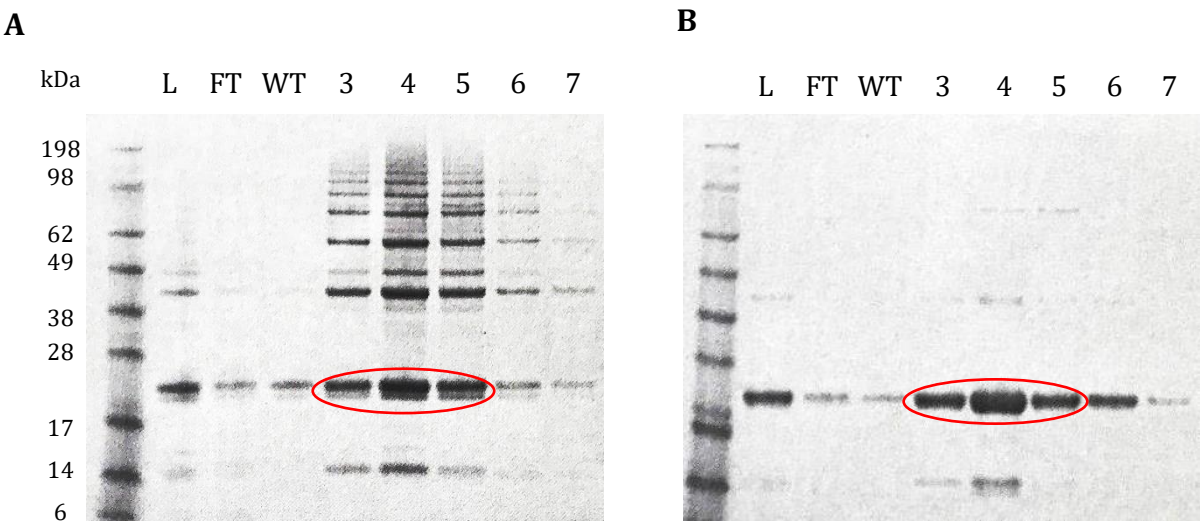

Figure 8 Gel analysis of the double mutant showing (**A**) unreduced column fractions, from left to right: the loading fraction (L), flow through (FT), wildtype enzyme (WT) and the column fractions from fraction 3 onwards. (**B**) The reduced fractions showing removal of doublet at 26 kDa (red circle) and aggregation of longer protein fragments.

The sustained presence of some larger aggregates after reduction suggests a higher concentration of reducing agent may be required. This was taken into account during subsequent activity measurements. The presence of an intramolecular disulfide bond may indicate covalent closure of the LID domain which could, in theory, prevent substrate access and thus render the enzyme inactive.

2.4.2 Mutant Activity

The ability of tAK_M to catalyse the formation of ATP from ADP was assessed via the luciferase/ luciferin coupled assay, in keeping with previous experiments (Chapter 1). Prior to reducing tAK_M, the luminescent light output was evaluated relative to tAK_{WT} (in solution) as shown in Figure 9.

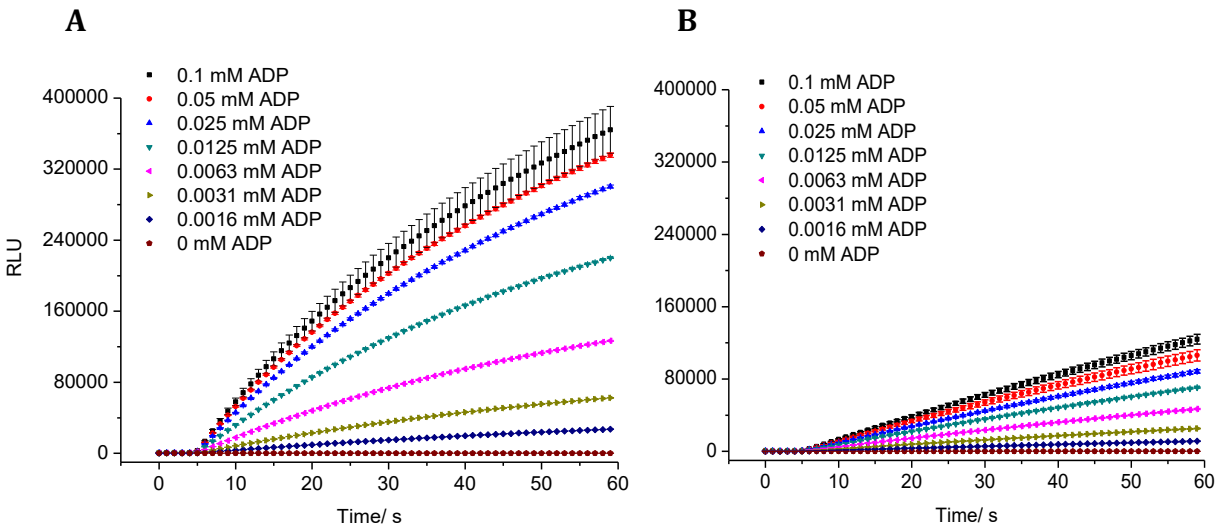

Figure 9 Luminescence output (RLU) plotted as a function of ADP concentration over time. This figure represents 40 ng of (**A**) tAK_{WT} and (**B**) tAK_M.

There is a substantial reduction (~66%) in luminescence output as a result of mutagenesis. When considering the change in initial rate of product turnover, there is a marked difference in the corresponding kinetic parameters as highlighted in Figure 10 and summarised in Table 2.

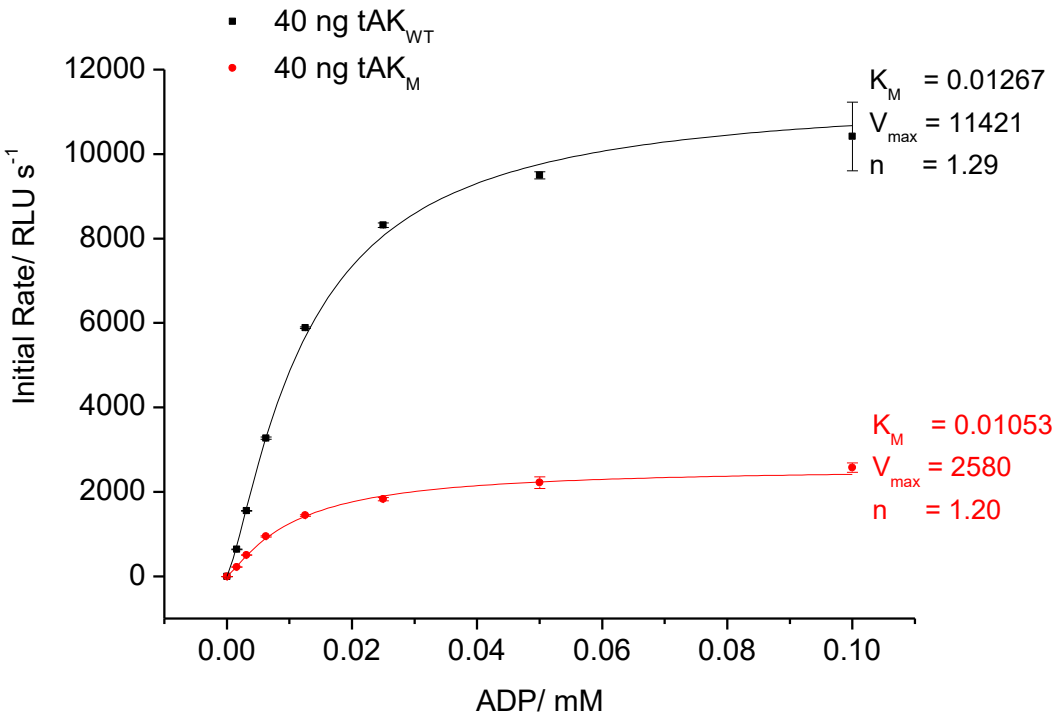

Figure 10 Comparison of initial rate of reaction (RLU s^{-1}) of tAK_{WT} (black) and tAK_M (red). The figure represents 40 ng of enzyme. Tangents were fitted according to a linear fit function between 5 and 15 s.

Table 2 Summary of calculated kinetic parameters for tAK_{WT} and tAK_M, the values presented represent the mean of varying concentrations of enzyme (40, 20, 10, 5 ng).

	k_{cat} (s^{-1})	K_M (mM)	k_{cat}/K_M (mM^{-1} s^{-1})
tAK_{WT}	0.138 ± 0.040	0.017 ± 0.003	8.45 ± 3.04
tAK_M	0.039 ± 0.009	0.015 ± 0.003	2.54 ± 0.15

The reduction in both rate of product turnover and catalytic efficiency may arise as a result of disulphide formation, as suggested by the gel analysis. The effect of reducing any potential disulphide bonds was evaluated in terms of enzyme activity using varying concentrations of DTT, shown in Figure 11.

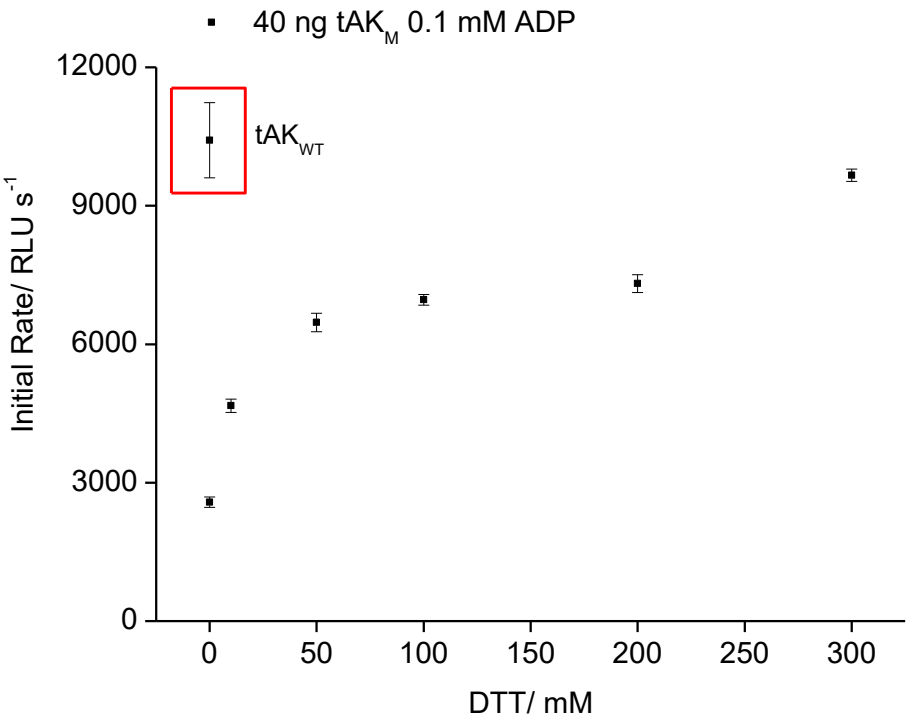

Figure 11 Effect of DTT on tAK$_M$ activity expressed as initial rate of reaction (RLU s^{-1}), compared to the activity of tAK$_{WT}$ (red box) at the same concentration (40 ng), utilising 0.1 mM ADP.

The plateau on the graph may be due to regeneration of the disulfide (in the presence of molecular oxygen), or as a result of oxidation of DTT to its corresponding ring system. Nonetheless, increasing concentrations of DTT appear to increase the activity of tAK$_M$, eventually enhancing the luminescent output > three-fold, resulting in an initial rate of reaction comparable to tAK$_{WT}$. Based on this, tAK$_M$ was reduced using excess DTT prior to conjugation in order to promote the retention of activity.

2.4.3 Bioconjugation

Thiol-mediated conjugation is expected to proceed via Michael addition from the cysteine residues onto the maleimide functionalised pyrene (Scheme 2).

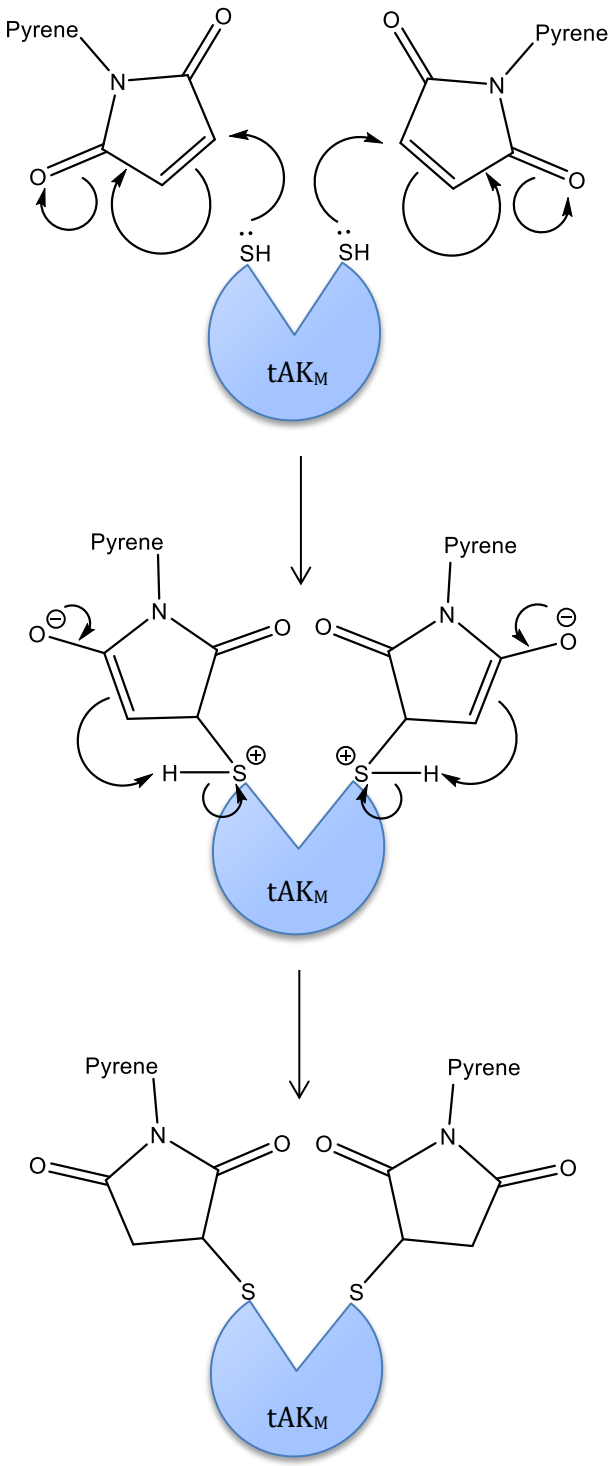

Scheme 2 Nucleophilic addition of *N*-(1-pyrene)maleimide to cysteine residues on tAK$_M$, resulting in thioether bond formation and assembly of the enzyme-fluorophore conjugate.

The monomer emission band (upon excitation at 340 nm) arising from an isolated pyrene (in the absence of substrate), appears at ~ 375 – 410 nm. The peaks associated with these wavelengths can be attributed to the π ⟶ π * transitions. Additionally, when two pyrene molecules come into close proximity, a broad peak appears at ~ 480 nm, corresponding to

the excimer (dimer) emission. This occurs via interaction of a ground state pyrene ring with an excited state pyrene ring. In order to confirm the most effective excitation wavelength for tAK_M conjugated to pyrene (tAK_{MC}), excitation/ emission scanning was performed as shown in Figures 12 and 13.

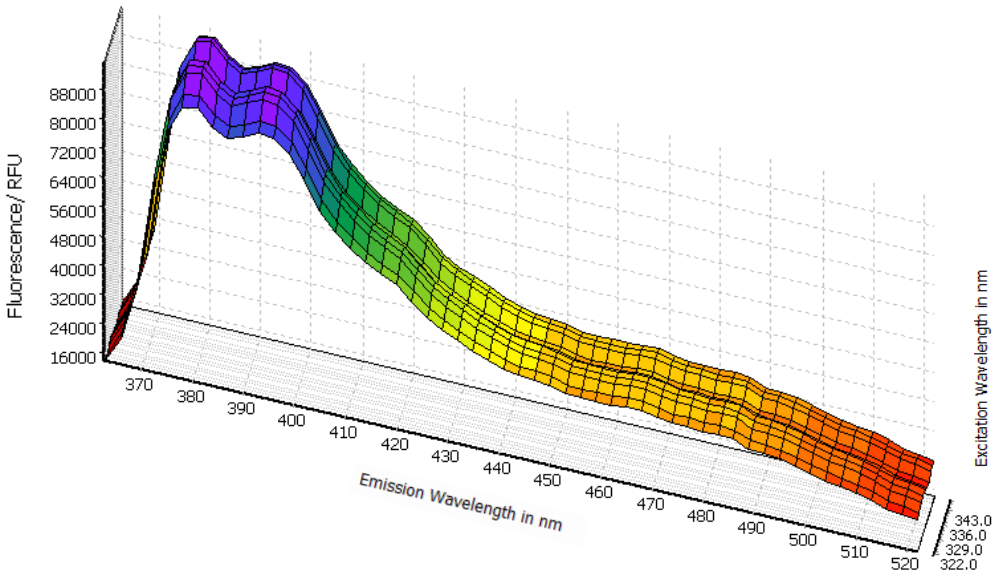

Figure 12 Fluorescence emission intensity of tAK_{MC}, plotted as relative fluorescence units (RFU), as a function of excitation wavelength, aimed at determining the optimum excitation wavelength for monomer emission from pyrene rings.

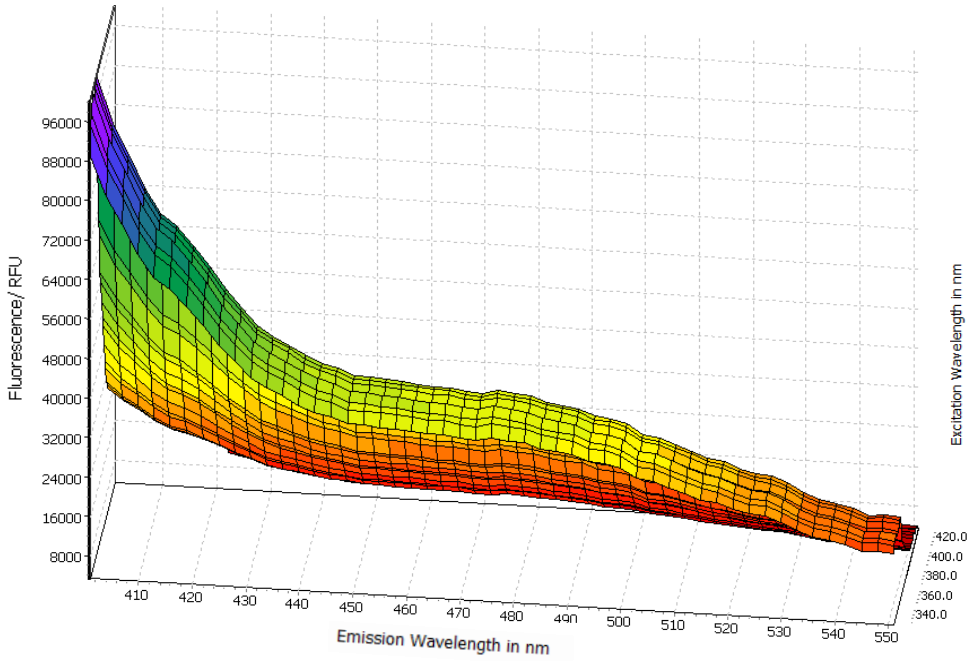

Figure 13 Fluorescence emission intensity of tAK_{MC} with an extended excitation spectrum, aimed at determining the optimum wavelength for excimer emission.

Wavelength scanning confirmed the appropriate excitation wavelength as 340 nm with a slit width of ± 8 nm, for both monomer (Figure 12) and excimer (Figure 13) fluorescence emission. Measuring the fluorescence intensity of tAK_{MC} in the absence of substrate exhibited a small peak in the excimer region (~ 480 nm), in addition to the peaks at lower wavelengths (associated with the monomer emission). This may be as a result of insufficient reduction of disulfide bonds, facilitating an increase in the spatial proximity of intramolecular pyrene rings. However, the change in spectra should still be apparent upon substrate binding. This expected change was monitored via the addition of 5 mM ADP as shown in Figure 14.

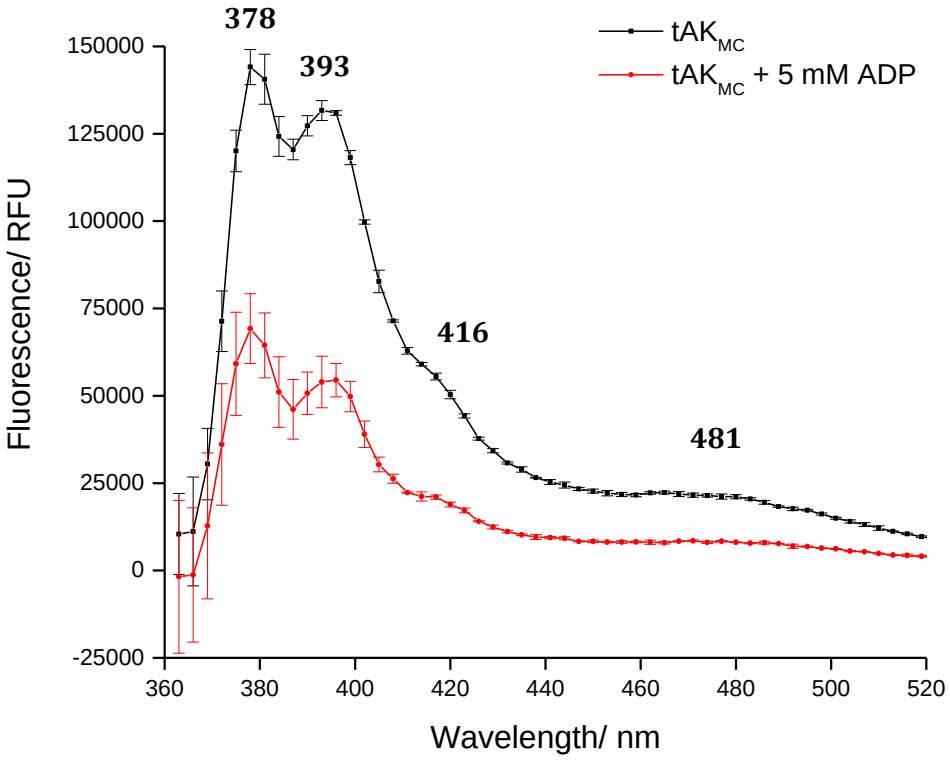

Figure 14 Fluorescence intensity of tAK_{MC} in the absence of substrate (black) and in the presence of 5 mM ADP (red). Excitation wavelength = 340 ± 8 nm.

As expected, the monomer emission occurs both in the presence and absence of substrate, while the intensity is reduced in the former. There appears to be a small peak in the range of the expected excimer emission (481 nm) in the absence of substrate. However, upon addition of ADP, the fluorescence intensity of both the monomer and the excimer signal decreases. This is in contrast to other studies whereby the intensity of the monomer emission is reduced, accompanied by a substantial increase in excimer emission at ~ 480 nm [76]. There

are a number of possible explanations for this. Firstly, the nature of the LID domain in tAK may influence any potential interactions between the fluorophores. Whilst previous studies have focused on AK isolated from *E. coli* (AK_e) (which has a relatively long LID domain), tAK isolated from *S. acidocaldarius* exists in a conformation with a shorter LID [77]. This, coupled to the chosen mutation sites, may affect the spatial proximity of the pyrene ligands and possibly the local secondary structure of the protein itself. Further analysis using molecular modelling (YASARA View [78,79]), permitted visualisation of the conformational change in tAK relative to other AKs. It has been reported that measurable fluorescence intensity as a result of excimer formation occurs when pyrene rings are ≤10 Å in separation [80]. Figures 15 and 16 show the difference in spatial arrangement of the previously reported mutation sites in AK_e, in the absence of substrate and in the presence of Ap5A (a catalytic transition state analogue) respectively.

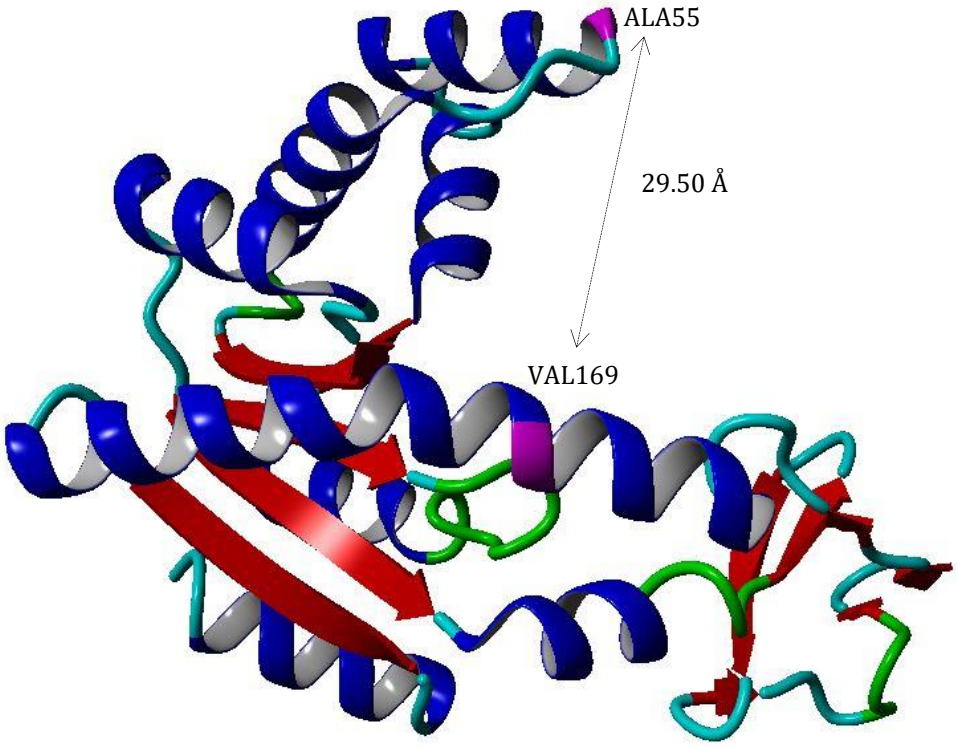

Figure 15 Crystallographic ribbon plot generated in YASARA View using PDB ID 4AKE showing the 29.50 Å distance (C^{α} – C^{α}) between alanine 55 and valine 169 (pink) in AK_e, both of which have previously been mutated to provide cysteine anchor sites for pyrene conjugation.

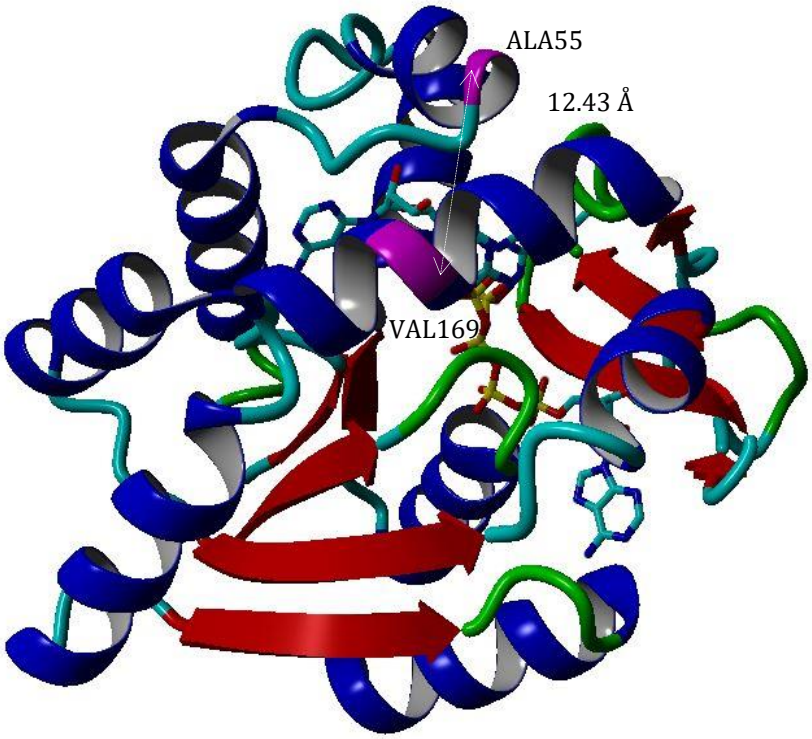

Figure 16 Crystallographic ribbon plot generated in YASARA View using PDB ID 1AKE showing the 12.43 Å distance (C^{α} – C^{α}) between alanine 55 and valine 169 (pink) in AK_e when bound to Ap5A (catalytic transition state analogue), representing the closed conformation.

The ~ 17 Å change in proximity of alanine 55 and valine 169 upon closure of the LID domain corresponds to a distance which may facilitate stacking interactions upon pyrene conjugation (post amino acid substitution, ALA/ VAL ⟶ CYS) [80]. The distance reported here represents the distance from the α carbons of the native amino acids, rather than the conjugated pyrene rings in the AK mutant, however the reported value for the proximal distance between the pyrene rings upon conjugation to the double-cysteine AK_e is 3.7 Å [76]. This is within the range of the predicted distance for observable excimer emission.

In contrast, when modelling the change in distance of the mutation sites in tAK upon substrate binding and subsequent LID closure, the resulting spatial arrangement may not be sufficient to facilitate pyrene – pyrene interactions. This is shown in Figures 17 and 18.

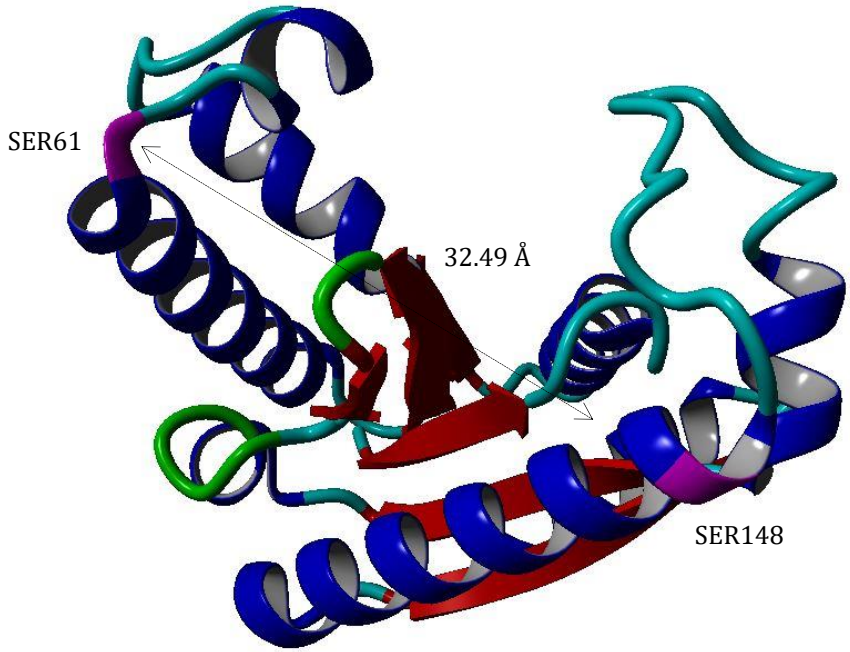

Figure 17 Crystallographic ribbon plot generated in YASARA View using PDB ID 1NKS showing the 32.49 Å distance (C^{α} – C^{α}) between serine 61 and serine 148 (pink) in tAK, in the absence of substrate.

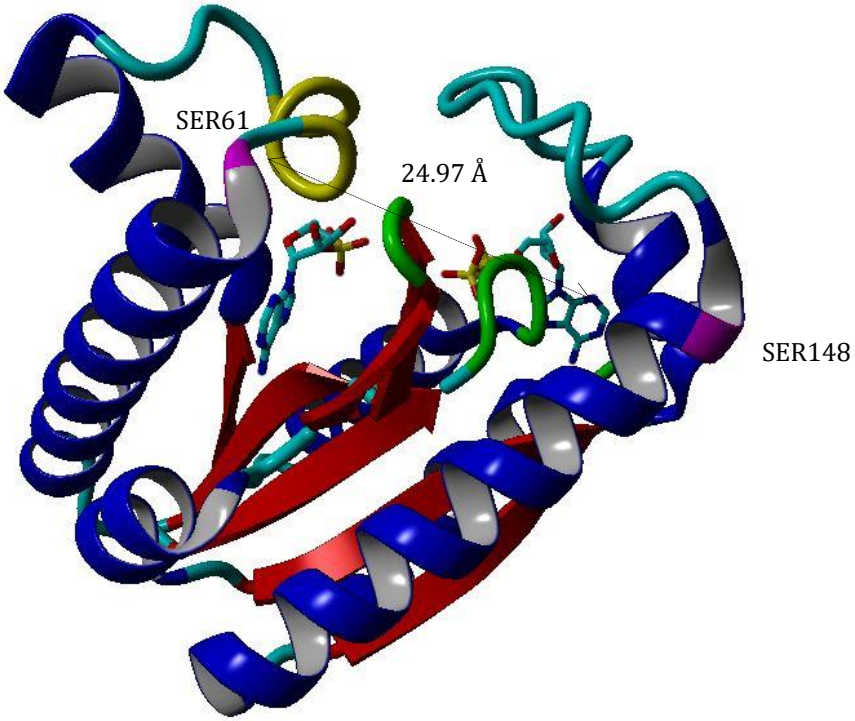

Figure 18 Crystallographic ribbon plot generated in YASARA View using PDB ID 1NKS showing the 24.97 Å distance (C^{α} – C^{α}) between serine 61 and serine 148 (pink) in tAK, when bound to ADP and AMP.

Upon substrate binding, the conformational change in tAK results in a ~7.5 Å change in distance between the mutation sites. Not only is this much smaller than previously observed in AK_e, the final separation of ~25 Å is likely too great a distance to facilitate effective π – π stacking interactions between conjugated pyrene molecules. A curious observation is the weak excimer signal observed in the fluorescence spectra in the absence of substrate (indicating tAK_{MC} in the open form). As previously stated, this may arise from insufficient intramolecular (or buried) disulfide reduction, which may hold the protein in a different conformation to the substrate-bound tAK_{MC}. However, this could equally be attributed to the flexibility of the α-helical scaffold to which the pyrene rings are attached. This flexibility may be lost upon substrate binding as a result of the conformational change, impairing any stacking interactions and eliminating the excimer signal. It may be argued that the excimer signal appears as a result of intermolecular pyrene interactions, rather than intramolecular stacking. However, previous studies using similar systems have proven this unlikely as only a minimal change in signal intensity was observed upon significant sample dilution [81].

Secondly, the absence of excimer signal may result from the specific spatial arrangement of the two pyrene molecules with respect to one another. It may be that the electron-rich pyrene rings are not in the correct orientation to facilitate excimer emission (regardless of whether spatial proximity is indeed the deciding factor). In order to facilitate effective π – π stacking interactions, the pyrene rings must be orientated face on. This configuration is enhanced by a number of non-covalent interactions from the surrounding microenvironment, for example C–H···π interactions between neighbouring amino acid residues and the pyrene rings. The mutations in the amino acid sequence and any subsequent changes in protein conformation may have reduced the capacity for stabilising interactions to take place, thus inhibiting the formation of the favourable ring configuration (as demonstrated in previous studies [76]).

2.4.3.1 Bioconjugate Activity

In order to investigate the nature of substrate binding and enzyme activity upon pyrene conjugation (relative to tAK_{WT} and tAK_M), activity assays using the luciferase/ luciferin system were performed on tAK_{MC}. Conjugation appeared to result in almost complete loss of enzymatic activity as shown in Figure 19.

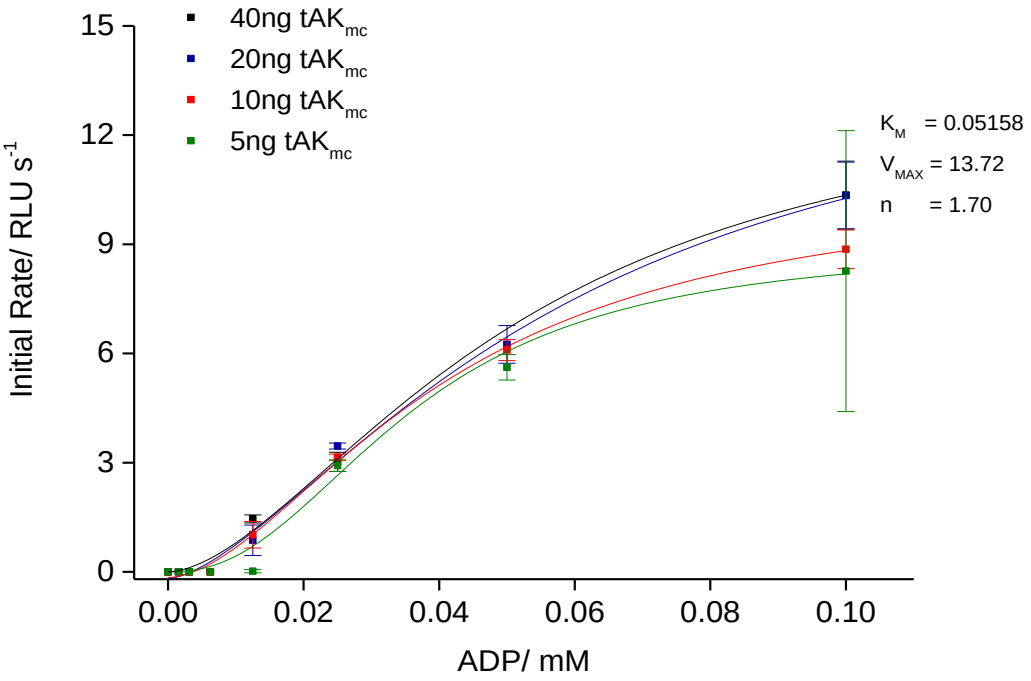

Figure 19 Comparison of initial rate of reaction (RLU s^{-1}) of tAK_{MC} as a function of substrate concentration. Tangents were fitted according to a linear fit function between 5 and 15 s. Kinetic parameters are labelled on the graph for 40 ng tAK_{MC}.

The effect of conjugation on tAK_M manifests as a large decrease in the initial rate of substrate turnover. Compared to the reduced tAK_M (Figure 11), there is ~1000-fold reduction in the initial rate of reaction. However, this may indeed arise as a result of conjugation (affecting the thermodynamic properties of the protein itself), or as a result of the conjugation conditions alone (i.e. in the presence of solvent). Figure 20 shows the effect of the experimental conditions on the reduced tAK_M without the addition of the pyrene ligands. Although the enzymatic activity is increased ~10-fold (relative to tAK_{MC}), the exposure of tAK_M to the conditions required to facilitate conjugation results in ~100-fold reduction in rate compared to the unconjugated tAK_M. The corresponding change in kinetic parameters are summarised in Table 3.

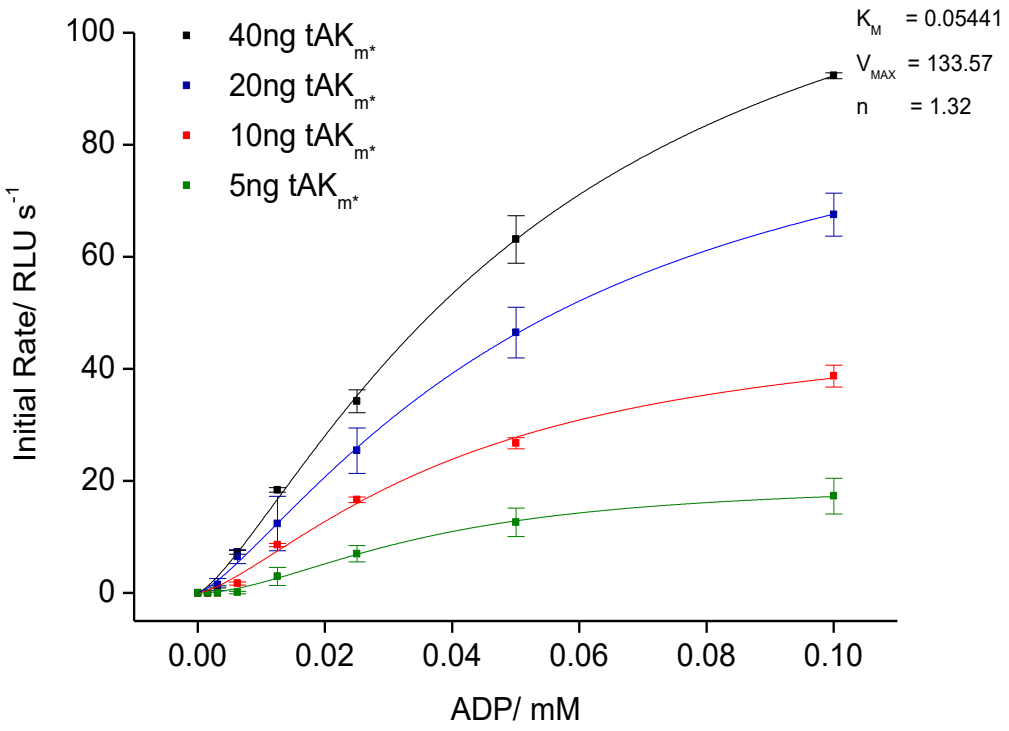

Figure 20 Comparison of initial rate of reaction (RLU s^{-1}) of tAK_M, exposed to the conjugation conditions (tAK_{M*}) as a function of substrate concentration. Tangents were fitted according to a linear fit function between 5 and 15 s. Kinetic parameters are labelled on the graph for 40 ng tAK_{M*}.

Table 3 Summary of calculated kinetic parameters for tAK_{MC} and tAK_{M*}. The values represent the mean of varying concentrations of enzymes (40, 20, 10, 5 ng), alongside the standard deviation.

	k_{cat} (s^{-1})	K_M (mM)	k_{cat}/K_M (mM^{-1} s^{-1})
tAK_{MC}	$3.816 \times 10^{-4} \pm 2.421 \times 10^{-4}$	0.047 ± 0.010	$9.10 \times 10^{-3} \pm 7.30 \times 10^{-3}$
tAK_{M*}	$1.679 \times 10^{-3} \pm 3.154 \times 10^{-4}$	0.047 ± 0.009	$3.73 \times 10^{-2} \pm 1.06 \times 10^{-2}$

The apparent increase in K_M of tAK_{MC} and tAK_{M*} likely indicates reduced substrate affinity. Although K_M cannot necessarily be considered a direct affinity constant (based on its derivation, Chapter 1, Section 1.1.3.2), the fact that V_{MAX} has been reduced so substantially indicates very slow turnover of product and therefore a small k_2 rate constant. If this constant is smaller than k_{-1}, the ratio of k_1: k_{-1} represents the equilibrium constant for the formation of the [ES] complex and as such, provides an indication of the enzyme's affinity for its substrate.

The increase in K_M in this case correlates to a reduced affinity of tAK towards ADP, resulting in weak substrate binding. This may have arisen as a result of changes to the secondary structure of the enzyme upon conjugation, or through partial enzyme inactivation as a result of the coupling conditions (i.e. the presence of DMSO).

2.5 Conclusions and Future Work

The research presented in this Chapter demonstrates how seemingly small structural changes to a protein can have large effects on the resulting physical and catalytic properties. The challenges associated with the genetic manipulation of a biological target (such as successful expression in a host strain, effective purification and retention of activity) can be extensive, yet they serve to highlight the evolutionarily perfected nature of bioactive proteins. The introduction of point mutations in tAK, resulting in the substitution of lysine for cysteine, was successful despite the formation of disulfide bridges. Upon reduction, the mutated enzyme was able to catalyse the formation of ATP at a similar rate to the wildtype enzyme. However, coupling of the mutant tAK to pyrene reporter probes reduced the activity of the enzyme substantially, likely as a result of both fluorophore attachment (hindering substrate access and/or inducing a change in the protein secondary structure), and the conditions used for conjugation. Additionally, the expected fluorescence signal from the interaction of the pyrene reporter ligands was absent upon substrate binding. Fluorescence signals were observed for the individual pyrene rings (monomer emission) in both the absence and presence of substrate. This may indicate insufficient conjugation (i.e. the attachment of a single ligand to each individual protein), or the generation of incorrectly orientated/ spatially arranged fluorophores.

The future development of this work will need to establish two critical parameters, firstly the potential alternative amino acids for successful mutagenesis (those not involved in substrate binding, exhibiting similar chemical and physical properties to cysteine and located in regions which come into close proximity (~10 Å) upon substrate binding). Secondly, the choice of fluorophore may need to be further investigated. The nature of the spacer arm (separating the protein and the delocalised ring system) can influence the stability and orientation of the pyrene molecules. The introduction of an amide bond in the linker arm between fluorophore and protein has been shown to facilitate stabilising interactions within the protein microenvironment. This has successfully resulted in face-on orientation of pyrene rings and subsequent fluorescence output, as a result of $\pi - \pi$ stacking interactions [76]. Finally the conjugation conditions should be optimised. For example, the choice of solvent (in order

to retain enzyme activity), the choice of reducing agent and/ or chemical denaturant (in order to reduce buried disulfide bonds) and the choice of specific reduction and conjugation conditions (as the presence of molecular oxygen can initiate disulfide reformation and quenching of pyrene fluorescence [80]). In addition to changing some of the fundamental parameters required for mutagenesis and conjugation, certain techniques may be employed in order to fully quantify and assess both experimental procedures. For example, mass spectrometry for the determination of single or multiple ligand functionalisation, circular dichroism for the evaluation of conjugation effects on protein structure, and column chromatography for the separation of unmodified and partially modified proteins from the doubly labelled mutant.

As an alternative to optical excitation of fluorescent reporter probes for the detection of proteinaceous activity, there are a number of other luminescent-based signalling approaches also capable of exploiting changes in the spatial arrangement of biomolecules. Bioluminescence-resonance energy transfer (BRET) relies on the non-radiative transfer of energy from a bioluminescent donor to a fluorescent acceptor. This process provides certain advantages over standard fluorescence measurements (and fluorescence-resonance energy transfer (FRET) based measurements), notably a larger Förster distance, allowing signal generation over longer distances (5-10 nm) [82]. As a common bioluminescent energy donor, luciferase has been utilised alongside green/ yellow fluorescent proteins to form BRET pairs for a multitude of biosensing applications [83-85]. Upon interaction of luciferase with coelenterazine (the substrate in this case), a characteristic fluorescence emission is observed which changes according to the spatial proximity of the donor/acceptor pair. By construction of BRET pairs fused to bioactive proteins, it is possible to monitor physical effects of substrate binding, for example any conformational changes within a protein. This could be implemented with tAK via genetic modification to form a BRET fusion protein as shown in Figure 21. As a development of the current clinical biosensor (WASHtAK), a BRET based system could provide valuable insight into hospital associated sterilisation procedures, based on the change in intensity of signal output at the two different wavelengths.

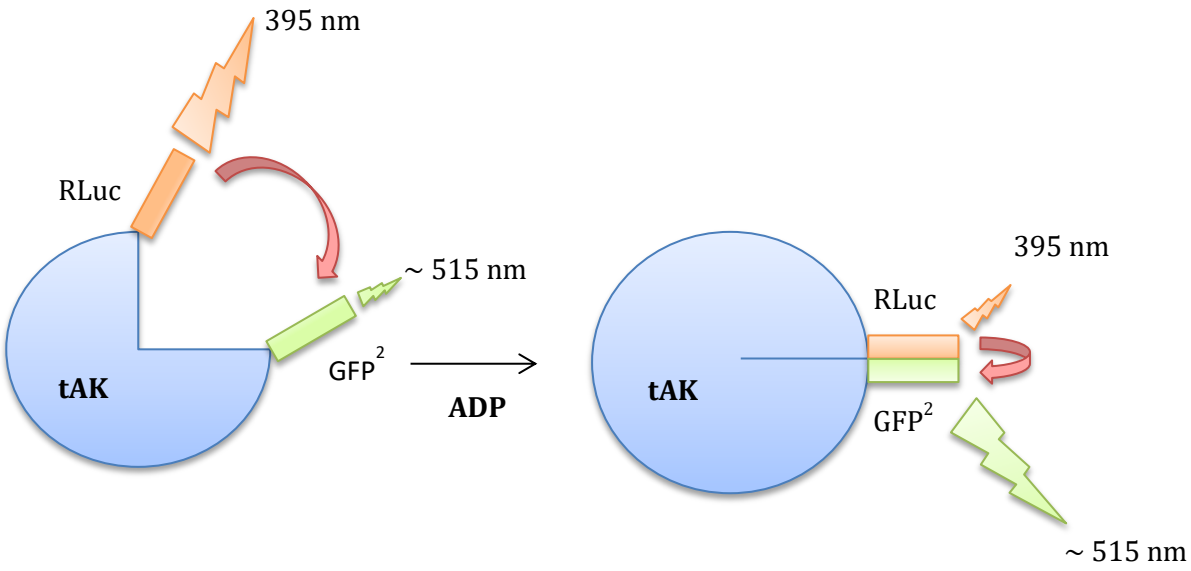

Figure 21 Schematic showing potential BRET system using *Renilla* luciferase (RLuc), green fluorescent protein^2 (GFP^2) and tAK. The binding of ADP causes a conformational change in tAK, decreasing the spatial proximity of the donor/acceptor pair, resulting in a measureable change in emission intensities upon energy transfer.

2.6 References

1 Clancy, S. & Brown, W. Translation: DNA to mRNA to Protein. *Nature Education* **1**, 101 (2008).

2 Berg JM, T. J., Stryer L. *Section 29.5, Eukaryotic Protein Synthesis Differs from Prokaryotic Protein Synthesis Primarily in Translation Initiation*. 5th edn, (W. H. Freeman and Company., 2002).

3 Edelheit, O., Hanukoglu, A. & Hanukoglu, I. Simple and efficient site-directed mutagenesis using two single-primer reactions in parallel to generate mutants for protein structure-function studies. *BMC Biotechnology* **9**, 61 (2009).

4 Plapp, B. V. Site-directed mutagenesis: a tool for studying enzyme catalysis. *Methods in Enzymology* **249**, 91-119 (1995).

5 Estell, D. A., Graycar, T. P. & Wells, J. A. Engineering an enzyme by site-directed mutagenesis to be resistant to chemical oxidation. *Journal of Biological Chemistry* **260**, 6518-6521 (1985).

6 Campas, M., Prieto-Simon, B. & Marty, J. L. A review of the use of genetically engineered enzymes in electrochemical biosensors. *Seminars in Cell and Developmental Biology* **20**, 3-9 (2009).

7 Li, Q., Yi, L., Marek, P. & Iverson, B. L. Commercial proteases: Present and future. *FEBS Letters* **587**, 1155-1163 (2013).

8 Estell, D. A. Engineering enzymes for improved performance in industrial applications. *Journal of Biotechnology* **28**, 25-30 (1993).

9 Lee, Y. & Rio, D. C. Mechanisms and Regulation of Alternative Pre-mRNA Splicing. *Annual Review of Biochemistry* **84**, 291-323 (2015).

10 Black, D. L. Mechanisms of alternative pre-messenger RNA splicing. *Annual Review of Biochemistry* **72**, 291-336 (2003).

11 Bökel, C. in *Drosophila: Methods and Protocols* (ed Christian Dahmann) 119-138 (Humana Press, 2008).

12 El-Gewely, M. R., Fenton, C., Kjeldsen, E. & Xu, H. in *Encyclopoedia of Life Sciences* (*eLS)* (John Wiley & Sons, Ltd, 2001).

13 Hutchison, C. A., Phillips, S., Edgell, M. H., Gillam, S., Jahnke, P. & Smith, M. Mutagenesis at a specific position in a DNA sequence. *Journal of Biological Chemistry* **253**, 6551-6560 (1978).

14 Braman, J., Papworth, C. & Greener, A. Site-directed mutagenesis using double-stranded plasmid DNA templates. *Methods in Molecular Biology* **57** (1996).

15 Lauerman, L. H. Advances in PCR technology. *Animal Health Research Reviews* **5**, 247-248 (2004).

16 Smith, C. Cloning and mutagenesis: tinkering with the order of things. *Nature Methods* **4**, 455-461 (2007).

17 Corley, R. B. *A Guide to Methods in the Biomedical Sciences*. illustrated edn, 53 - 56 (Springer Science & Business Media, 2004).

18 Dieffenbach, C. W., Lowe, T. M. & Dveksler, G. S. General concepts for PCR primer design. *PCR Methods and Applications* **3**, S30-37 (1993).

19 Lu, J., Johnston, A., Berichon, P., Ru, K.-l., Korbie, D. & Trau, M. PrimerSuite: A High-Throughput Web-Based Primer Design Program for Multiplex Bisulfite PCR. *Scientific Reports* **7**, 41328 (2017).

20 NCBI. Primer-BLAST, https://www.ncbi.nlm.nih.gov/tools/primer-blast/

21 Ye, J., Coulouris, G., Zaretskaya, I., Cutcutache, I., Rozen, S. & Madden, T. L. Primer-BLAST: A tool to design target-specific primers for polymerase chain reaction. *BMC Bioinformatics* **13**, 134-134 (2012).

22 The University of Queensland, D. I. Project 21 Manual: Experimental Procedures: Site-directed Mutagenesis, http://www.di.uq.edu.au/proj21proc

23 Lodge, J., Lund, P. & Minchin, S. *Gene Cloning*. 307- 309 (Taylor & Francis, 2007).

24 Hattman, S., Brooks, J. E. & Masurekar, M. Sequence specificity of the P1 modification methylase (M.Eco P1) and the DNA methylase (M.Eco dam) controlled by the Escherichia coli dam gene. *Journal of Molecular Biology* **126**, 367-380 (1978).

25 Marinus, M. G. & Løbner-Olesen, A. DNA Methylation. *EcoSal Plus* **6**, *PMC* 10.1128/ecosalplus.ESP-0003-2013 (2014).

26 Williams, R. J. Restriction endonucleases: classification, properties, and applications. *Molecular Biotechnology* **23**, 225-243 (2003).

27 Yoshida, N. & Sato, M. Plasmid uptake by bacteria: a comparison of methods and efficiencies. *Applied Microbiology and Biotechnology* **83**, 791-798 (2009).

28 Liu, X., Liu, L., Wang, Y., Wang, X., Ma, Y. & Li, Y. The Study on the factors affecting transformation efficiency of E. coli competent cells. *Pakistan Journal of Pharmaceutical Sciences* **27**, 679-684 (2014).

29 Aune, T. E. & Aachmann, F. L. Methodologies to increase the transformation efficiencies and the range of bacteria that can be transformed. *Applied Microbiology and Biotechnology* **85**, 1301-1313 (2010).

30 Evans, G. A. Molecular cloning: A laboratory manual. Second edition. Volumes 1, 2, and 3. Current protocols in molecular biology. Volumes 1 and 2. *Cell* **61**, 17-18.

31 Padmanabhan, S., Banerjee, S. & Mandi, N. *Screening of Bacterial Recombinants: Strategies and Preventing False Positives*. (InTech, 2011).

32 Walsh, C. T., Garneau-Tsodikova, S. & Gatto, G. J. Protein Posttranslational Modifications: The Chemistry of Proteome Diversifications. *Angewandte Chemie International Edition* **44**, 7342-7372 (2005).

33 Knorre, D. G., Kudryashova, N. V. & Godovikova, T. S. Chemical and Functional Aspects of Posttranslational Modification of Proteins. *Acta Naturae* **1**, 29-51 (2009).

34 Mann, M. & Jensen, O. N. Proteomic analysis of post-translational modifications. *Nature Biotechnology* **21**, 255-261 (2003).

35 Duan, G. & Walther, D. The Roles of Post-translational Modifications in the Context of Protein Interaction Networks. *PLOS Computational Biology* **11**, e1004049 (2015).

36 Wang, Y.-C., Peterson, S. E. & Loring, J. F. Protein post-translational modifications and regulation of pluripotency in human stem cells. *Cell Research* **24**, 143-160 (2014).

37 Audagnotto, M. & Dal Peraro, M. Protein post-translational modifications: In silico prediction tools and molecular modeling. *Computational and Structural Biotechnology Journal* **15**, 307-319 (2017).

38 Gajjala, P. R., Fliser, D., Speer, T., Jankowski, V. & Jankowski, J. Emerging role of post-translational modifications in chronic kidney disease and cardiovascular disease. *Nephrology Dialysis Transplantation* **30**, 1814-1824 (2015).

39 Sambataro, F. & Pennuto, M. Post-translational Modifications and Protein Quality Control in Motor Neuron and Polyglutamine Diseases. *Frontiers in Molecular Neuroscience* **10** (2017).

40 Tobin, P. H., Richards, D. H., Callender, R. A. & Wilson, C. J. Protein Engineering: A New Frontier for Biological Therapeutics. *Current drug metabolism* **15**, 743-756 (2014).

41 Woodley, J. M. Protein engineering of enzymes for process applications. *Current Opinion in Chemical Biology* **17**, 310-316 (2013).

42 Olson, E. J. & Tabor, J. J. Post-translational tools expand the scope of synthetic biology. *Current Opinion in Chemical Biology* **16**, 300-306 (2012).

43 Walsh, G. & Jefferis, R. Post-translational modifications in the context of therapeutic proteins. *Nature Biotechnology* **24**, 1241-1252 (2006).

44 Haspel, N., Moll, M., Baker, M. L., Chiu, W. & Kavraki, L. E. Tracing conformational changes in proteins. *BMC Structural Biology* **10**, S1 (2010).

45 Kahsai, A. W., Rajagopal, S., Sun, J. & Xiao, K. Monitoring protein conformational changes and dynamics using stable-isotope labeling and mass spectrometry. *Nature Protocols* **9**, 1301-1319 (2014).

46 Goh, C. S., Milburn, D. & Gerstein, M. Conformational changes associated with protein-protein interactions. *Current Opinion in Structural Biology* **14**, 104-109 (2004).

47 Chang, C.-W., Chou, C.-W. & Chang, D. T.-H. CCProf: exploring conformational change profile of proteins. *Database* **2016**, baw029-baw029 (2016).

48 Jeon, J., Nam, H. J., Choi, Y. S., Yang, J. S., Hwang, J. & Kim, S. Molecular evolution of protein conformational changes revealed by a network of evolutionarily coupled residues. *Molecular Biology and Evolution* **28**, 2675-2685 (2011).

49 Henzler-Wildman, K. A., Thai, V., Lei, M., Ott, M., Wolf-Watz, M., Fenn, T., Pozharski, E., Wilson, M. A., Petsko, G. A., Karplus, M., Hubner, C. G. & Kern, D. Intrinsic motions along an enzymatic reaction trajectory. *Nature* **450**, 838-844 (2007).

50 Arora, K. & Brooks, C. L., 3rd. Large-scale allosteric conformational transitions of adenylate kinase appear to involve a population-shift mechanism. *Proceedings of the National Acadamy of Sciences U S A* **104**, 18496-18501 (2007).

51 Jana, B., Adkar, B. V., Biswas, R. & Bagchi, B. Dynamic coupling between the LID and NMP domain motions in the catalytic conversion of ATP and AMP to ADP by adenylate kinase. *J Chemical Physics* **134**, 035101 (2011).

52 Brokaw, J. B. & Chu, J. W. On the roles of substrate binding and hinge unfolding in conformational changes of adenylate kinase. *Biophysical Journal* **99**, 3420-3429 (2010).

53 Pontiggia, F., Zen, A. & Micheletti, C. Small- and large-scale conformational changes of adenylate kinase: a molecular dynamics study of the subdomain motion and mechanics. *Biophysical Journal* **95**, 5901-5912 (2008).

54 Li, D., Liu, Ming S. & Ji, B. Mapping the Dynamics Landscape of Conformational Transitions in Enzyme: The Adenylate Kinase Case. *Biophysical Journal* **109**, 647-660 (2015).

55 Müller, C., Schlauderer, G., Reinstein, J. & Schulz, G. E. Adenylate kinase motions during catalysis: an energetic counterweight balancing substrate binding. *Structure* **4**, 147-156 (1996).

56 Müller, C. W. & Schulz, G. E. Structure of the complex between adenylate kinase from Escherichia coli and the inhibitor Ap5A refined at 1.9 Å resolution. *Journal of Molecular Biology* **224**, 159-177 (1992).

57 Ping, J., Hao, P., Li, Y. X. & Wang, J. F. Molecular dynamics studies on the conformational transitions of adenylate kinase: a computational evidence for the conformational selection mechanism. *Biomed Research International* **2013**, 628536 (2013).

58 Wolf-Watz, M., Thai, V., Henzler-Wildman, K., Hadjipavlou, G., Eisenmesser, E. Z. & Kern, D. Linkage between dynamics and catalysis in a thermophilic-mesophilic enzyme pair. *Nature Structural & Molecular Biology* **11**, 945-949 (2004).

59 Yuan, W., Yang, J., Kopečková, P. & Kopeček, J. Smart Hydrogels Containing Adenylate Kinase: Translating Substrate Recognition into Macroscopic Motion. *Journal of the American Chemical Society* **130**, 15760-15761 (2008).

60 Tobi, D. & Bahar, I. Structural changes involved in protein binding correlate with intrinsic motions of proteins in the unbound state. *Proceedings of the National Acadamy of Sciences U S A* **102**, 18908-18913 (2005).

61 Whitford, P. C., Gosavi, S. & Onuchic, J. N. Conformational Transitions in Adenylate Kinase: Allosteric Communication Reduces Misligation. *Journal of Biological Chemistry* **283**, 2042-2048 (2008).

62 Murphy, W. L., Dillmore, W. S., Modica, J. & Mrksich, M. Dynamic hydrogels: translating a protein conformational change into macroscopic motion. *Angewandte Chemie International Edition* **46**, 3066-3069 (2007).

63 Sui, Z., King, W. J. & Murphy, W. L. Dynamic Materials Based on a Protein Conformational Change. *Advanced Materials* **19**, 3377-3380 (2007).

64 Ehrick, J. D., Deo, S. K., Browning, T. W., Bachas, L. G., Madou, M. J. & Daunert, S. Genetically engineered protein in hydrogels tailors stimuli-responsive characteristics. *Nature Materials* **4**, 298-302 (2005).

65 Fujii, A., Hirota, S. & Matsuo, T. Reversible Switching of Fluorophore Property Based on Intrinsic Conformational Transition of Adenylate Kinase during Its Catalytic Cycle. *Bioconjugate Chemistry* **24**, 1218-1225 (2013).

66 Ungurs, M., Hesp, J. R., Poolman, T., McLuckie, G., O'Brien, S., Murdoch, H., Wells, P., Raven, N. D. H., Walker, J. T. & Sutton, J. M. Quantitative measurement of the efficacy of protein removal by

cleaning formulations; comparative evaluation of prion-directed cleaning chemistries. *Journal of Hospital Infection* **74**, 144-151 (2010).

67 Qiagen. QIAprep Miniprep Kit Handbook, https://www.qiagen.com/gb/resources/ (2015).

68 Qiagen. HiSpeed Plasmid Purification Handbook, https://www.qiagen.com/gb/resources

69 Technologies, A. QuikChange Lightning Site-Directed Mutagenesis Kit Instruction Manual, http://www.agilent.com/cs/library/usermanuals (2015).

70 Stratagene. XL10-Gold® Ultracompetent Cells Transformation Protocol, http://www.chem-agilent.com/pdf/strata/200314.pdf

71 Novagen. BugBuster®Protein Extraction Reagent User Protocol, http://www.merckmillipore.com/GB/en/product/BugBuster-Protein-Extraction-Reagent,EMD_BIO-70584

72 Bates, R. G. & Bower, V. E. Alkaline Solutions for pH Control. *Analytical Chemistry* **28**, 1322-1324 (1956).

73 Gomori, G. Preparation of buffers for use in enzyme studies. *Methods in Enzymology* **1**, 143–146 (1955).

74 Bradford, M. M. A rapid and sensitive method for the quantitation of microgram quantities of protein utilizing the principle of protein-dye binding. *Analytical Biochemistry* **72**, 248-254 (1976).

75 Invitrogen. Thiol-Reactive Probes Manuals and Protocols, https://www.thermofisher.com/order/catalog/product/P28

76 Fujii, A., Sekiguchi, Y., Matsumura, H., Inoue, T., Chung, W.-S., Hirota, S. & Matsuo, T. Excimer Emission Properties on Pyrene-Labeled Protein Surface: Correlation between Emission Spectra, Ring Stacking Modes, and Flexibilities of Pyrene Probes. *Bioconjugate Chemistry* **26**, 537-548 (2015).

77 Criswell, A. R., Bae, E., Stec, B., Konisky, J. & Phillips, G. N. Structures of thermophilic and mesophilic adenylate kinases from the genus Methanococcus. *Journal of Molecular Biology* **330**, 1087-1099 (2003).

78 Krieger, E. & Vriend, G. YASARA View - molecular graphics for all devices - from smartphones to workstations. *Bioinformatics* **30**, 2981-2982 (2014).

79 Krieger, E. & Vriend, G. New ways to boost molecular dynamics simulations. *Journal of Computational Chemistry* **36**, 996-1007 (2015).

80 Bains, G., Patel, A. B. & Narayanaswami, V. Pyrene: a probe to study protein conformation and conformational changes. *Molecules* **16**, 7909-7935 (2011).

81 Bains, G. K., Kim, S. H., Sorin, E. J. & Narayanaswami, V. The Extent of Pyrene Excimer Fluorescence Emission Is a Reflector of Distance and Flexibility: Analysis of the Segment Linking the LDL Receptor-Binding and Tetramerization Domains of Apolipoprotein E3. *Biochemistry* **51**, 6207-6219 (2012).

82 Dacres, H., Wang, J., Dumancic, M. M. & Trowell, S. C. Experimental Determination of the Förster Distance for Two Commonly Used Bioluminescent Resonance Energy Transfer Pairs. *Analytical Chemistry* **82**, 432-435 (2010).

83 Dacres, H., Dumancic, M. M., Horne, I. & Trowell, S. C. Direct comparison of fluorescence- and bioluminescence-based resonance energy transfer methods for real-time monitoring of thrombin-catalysed proteolytic cleavage. *Biosensors and Bioelectronics* **24**, 1164-1170 (2009).

84 Loening, A. M., Fenn, T. D., Wu, A. M. & Gambhir, S. S. Consensus guided mutagenesis of Renilla luciferase yields enhanced stability and light output. *Protein Engineering, Design and Selection* **19**, 391-400 (2006).

85 Dacres, H., Michie, M., Anderson, A. & Trowell, S. C. Advantages of substituting bioluminescence for fluorescence in a resonance energy transfer-based periplasmic binding protein biosensor. *Biosensors and Bioelectronics* **41**, 459-464 (2013).

Part B: Treatment of Infection

"If I had thought about it, I wouldn't have done the experiment. The literature was full of examples that said you can't do this."

Spencer F. Silver – Chemist, inventor of the Post-It Note.

Chapter 3: Recent Advances in Therapeutic Delivery Systems of Bacteriophage and Bacteriophage-Encoded Endolysins

3.1 Introduction

The purpose of this Chapter is to provide the theoretical basis of the research undertaken in the succeeding Chapters. This includes the clinical problem, potential biotherapeutic solutions and the current state of research in the context of bacterial infection control.

3.1.1 Antibiotic Resistance

The discovery and subsequent development of antibiotics has revolutionised modern medicine following the clinical introduction of penicillin almost 80 years ago [1]. Since then, over 20 classes of novel antibiotics have been brought to market, each with a unique mechanism of action (MOA), targeting a range of pathogenic bacteria. Despite the initial success of antibiotic therapy, bacterial evolution has been equally assiduous in the installation of biological countermeasures, aimed at resisting cellular destruction as a result of antibiotic exposure. There are a number of different mechanisms of resistance (MOR) exhibited by bacteria, resulting in partial or full protection from antibiotics. Aside from intrinsic resistance, bacteria can acquire resistance via horizontal gene transfer (HGT)[a], mutations in chromosomal genes (favoured by hypermutator bacterial strains), and as a consequence of selective pressures resulting from the presence of antimicrobial compounds or other contaminants [3]. The physical manifestation of these resistance mechanisms can be classified into three main strategies: reducing the intracellular concentration of drug (via uptake inhibition or antibiotic efflux), modification of the antibiotic target (via pre- or post-translational modification), and inactivation of the antibiotic compound (via enzymatic modification), as shown in Figure 1 [4,5]. A summary of some of the key classes of antibiotics and their respective MOA/ MOR is presented in Table 1[1,b].

[a] HGT refers to the transmission of genetic information between genomes from processes other than parent to offspring. HGT can occur through transduction, transformation and conjugation [2].
[b] Gram classification refers to the Gram staining process used to differentiate the two main classes of bacteria based on the differences in their cell wall constituents (peptidoglycan content). Gram-positive bacteria have thicker cell walls compared to Gram-negative bacteria, and thus retain the colour of the stain (crystal violet) [6].

Table 1 Summary of the common classes of antibiotics and their associated properties.

Antibiotic Class	Examples	Parent Structure	Activity	Mechanism of Action	Mechanism of Resistance
β - lactam	Penicillins Cephalosporins Carbapenems	4 - membered β - lactam ring	Broad-spectrum	Inhibition of cell wall synthesis	β – lactamase production (enzymatic hydrolysis of the β - lactam ring) [7]
Aminoglycoside	Streptomycin Gentamycin	Amino-modified glycoside	Broad-spectrum	Inhibition of protein synthesis	Cell membrane modification, antibiotic efflux, enzymatic modification of drug and drug target (ribosome) [8]
Tetracycline	Tetracycline Doxycycline	Linear, fused tetracyclic core structure	Broad-spectrum	Inhibition of protein synthesis	Antibiotic efflux, ribosomal protection proteins, and enzyme-catalysed drug inactivation [9]
Macrolide	Erythromycin Clarithomycin Azithromycin	Macrocyclic lactone ring	Broad-spectrum	Inhibition of protein synthesis	Ribosomal methylation or mutation and antibiotic efflux [10]
Glycopeptide	Vancomycin Telavancin Bleomycin	Glycosylated non-ribosomal peptide	Gram-positive bacteria	Inhibition of cell wall synthesis	Enzymatic modification of bacterial cell wall and thickening of cell wall [11]
Oxazolidone	Linezolid Eperezolid	Substituted oxazolidinone ring	Gram-positive bacteria	Inhibition of protein synthesis	Ribosomal (target) mutation [12]
Quinolone	Ciprofloxacin Levofloxacin	Bicyclic core structure related to 4-quinolone	Broad-spectrum	Inhibition of DNA synthesis	Antibiotic efflux and mutations in the target enzymes (DNA gyrase, topoisiomerase) [13]
Lipopeptide	Polymyxin B Colistin Daptomycin	Linear or cyclic peptide with lipophilic tail	Gram-positive bacteria	Depolarisation of cell membrane	Cell membrane (target) modification [14,15]

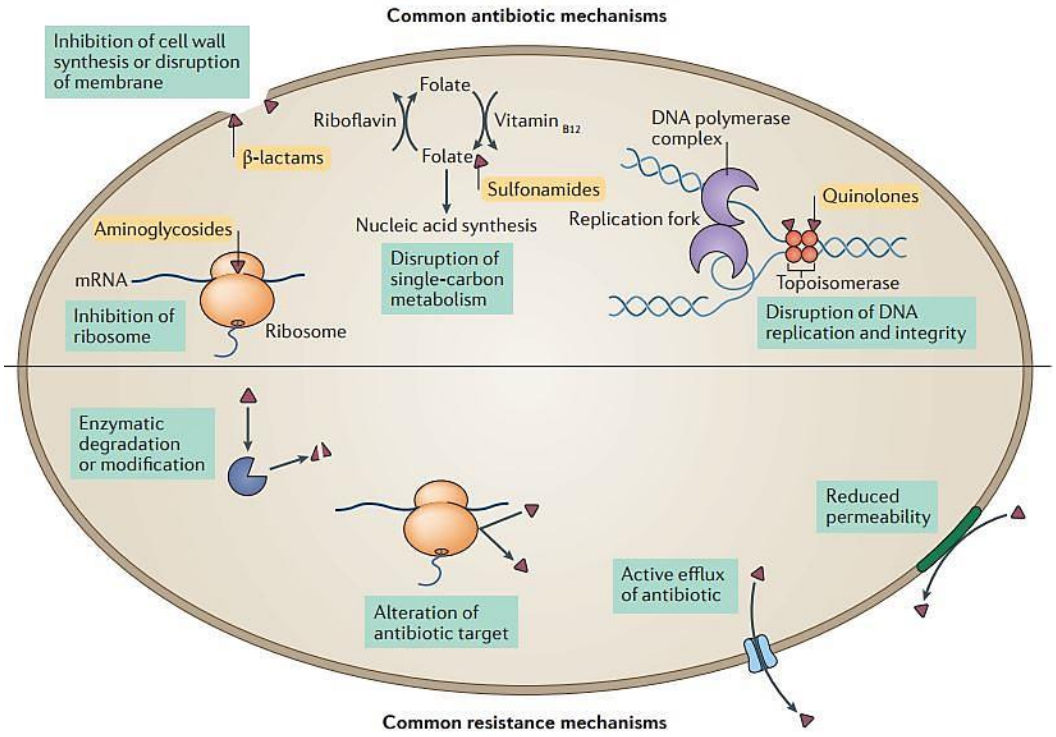

Figure 1 Summary of some of the common classes of antibiotics and their MOA (top), alongside the common bacterial strategies employed in order to resist antibiotics (bottom). Reprinted by permission from Macmillan Publishers Ltd: Nature Reviews Microbiology [5]. Copyright © 2017.

The threat posed by the spread of drug resistant pathogens is particularly ominous owing to the fact that the antibiotic pipeline has effectively run dry. There have been only two new classes of antibiotics discovered in the last 20 years, yet it is estimated that at least 700,000 people die globally each year as a result of resistant infections [16]. The factors driving the continued evolution of bacterial resistance have been associated with their overuse in both the medical and the agricultural sectors.

In the medical sense, antibiotics form the clinical basis of modern infection control, both in the hospital and in the community. However, their excessive and often inappropriate use has contributed to the selection of resistant bacterial variants. In many cases this is as a result of exposure to sub-lethal concentrations of antibiotic, (i.e. any concentration which is lower than the minimum inhibitory concentration (MIC) required to effectively inhibit bacterial growth). The generation of antibiotic concentration gradients within the body exerts a multitude of effects upon the bacterial population (both pathogenic and commensal), including the selection of resistance (*de novo* and pre-existing), the initiation of genotypic and

phenotypic alterations and changes in gene expression [17]. There are a number of causes of such exposure, including inefficient dosing strategies, poor drug pharmacokinetics and issues surrounding patient compliance [5]. With over 70 billion clinical doses administered worldwide in 2010 [18], it is unsurprising that the responsible distribution and consumption of antibiotics is a continuous cause for concern and as such, a highly debated topic. The appropriate prescribing of any drug is the responsibility of the qualified person (doctor, pharmacist, clinician etc.), while the appropriate consumption of the drug is the responsibility of the patient. However, this strategy is only effective if both parties are acting upon the correct advice. In developed countries, antibiotics are only available with a prescription, which aims to standardise and limit antibiotic distribution [19]. However, the advice given to patients upon prescription of antibiotic therapy has recently come under scrutiny. The current guidelines regarding the necessary duration of a course of antibiotics (as advocated by the World Health Organisation (WHO) and various governments across the world, including the UK [20]), insists that a patient must finish the full course of antibiotics as prescribed by their doctor. This is (and has been for many years) one of the most widely accepted, fundamental pieces of medical advice distributed to the general population. However, a paper published recently (July 2017) in the British Medical Journal by a number of prominent health and infectious disease specialists, suggests that the current guidelines are advocated in the absence of any clinical evidence [21]. The authors postulate that in direct contrast to the intended outcome (preventing the spread of resistance), the current notion of completing a full course of antibiotics is in fact resulting in gross over usage. With excessive use of antibiotics driving the evolution and spread of resistance, they suggest instead, that a patient should 'stop when they feel better', thus reducing prolonged, unnecessary administration. A detailed discussion regarding the ongoing debate as to the most effecting dosing strategies is outside the scope of this thesis, expert analysis is published elsewhere [22-25]. However, the prospect of a tangible, clinical division in the recommended advice given to patients, and the inevitable confusion this will cause, is yet another ambiguous element in multitude of deciding factors governing the spread of antibiotic resistance.

Aside from clinical use, the distribution of antibiotics within the agricultural sector accounts for an extortionate percentage of the global consumption. Annually, over 17 million kilograms of antibiotics are consumed in the US alone, 80% of which are used in the rearing of food animals [26]. Furthermore, the administration of antibiotics to livestock is often deliberately maintained at sub MIC levels (for example as feed additives aimed at increasing growth rates), which has a multitude of negative connotations as previously mentioned. The ability of bacterial zoonoses to effectively transmit antibiotic resistance genes to human

pathogens is poorly understood (largely owing to a lack of robust surveillance and epidemiological data). Nevertheless, the antibiotic reservoir created by the excessive, over-the-counter use of antibiotics in animal production is very much a threat to human health, as evidenced by the initial emergence of colistin resistance from a Chinese pig farm (which has now been documented in both clinical and agricultural samples [27,28]). As a consequence of their overuse, many antibiotics are no longer therapeutically effective (or indeed prophylactically effective) in controlling infection in livestock, thus last-resort antibiotics (used to treat resistant infections in humans), are used in the agricultural sector. The implications surrounding the use of medically important antimicrobials in the production of food animals has driven a call from the US Food & Drug Administration (FDA), to limit such use to therapeutic purposes only, under the supervision of licenced veterinarians [29]. Controlling the use of antibiotics outside of the clinic will be an important factor in retaining medical efficacy of the current treatment of bacterial infection.

Whilst the administration (including both appropriate and inappropriate use) and the dissemination of modern antibiotics has indeed fuelled the 'antibiotic crisis' as we know it, the acquisition of genetic elements inferring resistance to antibiotics (and the subsequent genetic mobility exhibited by bacteria), is not a new phenomenon. Studies have shown that the presence of antibiotic resistance genes predates modern, clinical use of antibiotics. Analysis of permafrost sediments dating back 30,000 years has identified ancient microbial DNA encoding resistance to β-lactam, tetracycline and glycopeptide antibiotics [30]. Furthermore, bacteria discovered in an isolated cave in New Mexico, devoid of any exposure to human activity for over 4 million years, have demonstrated resistance towards 14 commercially available antibiotics (the genetic and phenotypic presentation of resistance in keeping with modern variants) [31]. This research suggests that despite the modern selective pressure exhibited by the misuse of clinical antibiotics (whether this be overuse or under dosage), the future development of new antimicrobial drug compounds may in fact result in the inevitable selection of pre-existing resistance determinants, thereby limiting the effective lifetime of any new drug candidates. Based on the current trend, the average antibiotic encounters resistance within 2 years of marketing, and in some cases resistance is seen prior to clinical approval, for example in the case of tigecycline (likely as a result of structural similarities to tetracycline, of which tigecycline is a semi-synthetic analogue) [32,33]. Both the development of novel antibiotics/antimicrobials and the implementation of more effective treatment strategies must be globally prioritised in order to prevent a return to the pre-antibiotic era. The implications of a fast-approaching antibiotic void are vast, both in terms of treatment and prevention of infection. Certain surgical procedures would become unsafe and

otherwise easy-to-treat infections would prove fatal. Continuing on the current trajectory, it is estimated that by 2050 drug resistant infections will account for 10 million deaths worldwide (exceeding that of cancer), with a cumulative, global cost of antibiotic resistance exceeding $100 trillion (US) [16].

There are a number of factors affecting the clinical development of new drug candidates. The economic and regulatory issues governing the initial discovery, successful development and marketing of a new antibiotic are undoubtedly hindering investment from large pharmaceutical corporations. It has been estimated that the cost of bringing a new drug to market can reach $2.5 billion (US), and in the case of antibiotics; phase 3 development alone can reach $30 – 150 million depending on the nature of the infection. With this in mind, a standardised, numerical prediction of the net value of a new drug over a given time period, known as the net present value (NPV), must be evaluated against the risk of failure, in order to make any potential investment economically viable. Recent analysis has estimated the NPV of an antibiotic to be a negative value (up to -$50 million), predicting an overall financial loss upon market entry [26]. Antibiotics have a relatively low economic return compared to other more lucrative therapeutic areas, largely owing to their smaller contribution to the overall market value, thus the fine balance between the financial risk and the expected reward is an overwhelmingly unattractive venture for drug development companies.

Despite the stagnation in antimicrobial drug development in recent years, the emergence of multidrug resistant (MDR) bacterial pathogens (including those now resistant to last-resort antibiotics such as colistin, previously considered exempt from HGT [28]), is driving an urgent incentive for the establishment of global initiatives aimed at reviving antibiotic development. For example, the Innovative Medicines Institute (Europe) started the New Drugs for Bad Bugs campaign in 2013 [34], the UK initiated a Review on Antimicrobial Resistance in 2014 [16], the National Action Plan for Combating Antibiotic-Resistant Bacteria was released in the US in 2015 [35] and the WHO instigated the Global Action Plan on Antimicrobial Resistance [36]. Furthermore, the WHO has recently released a global priority list of antibiotic resistant bacteria, identifying the most important resistant bacteria for which urgent (new) treatment is sought. Of the two highest priority levels, nine bacterial species are classed as critical, and a further six are classified as high priority [37]. Alongside current interest in the discovery and development of new antibiotics, recent efforts are also aimed at the development of novel, alternative treatment options to be included in the 'antimicrobial arsenal' for use as single or adjunctive therapies alongside antibiotics.

3.1.2 Alternative Treatment of Infection

3.1.2.1 Alternative Drug Based Strategies

Alternative drug-based strategies aimed at controlling (and in some cases reversing) the presentation of antibiotic resistance in specific bacterial species and communities largely involve combination therapies; the administration of conventional antibiotics alongside additional small molecules, targeting certain features of the bacterial virulence machinery [38]. This may include efflux pump inhibitors (EPIs); small molecules which prevent cellular antibiotic expulsion associated with MDR. At least two broad-spectrum EPIs have been identified and extensively characterised (peptidomimetics and pyridopyrimidines), however there are no clinical EPIs currently approved for therapeutic use, owing to their high toxicity and a lack of understanding regarding their exact mechanism of action [39-41].

An alternative strategy involves the disruption of bacterial communication processes (quorum sensing). The ability of bacteria to communicate with one another has been implicated in both the onset of bacterial virulence and in the formation of biofilms (surface-bound communities of microbial cells protected and held in place by an exopolysaccharide (EPS) matrix). Disruption or quenching of these processes can be initiated via inhibition of the enzymes responsible for the synthesis of quorum sensing molecules. The antibacterial Triclosan works in this manner by inhibiting a key enzyme involved in the biosynthesis of acyl homoserine lactone (a primary quorum sensing mediator) [42]. In *Staphylococcus aureus* (*S. aureus*), the accessory gene regulator (agr) quorum sensing system regulates a number of key staphylococcal virulence factors (including enterotoxins, adhesins and exfoliative toxins) and as such, is considered an attractive target for the mediation of staphylococcal virulence [43]. The development of Savarin (a small molecule inhibitor, currently in preclinical development) successfully inhibited agr-dependent gene expression involved in dermonecrosis [44]. A key advantage in targeting bacterial communication processes is the limited effect on the development of resistance. Rather than affecting bacterial survival directly, quorum sensing inhibitors (QSIs), predominantly target virulence factors whilst acting synergistically with antibiotics. This is especially advantageous in the treatment of biofilms (which are notoriously difficult to penetrate using conventional antibiotics); QSIs can 'soften' a biofilm making it more susceptible to clearance via conventional drug therapy [45].

The development of resistance via the production of antibiotic inactivating enzymes, such as β-lactamases (which hydrolyse the β-lactam ring, destroying any antibiotic activity) and aminoglycoside modifying enzymes (which transfer functional groups to susceptible hydroxyl and amine moieties, again removing antibiotic activity), has also been the subject of significant investment into combating antibiotic resistance. One of the first examples of a clinically approved β-lactamase inhibitor is Clavulanic Acid. Exhibiting structural similarity to a traditional β-lactam antibiotic, Clavulanic Acid is a semisynthetic, suicide inhibitor (demonstrating competitive, irreversible binding), isolated from *Streptomyces*. Clinically administered alongside amoxicillin (co-amoxiclav), it inhibits enzymatic hydrolysis of the antibiotic, thus restoring antimicrobial efficacy. However, bacteria have subsequently evolved to produce previously unknown or rare β-lactamase enzymes which are largely unaffected by common β-lactamase inhibitors. Therefore the development of new and novel enzymatic suicide inhibitors is an ongoing strategy for many of the large pharmaceutical companies [46].

Attenuation of bacterial virulence and/or restoring the potency of existing antibiotics are two promising strategies aimed at increasing both the lifespan of current (and future) therapeutics, and reducing the development of antimicrobial resistance.

3.1.2.2 Bacteriophage

Alongside the development of additional drug based therapeutics, the use of biological antimicrobials has gained significant attention in recent years owing to the rise in global MDR. The use of biological entities to treat bacterial infection may encompass the development of antimicrobial viruses/ vaccines, enzymes, peptides or the administration of specific genetic material (such as genes aimed at reversing resistance). Of particular relevance to this thesis is the use of bacteriophage (phage) and phage-encoded endolysins. Phage (from the Greek *phagein*, meaning 'to eat'), are ubiquitous, predatory viruses of bacteria, outnumbering bacterial cells ten-fold. With an estimated environmental abundance of 10^{31}, phage provide a form of biological control, consistently regulating the global bacterial population [47].

'Officially' discovered in 1917 by Felix d'Herelle (the potential existence of antimicrobial viruses had been discovered independently by English bacteriologist Frederick William Twort in 1915 but was not pursued), phage were extensively studied in the former Soviet Union and Eastern Europe following their initial discovery [48]. One of the most prominent

institutions concerned with the therapeutic development of phage during this time (and is still very much in operation today), is the Eliava Institute in Tbilisi, Georgia. Established in 1923 by Giorgi Eliava (who was later executed by Stalin's secret police as a 'People's Enemy'), the Eliava Institute conducted a wealth of experiments into the therapeutic potential of phage treatment. Most notably, the prophylactic efficacy of phage to treat dysentery in children was evaluated in an extensive study in 1963/4 with over 30,000 test subjects included in the study [49]. Despite some promising initial findings from early experiments into phage therapy from the Eliava Institute and the Hirsfeld Institute in Wroclaw, Poland [50], parallel development of this potential new technology was absent in the Western world owing to the superior development of antibiotics. However, in light of the global dissemination of antibiotic resistance, coupled to a greater understanding of phage biology, there has been a scientific revival in phage-associated infection control. Advanced studies into phage therapy (to the point of human administration) were achieved the West in 2000 with the first phase I clinical trial published in the USA in 2009 [48,51].

Classification of phage (concerning the wide variation in viral morphology), is governed by the International Committee for Taxonomy of Viruses [52], a summary of the different families and their characteristics is presented elsewhere [53]. For the purpose of this thesis the most relevant is the *Caudovirales* order (which it is estimated that over 96% of phage belong), consisting of three distinct families: *Myoviridae*, *Siphoviridae* and *Podoviridae* [54]. The key features of this family of phage are double stranded, linear DNA, tailed particles (both contractile and non-contractile) and adhesion structures (baseplate and tail fibres/ spikes), as depicted in Figure 2 [55].

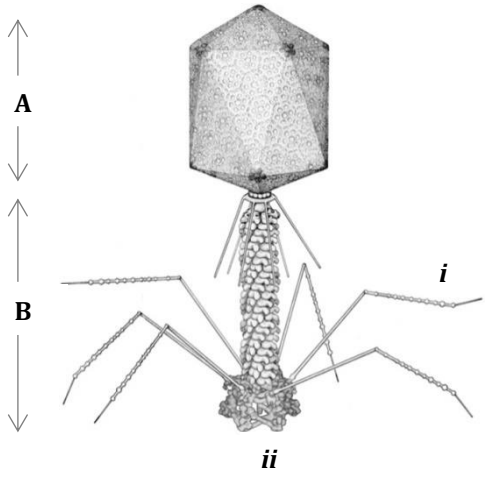

Figure 2 Representative structure of a tailed bacteriophage belonging to the *Caudovirales* order, consisting of (**A**) icosahedral head containing double stranded DNA, (**B**) sheathed tail comprising (***i***) multiple tail fibres and (***ii***) base plate. Adapted from [55]. Copyright © 2016 Yap *et al*.

There a number of key requirements and considerations associated with the use of phage as a biotherapeutic treatment option, including:

- Phage preparations should be fully characterised, including genome sequence and structure.
- The phage should be lytic (virulent) and non-transducing (discussed below).
- Phage-bacteria interactions should be understood, including the bacterial surface receptors required for phage adsorption.
- Animal models should be employed in order to confirm any *in vitro* efficacy.
- Phage preparations should be pure (i.e. have undergone lysate purification), and the preparation should conform to all safety and regulatory requirements [56].

Phage infect and replicate in the presence of bacteria in a number of different ways (depending on the nature of the phage), either they replicate via the standard viral infection cycle (lytic, resulting in bacterial lysis – as described in Section 3.2.4), or they can initiate a lysogenic, pseudo-lysogenic or chronic infection. Perhaps one of the most important considerations when prospecting phage for use as a therapeutic is the potential for transduction. Transduction originates during the lytic cycle, whereby certain phage demonstrate the ability to acquire fragments of bacterial DNA. During cell lysis the bacterial chromosome is cleaved into small segments which the newly assembling phage virions can mistakenly incorporate as opposed to, or in addition to phage DNA (owing to the low fidelity in bacteriophage DNA packaging) [57]. The resultant transducing phage are then able to infect further host strains and inject their genetic material (now containing bacterial DNA), which is incorporated into the host chromosome via recombination, yet is defective for replication of phage progeny (Figure 3 [58]). Whilst this mechanism relates to the lytic infection cycle, this phenomenon is relatively uncommon in lytic phage owing to the extensive degradation of the host genome during infection with virulent phage [59].

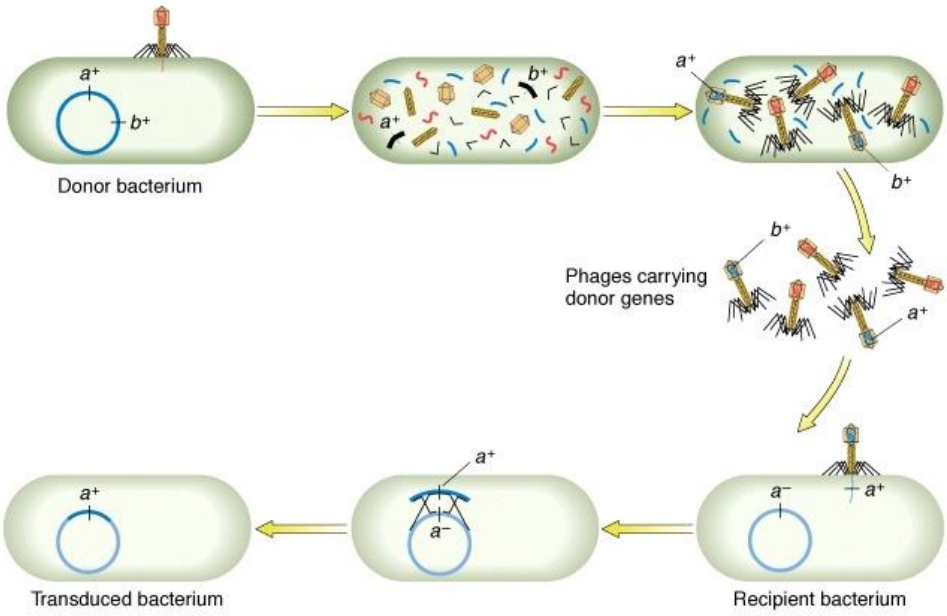

Figure 3 Schematic detailing the steps involved in transduction during the lytic phage infection cycle. Upon cell lysis phage acquire fragmented bacterial DNA (a^+/ b^+) from the donor bacterium. These donor genes may then be inserted into a recipient bacterium during phage infection, where they are incorporated into the bacterial genome via recombination, resulting in the formation of a transduced bacterium containing foreign bacterial DNA.

However, some phage (termed temperate) do not initiate the lytic infection cycle in the first instance, instead they inject their DNA into the host, which becomes incorporated into the bacterial chromosome as prophage, where it lies dormant in a latent state. During this time, the infected bacterium is resistant to further infection and the phage genome is transmitted through multiple bacterial generations at the point of cell division. This type of infection is referred to as lysogenic. It is possible for the viral prophage to become activated as a response to bacterial stress (such as DNA damage), in which case the lytic infection cycle is initiated. In this case, the prophage is excised from the bacterial chromosome and new phage virions are assembled according to the expression of lytic genes. Transduction can occur as a result of improper excision, resulting in the acquisition of neighbouring bacterial genes. Owing to the specific incision sites for the incorporation of prophage into the bacterial chromosome, temperate phage are only able to transduce specific host genes, this is referred to as specialised transduction, in contrast to generalised transduction (as previously described). The phage-assisted horizontal gene transfer of bacterial genes from one bacterium (donor) to another (transduced) can increase the virulence of the recipient, as a

result of the expression of gene products encoded by prophage during lysogeny. This has been demonstrated via the lysogenic conversion of multiple phage-encoding virulence factors including; diphtheria toxin, botulinum toxin, cholera toxin, certain staphylococcal virulence factors (such as enterotoxin A) and many more [60,61]. In light of the potential for phage to increase the fitness and survival of the bacterial host, it is therefore essential that temperate, transducing phage are eliminated from any potential therapeutic applications. Successful development of clinically relevant phage preparations has been demonstrated in a number of pre-clinical and clinical trials (discussed in Section 3.2.4).

3.1.2.3 Bacteriophage Endolysins

Whilst it is possible to source non-transducing, virulent phage, conforming to all safety and regulatory requirements for therapeutic application, perhaps a more convenient approach to antimicrobial therapy is the use of phage-encoded enzymes. This term may encompass depolymerases (involved in EPS breakdown) and lysins; ectolysins (responsible for peptidoglycan cleavage on the cell surface, assisting in phage DNA injection) and endolysins (responsible for intracellular peptidoglycan cleavage, facilitating the release of phage progeny) [62], the latter being the most relevant to this thesis. Devoid of any transducible genetic information, endolysins encoded by the phage genome are expressed during the late stages of the lytic infection cycle and are required for successful cell lysis. Despite the fact that phage endolysins are endogenous in their native form, they are also capable of achieving efficient bacterial lysis when applied extracellularly. Exhibiting the same specificity towards a bacterial host strain as the parent phage from which they are derived, endolysins are capable of causing rapid bacterial cell lysis and have thus far failed to initiate any form of bacterial resistance [63].

Endolysins are broadly categorised according to their structure as globular (consisting of a single catalytic domain), or modular (consisting of two or three domains including a catalytic domain and a cell wall binding domain, with or without an additional protein domain). As evolutionary advanced hydrolase enzymes, the specific activity of endolysins towards the peptidoglycan bacterial cell wall can be attributed to either; cleavage of the glycosidic linkages (glycosidases and transglycosidases), or cleavage of the peptide cross-bridges (amidases and endopeptidases) [64], the specific target sites are shown in Figure 4 [65,66]. A review detailing a number of different phage-encoded endolysins and their mechanism of action is published elsewhere [67].

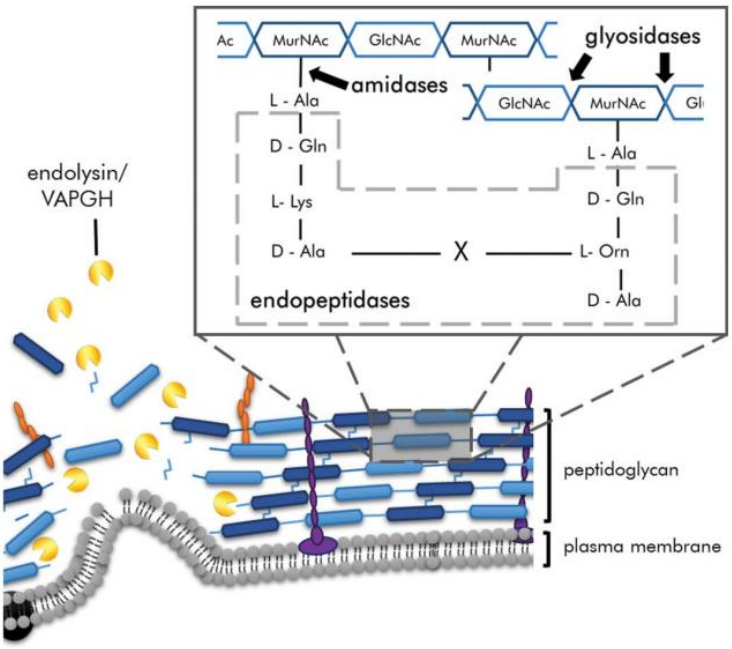

Figure 4 Schematic illustrating the peptidoglycan cell wall consisting of alternating sugar units: *N*-acetylmuramic acid (MurNAc) and *N*-acetylglucosamine (GlcNAc), crosslinked via peptide cross-bridges. The schematic highlights the various target sites of phage-encoded endolysins/ virion-associated peptidoglycan hydrolases (VAPGH). Reproduced from [66].

3.1.3 Therapeutic Delivery Systems

Both whole phage and phage-encoded endolysins have demonstrated significant potential in the clinical treatment of infection [62]. However, certain applications require an effective delivery system in order to protect and control the release of the therapeutic cargo. In addition to the specifications required for any bioactive compound/therapeutic agent, such as favourable ADMET parameters (Adsorption, Distribution, Metabolism, Excretion and Toxicity), all of which must be critically evaluated and optimised at the preclinical stage, the delivery vector must also conform to all current safety and regulatory requirements [68,69]. Some of the crucial factors governing the clinical success of a drug delivery system include biocompatibility, mechanical stability, degradation pathways and manufacturing cost [70].

The nature of the delivery system can have a significant effect on the properties of the therapeutic agent; this is especially relevant in the case of biological therapeutics. The delivery system may enhance or reduce clinical efficacy of the biological cargo, with respect

to crucial considerations such as biodistribution, pharmacokinetics or pharmacodynamics. For example, certain polymeric formulations can increase the exposure of therapeutic proteins, reducing the frequency of administration, thus potentially increasing patient compliance. On the other hand, fusion proteins (consisting of an antibody fused to a therapeutic protein), aimed at increasing the serum persistence of the therapeutic agent, have shown potential immunogenic properties [71]. A comprehensive review of past, present and future delivery technologies for a range of drug and therapeutic agents has been conducted by Tibbitt *et al* [72]. The following Section details specific strategies employed for the therapeutic delivery of phage and phage-encoded endolysins. This review aims to provide the theoretical reasoning and key considerations involved in the thermally triggered release of both phage and antimicrobial endolysins (as presented in the succeeding Chapters).

3.2 Publication

3.2.1 Declaration of Authorship

<table>
<tr><td colspan="10">This declaration concerns the article entitled:</td></tr>
<tr><td colspan="10">Recent Advances in Therapeutic Delivery Systems of Bacteriophage and Bacteriophage-Encoded Endolysins</td></tr>
<tr><td colspan="10">Publication status (tick one)</td></tr>
<tr><td>Draft manuscript</td><td></td><td>Submitted</td><td></td><td>In review</td><td></td><td>Accepted</td><td></td><td>Published</td><td>✓</td></tr>
<tr><td>Publication details (reference)</td><td colspan="9">Hathaway, H., Milo, S., Sutton, J. M. & Jenkins, A. T. A. Recent advances in therapeutic delivery systems of bacteriophage and bacteriophage-encoded endolysins. Therapeutic Delivery 8, 543-556, doi:10.4155/tde-2017-0040 (2017).</td></tr>
<tr><td>Candidate's contribution to the paper (detailed, and also given as a percentage).</td><td colspan="9">The candidate predominantly executed the…

Formulation of ideas: N/A
Design of methodology: N/A
Experimental work: N/A
Presentation of data in journal format:
Review was structured and written predominantly by the candidate (90%) with part written by second author (10%) and proof read by additional authors.</td></tr>
<tr><td>Statement from Candidate</td><td colspan="9">This paper reports on original research I conducted during the period of my Higher Degree by Research candidature.</td></tr>
<tr><td>Signed</td><td colspan="5">  </td><td>Date</td><td colspan="3">29.09.17</td></tr>
</table>

3.2.2 Copyright Agreement

This is a License Agreement between Hollie Hathaway ("You") and Future Science Ltd ("Future Science Ltd") provided by Copyright Clearance Center ("CCC"). The license consists of your order details, the terms and conditions provided by Future Science Ltd, and the payment terms and conditions.

License Number	4133580245818
License date	Jun 21, 2017
Licensed content publisher	Future Science Ltd
Licensed content title	Therapeutic delivery
Type of Use	Thesis/Dissertation
Format	Print, Electronic
Title or numeric reference of the portion(s)	Recent advances in therapeutic delivery systems of bacteriophage and bacteriophage-encoded endolysins
Author of portion(s)	Hollie Hathaway
Publication date of portion	21 June 2017
The requesting person/organization is:	Hollie Hathaway, University of Bath
Author/Editor	Hollie Hathaway
Title of New Work	Biomodification of Abiotic Surfaces for the Prevention of Hospital – Associated Infection
Publisher of New Work	University of Bath
Expected publication date	Oct 2017

3.2.3 Data Access Statement

This is a review article, and therefore all data underlying this study is cited in the references.

3.2.4 Published Article

Recent Advances in Therapeutic Delivery Systems of Bacteriophage and Bacteriophage-Encoded Endolysins

Hollie Hathaway[1*], Scarlet Milo[1], J. Mark Sutton[2], A. Toby A. Jenkins[1]

1. Department of Chemistry, University of Bath, UK, BA2 7AY
2. Technology Development Group, Public Health England, Porton Down, UK, SP4 0JG

*Corresponding Author: Email: holliejanehathaway@gmail.com, Tel: +44 (0) 1225 385100

Abstract

Antibiotics have been the cornerstone of clinical management of bacterial infection since their discovery in the early 20th century. However, their widespread and often indiscriminate use has now led to reports of multidrug resistance becoming globally commonplace. Bacteriophage therapy has undergone a recent revival in battle against pathogenic bacteria, as the self-replicating and co-evolutionary features of these predatory virions offer several advantages over conventional therapeutic agents. In particular, the use of targeted bacteriophage therapy from specialised delivery platforms has shown particular promise owing to the control of delivery location, administration conditions, and dosage of the therapeutic cargo. This review presents an overview of the recent formulations and applications of such delivery vehicles as an innovative and elegant tool for bacterial control.

Key Words: Bacteriophage, Endolysin, Encapsulation, Immobilisation, Stimuli-Responsive, Controlled Release, Complexation, Delivery System

Introduction

Following the discovery of penicillin in 1928 by Alexander Fleming and the subsequent development of modern antibiotics, the World has enjoyed a period of relative safety from the threat of bacterial infection. However, Fleming himself was discerningly cautious about the potential of modern antibiotics to keep this threat at bay, going on to describe the possibility of developed resistance in his 1945 Nobel lecture detailing the dangers of

"underdosage" [73]. This predicted evolution of multidrug resistant bacteria, and the subsequent decline in the production of novel antibiotics has driven a resurge of interest in the once forgotten viral therapies of the Eastern Bloc countries. Bacteriophage (phage) have been developed for therapeutic use since their discovery in the early 20th century, dominating antimicrobial treatment in the East where the antibiotic panacea failed to translate as effectively [74,75]. As ubiquitous predators of bacteria, phage exist in the biosphere alongside their host, continuously engaged in a biological game of cat and mouse, resulting in an estimated 50% reduction in the global bacterial population every 48 hours, arising from phage predation alone [76]. Phage propagate in bacteria through lytic development or lysogenic replication (Figure 5) [77]. For use as therapeutic agents, lytic phage (incapable of lysogenic infection and more potent than temperate phage) are identified by phenotypic and structural characterisation as well as genetic sequencing, in order to avoid any possible genetic transfer events, such as transduction.

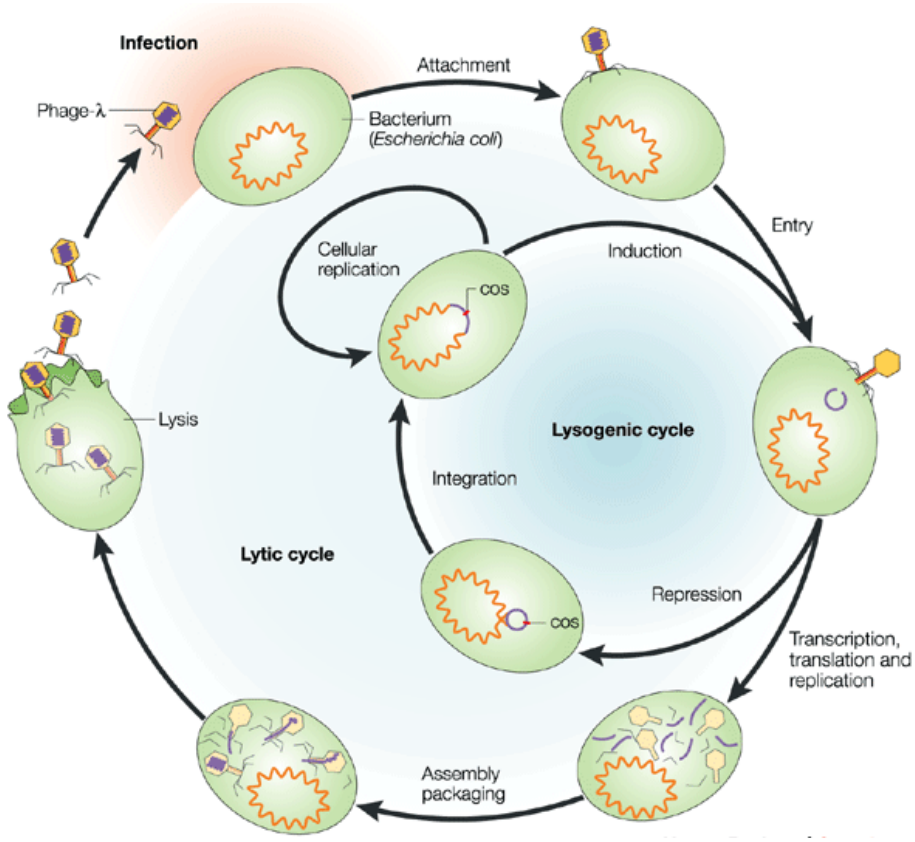

Figure 5 Standard viral replication cycles of bacteriophage. The closure of the newly formed circular DNA and corresponding cohesive site is denoted 'cos'. Reprinted by permission from Macmillan Publishers Ltd: Nature Reviews Genetics [77]. Copyright ©2013.

As host specific infectious agents, phage have been investigated as a form of bacterial biocontrol, with a range of applications in the medical, agricultural and biotechnology industries [78-81]. Owing to their high natural abundance, phage are relatively easily sourced and have been successfully isolated from all ecological environments in which bacteria are also present [82]. When used in combination as a *phage cocktail*, they are able to infect and destroy a multitude of bacterial species including both Gram-positive and Gram-negative strains. These self-replicating virions are also active against antibiotic resistant isolates such as *Pseudomonas aeruginosa* (*P. aeruginosa*), a multidrug resistant pathogen associated with a range of infectious diseases [83]. There have been a number of phage based products approved by the FDA within the agricultural sector including; ListSheild™ for use on ready to eat meat, seafood and food contact surfaces, SalmoFresh for poultry, fish and fruit and vegetables, EcoShield for red meat and LISTEX™ for meat, fish and cheese [84]. However, there are currently no licenced bacteriophage or bacteriophage derived products approved for human therapeutic use in the EU or the USA.

The need for regulated clinical trials and compliance with current manufacturing guidelines is a major complication in the implementation of sustainable phage therapy. The reliability of early studies from previously inaccessible countries (such as those within the former Soviet Union), have since been called into question based on factors such as lack of blinding and co-administration with antibiotics during early experimental therapy [85]. However in response to the ever-pressing requirement to develop new and more effective antimicrobials, the development of phage based products has recently seen some promising pre-clinical results, with a number of clinical trials underway. PhagoBurn (Trial Number NCT02116010 [86]), funded by the European Union is currently undergoing phase I/II trials utilising a phage cocktail to treat burn wound infections with results expected in March/April 2017. AmpliPhi Biosciences have a phage product AB-SA01 (Trial Number NCT02757755 [87]), active against *Staphylococcus aureus* (*S.aureus*) entering into phase II trials for the treatment of both chronic rhinosinusitis and bacterial skin infection. Previous clinical trials adhering to modern protocols have also seen success in the treatment of a range of infections, including venous leg ulcers, otitis and reduction of bacterial load in the nasal carriage [51,88,89]. In addition to regulatory and clinical requirements, the pharmacokinetics (PK) and pharmacodynamics (PD) of phage therapy must be considered. The administration of an antimicrobial at the site of infection must be both timely and in sufficient concentration to elicit a response, thus avoiding effects such as sub-lethal dose administration (with associated resistance development), immune response/ clearance, and diffusion limitations [90]. The physiological stability of such biological entities must be maintained during treatment, including the

prevention of neutralization (by antibodies or other such compounds), and protein degradation via localised environmental conditions [91]. The trials described above all focus on topical application of phage. One of the outstanding questions regarding their suitability for treatment of a wider range of infections is their suitability for systemic delivery. To be able to apply the phage distant to the site of infection necessitates a greater understanding of the clearance of phage from the body and strategies to maintain an effective concentration long enough for phage attachment to the pathogen and subsequent infection and amplification. Both the innate and adaptive immune system have a role in reducing the level of circulating phage. This has been discussed in detail recently and is outside of the scope of the current review [78]. This is likely to be a key determinant of therapeutic efficacy, but a number of the encapsulation and delivery methods described below also help to reduce immune clearance as well as enhancing other aspects of PK/PD. Therefore, the development of suitable delivery vehicles has received considerable attention recently in order to improve and maintain the pharmacological properties of therapeutic phage products *in vivo*.

A range of techniques have been employed in recent years utilizing various technologies (encapsulation, immobilization, conjugation etc.) to successfully exploit bacteriophage for a number of applications including; sensing and detection of infection, bacterial capture and phage-assisted delivery of therapeutic cargo [92-97]. The bacterial acquisition of specific genes via phage guided delivery, using CRISPR-Cas technology, for sensitization of previously drug resistant bacterial isolates [98,99], and the delivery of genes expressing novel antibacterial agents (SASPject; [100]) has demonstrated the versatility and extent to which phage have the potential to be utilized in modern medicine. This review will focus on the current advancements in delivery systems capable of housing phage for the specific therapeutic purpose of treating bacterial infection, with particular emphasis placed on the stabilisation and protective strategies required.

Encapsulation

The successful administration of a therapeutic agent to a target site often depends on a suitable delivery vehicle to ensure it reaches the infection site. An example of this is pulmonary delivery; an area in which phage have received considerable attention in recent years, owing to the increase in multidrug resistance amongst bacterial isolates, including those associated with pneumonia and tuberculosis. *Klebsiella pneumoniae* (*K. pneumoniae*) is a major cause of nosocomial pneumonia, especially amongst immunocompromised patients with reported mortality rates as high as 60% [101]. Whilst previously considered an

extracellular pathogen, this Gram-negative bacterium has shown the ability to become internalised *in vivo* by certain cell types including lung epithelial cells [102]. Therefore, effective treatment requires intracellular access, a concept referred to as the 'Trojan horse' approach, relying on a suitable vector to transport phage across the eukaryotic cell membrane, delivering the antimicrobial cargo directly into the infected cell. The ability of bacteria to colonise intracellularly, serving as a reservoir of infection and the inability of phage to enter myeloid cells, has previously rendered phage therapy ineffective for certain conditions. However the use of lipid-based carriers as a means of transportation across the cell membrane may offer the possibility of phage as a viable treatment option. Liposomal entrapment of the fully characterised lytic phage KPO1K2 appears to provide enhanced intracellular uptake into phagocytic cells in order to target engulfed *K. pneumoniae* present within macrophages. In the case of encapsulated phage, ~95% of the intracellular bacteria was eradicated within 24 hours compared to no significant difference in intracellular bacterial content using free phage (Figure 6) [103].

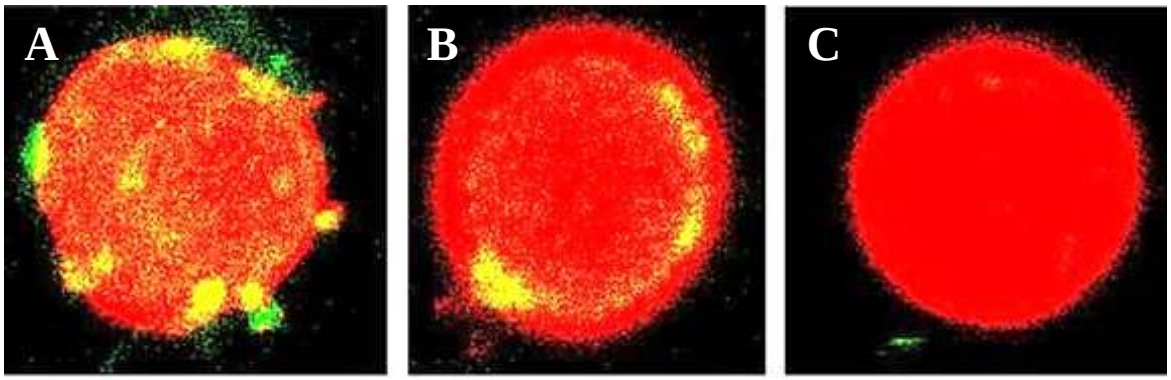

Figure 6 Confocal micrograph showing intracellular bacterial content using Live/Dead fluorescent staining **A)** Untreated macrophages, showing intracellular bacteria in yellow **B)** Infected macrophages treated with free phage, but with intracellular bacteria still evident **C)** Liposome treated macrophages with apparent intra cellular eradication of bacteria. Figure adapted from [103].

Liposomal entrapment has also been utilized for the potential intracellular treatment of tuberculosis via successful encapsulation of the mycobacteriophage TM4 or the reporter bacteriophage λeyfp into giant unilamellar vesicles (GUVs), by a variety of preparation techniques. Enhanced uptake into eukaryotic cells (THP-1 macrophages) was seen with encapsulated phage compared to free phage, and no sign of mechanical damage to the liposome was observed as a result of phage encapsulation [104].

Encapsulation of phage for the purpose of treating pulmonary-associated infection has shown additional benefits in terms of neutralisation protection. Cationic liposomal entrapment appears to offer a protective barrier from which phage are able to evade anti-phage antibodies. Antibodies produced by the mammalian immune system in response to phage therapy have shown the potential to render phage inactive, a problem which appears to be dependent both on the type of phage used and the delivery route chosen [105]. Liposome encapsulated phage (active against *K. pneumoniae*) incubated alongside bacteriophage antibodies from mouse serum, experienced complete protection from any degradative effects, whereas unencapsulated phage appeared to undergo complete neutralisation, with no active phage particles remaining after 3 hours incubation *in-vitro* [103].

Moreover, previous studies have shown that the efficacy of phage therapy in animal models is effective only after almost immediate administration post infection, whereas liposome entrapped phage appear to retain antibacterial activity against pulmonary associated infection even when treatment is delayed for up to 3 days post infection [106]. Furthermore, liposomal encapsulation of phage has demonstrated a greater degree of bio-distribution and bio-retention compared to free phage. This has been shown in *in vivo* experiments via the inoculation of mice with both free phage and phage encapsulated within phospholipid vesicles. Encapsulated phage were present at higher peak levels and concentrations were maintained longer, declining after 12 hours for encapsulated phage compared to 6 hours for free phage. Phage remained detectable for up to 4 days in blood, 6 days in the liver, lungs and kidney, and up to 14 days in the spleen following a single intraperitoneal injection, compared to undetectable levels after 48 hours in all four organs when using free phage (aqueous suspension) [107]. The maintenance of maximal concentration and length of persistence of phage in the circulation observed in this study, suggests that systemic treatment may be possible using such approaches.

Nanoemulsions consisting of phage within the aqueous core of a lipid suspension (water-in-oil-in-water), have gained attention, owing to the enhanced functional and structural stability of the entropically confined phage encased within such micelles. A positive correlation has been seen between the fatty acid chain length of the lipid micelle and the emulsion stability, manifested as an overall long term stability of up to 3 months at room temperature [108]. Alongside an increase in shelf life, the use of nanoemulsions has previously shown higher infectivity rates of bacteriophage when compared to aqueous phage suspensions, possibly as a result of the elimination of electrostatic repulsions between the negatively charged phage and bacteria [109,110].

Encapsulation of phage and the resulting protective effect has been exploited in the targeted delivery of bacteriophage K (active against *S. aureus*) to the intestine via oral delivery. Ensuring the successful delivery of phage (or any biological therapeutic) through the gastrointestinal (GI) tract relies on a protective strategy to prevent inactivation by stomach acid, an issue previously encountered with other encapsulation formulations, with detrimental effects observed as a function of microsphere size (<100 μm) and possible acid diffusion into the microspheres [111]. The utilisation of a microsphere delivery system consisting of alginate microspheres co-encapsulating calcium carbonate and phage K has shown to provide a more robust protective effect against simulated GI fluid than alginate microspheres alone. Moreover, the addition of protective additives such as maltodextrin (up to 20% w/v) to the microcapsules has shown to increase the viability of phage K after drying, thus allowing for dry form encapsulated phage preparation [112]. This was further investigated using alginate-whey protein microspheres with maltose as a protective agent against dehydration effects. The encapsulated phage K exhibited enhanced stability after drying, likely as a result of the high glass transition temperature of the disaccharide: preventing denaturation by alteration of the protein dynamics through physical confinement. In addition to any benefits offered by dry formulations in this instance (ease of storage, transport and administration), dry powders containing phage exhibited storage stability at both 4 °C and 23 °C with over 80% of the encapsulated phage retaining viability at the higher temperature after two weeks [113]. Similarly, *Escherichia coli* (*E. coli*) O157:H7 bacteriophage have been successfully encapsulated in chitosan-alginate microspheres, demonstrating stability and sustained release under simulated gastric conditions at pH 2 and 2.5. This has potential applications in the treatment of gastroenteritis infections such as haemorrhagic colitis [114].

Immobilisation

The surface anchoring of biological entities with retention of their original function can be problematic owing to conformational changes in tertiary protein structure (denaturation) and changes in water content caused by the binding of proteins and protein ensembles to what are often rigid supports. However, the therapeutic use of phage may require immobilisation on abiotic surfaces (such as medical devices including stents, tracheal tubes, catheters etc.) since such devices are particularly prone to bacterial biofilm formation: the ability of bacteria to colonise surfaces, forming dense and often impenetrable biofilms. A recent method targeted at successful phage immobilisation, has utilized plasma-associated activation of polytetrafluoroethylene (PTFE) and ultra-high molecular weight polyethylene (PE). Low temperature plasma treatment of such polymers created reactive acid groups

which were used as anchor points for phage attachment. Such immobilised phage retained activity against both *E. coli* and *S. aureus* despite confinement at the surface. Figure 7 shows the steps involved in amide formation and subsequent phage attachment. Furthermore, the surface-bound phage retained bactericidal activity for several months under specific conditions (high humidity/ aqueous environment) [115]. This technology demonstrates the potential of phage-coated surfaces as potent antimicrobial interfaces capable of targeting important human pathogens, with the potential to prevent biofilm formation.

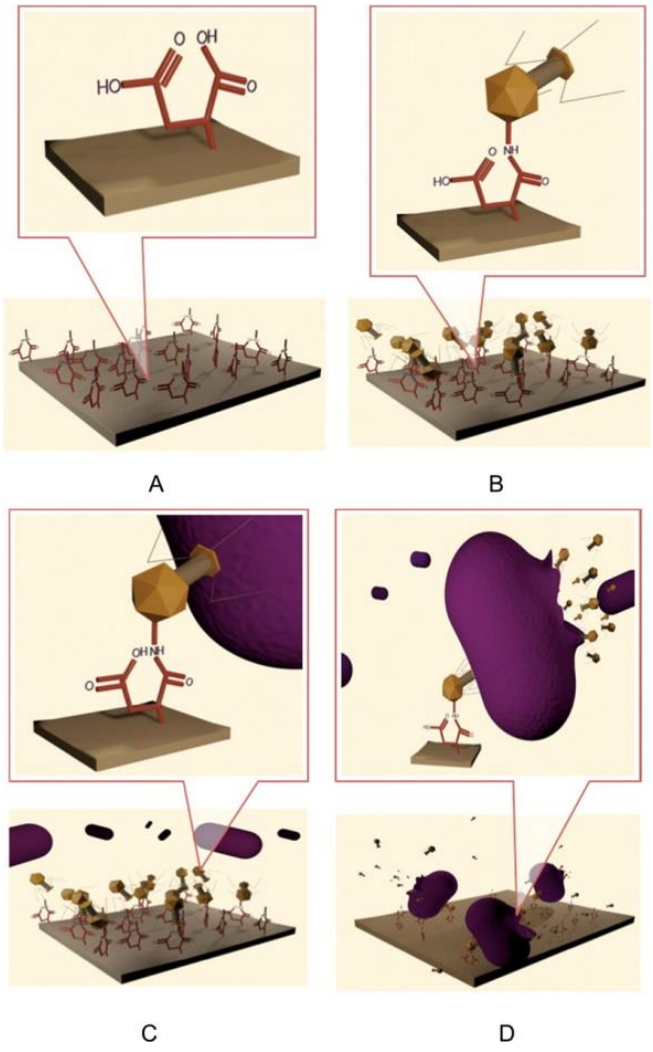

Figure 7 Steps involved in phage anchoring for the prevention of bacterial adhesion and biofilm formation. **A)** Plasma mediated formation of surface acid groups **B)** Phage attachment via amide bond formation **C)** Phage capture of bacterial cells **D)** Bacterial lysis post phage infection. Reprinted with permission from [115]. Copyright © 2013 American Chemical Society.

There are additional examples in the literature of successful phage binding to surfaces for purposes other than therapeutic treatment such as biosensors, bacterial capture platforms and antimicrobial coatings for food packaging [116-118]. Optimizing the parameters for successful phage immobilisation in terms of surface density, orientation, infectivity and stability is paramount in the development of any phage-based surface platform. Once established, this technology has the potential to be utilized for a range of applications, including antibacterial coatings and surfaces for therapeutic use.

Polymeric Formulations

Inactivation of phage as a result of environmental factors such as temperature, pH and UV is a major hurdle in the development of phage therapy, affecting both delivery route and stability. Phage-polymer ensembles have been shown to offer beneficial effects in terms of protein stability with respect to external conditions, offering the possibility of efficient storage and therapeutic use of phage for the treatment of infection. An example of this is the use of the naturally occurring polymer, poly-γ-glutamic acid (γ-PGA). Whilst the mechanism behind the protective effect is not yet fully understood, even in very low concentration ~1%, this biodegradable polymer has shown to effectively protect two different *E. coli* phage, MS2 and T2 (from the Leviviridae and Myoviridae families respectively), against temperatures of up to 60 °C, possibly as a result of physical protection of the viral particles. Protection against UV exposure was also seen with γ-PGA formulated phage, again possibly as a result of physical protection or refraction of the radiation. In the case of the T2 phage, a significant increase in survival rate was seen at a range of pH values via polymer stabilisation [119]. This is likely due to the pH sensitive nature of the polymer itself, which undergoes a conformational change at low pH where it exists in an alpha-helical conformation, potentially encasing the phage and protecting it from the acidic environment. γ-PGA exists in a linear random-coil conformation at neutral pH, hence the protective effects at higher pH are still poorly understood. However, further research may provide enhanced techniques for the protection of phage, with implications for both delivery and storage conditions.

Naturally occurring polymers such as proteins have shown potential to stabilise vaccine formulations, a concept which would have significant implications for the transportation and successful administration of human vaccines, especially in the developing world. Long term stability in elevated temperatures would drastically improve the often unreliable and expensive 'cold chain' transportation network required to distribute global immunisation treatment [120]. Building on this concept, recent efforts have taken the same approach using silk

proteins to stabilise phage against high temperatures, showing greater efficacy in protective effects when compared to a non-silk protein (bovine serum albumin). Results obtained showed 100% loss of viable phage in the absence of protein after one day incubation at 37°C, whereas the addition of various silk proteins (honeybee, hornet and silkworm), resulted in a maximum loss of 6% viable phage (Figure 8A). Indeed, the use of honeybee silk significantly enhanced phage survival even at 50 °C for up to 8 weeks (Figure 8B) [121]. A suggested reason for this is the increase in favourable protein-protein interactions, in preference of water-protein interactions within the hydration shell surrounding the phage.

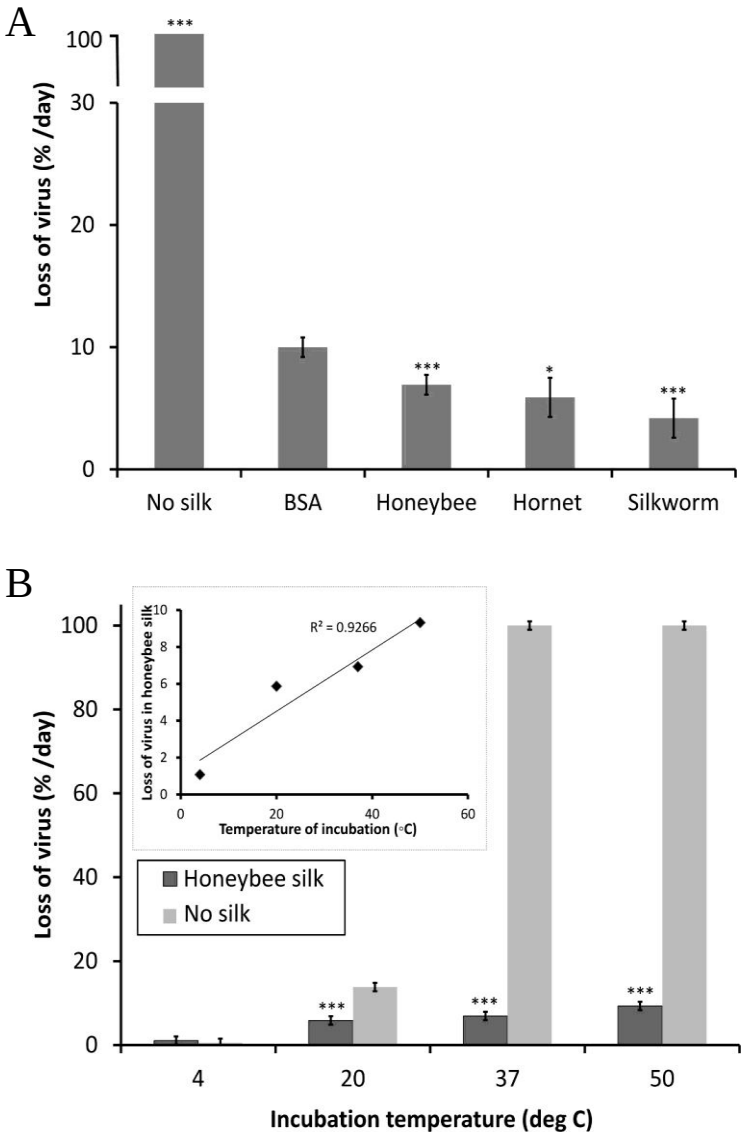

Figure 8 Loss of viral infectivity as a function of protein addition. **A)** After incubation at 37 °C with and without different proteins **B)** After incubation at various temperatures alongside honeybee silk. Inset highlights the correlation between viral viability and incubation temperature. Adapted with permission from [121]. Copyright © 2014 American Chemical Society.

Aerosol Formulations

Nebulization of drug formulations is a common methodology for the delivery of pharmaceutics and biopharmaceutics for inhalation directly to the lung. Patients suffering from cystic fibrosis (CF) are of particular concern, owing to their high susceptibility to infection. The administration of aerosolized phage via nebulization has previously been employed in a mouse model to evaluate the efficacy of phage therapy against a group of opportunistic pathogens: *Burkholderia cepacia* complex (BCC) organisms, capable of infecting immunocompromised patients. The results obtained showed a significant reduction in bacterial load within the lungs of immunocompromised and BCC infected mice (in some cases comparable to conventional antibiotics), using a range of different phage with varying multiplicities of infection (MOI) [122]. Further investigations into the use of nebulization as a delivery system for phage treatment has focused on *P. aeruginosa*, another common pathogen associated with CF, capable of causing respiratory failure in up to 95% of patients [123]. In this case, it was determined that the amount of phage delivered to the infection site which, for an infection such as this, concerns the lower respiratory tract, the choice of nebulizer also plays a significant part. It was concluded that a jet nebulizer is most effective, as 12% of the phage contained within particles and placed within the nebulizer, were small enough (< 4.7 μm) to be inhaled into the lower lung whilst retaining viability [124].

Another important consideration in the development of any therapeutic system is the potential for scale-up operations. In order to establish a viable delivery system, one must take into consideration a number of different factors including cost, feasibility of application, convenience and downstream processing steps. Whilst nebulization has shown promising results in terms of successful delivery, there are some concerns surrounding the expense and the complexity in the procedures associated with their use outside of the clinic (i.e. in a patient's home). As a potential alternative, recent efforts have focused on dry powder inhalers (DPIs), as a means of delivering phage in order to combat respiratory infection. Compared to nebulizers, DPIs are small, cheap, easy to operate and have been shown to successfully deliver a wide range of pharmaceuticals [125]. Aerosolized powders containing bacteriophages KS4-M and ϕKZ, targeting both BCC and *P. aeruginosa* respectively, demonstrated successful stabilisation of the lyophilized phage alongside retention of viability utilising a 60: 40 w/w matrix of lactose/lactoferrin [126].

In addition to freeze dried formulations for use in DPIs, spray drying has been investigated for pulmonary delivery of phage as it is a less energy intensive process and requires fewer

downstream processing steps. Using atomization as a potentially scalable process, two morphologically different phage, *Pseudomonas* phage LUZ19 and *Staphylococcus* phage Romulus, were successfully formulated into respirable powders in the presence of various excipients in order to protect the phage. Of those investigated, trehalose was found to be most effective in terms of protective effects, demonstrating increased stability at low temperature (4 °C). However, further investigation into thermal stability showed a pronounced effect on phage viability at higher temperature (25 °C) and high humidity. This is likely as a result of crystallization of the trehalose-phage amorphous matrix, thus highlighting the importance of suitable storage conditions of powder formulations containing phage particles [127]. In addition, the formation of phage-containing particles with the correct size parameters suitable for pulmonary delivery (between 1 and 5 μm) was found to be dependent on the type of phage, as previously postulated. Romulus-containing powders exhibited a higher percentage of suitably sized particles, when compared to podovirus LUZ19-containing particles. In contrast, the reduction in phage titre post spray drying (even in the presence of stabilising agents) was higher for Romulus phage (>2.5 log reduction), compared to LUZ19 (<1 log reduction), possibility as a consequence of shear stress on the long tail structure of the myovirus Romulus [128]. Therefore, the utilisation of dry powder phage therapy for treatment of pulmonary infection must rely on a compromise between particle size and phage survival, a fine balance which is evidently phage specific and very much dependent on production and storage conditions.

Stimuli-Responsive Systems

Alongside the stability and release-location of bacteriophage, the release-kinetics from the delivery matrix must also be considered. Stimuli-responsive systems should remain kinetically silent, unless a 'burst release' of the therapeutic agent is initiated in response to an external stimulus (e.g. temperature, pH, light, ultrasound or biomarker signals). Thereupon, adequate dosage of the antimicrobial is rapidly delivered to the correct physiological location in response to a successful bacterial infection. By avoiding systematic dosage of the often delicate biological cargo, triggered phage release systems can in principle avoid reduction in viable phage count commonly associated with exposure to biological fluids/ temperature fluctuations [129]. Moreover, triggered release systems can help ensure bacterial pathogens are not exposed to sub lethal doses of phage, making the phage more effective and slowing evolution of bacterial resistance.

Triggered-release phage systems are being developed with the potential for treatment of wound infection. Such systems are designed as modifications of existing wound dressing materials such as non-woven polymers, in order to incorporate stimuli-responsive phage delivery systems. One such system employs the thermally responsive polymer poly(*N*-isopropylacrylaminde) (PNIPAM), which undergoes a reversible, temperature-dependent phase transition at the lower critical solution temperature (LCST), manifesting as an unambiguous change in polymer volume. Control of the LCST was established via formulation with allylamine (ALA), allowing the system to undergo a transitional collapse at 34 °C. Impregnation of PNIPAM-co-ALA nanospheres with *S. aureus* phage K, and subsequent grafting to a non-woven polypropylene 'dressing' was achieved via amine coupling to plasma deposited maleic anhydride. Utilising the proximity of the polymer's morphological change to healthy skin temperature (32 °C), thermally-triggered release of phage K from the nanospheres was engineered to occur in response to infected skin, which often displays an increase in skin temperature as large as 3.6 °C. Incubation of phage-loaded nanospheres with *S. aureus* ST228 showed release of the phage cargo and subsequent cell lysis at 37 °C, whilst the bacterial lawn remained confluent at temperatures associated with healthy skin [130].

In addition to secondary physical stimuli, primary biomarker signals have been utilised to trigger the release of phage K for the treatment of infected skin wounds. Hyaluronidase (HAase) is an important virulence factor known to be secreted by pathogens associated with skin infection, including *S. aureus*. Degradation of hyaluronic acid (HA) in the skin by HAase is thought to aid bacterial invasion of tissue via cleavage of the β-1,4 position in HA, hence allowing the enzyme to act as a spreading factor within the process of bacterial pathogenesis [131]. A HA/HAase system has been developed comprising of a dual-layered hydrogel matrix which allowed HAase to trigger release of phage K for treatment of pathogenic skin infection [132]. Photo-cross-linked HA methacrylate (HAMA) hydrogels were used to cap and seal a lower reservoir layer of phage K containing agarose hydrogel. Clear visual signs of enzymatic degradation and subsequent phage release (ca. 10^5 PFU/ml) were observed when incubated with the supernatant of a wide range of *S. aureus* isolates. Both aforementioned examples of the incorporation a bacteriophage delivery system to a dressing platform exemplify the potential for future phage therapy, where phage virions are incorporated into a compatible carrier matrix.

Examples of photo-responsive systems utilizing bacteriophage, either within a 3 dimensional supramolecular hydrogel for cell culture and release [133], or in the derivation of a virus-like particle (VLP) for the photocaged delivery system of the anticancer drug doxorubicin [134],

demonstrate the wide-reaching applications of stimuli-responsive phage technologies. In particular, release systems based on VLPs have made a promising start within biomedical research for both diagnostic and therapeutic roles [135]. As the recombinantly expressed and non-infectious structural analogues of virus particles, VLPs still possess native viral recognition elements. When appropriately functionalised, the clinical tunability of such particles allows them to act as candidates for a multitude of medical purposes, including drug delivery applications and tumour imaging.

Bacteriophage Endolysins

In addition to using whole phage as a potential alternative to conventional antibiotics, there has been recent interest in using phage derived products, specifically endolysins as therapeutics. Encoded by the phage genome, these small molecules are transcribed and synthesised within the bacterial host's cytoplasm following phage infection. They are then translocated through the cytoplasmic membrane during the late stage of the infection cycle and are responsible for breaking down the bacterial cell wall, thus facilitating the release of the newly formed phage virions from the infected cell [136-138]. The primary benefit of using endolysins as opposed to whole phage lies with the elimination of genetic material from the therapeutic, thus eliminating the possibility of any genetic transfer events previously demonstrated with certain temperate phage [139]. Whilst bacteriophage undergoing consideration for medicinal use are incapable of such transduction, removal of phage genes entirely may help to subdue any concerns surrounding the opening of 'Pandora's Box' in terms of encouraging any phage assisted genetic mobilization. This may also help to speed regulatory acceptance of these new therapeutics. Furthermore, there are currently no identified resistance mechanisms towards phage lysins, indicative of the highly conserved, essential bacterial cell wall target sites of the phage-encoded enzymes [140]. Unlike many antibiotics, lysins are specific in their target bacterial strain and have shown the ability to eliminate staphylococcal biofilms including persister cells (dormant, drug tolerant variants) [141-143]. The primary disadvantage of using lysins compared with whole phage is that they are not amplified in the host cell, thus larger doses are required for antimicrobial effect.

A number of different endolysins have been isolated, characterised, and produced recombinantly, demonstrating lytic activity against a range of bacterial species (including *Acinetobacter baumanni*, *Bacillus anthracis* and *Streptococcus pyogenes* [144-147]). Owing to the specific advantages over whole phage therapy, there is currently an endolysin based medical device registered for human use. Staphefekt™, marketed by Micreos consists of an endolysin

active against *S. aureus* which can be used on intact skin for the treatment of conditions such as eczema, acne, rosacea and skin irritation. Whilst it is not licenced for use in open wounds or within the medical setting at present, future clinical trials are expected to explore the possibility of developing Staphefekt™ into a clinical treatment [148]. Similarly ContraFect Corporation have developed an endolysin, CF-301, in collaboration with The Rockefeller University for the treatment of *S. aureus* associated bloodstream infections. As the first lysin to enter clinical trials in the US, the recently completed phase I trial results in healthy volunteers have shown promising results with no adverse clinical safety signals observed. CF-301 has shown potency in combination with approved anti-staphylococcal agents and in the eradication of methicillin resistant *S .aureus* (MRSA) biofilms [149]. Additionally CF-301 has been granted Fast Track Designation from the FDA in order to expedite its clinical assessment, a clear indication of how lysins have the potential to fill unmet medical needs.

Additional protein engineering approaches have also enabled lysins to be developed for Gram-negative pathogens which are usually considered to be recalcitrant to endolysin treatment [150]. Artilysin®s, consisting of an endolysin and an amphipathic or polycationic lipopolysaccharide-destabilizing peptide, are able to successfully penetrate the outer membrane of Gram-negative bacterial cells. Through disruption of ionic and hydrophobic forces within the protective outer membrane, these engineered fusion proteins are then able degrade the peptidoglycan cell wall [151]. Artilysin®s have shown bactericidal efficacy both *in vitro* and *in vivo* against *P. aeruginosa* and *Acinetobacter baumanni* [152,153]. Similarly, 'artilysation' of endolysins effective against Gram-positive bacteria has shown to improve enzymatic and antibacterial activity compared to the wild type enzyme, through addition of a peptide selected to improve cell wall affinity [154].

However, as a relatively recent development, there are limited examples of successful delivery systems capable of carrying such antimicrobial cargo. One such study has successfully stabilized a staphylococcal endolysin, LysK (active against both methicillin and vancomycin resistant *S. aureus*), through complexation with polycationic polymers. Complexation resulted in increased activity, retention of specificity, and increased stability at physiological temperature. An increase in stability was also seen at 22 °C, with poly-$_L$-lysine and 10 mM NaCl, manifesting as an increase in the half-inactivation time from 2 days for the free enzyme, to 2 months for complexed LysK [155]. It is believed that the change in kinetic properties of LysK upon complexation is likely a result of charge redistribution in the bacterial cell wall, following interaction between the cationic polyelectrolytes and the negatively charged surface proteins enclosed within the wall itself.

As previously stated, stimuli-responsive materials are of particular interest as they allow for the controlled release of therapeutic cargo. The truncated form of LysK, denoted $CHAP_K$, consists of the single catalytic domain and has shown to exhibit lytic activity both *in vitro* and *in vivo* and against staphylococcal biofilms [143,156,157]. Exploiting synergistic effects with the bacteriocin lysostaphin, temperature responsive polymeric nanoparticles (PNIPAM) have demonstrated controlled release of the enzyme cocktail at an elevated temperature associated with infection *in vitro*. Formulated into a prototype wound dressing, nanoparticles containing the enzybiotics were anchored onto non-woven polypropylene via plasma activation of the surface and demonstrated statistically significant cell lysis at the elevated temperature (> 4 log reduction in cell count), compared to the lower temperature associated with uninfected skin (< 1 log reduction) [158].

Additional studies have investigated possible transportation methods for the delivery of endolysins to specific infections sites. The GI tract is capable of harbouring a range of pathogenic bacteria, many of which are difficult to treat (especially with a biopharmaceutical agent), owing to the harsh conditions found throughout the alimentary canal. Delivery of the endolysin CP25L, active against *Clostridium perfringens* (*C. perfringens*), to the GI tract has the potential to treat a range of diseases, including necrotic enteritis, gas gangrene and many common forms of food poisoning. Employing a dominant resident of the human intestinal flora, *Lactobacillus johnsonii* researchers have engineered this probiotic microbe to express CP25L, demonstrating successful production and secretion *in vitro* with retention of enzymatic lytic activity against *C. perfringens.* This engineered system provides a dual approach to targeting bacterial colonisation of the GI tract (initially via use of a probiotic microbe with the potential to be used as a competitive exclusion agent for the control of *C. perfringens* in its own right), and secondly through the secretion of an active endolysin with the potential for directed delivery to the gut [159,160].

Conclusion and Future Perspective

Current research into bacteriophage as an alternative or complementary treatment option for infectious diseases has shown encouraging results with a number of phage cocktails and products entering clinical trials. The development of phage therapy in Eastern Europe, in particular at the Eliava Institute in Tbilisi, Georgia, has laid the foundation for the potential implementation of global phage treatment in the 21st century. Recent research into phage delivery systems has shown advantages over the administration of unprotected phage including enhanced bioretention, stability and protection from harsh environmental

conditions or inactivating agents. Optimisation of such carrier/support systems has the potential to enhance phage therapy to treat a range of infections.

However, despite the current success in the development of phage based therapeutics and the relatively large number of phage products in the pipeline, one of the major hurdles for future phage therapy will be clinical approval. The need to address the antibiotic vacuum is currently driving a call for a more economically viable drug approval process, specifically to allow phage to enter clinical trials whilst being relieved of the rigid and time consuming regulatory framework associated with classical clinical trials [90]. In recognition of the unmet medical requirement for the development of novel antimicrobials, a recent (2015) amendment to the Federal Food, Drug and Cosmetic Act was introduced in the US proposing a modified pathway for the approval of antibacterial drugs within a highly defined, limited population. Denoted the Promise for Antibiotics and Therapeutics for Health (PATH) Act [161], this modification to current legislation may allow for the approval of certain antibacterial agents for use within a defined population for treatment of a serious infection, whilst circumventing restrictive, conventional clinical trials. This type of adaptive licencing, alongside possible implementation of compassionate use guidelines such as the Right to Try Act of 2015 [162] (allowing unlicensed phase I experimental drugs, biological products or devices to be used by patients diagnosed with a terminal illness), are encouraging signs that some obstacles facing future phage therapy are being addressed from a regulatory standpoint. The current clinical framework for conventional antibiotic approval may indeed prove unsuitable for whole phage which, as self-replicating biological entities are unlikely to conform to classical drug analysis. Following successful bacterial binding and infection, there is likely to be a significant increase in local phage concentration which may result in an underestimation of phage efficacy via standard PK/PD analysis. Conversely, phage endolysins which show a far greater similarity to chemical antibiotics may conform more successfully to current clinical assessment.

The future of bacteriophage therapy using targeted delivery systems looks promising for the treatment of serious, chronic and multidrug resistant bacterial infections, owing to the capability of controlling the pharmacokinetics/ dynamics of the phage, alongside offering protective and stabilising effects. However in order to continue driving the development of phage based therapeutics and the possible adaptation of regulatory pathways towards their approval, focus must be placed on stringent pre-clinical evaluation, with particular emphasis placed on phage concentration (MOI), biodistribution and suitable *in vivo* modelling. The current antibiotic crisis facing modern medicine appears to be shifting the paradigm in

favour of non-traditional therapy, affecting both development and approval strategies. Thus the next 5-10 years will be an intriguing time for bacteriophage research, offering the potential to see application within the clinical setting.

Executive Summary

Encapsulation

- Liposomal encapsulation can provide effective protection of phage from degradative effects including neutralisation by anti-phage antibodies and systematic clearance *in vivo*. Liposomes provide enhanced cellular uptake of phage in order to target intracellular diseases such as pneumonia and tuberculosis.
- Nanoemulsions can stabilise phage via aqueous encapsulation manifesting as an increase in shelf life and higher infectivity rates.
- Encapsulation within modified alginate microspheres provides a protective strategy capable of preventing phage inactivation under simulated gastric conditions. Addition of stabilising agents such as maltose and maltodextrin allow for the formulation of dry powders containing phage with retention of phage activity and stability.

Immobilisation

- Anchoring to surfaces via plasma activation has successfully immobilised active phage capable of causing bacterial lysis. Retention of activity was achieved for several months under the correct conditions.

Polymeric Formulations

- Complexation with naturally occurring polymers can provide protection against temperature, pH and UV, increasing both the versatility and long term stability of complexed phage. Increased activity and stability has also been seen with phage endolysins through complexation with polycationic polymers.

Aerosol Formulations

- Aerosol formulations for treatment of pulmonary infection can effectively incorporate phage, both in liquid form for use in nebulizers and in dry form for use in inhalers.
- By careful control of particle size, phage containing aerosols can successfully target pulmonary infection. However delivery formulation, storage conditions and the use of stabilisers must be considered individually for each phage administered in order to retain viability and stability.

Stimuli-Responsive Systems

- Controlled release of both phage and phage endolysins offers benefits in terms of preventing unnecessary administration of an antimicrobial and protection of the cargo from environmental conditions until it is required.
- Successful triggered release systems have been shown to release phage/ phage lysins as a response to various stimuli including temperature and bacterial toxin production for the treatment of wound infection.

Financial & Competing Interests Disclosure

The authors have no relevant affiliations or financial involvement with any organization or entity with a financial interest in or financial conflict with the subject matter or materials discussed in the manuscript. This includes employment, consultancies, honoraria, stock ownership or options, expert testimony, grants or patents received or pending, or royalties. No writing assistance was utilized in the production of this manuscript.

3.3 References

1 Lewis, K. Platforms for antibiotic discovery. *Nature Reviews Drug Discovery* **12**, 371-387 (2013).

2 Burmeister, A. R. Horizontal Gene Transfer. *Evolution, Medicine, and Public Health* **2015**, 193-194 (2015).

3 Berendonk, T. U., Manaia, C. M., Merlin, C., Fatta-Kassinos, D., Cytryn, E., Walsh, F., Burgmann, H., Sorum, H., Norstrom, M., Pons, M. N., Kreuzinger, N., Huovinen, P., Stefani, S., Schwartz, T., Kisand, V., Baquero, F. & Martinez, J. L. Tackling antibiotic resistance: the environmental framework. *Nature Reviews Microbiology* **13**, 310-317 (2015).

4 Blair, J. M. A., Webber, M. A., Baylay, A. J., Ogbolu, D. O. & Piddock, L. J. V. Molecular mechanisms of antibiotic resistance. *Nature Reviews Microbiology* **13**, 42-51 (2015).

5 Crofts, T. S., Gasparrini, A. J. & Dantas, G. Next-generation approaches to understand and combat the antibiotic resistome. *Nature Reviews Microbiology* **15**, 422-434 (2017).

6 Beveridge, T. J. Use of the gram stain in microbiology. *Biotech Histochem* **76**, 111-118 (2001).

7 Kong, K.-F., Schneper, L. & Mathee, K. Beta-lactam Antibiotics: From Antibiosis to Resistance and Bacteriology. *APMIS : acta pathologica, microbiologica, et immunologica Scandinavica* **118**, 1-36 (2010).

8 Garneau-Tsodikova, S. & Labby, K. J. Mechanisms of Resistance to Aminoglycoside Antibiotics: Overview and Perspectives. *MedChemComm* **7**, 11-27 (2016).

9 Roberts, M. C. Update on acquired tetracycline resistance genes. *FEMS Microbiology Letters* **245**, 195-203 (2005).

10 Leclercq, R. & Courvalin, P. Resistance to macrolides and related antibiotics in Streptococcus pneumoniae. *Antimicrobial Agents and Chemotherapy* **46**, 2727-2734 (2002).

11 Pootoolal, J., Neu, J. & Wright, G. D. Glycopeptide antibiotic resistance. *Annual review of pharmacology and toxicology* **42**, 381-408 (2002).

12 Bozdogan, B. & Appelbaum, P. C. Oxazolidinones: activity, mode of action, and mechanism of resistance. *International Journal of Antimicrobial Agents* **23**, 113-119 (2004).

13 Jacoby, G. A. Mechanisms of Resistance to Quinolones. *Clinical Infectious Diseases* **41**, S120-S126 (2005).

14 Bayer, A. S., Schneider, T. & Sahl, H.-G. Mechanisms of daptomycin resistance in Staphylococcus aureus: role of the cell membrane and cell wall. *Annals of the New York Academy of Sciences* **1277**, 139-158 (2013).

15 Cheng, Y. H., Lin, T. L., Pan, Y. J., Wang, Y. P., Lin, Y. T. & Wang, J. T. Colistin resistance mechanisms in Klebsiella pneumoniae strains from Taiwan. *Antimicrobial Agents and Chemotherapy* **59**, 2909-2913 (2015).

16 O'Neill, J. Tackling Drug-Resistant Infections Globally: Final Report and Recommendations, https://amr-review.org/sites/default/files/160525_Final%20paper_with%20cover.pdf (2016).

17 Andersson, D. I. & Hughes, D. Microbiological effects of sublethal levels of antibiotics. *Nature Reviews Microbiology* **12**, 465-478 (2014).

18 Van Boeckel, T. P., Gandra, S., Ashok, A., Caudron, Q., Grenfell, B. T., Levin, S. A. & Laxminarayan, R. Global antibiotic consumption 2000 to 2010: an analysis of national pharmaceutical sales data. *The Lancet Infectious Diseases* **14**, 742-750 (2014).

19 National Institute for Health and Care Excellence (NICE). Antimicrobial stewardship: systems and processes for effective antimicrobial medicine use, NICE Guideline (NG15), https://www.nice.org.uk/guidance/NG15/chapter/1-Recommendations#recommendations-for-prescribers (2015).

20 World Health Organisation - Marc Sprenger (Director of the WHO's secretariat for antimicrobial resistance). How to stop antibiotic resistance? Here's a WHO prescription, http://www.who.int/mediacentre/commentaries/stop-antibiotic-resistance/en/ (2015).

21 Llewelyn, M. J., Fitzpatrick, J. M., Darwin, E., SarahTonkin-Crine, Gorton, C., Paul, J., Peto, T. E. A., Yardley, L., Hopkins, S. & Walker, A. S. The antibiotic course has had its day. *The British Medical Journal* **358** (2017).

22 Scarpato, S. J., Timko, D. R., Cluzet, V. C., Dougherty, J. P., Nunez, J. J., Fishman, N. O. & Hamilton, K. W. An Evaluation of Antibiotic Prescribing Practices Upon Hospital Discharge. *Infection Control and Hospital Epidemiology* **38**, 353-355 (2016).

23 Goff, D. A., Kullar, R., Goldstein, E. J. C., Gilchrist, M., Nathwani, D., Cheng, A. C., Cairns, K. A., Escandón-Vargas, K., Villegas, M. V., Brink, A., van den Bergh, D. & Mendelson, M. A global call from five countries to collaborate in antibiotic stewardship: united we succeed, divided we might fail. *The Lancet Infectious Diseases* **17**, e56-e63 (2017).

24 Dallas, A., van Driel, M., van de Mortel, T. & Magin, P. Antibiotic prescribing for the future: exploring the attitudes of trainees in general practice. *British Journal of General Practice* **64**, e561-e567 (2014).

25 Trivedi, K. K., Dumartin, C., Gilchrist, M., Wade, P. & Howard, P. Identifying Best Practices Across Three Countries: Hospital Antimicrobial Stewardship in the United Kingdom, France, and the United States. *Clinical Infectious Diseases* **59**, S170-S178 (2014).

26 Luepke, K. H., Suda, K. J., Boucher, H., Russo, R. L., Bonney, M. W., Hunt, T. D. & Mohr, J. F. Past, Present, and Future of Antibacterial Economics: Increasing Bacterial Resistance, Limited Antibiotic Pipeline, and Societal Implications. *Pharmacotherapy: The Journal of Human Pharmacology and Drug Therapy* **37**, 71-84 (2017).

27 Al-Tawfiq, J. A., Laxminarayan, R. & Mendelson, M. How should we respond to the emergence of plasmid-mediated colistin resistance in humans and animals? *International Journal of Infectious Diseases* **54**, 77-84 (2017).

28 Liu, Y.-Y., Wang, Y., Walsh, T. R., Yi, L.-X., Zhang, R., Spencer, J., Doi, Y., Tian, G., Dong, B., Huang, X., Yu, L.-F., Gu, D., Ren, H., Chen, X., Lv, L., He, D., Zhou, H., Liang, Z., Liu, J.-H. & Shen, J. Emergence of plasmid-mediated colistin resistance mechanism MCR-1 in animals and human beings in China: a microbiological and molecular biological study. *The Lancet Infectious Diseases* **16**, 161-168.

29 US Food & Drug Administration. Guidance for Industry Evaluating the Safety of Antimicrobial New Animal Drugs with Regard to Their Microbiological Effects on Bacteria of Human Health Concern#152 (2003). https://www.fda.gov/downloads/AnimalVeterinary/GuidanceComplianceEnforcement/GuidanceforIndustry/UCM052519.pdf

30 D/'Costa, V. M., King, C. E., Kalan, L., Morar, M., Sung, W. W. L., Schwarz, C., Froese, D., Zazula, G., Calmels, F., Debruyne, R., Golding, G. B., Poinar, H. N. & Wright, G. D. Antibiotic resistance is ancient. *Nature* **477**, 457-461 (2011).

31 Bhullar, K., Waglechner, N., Pawlowski, A., Koteva, K., Banks, E. D., Johnston, M. D., Barton, H. A. & Wright, G. D. Antibiotic Resistance Is Prevalent in an Isolated Cave Microbiome. *Plos One* **7**, e34953 (2012).

32 Coates, A. R. M., Halls, G. & Hu, Y. Novel classes of antibiotics or more of the same? *British Journal of Pharmacology* **163**, 184-194 (2011).

33 Moore, A. M., Patel, S., Forsberg, K. J., Wang, B., Bentley, G., Razia, Y., Qin, X., Tarr, P. I. & Dantas, G. Pediatric Fecal Microbiota Harbor Diverse and Novel Antibiotic Resistance Genes. *Plos One* **8**, e78822 (2013).

34 Innovative Medicines Initiative. ND4BB New Drugs for Bad Bugs (2017). http://www.imi.europa.eu/sites/default/files/uploads/documents/Publications/IMI_AMR_2017%203%20LR.pdf

35 National Action Plan for the Combating Antibiotic-Resistant Bacteria (2015). https://www.cdc.gov/drugresistance/pdf/national_action_plan_for_combating_antibotic-resistant_bacteria.pdf

36 World Health Organisation. Global Action Plan on Antimicrobial Resistance (2015). http://www.wpro.who.int/entity/drug_resistance/resources/global_action_plan_eng.pdf

37 World Health Organisation. Global priority list of antibiotic-resistant bacteria to guide research, discovery, and development of new antibiotics (2017). http://www.who.int/medicines/publications/WHO-PPL-Short_Summary_25Feb-ET_NM_WHO.pdf?ua=1

38 Dickey, S. W., Cheung, G. Y. C. & Otto, M. Different drugs for bad bugs: antivirulence strategies in the age of antibiotic resistance. *Nature Reviews Drug Discovery* **16**, 457-471 (2017).

39 Sun, J., Deng, Z. & Yan, A. Bacterial multidrug efflux pumps: Mechanisms, physiology and pharmacological exploitations. *Biochemical and Biophysical Research Communications* **453**, 254-267 (2014).

40 Mullin, S., Mani, N. & Grossman, T. H. Inhibition of Antibiotic Efflux in Bacteria by the Novel Multidrug Resistance Inhibitors Biricodar (VX-710) and Timcodar (VX-853). *Antimicrobial Agents and Chemotherapy* **48**, 4171-4176 (2004).

41 Kalia, N. P. in *Drug Resistance in Bacteria, Fungi, Malaria, and Cancer* (eds Gunjan Arora, Andaleeb Sajid, & Vipin Chandra Kalia) 307-323 (Springer International Publishing, 2017).

42 Nigam, A., Gupta, D. & Sharma, A. Treatment of infectious disease: Beyond antibiotics. *Microbiological Research* **169**, 643-651 (2014).

43 Cheraghi, S., Pourgholi, L., Shafaati, M., Fesharaki, S. H., Jalali, A., Nosrati, R. & Boroumand, M. Molecular Analysis of Virulence Genes and the accessory gene regulator (agr) types Among Methicillin Resistant Staphylococcus aureus (MRSA) Strains. *Journal of Global Antimicrobial Resistance* (2017).

44 Sully, E. K., Malachowa, N., Elmore, B. O., Alexander, S. M., Femling, J. K., Gray, B. M., DeLeo, F. R., Otto, M., Cheung, A. L., Edwards, B. S., Sklar, L. A., Horswill, A. R., Hall, P. R. & Gresham, H. D. Selective Chemical Inhibition of agr Quorum Sensing in Staphylococcus aureus Promotes Host Defense with Minimal Impact on Resistance. *PLoS Pathogens* **10**, e1004174 (2014).

45 Bhardwaj, A. K., Vinothkumar, K. & Rajpara, N. Bacterial quorum sensing inhibitors: attractive alternatives for control of infectious pathogens showing multiple drug resistance. *Recent Patents on Anti-Infective Drug Discovery* **8**, 68-83 (2013).

46 Garber, K. A [beta]-lactamase inhibitor revival provides new hope for old antibiotics. *Nature Reviews Drug Discovery* **14**, 445-447 (2015).

47 Aziz, R. K., Dwivedi, B., Akhter, S., Breitbart, M. & Edwards, R. A. Multidimensional metrics for estimating phage abundance, distribution, gene density, and sequence coverage in metagenomes. *Frontiers in Microbiology* **6**, 381 (2015).

48 Wittebole, X., De Roock, S. & Opal, S. M. A historical overview of bacteriophage therapy as an alternative to antibiotics for the treatment of bacterial pathogens. *Virulence* **5**, 226-235 (2014).

49 Babalova, E., Katsitadze, K., Sakvarelidze, L., Imnaishvili, N., Sharashidze, T., Badashvili, V., Kiknadze, G., Meĭpariani, A., Gendzekhadze, N. & Machavariani, E. Preventive value of dried dysentery bacteriophage. *Zhurnal mikrobiologii, epidemiologii, i immunobiologii* **45**, 143-145 (1968).

50 Slopek, S., Weber-Dabrowska, B., Dabrowski, M. & Kucharewicz-Krukowska, A. Results of bacteriophage treatment of suppurative bacterial infections in the years 1981-1986. *Archivum immunologiae et therapiae experimentalis* **35**, 569-583 (1987).

51 Rhoads, D. D., Wolcott, R. D., Kuskowski, M. A., Wolcott, B. M., Ward, L. S. & Sulakvelidze, A. Bacteriophage therapy of venous leg ulcers in humans: results of a phase I safety trial. *Journal of Wound Care* **18**, 237-238, 240-233 (2009).

52 International Committee on Taxonomy of Viruses (ICTV). https://talk.ictvonline.org

53 Ackermann, H. W. Bacteriophage taxonomy. *Microbiology Australia* **32**, 90-94 (2011).

54 Calendar, R. *The Bacteriophages*. (Oxford University Press, USA, 2006).

55 Yap, M. L., Klose, T., Arisaka, F., Speir, J. A., Veesler, D., Fokine, A. & Rossmann, M. G. Role of bacteriophage T4 baseplate in regulating assembly and infection. *Proceedings of the National Academy of Sciences U S A* **113**, 2654-2659 (2016).

56 Skurnik, M. & Strauch, E. Phage therapy: Facts and fiction. *International Journal of Medical Microbiology* **296**, 5-14 (2006).

57 Neidleman, S. L. & Laskin, A. I. *Advances in Applied Microbiology*. (Elsevier Science, 1990).

58 University of Miami, Department of Biology. Microbial Genetics: Inheritance in Bacteria & Phages http://www.bio.miami.edu/dana/250/250SS16_5print.html

59 Waddell, T. E., Franklin, K., Mazzocco, A., Kropinski, A. M. & Johnson, R. P. in *Bacteriophages: Methods and Protocols, Volume 1: Isolation, Characterization, and Interactions* (eds Martha R. J. Clokie & Andrew M. Kropinski) 293-303 (Humana Press, 2009).

60 Feiner, R., Argov, T., Rabinovich, L., Sigal, N., Borovok, I. & Herskovits, A. A. A new perspective on lysogeny: prophages as active regulatory switches of bacteria. *Nature Reviews Microbiology* **13**, 641-650 (2015).

61 Coleman, D. C., Sullivan, D. J., Russell, R. J., Arbuthnott, J. P., Carey, B. F. & Pomeroy, H. M. Staphylococcus aureus bacteriophages mediating the simultaneous lysogenic conversion of beta-lysin, staphylokinase and enterotoxin A: molecular mechanism of triple conversion. *Journal of General Microbiology* **135**, 1679-1697 (1989).

62 Abedon, S. T., García, P., Mullany, P. & Aminov, R. Editorial: Phage Therapy: Past, Present and Future. *Frontiers in Microbiology* **8**, 981 (2017).

63 Fischetti, V. A. Bacteriophage endolysins: a novel anti-infective to control Gram-positive pathogens. *International Journal of Medical Microbiology* **300**, 357-362 (2010).

64 Young, R., Wang, I.-N. & Roof, W. D. Phages will out: strategies of host cell lysis. *Trends in Microbiology* **8**, 120-128 (2000).

65 Chapot-Chartier, M.-P. Interactions of the cell-wall glycopolymers of lactic acid bacteria with their bacteriophages. *Frontiers in Microbiology* **5**, 236 (2014).

66 Roach, D. R. & Donovan, D. M. Antimicrobial bacteriophage-derived proteins and therapeutic applications. *Bacteriophage* **5**, e1062590 (2015).

67 Drulis-Kawa, Z., Majkowska-Skrobek, G., Maciejewska, B., Delattre, A.-S. & Lavigne, R. Learning from Bacteriophages - Advantages and Limitations of Phage and Phage-Encoded Protein Applications. *Current Protein & Peptide Science* **13**, 699-722 (2012).

68 Li, A. P. Preclinical in vitro screening assays for drug-like properties. *Drug Discovery Today Technologies* **2**, 179-185 (2005).

69 Jain, K. K. in *Drug Delivery Systems* (ed Kewal K. Jain) 1-50 (Humana Press, 2008).

70 Coelho, J. F., Ferreira, P. C., Alves, P., Cordeiro, R., Fonseca, A. C., Góis, J. R. & Gil, M. H. Drug delivery systems: Advanced technologies potentially applicable in personalized treatments. *The EPMA Journal* **1**, 164-209 (2010).

71 Beals, J. M. & Shanafelt, A. B. Enhancing exposure of protein therapeutics. *Drug Discovery Today: Technologies* **3**, 87-94 (2006).

72 Tibbitt, M. W., Dahlman, J. E. & Langer, R. Emerging Frontiers in Drug Delivery. *Journal of the American Chemical Society* **138**, 704-717 (2016).

73 Sir Alexander Fleming - Nobel Lecture: Penicillin 1945. N*obelprize.org.* Nobel Media AB 2014. http://www.nobelprize.org/nobel_prizes/medicine/laureates/1945/fleming-lecture.html

74 Nobrega, F. L., Costa, A. R., Kluskens, L. D. & Azeredo, J. Revisiting phage therapy: new applications for old resources. *Trends in Microbiology* **23**, 185-191 (2015).

75 Twort, F. W. The Discovery of the Bacteriophage. *The Lancet* **205**, 845 (1925).

76 Hendrix, R. W. Bacteriophages: Evolution of the majority. *Theoretical Population Biology* **61**, 471-480 (2002).

77 Campbell, A. The future of bacteriophage biology. *Nature Reviews Genetics* **4**, 471-477 (2003).

78 Cisek, A. A., Dąbrowska, I., Gregorczyk, K. P. & Wyżewski, Z. Phage Therapy in Bacterial Infections Treatment: One Hundred Years After the Discovery of Bacteriophages. *Current Microbiology* **74**, 277-283 (2017).

79 Magnone, J. P., Marek, P. J., Sulakvelidze, A. & Senecal, A. G. Additive Approach for Inactivation of Escherichia coli O157:H7, Salmonella, and Shigella spp. on Contaminated Fresh Fruits and Vegetables Using Bacteriophage Cocktail and Produce Wash. *Journal of Food Protection* **76**, 1336-1341 (2013).

80 Schmelcher, M. & Loessner, M. J. Application of bacteriophages for detection of foodborne pathogens. *Bacteriophage* **4**, e28137 (2014).

81 Haq, I. U., Chaudhry, W. N., Akhtar, M. N., Andleeb, S. & Qadri, I. Bacteriophages and their implications on future biotechnology: a review. *Virology Journal* **9**, 9 (2012).

82 Weber-Dąbrowska, B., Jończyk-Matysiak, E., Żaczek, M., Łobocka, M., Łusiak-Szelachowska, M. & Górski, A. Bacteriophage Procurement for Therapeutic Purposes. *Frontiers in Microbiology* **7**, 1177 (2016).

83 Jassim, S. A. A. & Limoges, R. G. Natural solution to antibiotic resistance: bacteriophages 'The Living Drugs'. *World Journal of Microbiology & Biotechnology* **30**, 2153-2170 (2014).

84 Sarhan, W. A. & Azzazy, H. M. E. Phage approved in food, why not as a therapeutic? *Expert Review of Anti-infective Therapy* **13**, 91-101 (2015).

85 Kingwell, K. Bacteriophage therapies re-enter clinical trials. *Nature Reviews Drug Discovery* **14**, 515-516 (2015).

86 Evaluation of Phage Therapy for the Treatment of Escherichia Coli and Pseudomonas Aeruginosa Wound Infections in Burned Patients (PHAGOBURN). https://clinicaltrials.gov/ct2/show/NCT02116010

87 Ascending Dose Study of the Safety of AB-SA01 When Topically Applied to Intact Skin of Healthy Adults. https://clinicaltrials.gov/ct2/show/NCT02757755

88 Wright, A., Hawkins, C. H., Anggard, E. E. & Harper, D. R. A controlled clinical trial of a therapeutic bacteriophage preparation in chronic otitis due to antibiotic-resistant Pseudomonas aeruginosa; a preliminary report of efficacy. *Clinical Otolaryngology* **34**, 349-357 (2009).

89 Mann, N. H. The potential of phages to prevent MRSA infections. *Research in Microbiology* **159**, 400-405 (2008).

90 Cooper, C. J., Khan Mirzaei, M. & Nilsson, A. S. Adapting Drug Approval Pathways for Bacteriophage-Based Therapeutics. *Frontiers in Microbiology* **7**, 1209 (2016).

91 Ly-Chatain, M. H. The factors affecting effectiveness of treatment in phages therapy. *Frontiers in Microbiology* **5**, 51 (2014).

92 Srinivasan, S., Alexander, J. F., Driessen, W. H., Leonard, F., Ye, H., Liu, X., Arap, W., Pasqualini, R., Ferrari, M. & Godin, B. Bacteriophage Associated Silicon Particles: Design and Characterization of a Novel Theranostic Vector with Improved Payload Carrying Potential.

Journal of materials chemistry B, Materials for biology and medicine **1**, 10.1039/C1033TB20595A (2013).

93 Yata, T., Lee, K. Y., Dharakul, T., Songsivilai, S., Bismarck, A., Mintz, P. J. & Hajitou, A. Hybrid Nanomaterial Complexes for Advanced Phage-guided Gene Delivery. *Molecular Therapy — Nucleic Acids* **3**, e185 (2014).

94 Saboo, S., Tumban, E., Peabody, J., Wafula, D., Peabody, D. S., Chackerian, B. & Muttil, P. Optimized Formulation of a Thermostable Spray-Dried Virus-Like Particle Vaccine against Human Papillomavirus. *Molecular Pharmaceutics* **13**, 1646-1655 (2016).

95 van der Merwe, R. G., van Helden, P. D., Warren, R. M., Sampson, S. L. & Gey van Pittius, N. C. Phage-based detection of bacterial pathogens. *Analyst* **139**, 2617-2626 (2014).

96 Bhattarai, S. R., Yoo, S. Y., Lee, S. W. & Dean, D. Engineered phage-based therapeutic materials inhibit Chlamydia trachomatis intracellular infection. *Biomaterials* **33**, 5166-5174 (2012).

97 Hosseinidoust, Z., Olsson, A. L. J. & Tufenkji, N. Going viral: Designing bioactive surfaces with bacteriophage. *Colloids and Surfaces B: Biointerfaces* **124**, 2-16 (2014).

98 Yosef, I., Manor, M. & Qimron, U. Counteracting selection for antibiotic-resistant bacteria. *Bacteriophage* **6**, e1096996 (2016).

99 Yosef, I., Manor, M., Kiro, R. & Qimron, U. Temperate and lytic bacteriophages programmed to sensitize and kill antibiotic-resistant bacteria. *Proceedings of the National Academy of Sciences U S A* **112**, 7267-7272 (2015).

100 Fairhead, H. SASP gene delivery: a novel antibacterial approach. *Drug News Perspectives* **22**, 197-203 (2009).

101 Sahly, H. & Podschun, R. Clinical, bacteriological, and serological aspects of Klebsiella infections and their spondylarthropathic sequelae. *Clinical and Diagnostic Laboratory Immunology* **4**, 393-399 (1997).

102 Cortes, G., Alvarez, D., Saus, C. & Alberti, S. Role of lung epithelial cells in defense against Klebsiella pneumoniae pneumonia. *Infection and Immunity* **70**, 1075-1080 (2002).

103 Singla, S., Harjai, K., Katare, O. P. & Chhibber, S. Encapsulation of Bacteriophage in Liposome Accentuates Its Entry in to Macrophage and Shields It from Neutralizing Antibodies. *Plos One* **11** (2016).

104 Nieth, A., Verseux, C., Barnert, S., Suss, R. & Romer, W. A first step toward liposome-mediated intracellular bacteriophage therapy. *Expert Opinion on Drug Delivery* **12**, 1411-1424 (2015).

105 Lusiak-Szelachowska, M., Zaczek, M., Weber-Dabrowska, B., Miedzybrodzki, R., Klak, M., Fortuna, W., Letkiewicz, S., Rogoz, P., Szufnarowski, K., Jonczyk-Matysiak, E., Owczarek, B. & Gorski, A. Phage neutralization by sera of patients receiving phage therapy. *Viral Immunology* **27**, 295-304 (2014).

106 Singla, S., Harjai, K., Katare, O. P. & Chhibber, S. Bacteriophage-Loaded Nanostructured Lipid Carrier: Improved Pharmacokinetics Mediates Effective Resolution of Klebsiella pneumoniae-Induced Lobar Pneumonia. *Journal of Infectious Diseases* **212**, 325-334 (2015).

107 Singla, S., Harjai, K., Raza, K., Wadhwa, S., Katare, O. P. & Chhibber, S. Phospholipid vesicles encapsulated bacteriophage: A novel approach to enhance phage biodistribution. *Journal of Virological Methods* **236**, 68-76 (2016).

108 Balcao, V. M., Glasser, C. A., Chaud, M. V., del Fiol, F. S., Tubino, M. & Vila, M. Biomimetic aqueous-core lipid nanoballoons integrating a multiple emulsion formulation: A suitable housing system for viable lytic bacteriophages. *Colloids and Surfaces B-Biointerfaces* **123**, 478-485 (2014).

109 Esteban, P. P., Alves, D. R., Enright, M. C., Bean, J. E., Gaudion, A., Jenkins, A. T. A., Young, A. E. R. & Arnot, T. C. Enhancement of the Antimicrobial Properties of Bacteriophage-K via Stabilization using Oil-in-Water Nano-Emulsions. *Biotechnology Progress* **30**, 932-944 (2014).

110 Esteban, P. P., Jenkins, A. T. A. & Arnot, T. C. Elucidation of the mechanisms of action of Bacteriophage K/nano-emulsion formulations against S. aureus via measurement of particle size and zeta potential. *Colloids and Surfaces B: Biointerfaces* **139**, 87-94 (2016).

111 Ma, Y. S., Pacan, J. C., Wang, Q., Xu, Y. P., Huang, X. Q., Korenevsky, A. & Sabour, P. M. Microencapsulation of bacteriophage Felix O1 into chitosan-alginate microspheres for oral delivery. *Applied Environmental Microbiology* **74**, 4799-4805 (2008).

112 Ma, Y. S., Pacan, J. C., Wang, Q., Sabour, P. M., Huang, X. Q. & Xu, Y. P. Enhanced alginate microspheres as means of oral delivery of bacteriophage for reducing Staphylococcus aureus intestinal carriage. *Food Hydrocolloids* **26**, 434-440 (2012).

113 Tang, Z., Huang, X., Sabour, P. M., Chambers, J. R. & Wang, Q. Preparation and characterization of dry powder bacteriophage K for intestinal delivery through oral administration. *LWT - Food Science and Technology* **60**, 263-270 (2015).

114 Kim, S., Jo, A. & Ahn, J. Application of chitosan-alginate microspheres for the sustained release of bacteriophage in simulated gastrointestinal conditions. *International Journal of Food Science and Technology* **50**, 913-918 (2015).

115 Pearson, H. A., Sahukhal, G. S., Elasri, M. O. & Urban, M. W. Phage-Bacterium War on Polymeric Surfaces: Can Surface-Anchored Bacteriophages Eliminate Microbial Infections? *Biomacromolecules* **14**, 1257-1261 (2013).

116 Olsson, A. L. J., Wargenau, A. & Tufenkji, N. Optimizing Bacteriophage Surface Densities for Bacterial Capture and Sensing in Quartz Crystal Microbalance with Dissipation Monitoring. *Acs Applied Materials & Interfaces* **8**, 13698-13706 (2016).

117 Tawil, N., Sacher, E., Mandeville, R. & Meunier, M. Strategies for the Immobilization of Bacteriophages on Gold Surfaces Monitored by Surface Plasmon Resonance and Surface Morphology. *The Journal of Physical Chemistry C* **117**, 6686-6691 (2013).

118 Wang, C., Sauvageau, D. & Elias, A. Immobilization of Active Bacteriophages on Polyhydroxyalkanoate Surfaces. *ACS Applied Materials & Interfaces* **8**, 1128-1138 (2016).

119 Khalil, R. I., Irorere, U. V., Radecka, I., Burns, T. A., Kowalczuk, M., Mason, L. J. & Khechara, P. M. Poly-γ-Glutamic Acid: Biodegradable Polymer for Potential Protection of Beneficial Viruses. *Materials* **9** (2016).

120 Zhang, J., Pritchard, E., Hu, X., Valentin, T., Panilaitis, B., Omenetto, F. G. & Kaplan, D. L. Stabilization of vaccines and antibiotics in silk and eliminating the cold chain. *Proceedings of the National Academy of Sciences* **109**, 11981-11986 (2012).

121 Sutherland, T. D., Sriskantha, A., Church, J. S., Strive, T., Trueman, H. E. & Kameda, T. Stabilization of Viruses by Encapsulation in Silk Proteins. *ACS Applied Materials & Interfaces* **6**, 18189-18196 (2014).

122 Semler, D. D., Goudie, A. D., Finlay, W. H. & Dennis, J. J. Aerosol Phage Therapy Efficacy in Burkholderia cepacia Complex Respiratory Infections. *Antimicrobial Agents and Chemotherapy* **58**, 4005-4013 (2014).

123 Hansen, C. R., Pressler, T., Koch, C. & Høiby, N. Long-term azitromycin treatment of cystic fibrosis patients with chronic Pseudomonas aeruginosa infection; an observational cohort study. *Journal of Cystic Fibrosis* **4**, 35-40 (2005).

124 Sahota, J. S., Smith, C. M., Radhakrishnan, P., Winstanley, C., Goderdzishvili, M., Chanishvili, N., Kadioglu, A., O'Callaghan, C. & Clokie, M. R. Bacteriophage Delivery by Nebulization and Efficacy Against Phenotypically Diverse Pseudomonas aeruginosa from Cystic Fibrosis Patients. *Journal of Aerosol Medicine and Pulmonary Drug Delivery* **28**, 353-360 (2015).

125 Bosquillon, C., Lombry, C., Préat, V. & Vanbever, R. Influence of formulation excipients and physical characteristics of inhalation dry powders on their aerosolization performance. *Journal of Controlled Release* **70**, 329-339 (2001).

126 Golshahi, L., Lynch, K. H., Dennis, J. J. & Finlay, W. H. In vitro lung delivery of bacteriophages KS4-M and PhiKZ using dry powder inhalers for treatment of Burkholderia cepacia complex and Pseudomonas aeruginosa infections in cystic fibrosis. *Journal of Applied Microbiology* **110**, 106-117 (2011).

127 Vandenheuvel, D., Meeus, J., Lavigne, R. & Van den Mooter, G. Instability of bacteriophages in spray-dried trehalose powders is caused by crystallization of the matrix. *International Journal of Pharmaceutics* **472**, 202-205 (2014).

128 Vandenheuvel, D., Singh, A., Vandersteegen, K., Klumpp, J., Lavigne, R. & Van den Mooter, G. Feasibility of spray drying bacteriophages into respirable powders to combat pulmonary bacterial infections. *European Journal of Pharmaceutics and Biopharmaceutics* **84**, 578-582 (2013).

129 Dixon, D. V., Hosseinidoust, Z. & Tufenkji, N. Effects of environmental and clinical interferents on the host capture efficiency of immobilized bacteriophages. *Langmuir* **30**, 3184-3190 (2014).

130 Hathaway, H., Alves, D. R., Bean, J., Esteban, P. P., Ouadi, K., Mark Sutton, J. & Jenkins, A. T. Poly(N-isopropylacrylamide-co-allylamine) (PNIPAM-co-ALA) nanospheres for the thermally triggered release of Bacteriophage K. *European Journal of Pharmaceutics and Biopharmaceutics* **96**, 437-441 (2015).

131 Starr, C. R. & Engleberg, N. C. Role of hyaluronidase in subcutaneous spread and growth of group A streptococcus. *Infection and Immunity* **74**, 40-48 (2006).

132 Bean, J. E., Alves, D. R., Laabei, M., Esteban, P. P., Thet, N. T., Enright, M. C. & Jenkins, A. T. A. Triggered Release of Bacteriophage K from Agarose/Hyaluronan Hydrogel Matrixes by Staphylococcus aureus Virulence Factors. *Chemistry of Materials* **26**, 7201-7208 (2014).

133 Chen, L., Zhao, X., Lin, Y., Su, Z. & Wang, Q. Dual stimuli-responsive supramolecular hydrogel of bionanoparticles and hyaluronan. *Polymer Chemistry* **5**, 6754-6760 (2014).

134 Chen, Z., Li, N., Chen, L., Lee, J. & Gassensmith, J. J. Dual Functionalized Bacteriophage Qbeta as a Photocaged Drug Carrier. *Small* **12**, 4563-4571 (2016).

135 Schwarz, B. & Douglas, T. Development of virus-like particles for diagnostic and prophylactic biomedical applications. *Wiley Interdisciplinary Reviews: Nanomedicine and Nanobiotechnology* **7**, 722-735 (2015).

136 Fischetti, V. A., Nelson, D. & Schuch, R. Reinventing phage therapy: are the parts greater than the sum? *Nature Biotechnology* **24**, 1508-1511 (2006).

137 Pastagia, M., Schuch, R., Fischetti, V. A. & Huang, D. B. Lysins: the arrival of pathogen-directed anti-infectives. *Journal of Medical Microbiology* **62**, 1506-1516 (2013).

138 Pohane, A. A. & Jain, V. Insights into the regulation of bacteriophage endolysin: multiple means to the same end. *Microbiology* **161**, 2269-2276 (2015).

139 Moon, B. Y., Park, J. Y., Robinson, D. A., Thomas, J. C., Park, Y. H., Thornton, J. A. & Seo, K. S. Mobilization of Genomic Islands of Staphylococcus aureus by Temperate Bacteriophage. *Plos One* **11**, e0151409 (2016).

140 Ajuebor, J., McAuliffe, O., O'Mahony, J., Ross, R. P., Hill, C. & Coffey, A. Bacteriophage endolysins and their applications. *Science Progress* **99**, 183-199 (2016).

141 Gutierrez, D., Ruas-Madiedo, P., Martínez, B., Rodríguez, A. & García, P. Effective removal of staphylococcal biofilms by the endolysin LysH5. *Plos One* **9**, e107307 (2014).

142 Singh, P. K., Donovan, D. M. & Kumar, A. Intravitreal injection of the chimeric phage endolysin Ply187 protects mice from Staphylococcus aureus endophthalmitis. *Antimicrobial Agents and Chemotherapy* **58**, 4621-4629 (2014).

143 Fenton, M., Keary, R., McAuliffe, O., Ross, R. P., O'Mahony, J. & Coffey, A. Bacteriophage-Derived Peptidase CHAP(K) Eliminates and Prevents Staphylococcal Biofilms. *International Journal of Microbiology* **2013**, 625341 (2013).

144 Shen, Y., Koeller, T., Kreikemeyer, B. & Nelson, D. C. Rapid degradation of Streptococcus pyogenes biofilms by PlyC, a bacteriophage-encoded endolysin. *Journal of Antimicrobial Chemotherapy* **68**, 1818-1824 (2013).

145 Schuch, R., Nelson, D. & Fischetti, V. A. A bacteriolytic agent that detects and kills Bacillus anthracis. *Nature* **418**, 884-889 (2002).

146 Lai, M.-J., Soo, P.-C., Lin, N.-T., Hu, A., Chen, Y.-J., Chen, L.-K. & Chang, K.-C. Identification and characterisation of the putative phage-related endolysins through full genome sequence analysis in Acinetobacter baumannii ATCC 17978. *International Journal of Antimicrobial Agents* **42**, 141-148 (2013).

147 Lai, M.-J., Liu, C.-C., Jiang, S.-J., Soo, P.-C., Tu, M.-H., Lee, J.-J., Chen, Y.-H. & Chang, K.-C. Antimycobacterial Activities of Endolysins Derived From a Mycobacteriophage, BTCU-1. *Molecules* **20**, 19277-19290 (2015).

148 Herpers, B. Endolysins: redefining antibacterial therapy. *Future Microbiology* **10**, 309-311 (2015).

149 Schuch, R., Lee, H. M., Schneider, B. C., Sauve, K. L., Law, C., Khan, B. K., Rotolo, J. A., Horiuchi, Y., Couto, D. E., Raz, A., Fischetti, V. A., Huang, D. B., Nowinski, R. C. & Wittekind, M. Combination therapy with lysin CF-301 and antibiotic is superior to antibiotic alone for treating methicillin-resistant Staphylococcus aureus-induced murine bacteremia. *The Journal of Infectious Diseases* **209**, 1469-1478 (2014).

150 Briers, Y. & Lavigne, R. Breaking barriers: expansion of the use of endolysins as novel antibacterials against Gram-negative bacteria. *Future Microbiology* **10**, 377-390 (2015).

151 Briers, Y., Walmagh, M., Van Puyenbroeck, V., Cornelissen, A., Cenens, W., Aertsen, A., Oliveira, H., Azeredo, J., Verween, G., Pirnay, J.-P., Miller, S., Volckaert, G. & Lavigne, R. Engineered Endolysin-Based "Artilysins" To Combat Multidrug-Resistant Gram-Negative Pathogens. *Mbio* **5** (2014).

152 Defraine, V., Schuermans, J., Grymonprez, B., Govers, S. K., Aertsen, A., Fauvart, M., Michiels, J., Lavigne, R. & Briers, Y. Efficacy of Artilysin Art-175 against Resistant and Persistent Acinetobacter baumannii. *Antimicrobial Agents and Chemotherapy* **60**, 3480-3488 (2016).

153 Gerstmans, H., Rodriguez-Rubio, L., Lavigne, R. & Briers, Y. From endolysins to Artilysin (R) s: novel enzyme-based approaches to kill drug-resistant bacteria. *Biochemical Society Transactions* **44**, 123-128 (2016).

154 Rodriguez-Rubio, L., Chang, W. L., Gutierrez, D., Lavigne, R., Martinez, B., Rodriguez, A., Govers, S. K., Aertsen, A., Hirl, C., Biebl, M., Briers, Y. & Garcia, P. 'Artilysation' of endolysin lambda Sa2lys strongly improves its enzymatic and antibacterial activity against streptococci. *Scientific Reports* **6** (2016).

155 Filatova, L. Y., Donovan, D. M., Becker, S. C., Lebedev, D. N., Priyma, A. D., Koudriachova, H. V., Kabanov, A. V. & Klyachko, N. L. Physicochemical characterization of the staphylolytic LysK enzyme in complexes with polycationic polymers as a potent antimicrobial. *Biochimie* **95**, 1689-1696 (2013).

156 Fenton, M., Casey, P. G., Hill, C., Gahan, C. G. M., Ross, R. P., McAuliffe, O., O'Mahony, J., Maher, F. & Coffey, A. The truncated phage lysin CHAP(k) eliminates Staphylococcus aureus in the nares of mice. *Bioengineered Bugs* **1**, 404-407 (2010).

157 Fenton, M., Ross, R. P., McAuliffe, O., O'Mahony, J. & Coffey, A. Characterization of the staphylococcal bacteriophage lysin CHAP(K). *Journal of Applied Microbiology* **111**, 1025-1035 (2011).

158 Hathaway, H., Ajuebor, J., Stephens, L., Coffey, A., Potter, U., Sutton, J. M. & Jenkins, A. T. A. Thermally triggered release of the bacteriophage endolysin CHAPK and the bacteriocin lysostaphin for the control of methicillin resistant Staphylococcus aureus (MRSA). *Journal of Controlled Release* **245**, 108-115 (2017).

159 La Ragione, R. M., Narbad, A., Gasson, M. J. & Woodward, M. J. In vivo characterization of Lactobacillus johnsonii FI9785 for use as a defined competitive exclusion agent against bacterial pathogens in poultry. *Letters in Applied Microbiology* **38**, 197-205 (2004).

160 Gervasi, T., Horn, N., Wegmann, U., Dugo, G., Narbad, A. & Mayer, M. J. Expression and delivery of an endolysin to combat Clostridium perfringens. *Applied Microbiology and Biotechnology* **98**, 2495-2505 (2014).

161 114th USA Congress (2015-2016). S.185 - Promise for Antibiotics and Therapeutics for Health (PATH) Act. https://www.congress.gov/bill/114th-congress/senate-bill/185

162 114th Congress (2015-2016). H.R.3012 - Right to Try Act of 2015. https://www.congress.gov/bill/114th-congress/house-bill/3012

Chapter 4: Poly(*N*-isopropylacrylamide-*co*-allylamine) (PNIPAM-*co*-ALA) Nanospheres for the Thermally Triggered Release of Bacteriophage K

4.1 Introduction

The research presented in this Chapter is based on the utilisation of bacteriophage for the treatment of wound infection. As discussed in Chapter 3, phage have been used in the treatment of a wide variety of bacterial infections, demonstrating clinical success in their application. This Chapter describes a stimuli-responsive carrier matrix for the controlled delivery of bacteriophage K, based upon the physiological change in skin temperature associated with wound infection (Figure 1). This research aims to provide a proof of concept, prototype wound dressing, housing staphylococcal phage encapsulated within polymeric nanoparticles, anchored onto non-woven polypropylene via plasma activation. Conceptually, this work is concerned with the prevention of any unnecessary administration of an antimicrobial, whilst reducing the need for continuous wound inspection and dressing changes. This aims to decrease patient discomfort and reduce clinical intervention.

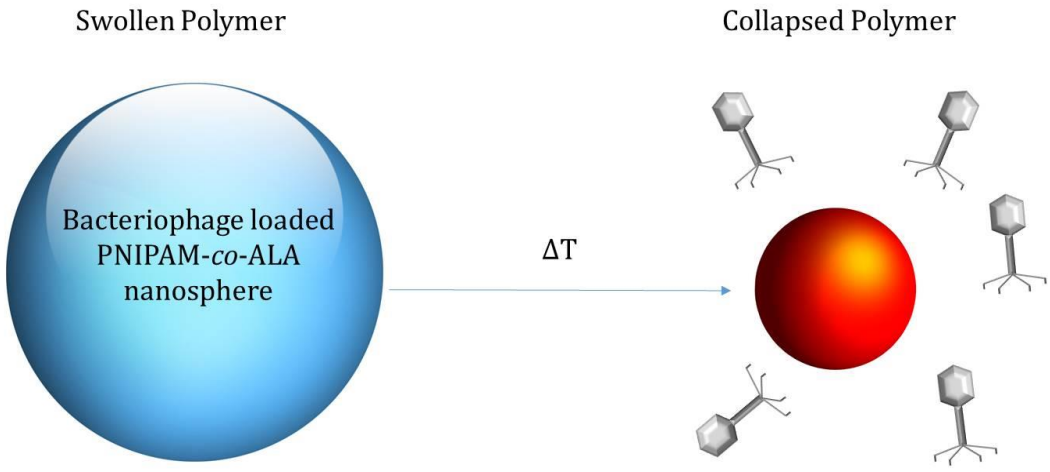

Figure 1 Schematic representation of the thermally triggered release of bacteriophage from PNIPAM-*co*-ALA nanospheres, arising as a result of the entropically driven collapse of the polymeric particles at higher temperature.

4.1.1 Cutaneous Wounds

As the largest organ in the human body, the skin comprises of multiple, histological layers which, alongside controlling thermoregulation, maintaining fluid homeostasis and regulating metabolic processes, acts as a primary external defence system, preventing entry of pathogenic organisms. Should an epithelial breach in the skin occur (for example as a result of a cut, graze or burn), the resultant wound must undergo a complex healing process in order to regain structural integrity and prevent infection. In 2013, the annual NHS cost of wound management was reported as £5.3 billion, representing 4% of the total expenditure on public health in the UK, comparable to the cost of managing obesity in the same year [1]. The classical (uninterrupted) wound healing process is detailed in Figure 2 [2].

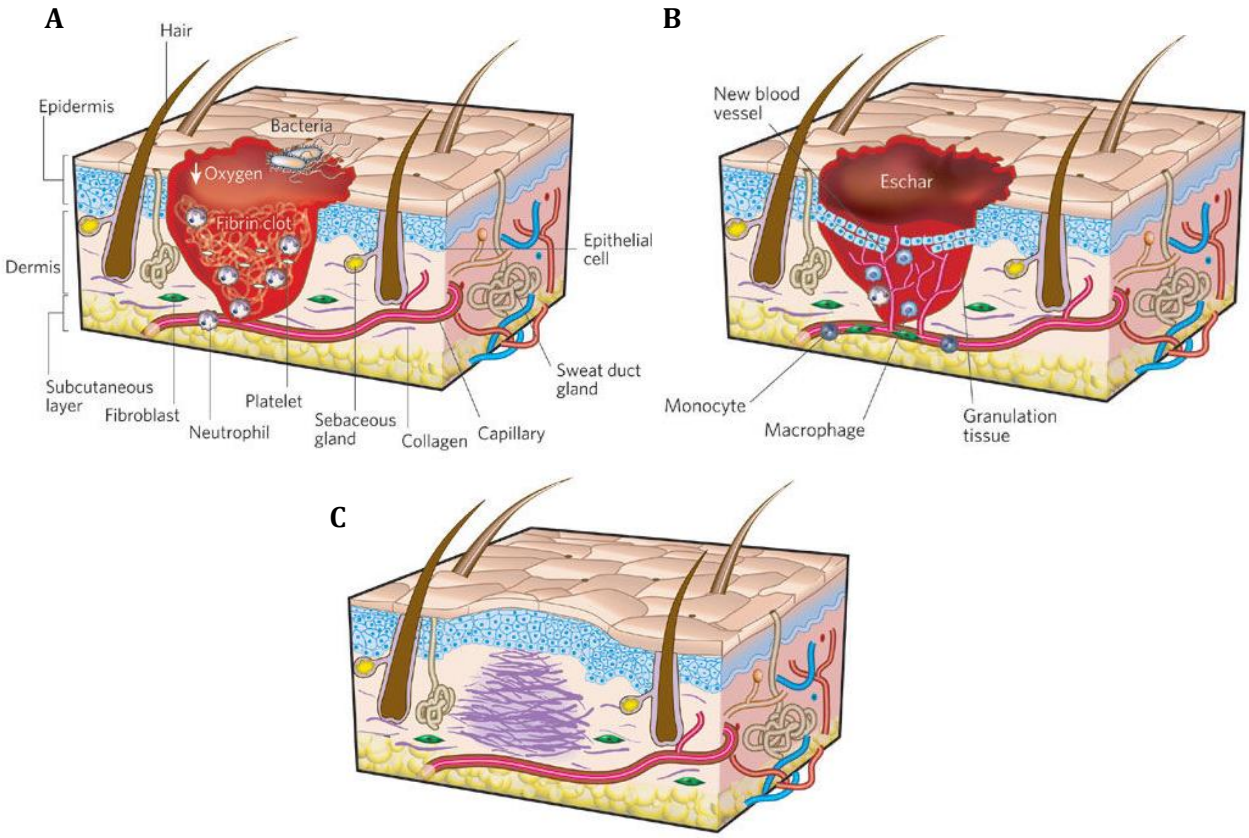

Figure 2 Schematic representing the classical wound healing process following injury. **A**) **Inflammation**; commences immediately after injury (alongside haemostasis), a fibrin clot forms and the wound environment becomes hypoxic. Neutrophils, platelets and bacteria are present within the wound. **B) Proliferation;** involving re-epithelialisation, angiogenesis and granulation. The fibrin clot is replaced with an eschar (scab) and new blood vessels populate the area, re-vascularising the wound. **C) Maturation;** can occur for up to 2 years post injury and involves development of the normal epithelium and maturation of the scar tissue. Adapted by permission from Macmillan Publishers Ltd: Nature [2]. Copyright ©2008.

4.1.1.1 Wound Classification

Wounds that heal according to the carefully regulated, systematic cascade within a predicted timeframe (as detailed in Section 4.1.1) are referred to as acute wounds. This term may encompass surgical site wounds or traumatic wounds such as burns. Whilst there may be certain factors (such as infection) which temporarily affect the normal healing process, with appropriate and timely intervention (which is often minimal), an acute wound is expected to heal according to the classical wound healing timeline, resulting in successful tissue regeneration [3].

In contrast, a chronic wound is defined as a wound which has failed to heal in a timely and orderly manner, in order to re-establish anatomical and functional integrity over a 3 month period [4]. Chronic wounds do not conform to the linear progression of classical wound healing, rather, they exhibit a prolonged inflammatory phase, becoming trapped in a continuous cycle of tissue renewal and breakdown, thereby preventing the continuation of the normal wound healing process [5]. There are a number of reasons why a wound may fail to heal correctly (both local and systemic factors), however chronic wounds are often associated with an underlying condition (such as diabetes or obesity) and are rarely seen in individuals who are otherwise healthy. The burden associated with treating chronic wounds is rapidly increasing (chronic wounds have been referred to as 'the silent epidemic'), owing to the aging population, increasing healthcare costs and a global increase in the incidence of diabetes and obesity [6]. In the USA alone, it has been reported that chronic wounds carry an annual cost of $25 billion. Furthermore, it has been estimated that 1 -2% of the population in developed countries will develop a chronic wound in their lifetime [7]. The Wound Healing Society classifies chronic wounds into 4 categories: diabetic ulcers, venous ulcers, pressure ulcers and arterial insufficiency ulcers [8]. A detailed discussion surrounding the pathophysiology of chronic wounds is presented elsewhere [9].

4.1.2 Wound Infection

Healthy skin is permanently colonised by a number of bacterial species with a reported 10^3 - 10^4 microorganisms per cm^2 skin (rising to 10^6 in moist areas) [10]. Exhibiting a symbiotic relationship with the host and contributing to a healthy skin microflora, microbial colonisation at the point of injury can play a significant role in subsequent wound healing. In some cases, opportunistic and pathogenic organisms located in close proximity to the wound gain entry to the surrounding tissues and initiate an infection, thus impairing successful

wound healing. The nature of the infection can vary; it may be localised (requiring minimal intervention) or it may spread to surrounding tissues, causing a deep or systemic infection (requiring significant clinical intervention). One of the most challenging aspects of wound management is the clinical definition and assessment of the wound itself. It is important to note that contamination of a wound (either by opportunistic members of the normal skin flora, exogenous bacteria introduced from the environment or endogenous bacteria from surrounding mucosal membranes), does not necessarily result in infection. However, the sustained presence of proliferating microorganisms residing within a wound eventually increases the bacterial burden to a critical level (critical colonisation), which is sufficient to overcome the host inflammatory response, thus resulting in infection. The extent of the infection, relative to the nature of the wound often dictates the healing process; therefore, both of these variables must be established in order to initiate effective treatment. To date, there is no universally accepted classification system for skin and soft tissue infections (SSTIs), likely owing to the vast number of variables associated with clinical presentation (such as the anatomical location, rate of progression, degree of necrosis, aetiological agent(s) responsible and severity of both the wound and the infection) [11].

4.1.2.1 Acute Wound Infection

In 2013 the FDA defined the term acute bacterial skin and skin structure infection (ABSSSI) and published guidelines on the clinical presentation of such infections. This term encompasses cellulitis, major skin abscesses, wound infections (with a minimum lesion surface area of 75 cm^2) and erysipelas [12]. In terms of diagnosis, the most effective techniques (and the point at which they are initiated or deemed necessary) for microbiological analysis of an infected wound, alongside the most appropriate wound management strategy, are two critical factors debated amongst clinicians [13,14]. Cultures obtained from surface swabs often only identify commensal colonising microbes, failing to represent the specific pathogen(s) responsible for infection, and the sensitivity of blood cultures is low. Tissue biopsies, radiological imaging and ultrasonography are the most valuable tools in diagnosis of ABSSSIs [15]. However, the clinical identification of the pathogen(s) responsible for an ABSSSI is often neglected in favour of commencing antibiotic therapy in cases of suspected (or confirmed yet unidentified) wound infection. This largely involves the administration of broad-spectrum antibiotics and arguably, often subjective monitoring of the therapeutic impact [16]. Recent evidence suggests that a 5-7 day course of antimicrobial therapy is sufficient to treat uncomplicated SSTIs, however clinically; courses of up to 2 weeks are often prescribed [17]. Not only does this contribute to drug resistance (as discussed in Chapter 3), it is also associated

with enhanced drug toxicity and the development of secondary infections (for example infections caused by *Clostridium difficile*) [18,19].

Globally, the most common pathogen associated with ABSSSIs is *S. aureus*, including MRSA [15]. Potential resistance to antibiotic therapy offers an additional challenge in the successful treatment of such infections. In fact, inappropriate treatment of MRSA-associated infections is a significant factor in the development of recurrent infection, such that the 2013 FDA guidelines specify certain considerations for the development of new drugs for complicated ABSSSIs [12,20]. MRSA infections result in extended hospitalisation, increased mortality and a significant increase in associated cost. It has been reported that for surgical site infections caused by *S. aureus*, the average, excess hospital charges associated with MRSA compared to a susceptible infection is ~$14,000 per case [21].

4.1.2.2 Chronic Wound Infection

The complexity of infection is complicated further in the case of chronic or non-healing wounds. A recent systematic review and meta-analysis of published literature conducted by Malone *et al*, analysed 185 chronic wounds and identified bacterial biofilms in 78.2% of the wounds. Further analysis of current *in vitro* and animal models resulted in a final conclusion stating that bacterial biofilms are ubiquitous in human, non-healing chronic wounds [22]. The establishment of bacterial biofilms in chronic wounds causes a number of complications with respect to effective treatment. The protective nature of a biofilm enables microbial cells to evade the host immune response, alongside providing an environment in which bacteria are often more virulent and resistant to antibiotic treatment [23]. Indeed, bacteria within a biofilm often exhibit increased tolerance to systemic antibiotic treatment, owing to their reduced metabolic activity (certain classes of antibiotics: β-lactams, aminoglycosides and quinolones are only effective against actively dividing cells) [24].

Furthermore, the aetiology of chronic infections often differs from acute infections. In addition to commensal microbes, opportunistic pathogens (especially Gram-negative species such as *P. aeruginosa*), play a greater role in chronic infections and impaired wound healing [25]. The formation of polymicrobial biofilms can lead to enhanced virulence; a study conducted by Korgaonkar *et al* demonstrated the synergistic interaction between *P. aeruginosa* and *S. aureus* in a polymicrobial biofilm, resulting in the production of extracellular, lytic virulence factors [26]. The propensity towards infection (and the subsequent formation of biofilms),

alongside the rise in MDR (as discussed in Chapter 3) makes effective treatment of chronic wounds notoriously difficult to implement and sustain.

4.1.3 Temperature as an Indication of Infection

Alongside the microbiological characterisation/assessment of a wound, there are other physical characteristics associated with the development of infection. As indirect indicators of infection, these features may include an increase in wound pH, a change in wound exudate or an increase in surface temperature, the latter being the most relevant to this thesis [27]. A number of different studies have evaluated the change in temperature of a wound (both acute and chronic) and how it correlates to wound healing [28,29]. An initial, localised increase in wound temperature (via inflammation), is often associated with successful healing [30].

However, a prolonged or significant increase in temperature has been correlated with the development of infection. A study involving 112 patients over a 6 month period used infrared thermography to measure the periwound temperature of leg and foot ulcers, in order to evaluate surface temperature as an indicator of infection. Patients presenting with an elevated periwound temperature were eight times more likely to be diagnosed with a deep infection [31]. Furthermore, a clinical pilot study identified a statistically significant relationship between skin temperature and wound infection, manifesting as a difference of 3 – 4 °C between a chronically infected wound and normal tissue [32].

One of the most challenging aspects of evaluating temperature as a marker for infection is eliminating any temperature fluctuations associated with the normal healing process. A study aimed at quantifying the temperature gradient of healing wounds, post infection (i.e. inflamed but uninfected) reported a temperature change of ±2 °C, whereas the temperature of healthy skin is reported to fluctuate by ±1 °C [33,34]. Therefore, despite the observed increase in skin temperature as a result of an inflammatory response to wound healing, an infection appears to increase the temperature further, providing a significant physical change associated with infection. A recent study conducted by Chanmugam *et al*, confirmed this by using long-wave infrared thermography to measure the difference in the relative temperature maximum of normal healing wounds (control group), wounds with associated inflammation and clinically infected wounds. The results indicated a temperature fluctuation of ±1.1 - 1.2 °C in normal healing wounds, a temperature gradient of ±1.5 - 2.2 °C in inflamed wounds and a maximum temperature differential of infected wounds of +4 - 5 °C (Figure 3) [35].

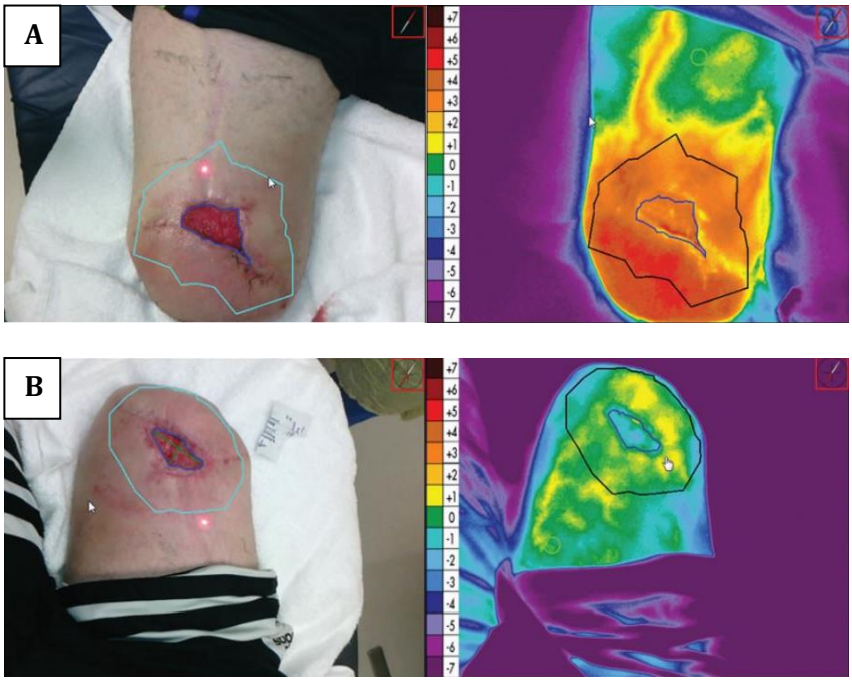

Figure 3 Long-wave infrared thermography showing the change in temperature gradient of an open wound on an amputation site **(A)** at the point of infection, pre-antibiotic treatment, exhibiting a relative, wound bed temperature maximum of +5 °C **(B)** free from infection, post-antibiotic treatment, exhibiting a relative, wound bed temperature maximum of +0.8 °C. Reprinted from [35] with permission from Wolters Kluwer Health, Inc. Copyright © 2017.

The research described henceforth in the succeeding publication aims to utilize a change in temperature, in order to deliver a biological antimicrobial agent (as an alternative to antibiotics), in a timely and controlled manner. This proof of concept technology may be developed further for use in a wound dressing owing to the temperature-associated presentation of infection in cutaneous wounds (predominantly chronic wounds).

4.2 Extended Methodology

4.2.1 Principles of Bacterial Growth

In order to study and quantify bacterial growth, cells are cultured in liquid medium (which provides optimum growth conditions and contains all the necessary nutrients required for reproduction). Aliquots are subsequently plated onto solid agar medium in order to quantify bacterial cell numbers. During cultivation in liquid media, bacteria exhibit four distinct

growth phases, which can be monitored according to the change in cell density over time. The first phase in the bacterial growth curve is referred to as the initial lag phase, whereby the cells are preparing for reproduction (i.e. via DNA replication and enzyme production). The second is the exponential growth phase, during which time the cells begin dividing (via binary fission) and cell numbers increase exponentially. Following the exponential phase the cells enter a stationary phase, during which the rate of cell growth (division) is equalled by the rate of cell death, resulting in a plateau with no net increase in cell numbers. Finally, upon depletion of available nutrients and accumulation of waste products, the cells enter the death phase where bacterial cell count begins to decline. Cell density may be assessed photometrically using optical density (OD) measurements, which correlate the degree of light scattering (or turbidity) to cell density. The bacterial growth curve as a function of both cell count and OD is shown graphically in Figure 4.

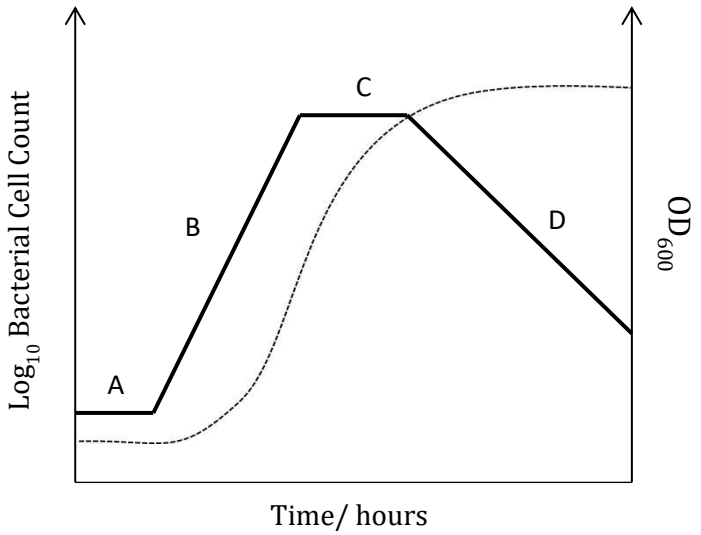

Figure 4 Bacterial growth curve showing the change in bacterial cell count over time (solid line) and the corresponding change in optical density at 600 nm (dotted line). The graph shows **(A)** the lag phage, **(B)** the exponential growth phase, **(C)** the stationary phase and **(D)** the death phase. The OD does not decline during the death phase as dead cells will still scatter light and exhibit turbidity in solution.

4.2.1.1 Quantifying Bacterial Cell Count

A measure of bacterial cell count is the colony forming unit (CFU). This refers to a single colony (grown on an agar plate) which has arisen from a singular viable cell, resulting in a cluster of cells derived from the same parent, which are genetically identical (forming a clone). Colonies can be obtained via plating onto nutrient agar, following dilution from liquid

culture [36]. Following incubation, plates with 30 – 300 colonies may be used in order to calculate the number of CFU per unit volume (CFU/ ml), providing an estimate of the number of cells in the original culture, according to the following equation:

$$\text{CFU/ ml} = \frac{\text{Number of Colonies}}{\text{d} \times \text{V}} \quad (1)$$

Where d is the dilution factor (from original culture) and V is the volume of inoculum (ml).

4.2.2 Principles of Bacteriophage Propagation

Phage propagate within a bacterial host (as described in Chapter 3). In order to obtain pure phage lysate, the phage and corresponding bacterial host strain are incubated together to facilitate phage infection and replication. There are a number of methods of obtaining phage lysate, however the research presented in the succeeding publication utilises the double layer method. Following overnight incubation of phage/ host cultures, soft agar is added (which facilitates an even distribution of bacteria and phage, providing optimum visualisation of phage activity). The solution is then poured onto agar plates and incubated overnight. Buffer containing chloroform is then added to the plates displaying confluent lysis (clearance of bacteria) in order to kill any resistant isolates. The plates are incubated again in order to extract the phage and the solution is removed from the plate. Finally, the lysate is centrifuged and filter-sterilised in order to remove any cell debris and stored at 4 °C, for use experimentally or for further propagation.

4.2.2.1 Quantifying Phage Titre

The titre (or concentration) of a phage solution can be quantified via the spot test. Phage form plaques (zones of bacterial clearance) when spotted onto a bacterial lawn. The number of plaque forming units (PFU) on a bacterial lawn can be quantified, which provides an estimate of the number of phage in the starting lysate. The spot test involves the addition of 100 µl of growing host culture to 3 ml of soft agar, which is then poured onto agar plates and left to dry. The phage lysate is then serially diluted 10-fold in buffer and 10 µl aliquots are spotted onto the bacterial lawns. The plates are then incubated overnight (Figure 5).

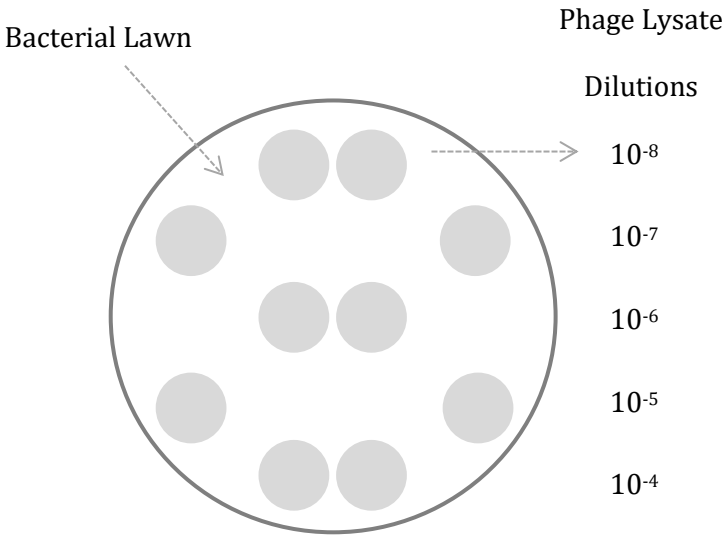

Figure 5 Schematic outlining the spot test method for bacteriophage titration.

The number of plaques is counted and the PFU per ml can be quantified according to the following equation:

$$\text{PFU/ ml} = \frac{\text{Number of Plaques}}{\text{d} \times \text{V}} \quad (2)$$

Where d is the dilution factor (from original lysate) and V is the volume of inoculum (ml).

4.3 Publication

4.3.1 Declaration of Authorship

<table>
<tr><td colspan="10">This declaration concerns the article entitled:</td></tr>
<tr><td colspan="10">Poly(N-isopropylacrylamide-co-allylamine) (PNIPAM-co-ALA) Nanospheres for the Thermally Triggered Release of Bacteriophage K</td></tr>
<tr><td colspan="10">Publication status (tick one)</td></tr>
<tr><td>Draft manuscript</td><td></td><td>Submitted</td><td></td><td>In review</td><td></td><td>Accepted</td><td></td><td>Published</td><td>✓</td></tr>
<tr><td>Publication details (reference)</td><td colspan="9">Hathaway, H., Alves, D. R., Bean, J., Esteban, P. P., Ouadi, K., Sutton, J. M. & Jenkins, A. T. A. Poly(N-isopropylacrylamide-co-allylamine) (PNIPAM-co-ALA) nanospheres for the thermally triggered release of Bacteriophage K. European Journal of Pharmaceutics and Biopharmaceutics 96, 437-441, doi:10.1016/j.ejpb.2015.09.013 (2015).</td></tr>
<tr><td>Candidate's contribution to the paper (detailed, and also given as a percentage).</td><td colspan="9">The candidate predominantly executed the…

Formulation of ideas:
Conceptually this study was designed by the candidate, including trouble shooting and development of the concept into the presented form (100%).
Design of methodology:
All methodology was decided upon by the candidate (100%).
Experimental work:
All experimental work except initial bacteriophage preparation was undertaken by candidate. Some research was undertaken in conjunction with other authors (90%).
Presentation of data in journal format:
Manuscript was written and prepared by candidate. Proof reading given by some of the other authors (90%).</td></tr>
<tr><td>Statement from Candidate</td><td colspan="9">This paper reports on original research I conducted during the period of my Higher Degree by Research candidature.</td></tr>
<tr><td>Signed</td><td colspan="5">  </td><td>Date</td><td colspan="3">29.09.17</td></tr>
</table>

4.3.2 Copyright Agreement

Copyright Agreement

This Agreement between Hollie Hathaway ("You") and Elsevier ("Elsevier") consists of your license details and the terms and conditions provided by Elsevier and Copyright Clearance Center.

License Number	4126550167309
License date	Jun 12, 2017
Licensed Content Publisher	Elsevier
Licensed Content Publication	European Journal of Pharmaceutics and Biopharmaceutics
Licensed Content Title	Poly(N-isopropylacrylamide-co-allylamine) (PNIPAM-co-ALA) nanospheres for the thermally triggered release of Bacteriophage K
Licensed Content Author	Hollie Hathaway
Licensed Content Date	Oct 1, 2015
Licensed Content Volume	96
Licensed Content Issue	n/a
Licensed Content Pages	5
Start Page	437
End Page	441
Type of Use	reuse in a thesis/dissertation
Portion	full article
Format	both print and electronic
Title of your thesis/dissertation	Biomodification of Abiotic Surfaces for the Prevention of Hospital-Associated Infection
Expected completion date	Oct 2017
Estimated size (number of pages)	200

4.3.3 Data Access Statement

All data created during this research is openly available from the University of Bath data archive at https://doi.org/10.15125/BATH-00335.

4.3.4 Published Article

Poly(*N*-isopropylacrylamide-*co*-allylamine) (PNIPAM-*co*-ALA) Nanospheres for the Thermally Triggered Release of Bacteriophage K

Hollie Hathaway[1], Diana R. Alves[1], Jessica Bean[1], Patricia P. Esteban[2], Khadija Ouadi[3], J. Mark Sutton[4], A. Toby A. Jenkins[1]*

1. Department of Chemistry, University of Bath, UK, BA2 7AY
2. Department of Chemical Engineering, University of Bath, UK, BA2 7AY
3. Department of Biology and Biochemistry, University of Bath, UK, BA2 7AY
4. Technology Development Group, Public Health England, Porton Down, Salisbury, Wiltshire, UK, SP4 0JG

*Corresponding Author: Email: a.t.a.jenkins@bath.ac.uk, Tel: +44 (0) 1225 386118

Abstract

Due to the increased prevalence of resistant bacterial isolates which are no longer susceptible to antibiotic treatment, recent emphasis has been placed on finding alternative modes of treatment of wound infections. Bacteriophage have long been investigated for their antimicrobial properties, yet the utilization of phage therapy for the treatment of wound infections relies on a suitable delivery system. Poly(*N*-isopropylacrylamide) (PNIPAM) is a thermally responsive polymer which undergoes a temperature dependent phase transition at a critical solution temperature. Bacteriophage K has been successfully formulated with PNIPAM nanospheres copolymerized with allylamine (PNIPAM-*co*-ALA). By utilizing a temperature responsive polymer it has been possible to engineer the nanospheres to collapse at an elevated temperature associated with a bacterial skin infection. The nanogels were reacted with surface deposited maleic anhydride in order to anchor the nanogels to non-woven fabric. Bacteriophage incorporated PNIPAM-*co*-ALA nanospheres demonstrated successful bacterial lysis of a clinically relevant bacterial isolate - *Staphylococcus aureus* ST228 at 37 °C, whilst bacterial growth was unaffected at 25 °C, thus providing a thermally triggered release of bacteriophage.

Keywords: PNIPAM, Bacteriophage, Thermal Release

Introduction

The triggered release of a pharmaceutically active substance (small molecule, protein, virus) from a particle has been the subject of much interest in recent years as the utilization of such a device clinically could be used to provide dosing of a drug or drug candidate both where, and when it is needed and at a high local concentration [37,38]. Triggered delivery can mean that an agent is only released following a pathological change in the patient, preventing unnecessary usage of a drug, but also ensuring that it is provided at a sufficiently high dosage in-situ to be pharmacologically effective. Systemic antibiotics to combat bacterial infection have to be used at relatively high dosages to give a sufficiently high concentration within blood / tissue at the infection site in order to prevent further bacterial growth. Indeed, should the concentration of an antibiotic be too low at the site of infection, the effect can be to increase the rate of evolution of antibiotic resistance and virulence within the infecting organism [39].

The delivery of a drug to a target site via a carrier particle or matrix can allow the slow, passive diffusion of that drug from the carrier matrix, with the diffusion rate being controlled by the matrix viscosity and size of the drug (based on Fick's laws). Examples of such systems for topical application of drugs include skin patches for nicotine administration and transdermal pain relief delivery [40,41]. Alternatively, a burst response can be engineered, which though still ultimately diffusion controlled would deliver the drug at a much higher rate. The initiation of the burst response might utilize an external trigger, which in a wound site could be a molecule released by the infective bacteria: secretion toxins, enzymes, signalling molecules etc. [42-44], changes in the host immune response (e.g. cytokines) or a more general host tissue response such as pH or temperature change [45,46].

Poly (*N*-isopropylacrylamide) (PNIPAM) is a thermally responsive polymer which undergoes a fully reversible temperature dependent phase transition at a lower critical solution temperature (LCST) which manifests as a change in polymer volume. Following the entropically favoured expulsion of water at the LCST, the polymer undergoes a characteristic morphological change from a random coil structure to a hydrophobic globule structure [47]. The LCST of PNIPAM can vary from 32 °C to 36 °C depending on a number of factors including polymer concentration, the presence of surfactants and the use of copolymers [48]. The fact that the LCST is near to body temperature of 37 °C means that PNIPAM has been relatively well researched and utilized within the bioengineering industry as a drug delivery platform [49]. PNIPAM nanospheres copolymerized with allylamine (PNIPAM-*co*-ALA) made in previous

work were measured using Dynamic Light Scattering (DLS) to change from a mean diameter of 210 nm at 33 °C to 70 nm at 37 °C [50]. This decrease in size was previously utilized to release silver ions, the putative aim being to exploit the potentially antimicrobial properties of silver in a future wound dressing.

Bacteriophage (phage) are viruses which reproduce via infection of specific bacterial hosts. They are capable of attaching themselves to specific receptors located on the surface of a bacterial cell, injecting their genetic information (in the form of DNA or RNA) into the cell taking advantage of the bacterium's cellular machinery in order to replicate in vivo, ultimately resulting in the rupture and destruction of the bacterium [51]. First discovered and used clinically in the 1930s in the former Soviet Union, their potential utility as antimicrobial agents is being re-examined with the rapid evolution of antibiotic resistance in many common infectious bacterial organisms such as *Staphylococcus aureus* (*S. aureus*) [52]. The potential advantages of phage are that they co-exist with their host bacteria, so strains which are active against target bacteria can be prospected for and isolated with relative ease. Moreover they are fairly host strain specific, and are normally harmless to host eukaryotic cells. However the regulatory environment surrounding the clinical application of phage is only slowly adjusting to the utilization of a biological agent for infection control, in part because some types of phage can deliver host virulence or antibiotic resistance factors via lysogenic conversion: an example being the shiga toxin in *Escherichia coli* and the mecA resistance cassette in methicillin resistant *S. aureus* [53,54]. However, by careful selection of phage phenotypes and genotypes, lysogenic strains can be avoided and current indications are that phage may have an important role in the future armoury of antimicrobial substances.

One important consideration when utilizing phage to destroy pathogenic bacteria is the multiplicity of infection (MOI), the ratio of phage to bacteria. The concentration of phage must be high enough to ensure rapid infection, multiplication and lysis of the target bacteria before non-susceptible bacteria present at the point of infection utilize the space and resources provided by death of their co-infecting cells [55]. Much of the current effort in phage therapy is concerned with topical delivery, for example in chronic otitis media (ear infection) and wounds. Delivering phage via a wound dressing requires the phage to be contained within a reservoir until required, ideally only when their target bacterial hosts are present and at a sufficient density to provide an environment for efficient phage propagation.

In this paper, bacteriophage have been formulated with PNIPAM-*co*-ALA nanospheres and the particles grafted via a plasma deposited film of maleic anhydride to non-woven

polypropylene. Allylamine was chosen as the copolymer in order to control the LCST and to provide readily available functional groups for the surface anchoring of the nanoparticles. The use of plasma deposited maleic anhydride for attachment of particles / proteins / molecules to surfaces has been discussed in detail elsewhere [56-58]. The infectivity of the phage was assessed against a clinically relevant Methicillin Resistant *S. aureus* (MRSA) strain (ST228). The bacteria itself is a multiple-antibiotic resistant, gentamicin resistant SCC*mec* (Staphylococcal chromosomal cassette *mec*) I strain of MRSA from clonal complex (CC) 5 [59], one of the most clinically relevant clonal complexes worldwide [60]. This clonal lineage is of particular interest clinically due to previously documented instances in which the clone has exhibited sporadic periods of extremely high transmissibility [61].

Materials and Methods

Materials

N-isopropylacrylamide, allylamine, ethylene-glycol diacrylate, sodium persulphate, sodium dodecylsulfate (SDS), poly(ethylene glycol) (PEG), sodium chloride, magnesium sulphate, calcium chloride and tris-hydrochloride (pH 7.5) were all purchased from Sigma-Aldrich (Poole, Dorset, UK).

Bacteriophage K (phage K) was obtained from D. Alves (University of Bath) from a previously sourced collection. Tryptic Soy Broth (TSB) and Tryptic Soy Agar (TSA) were purchased from Sigma-Aldrich (Poole, Dorset, UK). Luria-Bertani broth (LB) was purchased from Invitrogen Life Technologies Ltd, Paisley, UK and Bacteriological agar was purchased from Thermo Scientific, Hampshire, UK. Pseudomonal and Staphylococcal bacterial isolates used in experimental work were obtained from a bacterial strain collection belonging to the Biophysical Chemistry Research Group housed at the University of Bath and the University Hospital of Lausanne respectively.

Bacteria, Bacteriophage and Growth Conditions

For this study *S. aureus* ST228 and *P. aeruginosa* PAO1 isolates were used. The isolate of ST228 used was isolated from a patient soft tissue infection. The strain was PVL negative and is PFGE subtype Db. Bacteria from TSA plates were grown at 37 °C with continual shaking (170 rpm) in TSB. TSB-soft-agar containing 0.65% of bacteriological agar and SM buffer (5 M NaCl, 1 M $MgSO_4$, 1 M Tris–HCl [pH 7.5], 0.1% gelatine solution) were used for bacteriophage

propagation and plaque count assays. Note that media was supplemented with 1 mM $CaCl_2$ and $MgSO_4$ to improve phage adsorption [62]. Bacterial aliquots were stocked at -80 °C in broth containing 15% glycerol (v/v).

Bacteriophage Propagation and Purification

Phage K was propagated in the prophage-free isolate *S. aureus* RN4220 in order to avoid any potential contamination with mobilized phage. Briefly, 100 µl of phage lysate and 100 µl of host growing culture were mixed and left for 5 min at room temperature. 3 ml of soft-agar was added and poured onto TSA plates. The following day, after an overnight incubation at 37 °C, plates displaying confluent lysis were selected and 3 ml of SM buffer and 2% chloroform were added before incubating at 37 °C for 4 h. High titre (or concentration) phage solution was removed from the plates, and centrifuged (8,000 x g, 10 min) to remove cell debris, then filter sterilized (pore size, 0.22 µm) and stored at 4 °C. By dilution of phage titre it was thus possible to observe plaques that would have been formed by an individual phage, allowing both phage concentration to be estimated and lytic activity to be quantified.

Phage K lysate purification was performed by adding 1 M NaCl and left at 4 °C overnight. The following day the solution was centrifuged (4000 rpm, 1 h) and the supernatant was carefully transferred to a new tube. 10% (w/v) PEG (m.w. 8000) was added to the lysate and left at 4 °C overnight. The solution was then centrifuged (4000 rpm, 30 min) to obtain a PEG-phage pellet. The pellet was resuspended gently in 1 ml of SM buffer and vortexed thoroughly.

PNIPAM-*co*-ALA Nanosphere Preparation

PNIPAM-*co*-ALA nanospheres were synthesized via precipitation polymerization, (Scheme 1, Supplementary Information). To a round bottomed flask containing 57.5 ml deionised water, 0.96 g N-isopropylacrylamide (10% molar ratio), 65.5 µl allylamine, 20.8 µl ethylene-glycol diacrylate (cross-linker, 1% molar ratio) and 0.0185 g SDS were added. The solution was freeze-thawed three times and purged with N_2. The solution was heated to 70 °C with stirring for 10 min, after which 0.03875 g of initiator (sodium persulphate) in 5 ml of deionised water was added and the reaction was allowed to proceed for 4 h. The gels were purified by dialysis (using 10 kDa MWCO dialysis membranes) in deionised water for 7 days.

Electron Microscopy

Phage particles in water were deposited on carbon coated copper grids and negatively stained with 1% uranyl acetate (pH 4). Visualization was performed using a transmission electron microscope (TEM) (JEOL JEM1200EXII) operated at 120 kV.

Dynamic Light Scattering and Zeta Potential Measurements

Particles were sized and characterized using a Zetasizer Nanoscale light scattering device (Malvern Instruments, Malvern, UK), which allowed measurements to be made as temperature was varied.

Grafting of PNIPAM-*co*-ALA Nanospheres to Non-Woven Polypropylene

Non-woven polypropylene (2 x 2 cm squares) were washed in isopropyl alcohol, dried and placed in a radio-frequency plasma reactor. Pressure was reduced to 0.001 mb, and maleic anhydride vapour introduced in a continual flow. RF radiation was coupled into the reactor via an inductive loop to create a plasma. The plasma was pulsed: 1 ms on / 40 ms off for 10 min. The deposition of anhydride groups was observed using Fourier Transform Infrared spectroscopy (FT-IR). Full details of this procedure are described elsewhere [63,64]. The plasma modified fabrics were then immediately placed in a suspension of the PNIPAM-*co*-ALA nanospheres at room temperature for 60 min. The formation of amides, indicative of the coupling of free amines in the PNIPAM-*co*-ALA nanospheres via nucleophilic attack to the plasma deposited maleic anhydride film was ascertained by FT-IR.

Addition of Phage to Fabric Grafted Nanospheres

Bacteriophage K of titre 10^9 PFU/ml was incorporated into the anchored gel matrix via soaking in 500 µl of phage solution for 4 h at 25 °C. The fabric was washed 3 times in deionised water to remove unbound phage and allowed to dry. Control experiments were undertaken by replacing the phage solution with SM buffer.

Bacterial Confluent Lysis Preparation and Deposition of PNIPAM-*co*-ALA Nanospheres

TSA culture plates were spread evenly with 100 µl of bacterial suspension. The plates were allowed to dry in aseptic conditions for 1 h. The nanogel-fabric swatches incorporating the

phage particles were placed onto the agar plates and incubated for 24 h. The plates were incubated upside down in order to prevent any condensation that could interfere with the phage release. Half of the plates were incubated at 37 °C (above the LCST) and half at 25 °C (below LCST). Spots (10 µl) of the phage solution were also added to individual plates in order to assess successful phage replication and growth inhibition at both temperatures without the use of nanospheres or fabric, via the appearance of plaques. Control experiments were undertaken using phage K resistant *P. aeruginosa* PA01. The thermal release of bacteriophage from the nanosphere grafted non-woven fabrics was observed as the formation of an inhibitory zone on and around the bacterial culture plate.

Results and Discussion

PNIPAM-*co*-ALA Nanospheres

The DLS measurements of the nanospheres showed an LCST at around 34 °C with the diameter of the particles decreasing from 400 nm +/- 50 nm to 170 nm +/- 30 nm, as shown in Figure 6. The collapse of the nanoparticles at 34 °C is clinically relevant as it corresponds to an elevated temperature associated with a bacterial skin infection. Whilst healthy skin has a surface temperature of around 32 °C, infected skin presents an increase in temperature of around 3.6 °C (in the case of infected leg ulcers [32]).

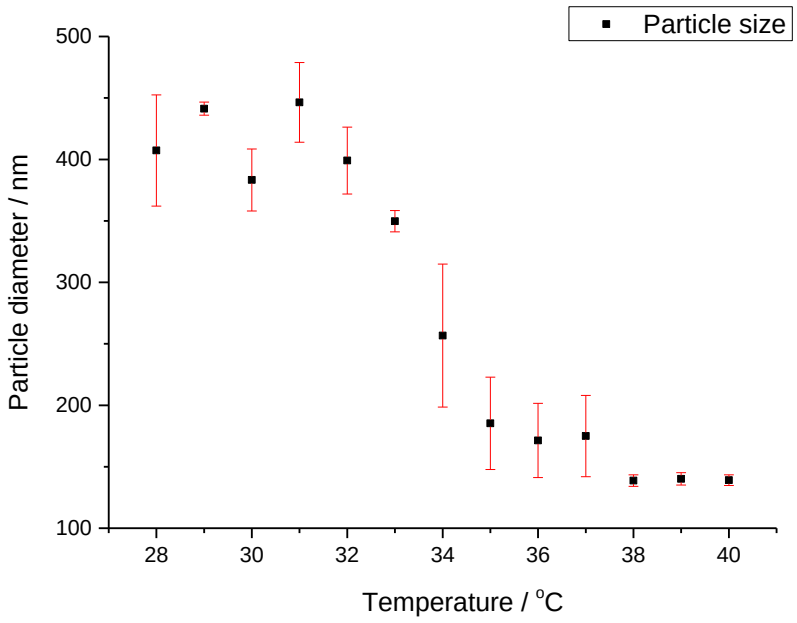

Figure 6 DLS measurement of PNIPAM-*co*-ALA nanoparticles prior to coupling to non-woven polypropylene and phage addition.

Zeta potential analysis showed a sharp increase in potential at the LCST, owed to the increase in overall surface area of the collapsed nanospheres (Figure 7).

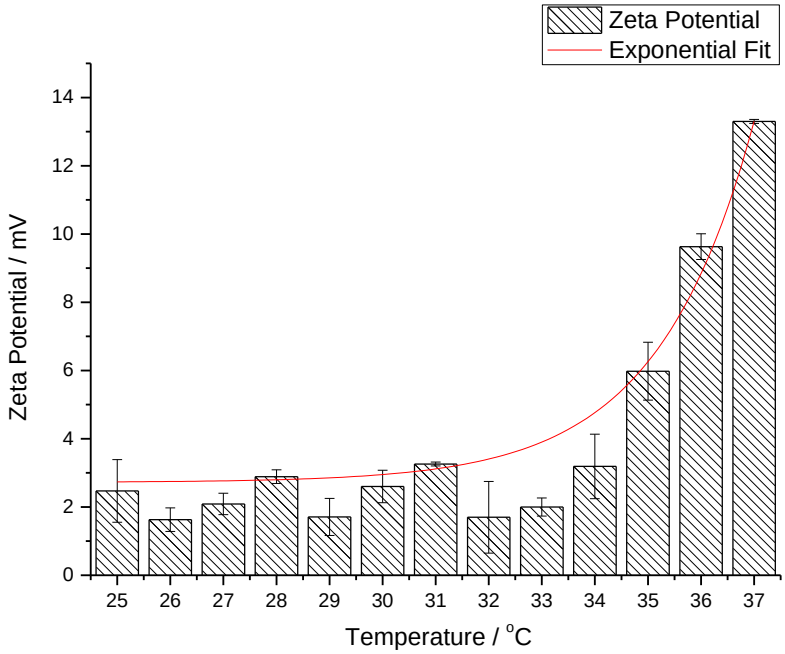

Figure 7 Zeta potential measurement of PNIPAM-*co*-ALA nanoparticles prior to coupling to non-woven polypropylene and phage addition.

Both measurements show the LCST clearly at 34 °C, the effect of which can also be clearly seen by eye (Figure 8).

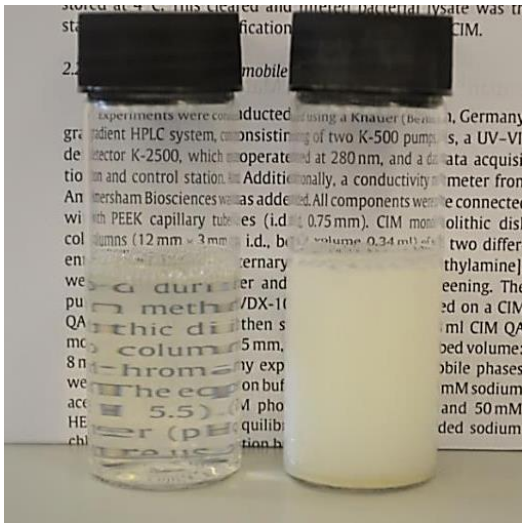

Figure 8 PNIPAM-*co*-ALA nanospheres in the swollen state (left) and collapsed state (right), the visible change is accounted for due to a change in refractive indices between the polymer and the solvent upon collapsing.

Bacteriophage activity was measured in terms of its ability to form zones of clearance (plaques) in lawns of *S. aureus*. A standard phage titre of 10^9 PFU/ml was determined for phage K, when measured on a susceptible strain of *S. aureus* ST228. Non-infectivity of phage K to *P. aeruginosa* PAO1 (control) was also confirmed. Transmission Electron Microscopy (TEM) confirmed the morphology of phage K (Figure 9).

Figure 9 TEM image of phage K. Note the icosahedral head, tail fibre and base plate containing host bacterial recognition moieties.

Attachment of PNIPAM-*co*-ALA Nanospheres to Non-Woven Polypropylene

Plasma modification of non-woven polypropylene with maleic anhydride (MA) was confirmed by FT-IR (Figure 1, Supplementary Information). The absorption peak at 1780 cm^{-1} indicative of the anhydride group is a reliable indicator of successful deposition of MA. The attachment of the PNIPAM-*co*-ALA nanospheres to the MA modified polypropylene was again confirmed by FT-IR (Figure 2, Supplementary Information) and also qualitatively implied via the subsequent thermal triggered release of phage at temperatures above the LCST.

Measurement of Thermally Triggered Release of Bacteriophage k from PNIPAM-*co*-ALA Nanospheres

The thermally triggered release of phage K was measured qualitatively via the formation of zones of clearing under and around the phage-PNIPAM-*co*-ALA non-woven polypropylene swatches found on confluent lawns of *S. aureus* ST228 (Figure 10).

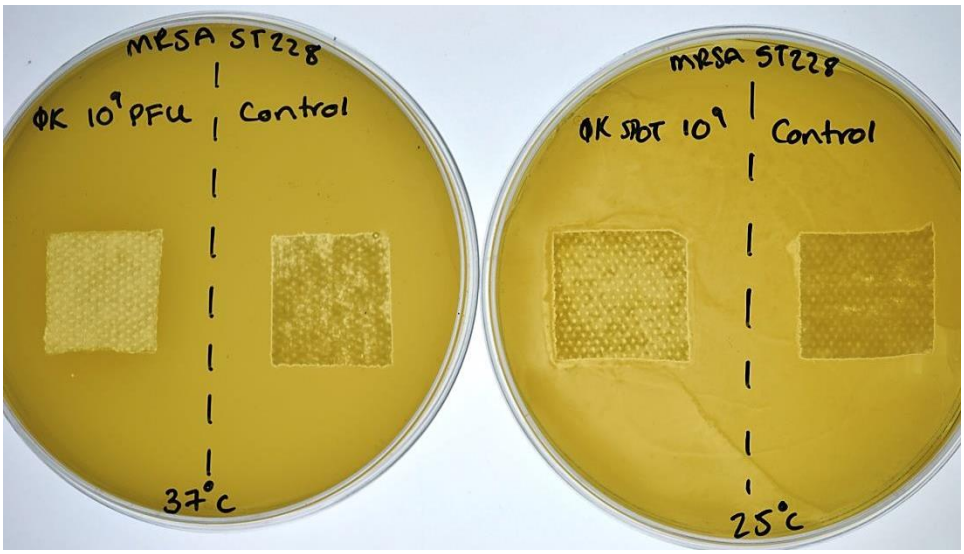

Figure 10 Confluent lawns of *S. aureus* ST228 at 37 °C (left) and 25 °C (right). A clear zone of bacteria where the phage modified PNIPAM-*co*-ALA modified non-woven polypropylene is clearly seen at 37 °C. The control in each case is the PNIPAM-*co*-ALA modified non-woven polypropylene without phage added.

The clearance of the *S. aureus* ST228 by released phage at 37 °C is clearly visible in Figure 10 (left), with the attached PNIPAM-*co*-ALA nanospheres collapsed and by implication, its cargo of phage k released. The transparency of the polypropylene swatch containing phage K at 37 °C is indicative of an absence of bacterial growth under the swatch itself. At 25 °C (right), below the LCST, the bacterial growth is little affected by the placing of the phage-PNIPAM-*co*-ALA non-woven polypropylene on the bacterial lawn, indicating that the immobilized phage are not released due to the retention of the swollen polymer state. The result of the phage containing swatch incubated at 25 °C is comparable to that of the control swatch incubated at 37 °C. Further control measurements were made on lawns of *P. aeruginosa* PAO1 (Figure 11). *P. aeruginosa* is not infected by phage K, so its inclusion was to ensure that the clear zone seen with *S. aureus* (Figure 10) was due to the release of phage and not by any other interfering process.

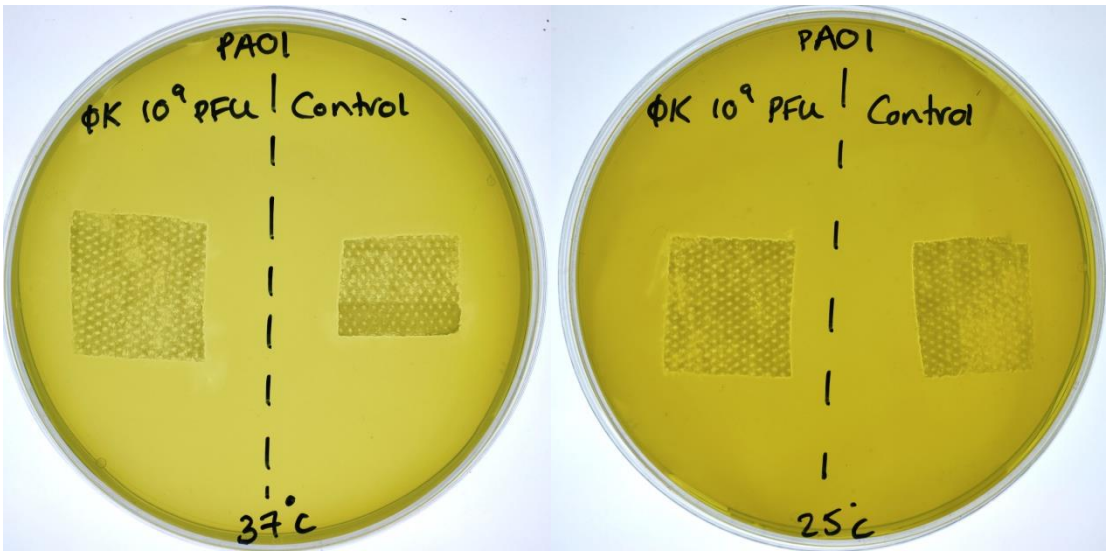

Figure 11 Control experiments with phage K modified PNIPAM-*co*-ALA nanospheres anchored onto non-woven polypropylene grown on a *P. aeruginosa* PAO1 lawn. No attenuation of bacterial growth was observed.

Whilst the optimum conditions for bacterial growth exist at 37 °C, confluent bacterial growth was assessed at 25 °C in order to confirm the successful infectivity of phage K under these conditions. This was undertaken to ensure the absence of bacterial lysis at 25 °C was not as a result of an inability of the phage to replicate. The results of this are included in the Supplementary Information for clarity, demonstrating successful bacterial lysis even at a reduced temperature (Figure 3 – Supplementary Information).

Conclusion

In summary this work has demonstrated a new and previously unreported application of a thermoresponsive polymer, engineered to provide a biologically significant trigger for the administration of bacteriophage. The importance of controlled release when evaluating treatment for bacterial infection is of the utmost importance in preventing the spread of resistance towards current and new therapies. By exploiting and developing the physical and chemical properties of new and existing 'smart materials', such as PNIPAM, it has been possible to selectively control the release of a new and potentially viable alternative treatment for bacterial infection, whilst avoiding the presentation of the continual selective pressure so often faced by bacteria due to improper administration of antimicrobials. Alongside the development of the carrier matrix for the bacteriophage, we have also

successfully covalently anchored the delivery system onto a simulated dressing platform via plasma deposition with the intention of a bandage/ wound dressing application.

Supplementary Information

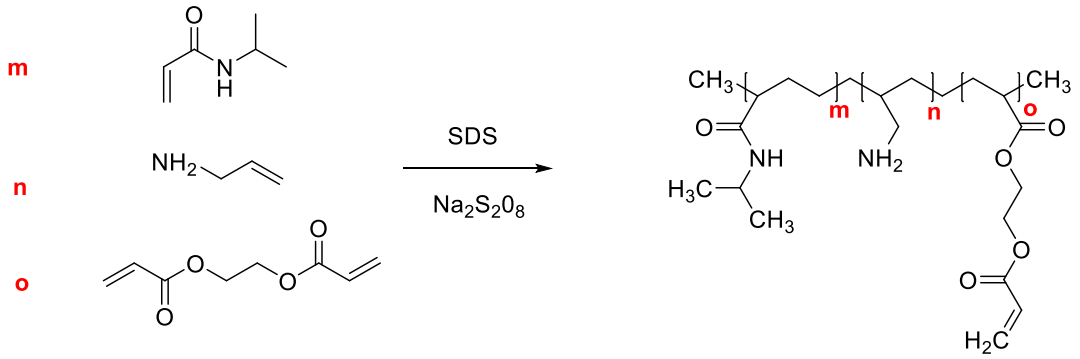

Supplementary Scheme 1 Precipitation polymerization of PNIPAM-*co*-ALA nanogels.

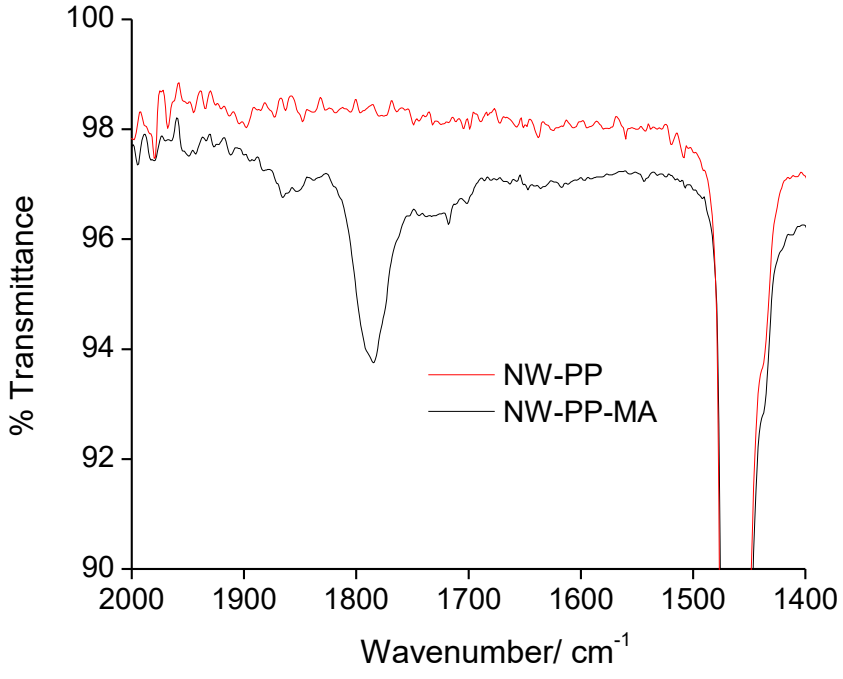

Supplementary Figure 1 FT-IR of non-woven polypropylene (NW-PP) prior to and following plasma deposition of maleic anhydride (NW-PP-MA). The peak at 1780 cm^{-1} in the NW-PP-MA spectra corresponding to the C=O carbonyl stretch of the anhydride moiety.

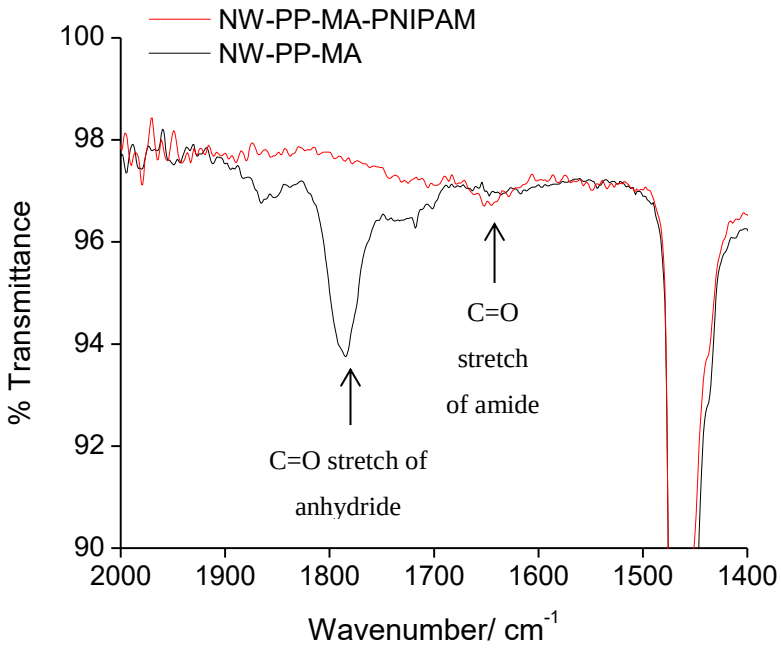

Supplementary Figure 2 FT-IR of maleic anhydride deposited non-woven polypropylene (NW-PP-MA) prior to and following addition of PNIPAM nanospheres (NW-PP-MA-PNIPAM). The shift in the C=O peak from 1780 cm^{-1} in the deposited anhydride to 1662 cm^{-1} after reaction with PNIPAM is indicative of the C=O stretch in the newly formed amide link.

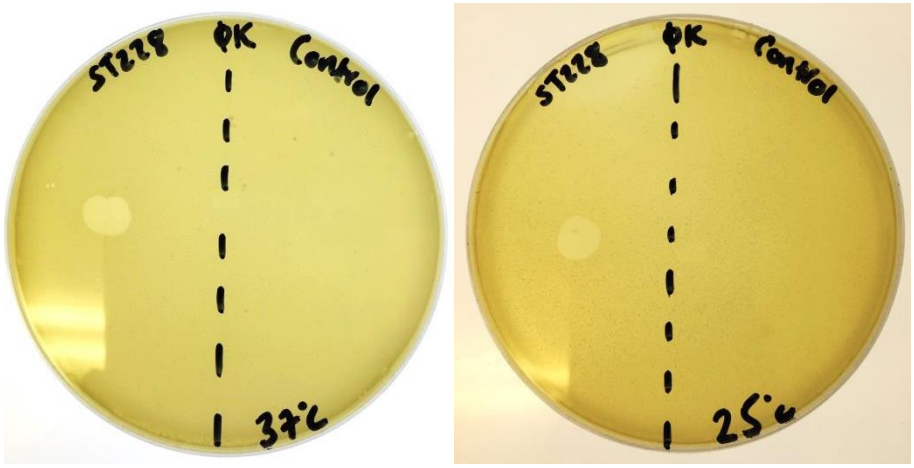

Supplementary Figure 3 10 µl of phage K spotted onto a lawn of *S. aureus* ST228 and incubated at 37 °C (left) and 25 °C (right) in order to demonstrate successful infection. The control in each case was a 10 µl spot of SM buffer only.

Author Information

Corresponding Author
* Dr. Toby Jenkins , Department of Chemistry, University of Bath, Claverton Down, Bath and North East Somerset, BA2 7AY
Tel: +44 (0) 1225 386118,
Email: a.t.a.jenkins@bath.ac.uk

Notes

The authors declare no competing financial interest. The manuscript was written through contributions of all authors.

Funding Sources

We thank the Annette Trust, the Engineering & Physical Sciences Research Council (EP/I027602/1) and the Biotechnology & Biological Sciences Research Councils (iCASE) for funding this work.

Acknowledgements

The authors wish to acknowledge Dr. Dominique Blanc and the staff of the Service of Hospital Preventive Medicine at Lausanne University Hospital for providing us access to their collection of ST228 isolates, as well as providing meta-data for each isolate.

4.4 Additional Results

Owing to the specific requirements for publication, it was not possible to include multiple images demonstrating similar results within the preceding article. However, for the purpose of clarity, additional images are presented below, aimed at providing further evidence of the thermally triggered release of bacteriophage, as detailed in the publication. Figure 12 shows the same set of plates shown in Figure 10 but with natural light behind, highlighting the transparency of the swatch containing phage at 37 °C.

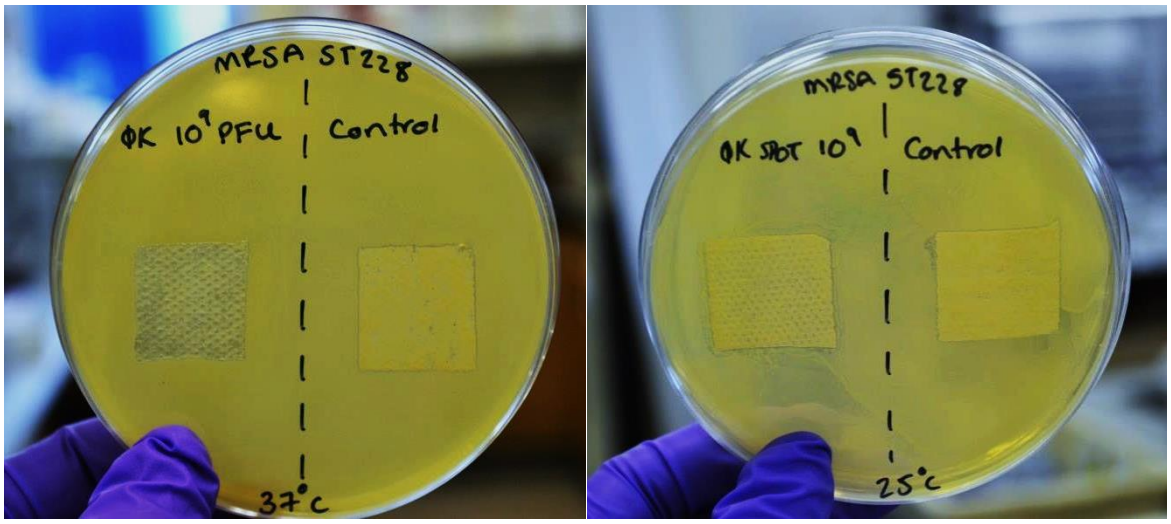

Figure 12 MRSA bacterial lawns showing temperature dependent release of bacteriophage K. The absence of bacterial growth under the PNIPAM-*co*-ALA fabric swatch at 37 °C (left), results from the antimicrobial activity of the phage released from the polymer matrix. The consistent bacterial growth seen under the swatch at 25 °C (right) indicates retention of the phage within the swollen nanoparticles.

Additional experiments were undertaken aimed at increasing the encapsulation efficiency of the phage within the nanoparticles. As oppose to relying on diffusion of the phage into the surface-anchored particles in their swollen state, the addition of phage to the collapsed polymer was investigated. However, the addition of phage to the nanoparticle solution above the LCST (40 °C) resulted in polymer precipitation (Figure 13).

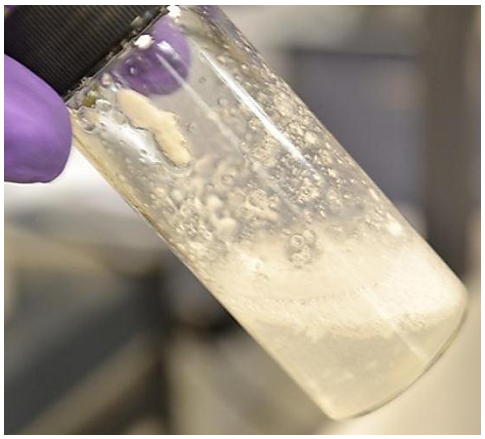

Figure 13 Solution of PNIPAM-*co*-ALA nanoparticles and bacteriophage K, showing polymer precipitation at 40 °C.

A possible explanation for this is the effect on the entropy of mixing upon addition of phage solution. Above the LCST the solvent-polymer interactions are replaced by favourable polymer-polymer interactions (Figure 14). Upon addition of aqueous phage, the apolar isopropyl units on the polymer chains facilitate ordering of the water molecules, resulting in a large negative contribution to the entropy of mixing ($\Delta S_{M)}$. The ΔS_M contribution is reflected in the Gibbs free energy of mixing (ΔG_M), resulting in a positive ΔG_M and the polymer precipitates [65].

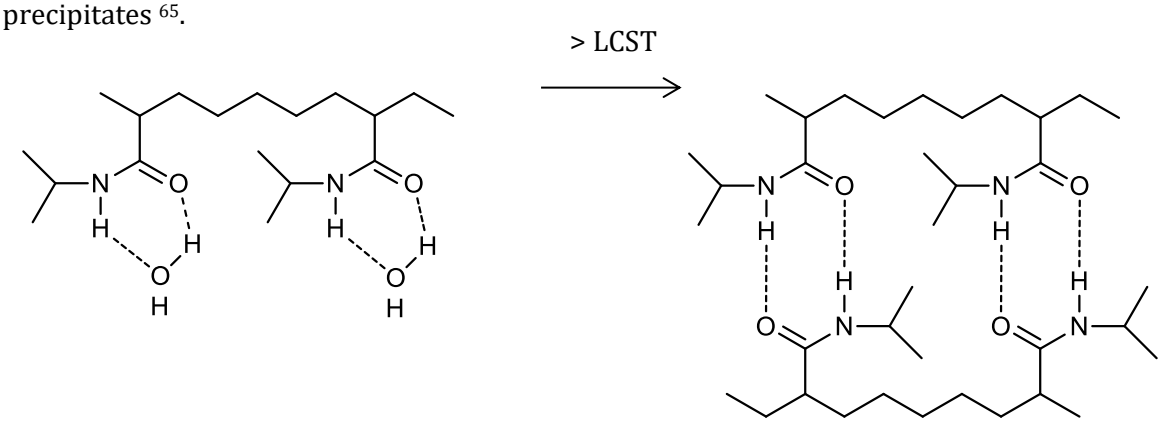

Figure 14 The change in hydrophilicity of the PNIPAM polymer above the LCST, resulting in the entropically driven expulsion of water from the hydrated polymer and the formation of favourable polymer-polymer interactions.

The observed polymer precipitation indicates that encapsulation in aqueous solution should be undertaken at the LCST or below it. It has been suggested that PNIPAM exists in a number of thermodynamically stable intermediate states during the transitional collapse of the polymer at the LCST, which may provide a stable polymeric solution in which to encapsulate phage [66].

4.5 Conclusions and Future Work

The research presented in the preceding publication describes an early, proof of concept formulation for the controlled release of a biological therapeutic from a thermoresponsive, polymeric platform. The study has focused on the potential incorporation of such technology into a dressing-based system, owing to the increase in skin temperature as a result of infection (the advantages of stimuli-responsive systems are discussed in Chapter 3). There are undoubtedly some limitations to the study presented, however as mentioned, this research is intended as a preliminary study into the retention of biological activity of encapsulated phage within a stimuli-responsive delivery system. Alongside the reported application, the technology underpinning this research has the capacity to be utilised for other biotherapeutic applications (this may include the utilisation of phage as transport vectors for the delivery of genetic material in order to sensitize bacteria to antibiotics, i.e. using the CRISPR-Cas system [67]). Nonetheless, there are a number of crucial considerations which, if addressed would enhance the reported study in its current form and intended outcome. Firstly, quantitative data establishing the rate and extent of phage release from the nanoparticles would potentially provide an understanding of the fundamental properties of the current system. This may include insight into the responsiveness of the nanoparticles, the diffusion profile of the phage into the surrounding matrix and any inhibition of biological function as a result of polymeric confinement. The stability of the phage preparation within the nanoparticles should also be evaluated in order to establish the long term viability of the encapsulated phage. Finally, the precise mechanism of phage entrapment/ encapsulation within the PNIPAM nanoparticles should be investigated. Despite the observed success in the controlled release of phage, an understanding of the polymeric immobilisation may offer the potential for enhanced stability/ delivery.

Alongside specific improvements to the research presented, further development of this technology, aimed at advancing the current study should focus on the following aspects in order to potentiate clinical implementation of such a system.

4.5.1 Bacterial Resistance

Owing to the selective pressure exerted as a result of phage predation, bacteria have evolved numerous strategies in order to resist infection. Some of the key evasion tactics include prevention of phage attachment (via modification of cell surface receptors, production of EPS or production of competitive inhibitors), degradation of phage DNA (via restriction-

modification systems) and installation of abortive infection pathways (preventing phage multiplication by initiating 'cell suicide') [68]. However, as co-evolutionary predators, phage have simultaneously evolved in order to overcome this resistance (largely via point mutations, arising as a result of complex phage-bacterium population dynamics) [69]. A dynamic equilibrium exists between phage and their bacterial hosts, which has been described as an antagonistic-coexistence paradigm. The selection of evolved phage (present as a result of bacterial resistance mechanisms) therefore ensures the survival of the phage population, whilst influencing the genetic diversity of both phage and bacteria [70]. The likelihood of bacteria becoming resistant to the therapeutic administration of phage is considered low, owing to the detrimental effects associated with the fitness of the host. Bacteria exhibiting resistance to phage demonstrate an increased susceptibility to other phage, an altered competitive ability and are subject to an enhanced cost of deleterious mutations [71]. Despite this, any potential encouragement of resistance as a result of phage therapy must be avoided at all costs. A common strategy aimed at overcoming resistance focuses on the use of a phage cocktail. This requires a mixture of different phage, displaying unrelated modes of infection in order to ensure bacterial lysis, based on the extremely unlikely development of resistance to multiple (if not all) phage isolates within a cocktail. This has been previously demonstrated in a cocktail of modified phage K derivatives, capable of circumventing multiple resistance mechanisms exhibited by a number of clinical *S. aureus* strains [72]. In addition, phage have exhibited synergy with antibiotics, offering the possibility of simultaneously reducing resistance to both [73]. Utilisation of a phage cocktail or a phage/antibiotic cocktail within a thermoresponsive delivery platform may offer increased longevity of the therapeutic system.

4.5.2 Phage Host Range

The specificity of phage provides certain benefits with regards to targeted biocontrol (unlike broad-spectrum antibiotics, phage do not disrupt the commensal microflora of the host). However, when considering a polymicrobial infection (i.e. a mixed species biofilm within a chronic wound), a single phage preparation is not sufficient to effectively eliminate all pathogenic organisms. The use of polyvalent phage (as oppose to highly strain specific phage) provides a larger therapeutic window, especially if the pathogenic bacterial species has yet to be formally identified prior to clinical intervention. Polyvalent phage exhibit a broader host range, often targeting multiple strains within a species and, in some cases, multiple species within a genus. Phage K (used in the study in question), is a polyvalent phage, effective against both coagulase-positive and -negative staphylococci [74]. Additionally, phage K lacks the

specific recognition site (GATC) for restriction modification by specific host endonucleases, thus exhibiting an effective counter-resistance strategy [75]. However, in order to increase the therapeutic window further, a phage cocktail consisting of a number of different phage isolates should be employed. Expanding the host range of a phage cocktail provides an effective means of targeting multiple bacterial isolates, ranging from Gram-positive to – negative species. This would be especially beneficial in the case of a mixed species wound infection.

4.5.3 Biofilm Formation

As discussed in Section 4.1.22, biofilm-associated infections are commonplace in SSTIs. In the current application, the increase in wound temperature as an indication of infection predominantly relates to chronic wounds, which are especially susceptible to the formation of biofilms. The use of phage to treat biofilm-associated infections has been widely investigated [76,77]. Whilst biofilms are substantially more difficult to treat with conventional antibiotics and biocides (largely owing to the protective nature of the EPS and the presence of metabolically inactive persister cells), phage exhibit unique characteristics which have shown promise in the penetration and eradication of biofilms. The infectivity of phage and the production of EPS degrading enzymes has shown increased efficacy in the targeting of bacterial biofilms. In order to effectively model an infected wound scenario (and any temperature-associated effects) it would be beneficial to test the phage-PNIPAM system on a biofilm (preferably mixed-species). In addition, whilst phage are capable of producing EPS degrading enzymes, this occurs largely inside the bacterial cell prior to lysis, thus relying on initial penetration of the biofilm and the successful establishment of phage infection [78]. Perhaps an additional consideration would be the incorporation of a biofilm disrupting agent (i.e. proteinase K), in order to facilitate rapid phage penetration into the biofilm in the first instance [79].

4.5.4 Immune/ Cytotoxic Response

An essential consideration regarding the potential implementation of any medical product/ device is the effect of the combined components on the host. As naturally occurring biological entities, phage are (in themselves) largely harmless to humans. There is some evidence to suggest the administration of therapeutic phage can result in the generation of antibodies via interaction with the adaptive immune system, however the clearance of phage (upon

intravenous administration), is thought to occur before the substantial production of antibodies. Furthermore, this phenomenon is largely associated with systemic phage therapy, topical application of phage has not shown any adverse effects and both animal and clinical trials have not demonstrated in any serious immunological effects [80,81].

Perhaps a more concerning feature associated with the therapeutic administration of phage is the simultaneous lysis of numerous bacterial cells *in vivo*. The rapid release of endotoxins and liposaccharides from lysed pathogenic bacteria can produce a significant immune response and has been associated with cytokine cascades, potentially resulting in increased morbidity and mortality [82]. Efforts to circumvent adverse immune reactions have focused on genetic engineering, aimed at retaining the bactericidal properties of phage whilst removing the requirement for bacterial lysis. This approach has been demonstrated for temperate phage via expression of lethal but non-lytic proteins, and for lytic phage resulting in non-lytic, non-replicative lethal variants [83]. The gene encoding the endolysin (responsible for cellular lysis) was inactivated in a temperate *S. aureus* phage, which resulted in full retention of bactericidal activity and survival of all MRSA-infected mice in an *in vivo* study (n = 8) [84]. This appears to be a promising strategy for the future development of phage technology, which, in light of the lengthy and complex regulatory framework associated with phage therapy, may potentially expedite approval pathways.

Topical administration of phage has, thus far, failed to report any localised cytotoxic effects (although this may be a function of inadequate cytotoxicity studies rather than an absence of effect) [85]. A study conducted recently has demonstrated promising results in the administration of a phage cocktail for treatment of *S. aureus* infection in the frontal sinus region of sheep. Safety data reported no inflammatory infiltration or tissue damage to the sinus mucosa, despite twice-daily phage application over a 20 day period [86]. Nonetheless, owing to the wide variation in phage structure, activity and preparation (especially in the case of modified phage), all phage formulations should be fully characterised in terms of host response, regardless of previous studies.

In addition to any immune or cytotoxic effects associated with the administration of phage, the current thermoresponsive system relies on the implementation of a polymeric delivery system, which may present additional host-associated effects. In-depth cytotoxicity studies of PNIPAM (formed by free radical polymerisation) and PNIPAM coated substrates have been conducted on a range of cell lines (it is well known that the NIPAM monomer is toxic). PNIPAM coated surfaces (using synthesised PNIPAM) were not cytotoxic to all 4 cell types

tested (fibroblasts, endothelial, epithelial and smooth muscle cells). Synthesised PNIPAM and commercially produced PNIPAM did not appear to affect cell viability. Of the cell lines tested, only endothelial cells demonstrated increased sensitivity to commercially available PNIPAM coated surfaces; however this was attributed to residual presence of the monomer [87]. This research highlights the importance of polymer purity and the choice of cell line. PNIPAM nanoparticles have been tested on a dermal cell line; results of this study indicated the nanoparticles were localised and internalised in lysosomes within 24 h and no cytotoxic or genotoxic responses were observed [88]. Whilst these studies indicate promising results regarding the biocompatibility of PNIPAM as a drug delivery vehicle, the precise polymeric system (including the allylamine copolymer) reported in this study has yet to be tested. Furthermore, the stability of the nanoparticles on the non-woven fabric should be evaluated, in order to establish the degree of particle detachment from the plasma activated surface, which may affect the cytotoxicity of the system. There have been numerous studies conducted on the safety and tolerance of therapeutic nanoparticles detailing various complex biological interactions (including interaction with the innate immune system), which are largely dictated by the characteristics of the nanoparticles (size, shape, deformability etc.). A detailed review of some of the key considerations is presented by Boraschi *et al* [89].

Additional studies aimed at optimising the research presented, focused on the aforementioned variables, could in theory, provide an effective means of controlling the release of an enhanced bacteriophage cocktail, from a fully biocompatible delivery system for the treatment of chronic wounds.

4.6 References

1 Guest, J. F., Ayoub, N., McIlwraith, T., Uchegbu, I., Gerrish, A., Weidlich, D., Vowden, K. & Vowden, P. Health economic burden that wounds impose on the National Health Service in the UK. *BMJ Open* **5** (2015).

2 Gurtner, G. C., Werner, S., Barrandon, Y. & Longaker, M. T. Wound repair and regeneration. *Nature* **453**, 314-321 (2008).

3 Li, J., Chen, J. & Kirsner, R. Pathophysiology of acute wound healing. *Clinics in Dermatology* **25**, 9-18 (2007).

4 Werdin, F., Tennenhaus, M., Schaller, H.-E. & Rennekampff, H.-O. Evidence-based Management Strategies for Treatment of Chronic Wounds. *Eplasty* **9**, e19 (2009).

5 Harper, D., Young, A. & McNaught, C.-E. The physiology of wound healing. *Surgery - Oxford International Edition* **32**, 445-450.

6 Sen, C. K., Gordillo, G. M., Roy, S., Kirsner, R., Lambert, L., Hunt, T. K., Gottrup, F., Gurtner, G. C. & Longaker, M. T. Human Skin Wounds: A Major and Snowballing Threat to Public Health and the Economy. *Wound repair and regeneration : official publication of the Wound Healing Society [and] the European Tissue Repair Society* **17**, 763-771 (2009).

7 Gottrup, F. A specialized wound-healing center concept: importance of a multidisciplinary department structure and surgical treatment facilities in the treatment of chronic wounds. *The American Journal of Surgery* **187**, 38s-43s (2004).

8 The Wound Healing Society. Chronic Wound Care Guidelines. http://woundheal.org/documents/final_pocket_guide_treatment.aspx

9 Frykberg, R. G. & Banks, J. Challenges in the Treatment of Chronic Wounds. *Advances in Wound Care* **4**, 560-582 (2015).

10 Greene, J. N. The Microbiology of Colonization, including Techniques for Assessing and Measuring Colonization. *Infection Control and Hospital Epidemiology* **17**, 114-118 (1996).

11 Esposito, S., Bassetti, M., Concia, E., De Simone, G., De Rosa, F. G., Grossi, P., Novelli, A., Menichetti, F., Petrosillo, N., Tinelli, M., Tumbarello, M., Sanguinetti, M., Viale, P., Venditti, M. & Viscoli, C. Diagnosis and management of skin and soft-tissue infections (SSTI). A literature review and consensus statement: an update. *Journal of Chemotherapy* **29**, 197-214 (2017).

12 U.S. Department of Health and Human Services Food and Drug Administration Center for Drug Evaluation and Research (CDER). Guidance for Industry Acute Bacterial Skin and Skin Structure Infections: Developing Drugs for Treatment (2013). https://www.fda.gov/downloads/Drugs/Guidances/ucm071185.pdf

13 Jhass, P., Siaw-Sakyi, V. & Wild, T. Wound infection risk evaluation – a new prediction score – WIRE. *Wound Medicine* **16**, 34-39 (2017).

14 Bowler, P. G., Duerden, B. I. & Armstrong, D. G. Wound Microbiology and Associated Approaches to Wound Management. *Clinical Microbiology Reviews* **14**, 244-269 (2001).

15 Russo, A., Concia, E., Cristini, F., De Rosa, F. G., Esposito, S., Menichetti, F., Petrosillo, N., Tumbarello, M., Venditti, M., Viale, P., Viscoli, C. & Bassetti, M. Current and future trends in

antibiotic therapy of acute bacterial skin and skin-structure infections. *Clinical Microbiology and Infection* **22,** 27-36 (2016).

16 Cutting, K. F. & White, R. Defined and refined: criteria for identifying wound infection revisited. *British Journal of Community Nursing* **9**, 6-15 (2004).

17 Schuler, C. L., Courter, J. D., Conneely, S. E., Frost, M. A., Sherenian, M. G., Shah, S. S. & Gosdin, C. H. Decreasing Duration of Antibiotic Prescribing for Uncomplicated Skin and Soft Tissue Infections. *Pediatrics* **137**, e20151223 (2016).

18 Brown, K. A., Khanafer, N., Daneman, N. & Fisman, D. N. Meta-analysis of antibiotics and the risk of community-associated Clostridium difficile infection. *Antimicrobial Agents and Chemotherapy* **57**, 2326-2332 (2013).

19 Walsh, T. L., Chan, L., Konopka, C. I., Burkitt, M. J., Moffa, M. A., Bremmer, D. N., Murillo, M. A., Watson, C. & Chan-Tompkins, N. H. Appropriateness of antibiotic management of uncomplicated skin and soft tissue infections in hospitalized adult patients. *BMC Infectious Diseases* **16**, 721 (2016).

20 Lipsky, B. A., Napolitano, L. M., Moran, G. J., Vo, L., Nicholson, S. & Kim, M. Inappropriate initial antibiotic treatment for complicated skin and soft tissue infections in hospitalized patients: incidence and associated factors. *Diagnostic Microbiology and Infectious Disease* **79**, 273-279 (2014).

21 Engemann, J. J., Carmeli, Y., Cosgrove, S. E., Fowler, V. G., Bronstein, M. Z., Trivette, S. L., Briggs, J. P., Sexton, D. J. & Kaye, K. S. Adverse Clinical and Economic Outcomes Attributable to Methicillin Resistance among Patients with Staphylococcus aureus Surgical Site Infection. *Clinical Infectious Diseases* **36**, 592-598 (2003).

22 Malone, M., Bjarnsholt, T., McBain, A. J., James, G. A., Stoodley, P., Leaper, D., Tachi, M., Schultz, G., Swanson, T. & Wolcott, R. D. The prevalence of biofilms in chronic wounds: a systematic review and meta-analysis of published data. *Journal of Wound Care* **26**, 20-25 (2017).

23 Bjarnsholt, T., Kirketerp-Moller, K., Jensen, P. O., Madsen, K. G., Phipps, R., Krogfelt, K., Hoiby, N. & Givskov, M. Why chronic wounds will not heal: a novel hypothesis. *Wound Repair and Regeneration* **16**, 2-10 (2008).

24 Malik, D. J., Sokolov, I. J., Vinner, G. K., Mancuso, F., Cinquerrui, S., Vladisavljevic, G. T., Clokie, M. R. J., Garton, N. J., Stapley, A. G. F. & Kirpichnikova, A. Formulation, stabilisation and encapsulation of bacteriophage for phage therapy. *Advances in Colloid and Interface Science* (2017).

25 Kirketerp-Møller, K., Jensen, P. Ø., Fazli, M., Madsen, K. G., Pedersen, J., Moser, C., Tolker-Nielsen, T., Høiby, N., Givskov, M. & Bjarnsholt, T. Distribution, Organization, and Ecology of Bacteria in Chronic Wounds. *Journal of Clinical Microbiology* **46**, 2717-2722 (2008).

26 Korgaonkar, A., Trivedi, U., Rumbaugh, K. P. & Whiteley, M. Community surveillance enhances Pseudomonas aeruginosa virulence during polymicrobial infection. *Proceedings of the National Academy of Sciences* **110**, 1059-1064 (2013).

27 Power, G., Moore, Z. & O'Connor, T. Measurement of pH, exudate composition and temperature in wound healing: a systematic review. *Journal of Wound Care* **26**, 381-397 (2017).

28 Lavery, L. A., Higgins, K. R., Lanctot, D. R., Constantinides, G. P., Zamorano, R. G., Armstrong, D. G., Athanasiou, K. A. & Agrawal, C. M. Home monitoring of foot skin temperatures to prevent ulceration. *Diabetes Care* **27**, 2642-2647 (2004).

29 Armstrong, D. G., Lipsky, B. A., Polis, A. B. & Abramson, M. A. Does dermal thermometry predict clinical outcome in diabetic foot infection? Analysis of data from the SIDESTEP* trial. *International Wound Journal* **3**, 302-307 (2006).

30 Dini, V., Salvo, P., Janowska, A., Di Francesco, F., Barbini, A. & Romanelli, M. Correlation Between Wound Temperature Obtained With an Infrared Camera and Clinical Wound Bed Score in Venous Leg Ulcers. *Wounds* **27**, 274-278 (2015).

31 Woo, K. Y. & Sibbald, R. G. A cross-sectional validation study of using NERDS and STONEES to assess bacterial burden. *Ostomy Wound Manage* **55**, 40-48 (2009).

32 Fierheller, M. & Sibbald, G. A Clinical Investigation into the Relationship between Increased Periwound Skin Temperature and Local Wound Infection in Patients with Chronic Leg Ulcers. *Advances in Skin & Wound Care* **23**, 369-378 (2010).

33 Uematsu, S., Edwin, D. H., Jankel, W. R., Kozikowski, J. & Trattner, M. Quantification of thermal asymmetry. Part 1: Normal values and reproducibility. *Journal of Neurosurgy* **69**, 552-555 (1988).

34 Romano, C. L., Romano, D., Dell'Oro, F., Logoluso, N. & Drago, L. Healing of surgical site after total hip and knee replacements show similar telethermographic patterns. *Journal of Orthopaedics and Traumatology* **12**, 81-86 (2011).

35 Chanmugam, A., Langemo, D., Thomason, K., Haan, J., Altenburger, E. A., Tippett, A., Henderson, L. & Zortman, T. A. Relative Temperature Maximum in Wound Infection and Inflammation as Compared with a Control Subject Using Long-Wave Infrared Thermography. *Advances in Wound Care* **30**, 406-414 (2017).

36 Breed, R. S. & Dotterrer, W. D. The Number of Colonies Allowable on Satisfactory Agar Plates. *Journal of Bacteriology* **1**, 321-331 (1916).

37 Radovic-Moreno, A. F., Lu, T. K., Puscasu, V. A., Yoon, C. J., Langer, R. & Farokhzad, O. C. Surface Charge-Switching Polymeric Nanoparticles for Bacterial Cell Wall-Targeted Delivery of Antibiotics. *ACS Nano* **6**, 4279-4287 (2012).

38 Ge, J., Neofytou, E., Cahill, T. J., Beygui, R. E. & Zare, R. N. Drug Release from Electric-Field-Responsive Nanoparticles. *ACS Nano* **6**, 227-233 (2012).

39 Andersson, D. I. & Hughes, D. Evolution of antibiotic resistance at non-lethal drug concentrations. *Drug Resistance Updates* **15**, 162-172 (2012).

40 Donnelly, R. F., McCarron, P. A., Morrow, D. I. J. & Woolfson, A. D. Fast-drying multi-laminate bioadhesive films for transdermal and topical drug delivery. *Drug Development and Industrial Pharmacy* **39**, 1818-1831 (2013).

41 Inui, N., Kato, T., Uchida, S., Chida, K., Takeuchi, K., Kimura, T. & Watanabe, H. Novel Patch for Transdermal Administration of Morphine. *Journal of Pain and Symptom Management* **44**, 479-485 (2012).

42 Pornpattananangkul, D., Zhang, L., Olson, S., Aryal, S., Obonyo, M., Vecchio, K., Huang, C.-M. & Zhang, L. Bacterial Toxin-Triggered Drug Release from Gold Nanoparticle-Stabilized Liposomes for the Treatment of Bacterial Infection. *Journal of the American Chemical Society* **133**, 4132-4139 (2011).

43 Komnatnyy, V. V., Chiang, W.-C., Tolker-Nielsen, T., Givskov, M. & Nielsen, T. E. Bacteria-triggered release of antimicrobial agents. *Abstracts of Papers of the American Chemical Society* **247** (2014).

44 Bean, J. E., Alves, D. R., Laabei, M., Esteban, P. P., Thet, N. T., Enright, M. C. & Jenkins, A. T. A. Triggered Release of Bacteriophage K from Agarose/Hyaluronan Hydrogel Matrixes by Staphylococcus aureus Virulence Factors. *Chemistry of Materials* **26**, 7201-7208 (2014).

45 Pavlukhina, S., Lu, Y., Patimetha, A., Libera, M. & Sukhishvili, S. Polymer Multilayers with pH-Triggered Release of Antibacterial Agents. *Biomacromolecules* **11**, 3448-3456 (2010).

46 McCoy, C. P., Brady, C., Cowley, J. F., McGlinchey, S. M., McGoldrick, N., Kinnear, D. J., Andrews, G. P. & Jones, D. S. Triggered drug delivery from biomaterials. *Expert Opinion on Drug Delivery* **7**, 605-616 (2010).

47 Wu, C. A comparison between the 'coil-to-globule' transition of linear chains and the "volume phase transition" of spherical microgels. *Polymer* **39**, 4609-4619 (1998).

48 Gong, Z.-l., Tang, D.-y. & Guo, Y.-d. The fabrication and self-flocculation effect of hybrid TiO2 nanoparticles grafted with poly(N-isopropylacrylamide) at ambient temperature via surface-initiated atom transfer radical polymerization. *Journal of Materials Chemistry* **22**, 16872-16879 (2012).

49 Guan, Y. & Zhang, Y. PNIPAM microgels for biomedical applications: from dispersed particles to 3D assemblies. *Soft Matter* **7**, 6375-6384 (2011).

50 James, C., Johnson, A. L. & Jenkins, A. T. A. Antimicrobial surface grafted thermally responsive PNIPAM-co-ALA nano-gels. *Chemical Communications* **47**, 12777-12779 (2011).

51 Hendrix, R. W. Bacteriophages: Evolution of the majority. *Theoretical Population Biology* **61**, 471-480 (2002).

52 Nobrega, F. L., Costa, A. R., Kluskens, L. D. & Azeredo, J. Revisiting phage therapy: new applications for old resources. *Trends in Microbiology* **23**, 185-191 (2015).

53 Parracho, H. M., Burrowes, B. H., Enright, M. C., McConville, M. L. & Harper, D. R. The role of regulated clinical trials in the development of bacteriophage therapeutics. *Journal of molecular and genetic medicine : an international journal of biomedical research* **6**, 279-286 (2012).

54 Penades, J. R., Chen, J., Quiles-Puchalt, N., Carpena, N. & Novick, R. P. Bacteriophage-mediated spread of bacterial virulence genes. *Current Opinion in Microbiology* **23**, 171-178 (2015).

55 Kasman, L. M., Kasman, A., Westwater, C., Dolan, J., Schmidt, M. G. & Norris, J. S. Overcoming the phage replication threshold: a mathematical model with implications for phage therapy. *Journal of Virology* **76**, 5557-5564 (2002).

56 Foerch, R., Chifen, A. N., Bousquet, A., Khor, H. L., Jungblut, M., Chu, L.-Q., Zhang, Z., Osey-Mensah, I., Sinner, E.-K. & Knoll, W. Recent and expected roles of plasma-polymerized films for biomedical applications. *Chemical Vapor Deposition* **13**, 280-294 (2007).

57 Mishra, G. & McArthur, S. L. Plasma Polymerization of Maleic Anhydride: Just What Are the Right Deposition Conditions? *Langmuir* **26**, 9645-9658 (2010).

58 Pearson, H. A., Sahukhal, G. S., Elasri, M. O. & Urban, M. W. Phage-Bacterium War on Polymeric Surfaces: Can Surface-Anchored Bacteriophages Eliminate Microbial Infections? *Biomacromolecules* **14**, 1257-1261 (2013).

59 Monecke, S., Ehricht, R., Slickers, P., Wiese, N. & Jonas, D. Intra-strain variability of methicillin-resistant Staphylococcus aureus strains ST228-MRSA-I and ST5-MRSA-II. *European Journal of Clinical Microbiology & Infectious Diseases* **28**, 1383-1390 (2009).

60 Stefani, S., Chung, D. R., Lindsay, J. A., Friedrich, A. W., Kearns, A. M., Westh, H. & MacKenzie, F. M. Meticillin-resistant Staphylococcus aureus (MRSA): global epidemiology and harmonisation of typing methods. *International Journal of Antimicrobial Agents* **39**, 273-282 (2012).

61 Vogel, V., Falquet, L., Calderon-Copete, S. P., Basset, P. & Blanc, D. S. Short Term Evolution of a Highly Transmissible Methicillin-Resistant Staphylococcus aureus Clone (ST228) in a Tertiary Care Hospital. *Plos One* **7** (2012).

62 Verma, V., Harjai, K. & Chhibber, S. Restricting ciprofloxacin-induced resistant variant formation in biofilm of Klebsiella pneumoniae B5055 by complementary bacteriophage treatment. *Journal of Antimicrobial Chemotherapy* **64**, 1212-1218 (2009).

63 Schiller, S., Hu, J., Jenkins, A. T. A., Timmons, R. B., Sanchez-Estrada, F. S., Knoll, W. & Forch, R. Chemical structure and properties of plasma-polymerized maleic anhydride films. *Chemistry of Materials* **14**, 235-242 (2002).

64 Jenkins, A. T. A., Hu, J., Wang, Y. Z., Schiller, S., Foerch, R. & Knoll, W. Pulsed plasma deposited maleic anhydride thin films as supports for lipid bilayers. *Langmuir* **16**, 6381-6384 (2000).

65 Wu, C. A comparison between the `coil-to-globule' transition of linear chains and the “volume phase transition” of spherical microgels1Dedicated to the 80th birthday of Professor Renyuan Qian.1. *Polymer* **39**, 4609-4619 (1998).

66 Ottaviani, M. F., Winnik, F. M., Bossmann, S. H. & Turro, N. J. Phase Separation of Poly(N-isopropylacrylamide) in Mixtures of Water and Methanol: A Spectroscopic Study of the Phase-Transition Process with a Polymer Tagged with a Fluorescent Dye and a Spin Label. *Helvetica Chimica Acta* **84**, 2476-2492 (2001).

67 Goren, M., Yosef, I. & Qimron, U. Sensitizing pathogens to antibiotics using the CRISPR-Cas system. *Drug Resistance Updates* **30**, 1-6 (2017).

68 Labrie, S. J., Samson, J. E. & Moineau, S. Bacteriophage resistance mechanisms. *Nauture Reviews Microbiology* **8**, 317-327 (2010).

69 Keen, E. Phage Therapy: Concept to Cure. *Frontiers in Microbiology* **3** (2012).

70 Samson, J. E., Magadan, A. H., Sabri, M. & Moineau, S. Revenge of the phages: defeating bacterial defences. *Nauture Reviews Microbiology* **11**, 675-687 (2013).

71 Ormala, A. M. & Jalasvuori, M. Phage therapy: Should bacterial resistance to phages be a concern, even in the long run? *Bacteriophage* **3**, e24219 (2013).

72 Kelly, D., McAuliffe, O., O'Mahony, J. & Coffey, A. Development of a broad-host-range phage cocktail for biocontrol. *Bioengineered Bugs* **2**, 31-37 (2011).

73 Jo, A., Ding, T. & Ahn, J. Synergistic antimicrobial activity of bacteriophages and antibiotics against Staphylococcus aureus. *Food Science and Biotechnology* **25**, 935-940 (2016).

74 O'Flaherty, S., Ross, R. P., Meaney, W., Fitzgerald, G. F., Elbreki, M. F. & Coffey, A. Potential of the Polyvalent Anti-Staphylococcus Bacteriophage K for Control of Antibiotic-Resistant Staphylococci from Hospitals. *Applied Environmental Microbiology* **71**, 1836-1842 (2005).

75 O'Flaherty, S., Coffey, A., Edwards, R., Meaney, W., Fitzgerald, G. F. & Ross, R. P. Genome of Staphylococcal Phage K: a New Lineage of Myoviridae Infecting Gram-Positive Bacteria with a Low G+C Content. *Journal of Bacteriology* **186**, 2862-2871 (2004).

76 Azeredo, J. & Sutherland, I. W. The use of phages for the removal of infectious biofilms. *Current Pharmaceutical Biotechnology* **9**, 261-266 (2008).

77 Chan, B. K. & Abedon, S. T. Bacteriophages and their enzymes in biofilm control. *Current Pharmaceutical Design* **21**, 85-99 (2015).

78 Harper, D. R., Parracho, H. M. R. T., Walker, J., Sharp, R., Hughes, G., Werthén, M., Lehman, S. & Morales, S. Bacteriophages and Biofilms. *Antibiotics* **3**, 270-284 (2014).

79 Lister, J. L. & Horswill, A. R. Staphylococcus aureus biofilms: recent developments in biofilm dispersal. *Frontiers in Cellular and Infection Microbiology* **4** (2014).

80 Merril, C. R., Scholl, D. & Adhya, S. L. The prospect for bacteriophage therapy in Western medicine. *Nature Reviews Drug Discovery* **2**, 489-497 (2003).

81 Nilsson, A. S. Phage therapy—constraints and possibilities. *Upsala Journal of Medical Sciences* **119**, 192-198 (2014).

82 Lu, T. K. & Koeris, M. S. The next generation of bacteriophage therapy. *Current Opinion in Microbiology* **14**, 524-531 (2011).

83 Pires, D. P., Cleto, S., Sillankorva, S., Azeredo, J. & Lu, T. K. Genetically Engineered Phages: a Review of Advances over the Last Decade. *Microbiology and Molecular Biology Reviews* **80**, 523-543 (2016).

84 Paul, V. D., Sundarrajan, S., Rajagopalan, S. S., Hariharan, S., Kempashanaiah, N., Padmanabhan, S., Sriram, B. & Ramachandran, J. Lysis-deficient phages as novel therapeutic agents for controlling bacterial infection. *BMC Microbiology* **11**, 195 (2011).

85 Henein, A. What are the limitations on the wider therapeutic use of phage? *Bacteriophage* **3**, e24872 (2013).

86 Drilling, A. J., Ooi, M. L., Miljkovic, D., James, C., Speck, P., Vreugde, S., Clark, J. & Wormald, P. J. Long-Term Safety of Topical Bacteriophage Application to the Frontal Sinus Region. *Frontiers in Cellular and Infection Microbiology* **7**, 49 (2017).

87 Cooperstein, M. A. & Canavan, H. E. Assessment of cytotoxicity of (N-isopropyl acrylamide) and Poly(N-isopropyl acrylamide)-coated surfaces. *Biointerphases* **8**, 19 (2013).

88 Naha, P. C., Bhattacharya, K., Tenuta, T., Dawson, K. A., Lynch, I., Gracia, A., Lyng, F. M. & Byrne, H. J. Intracellular localisation, geno- and cytotoxic response of polyN-isopropylacrylamide (PNIPAM) nanoparticles to human keratinocyte (HaCaT) and colon cells (SW 480). *Toxicology Letters* **198**, 134-143 (2010).

89 Boraschi, D., Italiani, P., Palomba, R., Decuzzi, P., Duschl, A., Fadeel, B. & Moghimi, S. M. Nanoparticles and innate immunity: new perspectives on host defence. *Seminars in Immunology* (2017).

Chapter 5: Thermally Triggered Release of the Bacteriophage Endolysin $CHAP_K$ and the Bacteriocin Lysostaphin for the Control of Methicillin Resistant *Staphylococcus aureus* (MRSA)

5.1 Introduction

This research is presented as an extension of the previous study reported in Chapter 4; the utilisation of skin temperature as an indication of infection, in order to facilitate the delivery of an antimicrobial formulation from a thermoresponsive polymeric platform (Figure 1). Exploiting a formidable bacterial defence strategy (the production of bacteriocins), alongside utilisation of a key component involved in phage-mediated biocontrol of bacterial population dynamics (the production of phage-encoded endolysins), the potential to control infection has been investigated. This study details the formulation of an enzybiotic cocktail consisting of a phage-encoded endolysin ($CHAP_K$) and a bacteriocin (lysostaphin). Cooperative effects in terms of synergistic interaction have been evaluated, with the intention of developing an effective cocktail, exhibiting greater antimicrobial efficacy than the sum of the individual components. The primary advantage associated with the use of bactericidal enzymes, surrounds avoiding the implementation of self-replicating biological agents, thus eliminating any potential transduction of genetic material. The aims of this research are largely based on those underpinning the previous publication, with the additional benefit of potentially circumventing some of the complex regulatory and approval issues surrounding the use of whole phage.

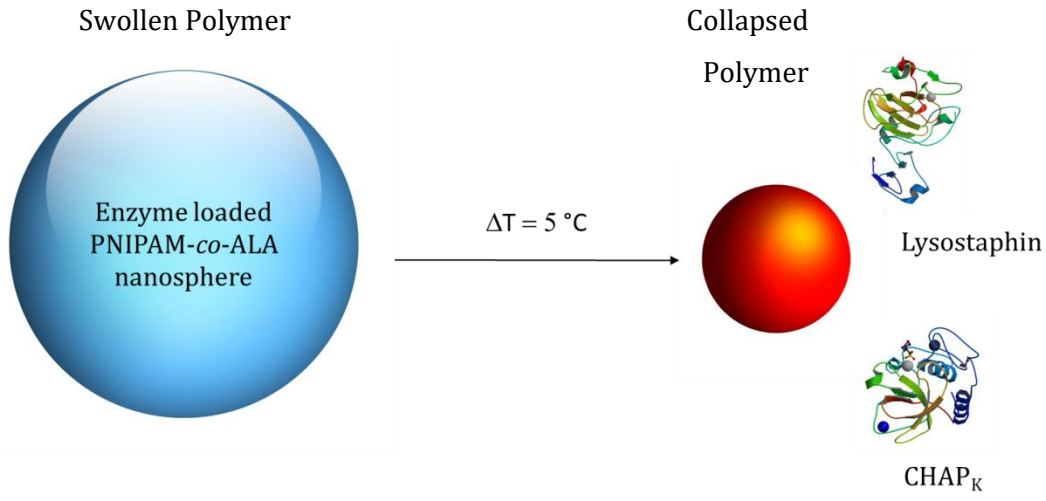

Figure 1 Schematic illustrating the thermally triggered release of an enzybiotic cocktail, consisting of a bacteriophage-encoded endolysin ($CHAP_K$) and a staphylococcal bacteriocin (lysostaphin) from PNIPAM-*co*-ALA nanospheres.

5.1.1 $CHAP_K$

Phage-encoded endolysins have been the subject of considerable interest in recent years, owing to the rise in multi-drug resistance and the developmental decline of novel antibiotics. Endolysin classification, characterisation and clinical development are discussed in Chapter 3. $CHAP_K$, the truncated form of LysK exhibits a relatively broad lytic spectrum, which includes staphylococcal, micrococcal and streptococcal species. As a peptidoglycan hydrolase enzyme, $CHAP_K$ cleaves the bond between $_D$-alanine and the first glycine in the pentaglycine cross-bridge of *S. aureus* peptidoglycan. However, in the case of streptococcal peptidoglycan, there are no glycine residues; instead, the cleavage site appears to be between $_D$-alanine and $_L$-alanine in the cross-bridge. It is therefore speculated that the absence of the cell wall-binding domain (i.e. the SH3b domain found in LysK), may facilitate the recognition of a common moiety in the structure of the peptidoglycan cell wall of multiple bacterial species [1]. This enhanced lytic activity (relative to the parent enzyme), offers an extended spectrum of antimicrobial activity against multiple Gram-positive species, including coagulase-negative strains, for example *Staphylococcus epidermidis* (*S. epidermidis*). $CHAP_K$-mediated peptidoglycan bond cleavage involves a catalytic triad consisting of cysteine, histidine and glutamate (Figure 2 [2]).

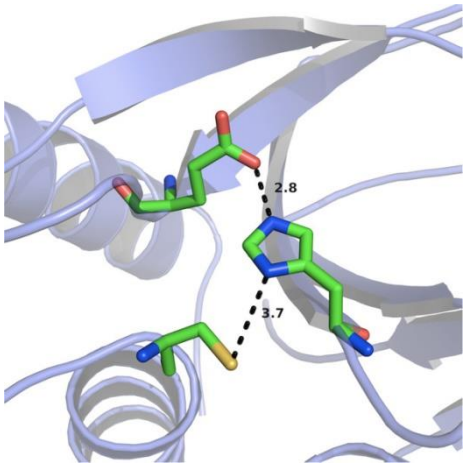

Figure 2 The catalytic triad of responsible for $CHAP_K$–mediated peptidoglycan hydrolysis. The triad consists of Cys54, located on the second α-helix (bottom), His117, located on β-strand C (middle) and Glu134, located on β-strand D (top). Distances are shown in Å. Reproduced from [2]. Copyright © 2014 Sanz-Gaitero *et al*.

The proposed mechanism involves 2 sequential proton transfer steps: His117 (from the protonated imidazole ring) to Glu134, followed by Cys54 to His117. The deprotonation of Cys54 then facilitates nucleophilic attack on the peptide bond in the cell wall, resulting in the

formation of an acyl-enzyme intermediate, which may be hydrolysed to release the newly cleaved peptidoglycan.

$CHAP_K$ retains lytic activity over a broad pH range (6 – 11), a broad temperature range (5 – 40 °C) and is stable for up to 1 month when stored at 4 °C and up to 1 year when stored at -80 °C [3]. The ability to withstand conditions which would otherwise inactive other phage endolysins and the ability to target multiple bacterial strains, regardless of their origin, antibiotic resistance profile or ability to form biofilms, makes $CHAP_K$ a promising candidate in the design of novel biotherapeutic antimicrobials.

5.1.2 Bacteriocins

Bacteriocins are highly specific, ribosomally synthesised antimicrobial peptides or proteins produced by both Gram-positive and -negative bacteria. In fact, over 99% of bacteria produce at least one type of bacteriocin [4]. Microbial production of such proteinaceous species provides a means of out-competing neighbouring bacteria (for both space and resources), via cellular destruction of closely related competitor strains. The heterogeneous nature of bacteriocins gives rise to variation in their specific mode of action; the most common mechanisms involve the formation of pores in the cell membrane and dissipation of membrane potential, inhibition of nucleic acid synthesis and prevention of peptidoglycan synthesis [5]. The producing strain remains unaffected by the presence of their synthesised bacteriocins, owing to the simultaneous expression of immunity proteins. This form of biocontrol is yet another crucial factor involved in controlling the complex ecology of bacterial communities. Recent studies have demonstrated promising results regarding the therapeutic potential of bacteriocins as protein antibiotics; a detailed review of the current state of research has been published by Behrens *et al* [6].

In addition to their current development as therapeutic agents, bacteriocins have been widely investigated for use in the food industry. Nisin is produced by the bacteria *Lactococcus lactis* and is classed as a broad-spectrum bacteriocin (from the class lantibiotics, owing to the presence of the uncommon amino acid lanthionine). Nisin has been approved by the FDA for use in pasteurized processed cheese, for the control of lactic acid bacteria (known to spoil food preparations). Further discussion on the application of bacteriocins in the food industry is published elsewhere [7]. However, recognition of the potent antimicrobial properties of certain bacteriocins by regulatory authorities is an encouraging first step for their future therapeutic development.

5.1.2.1 Lysostaphin

Lysostaphin, first identified in 1964, is a bacteriocin (although may be referred to as a bacteriolysin), exhibiting potent and specific activity against clinically relevant staphylococcal species (predominantly *S. aureus* and *S. epidermidis*) [5]. Produced by a key environmental competitor of *S. aureus* (discussed further in Section 5.2), it has demonstrated efficacy against both MSSA and MRSA and is capable of killing both active and quiescent bacteria. Lysostaphin has been extensively investigated for the control of *S. aureus* both *in vitro* and *in vivo*, including biofilm associated infections [8]. Additionally, this potent peptidoglycan hydrolase enzyme has shown greater antibiotic efficacy than vancomycin *in vitro* [9]. Furthermore, enhanced antimicrobial effects have been demonstrated when using lysostaphin in conjunction with conventional antibiotics [10]. Of particular relevance to this thesis is the development of a lysostaphin impregnated chitosan-collagen hydrogel for use in MRSA-infected burn wounds. The study, conducted by Cui *et al*, aimed to test the novel antimicrobial hydrogel formulation on MRSA-infected third degree burns in a rabbit model [11]. The results showed 100% wound healing over a 2 week period and complete eradication of infection after 2 weeks, thereby demonstrating the promising potential of lysostaphin for treatment of burn wound infections.

Lysostaphin initiates bacterial cell lysis via catalysis of cell wall hydrolysis, however it has a slightly different target site in the pentaglycine cross bridge compared to $CHAP_K$. The cleavage point in this case is between the third and fourth glycine residues (Figure 3 [12]).

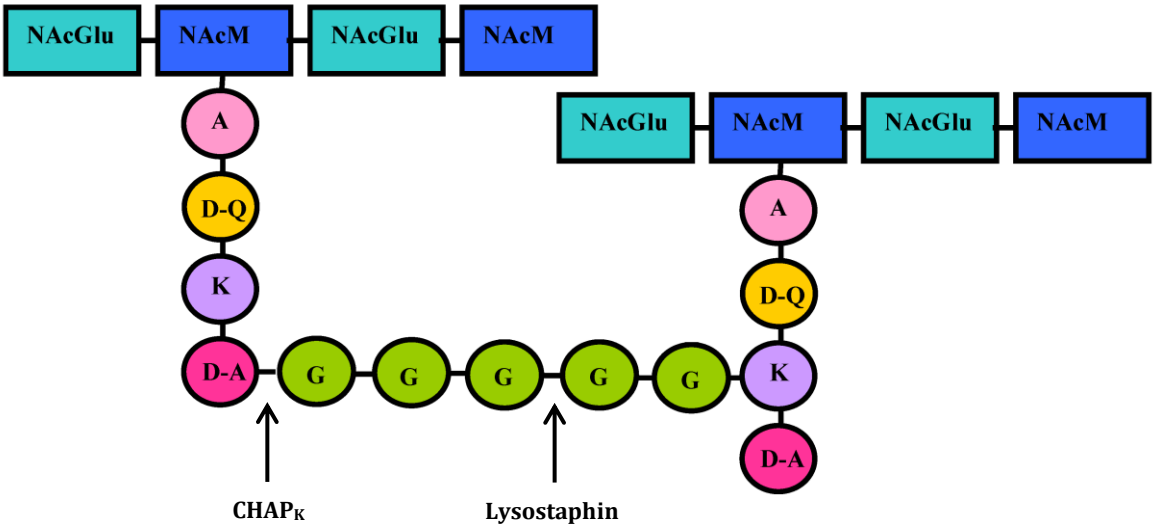

Figure 3 Structure of the peptidoglycan cell wall of *S. aureus*, highlighting the cleavage site for lysostaphin relative to $CHAP_K$. Adapted from [12]. Copyright © 2010 Bastos *et al*.

As a member of the M23 metalloendopeptidase family, the active site of lysostaphin is centred around a Zn^{2+} ion, which is coordinated to histidine 279, aspartate 283, histidine 362 and a water molecule (in the active form of the enzyme) [13]. The proposed mechanism involves the abstraction of a proton from water by the first histidine residue, resulting in the formation of a nucleophilic hydroxide ion which attacks the carbonyl carbon in the peptidoglycan peptide bond. The second chelated-histidine is thought to stabilise the tetrahedral transition state [14].

5.2 Extended Methodology

5.2.1 Minimum Inhibitory Concentration

A stock solution of the antimicrobial to be tested (i.e. antibiotic or enzyme) was made up to twice the starting concentration required (i.e. in order to start with 64 µg/ml in the MIC experiment, a 128 µg/ ml stock solution was prepared). Overnight bacterial cultures were subcultured 1:1000 in TSB. To a 96 well plate, 100 µl of TSB was added to columns 2 - 12 and 100 µl of antimicrobial stock solution was added to columns 1 and 2. Using a multichannel pipette, 100 µl was taken from the wells in column 2 and serially diluted across the plate to column 10 (columns 11 and 12 were reserved for negative controls in the absence of antibiotic and bacteria respectively). The additional 100 µl in column 10 was discarded after dilution. 100 µl of bacterial subculture was added to every well except those in column 12. The plate was then incubated overnight at 37 °C and the MIC was determined the following day. The MIC was defined as the lowest concentration of antimicrobial capable of inhibiting the growth of bacteria (assessed as a function of OD at 600 nm using a microtitre plate reader). Each antimicrobial concentration was therefore tested 8 times (based on the number of rows in a 96 well plate).

5.2.2 Checkerboard Assay

Stock solutions of $CHAP_K$ and lysostaphin were made up to 4 times the starting concentration to be tested; in this case 256 µg/ml and 1 µg/ml respectively. Overnight bacterial cultures were subcultured 1:1000 in TSB. To a 96 well plate, 100 µl of TSB was added to each well except those in column 1. 100 µl of the lysostaphin stock solution was added to columns 1 and 2. Using a multichannel pipette, 100 µl was taken from the wells in column 2 and serially diluted across the plate; the excess 100 µl in the final column was discarded after dilution. 100 µl of the $CHAP_K$ stock solution was then added to each well in row A. Using a multichannel

pipette 100 µl was taken from the wells in row A and serially diluted down the plate; the excess 100 µl in the final row was discarded after dilution. 100 µl of bacterial culture was then added to each well (with the exception of those reserved for controls) and the plate was then incubated overnight at 37 °C. Synergy was assessed visually the following day, demonstrated by an absence of bacterial growth and the calculation of inhibition concentrations (Section 5.3).

5.2.3 Bradford Assay

Bovine serum albumin (BSA) (Sigma Aldrich) was serially diluted 1:2 from stock (2 mg/ml) in DI water to create a range of BSA concentrations. 10 µl of each dilution was added to a microtitre plate in triplicate, alongside DI water (used as a blank sample). Coomassie Plus Reagent (Thermo Scientific™, ThermoFisher) was equilibrated to room temperature and 300 µl was added to each well. The plate was mixed on a shaker plate at 600 rpm for 30 s at room temperature and held at room temperature for a further 10 min. The absorbance at 595 nm was then measured using a microtitre plate reader. The absorbance from the blank samples (DI water and Coomassie Plus Reagent), was subtracted from the sample measurements and the values were used to prepare a standard curve (BSA concentration vs. absorbance). The samples containing unknown concentrations of protein (in this case $CHAP_K$), were then diluted 1:10 and 1:20 in DI water. 10 µl of each was added to a microtitre plate in triplicate, followed by 300 µl of Coomassie Plus reagent. The process was repeated as before and absorbance measurements were taken. The absorbance readings of the samples containing $CHAP_K$ were then correlated to the standard curve and the concentration was determined.

5.3 Publication

5.3.1 Declaration of Authorship

<table>
<tr><td colspan="10">This declaration concerns the article entitled:</td></tr>
<tr><td colspan="10">Thermally Triggered Release of the Bacteriophage Endolysin $CHAP_K$ and the Bacteriocin Lysostaphin for the Control of Methicillin Resistant Staphylococcus aureus (MRSA)</td></tr>
<tr><td colspan="10">Publication status (tick one)</td></tr>
<tr><td>Draft manuscript</td><td></td><td>Submitted</td><td></td><td>In review</td><td></td><td>Accepted</td><td></td><td>Published</td><td>✓</td></tr>
<tr><td>Publication details (reference)</td><td colspan="9">Hathaway, H., Ajuebor, J., Stephens, L., Coffey, A., Potter, U., Sutton, J. M. & Jenkins, A. T. A. Thermally triggered release of the bacteriophage endolysin $CHAP_K$ and the bacteriocin lysostaphin for the control of methicillin resistant Staphylococcus aureus (MRSA). Journal of Controlled Release 245, 108-115, doi:http://dx.doi.org/10.1016/j.jconrel.2016.11.030 (2017).</td></tr>
<tr><td>Candidate's contribution to the paper (detailed, and also given as a percentage).</td><td colspan="9">The candidate predominantly executed the…

Formulation of ideas:
Concept and research development was instigated by the candidate, including the initiation of relevant collaborations (100%).
Design of methodology:
Experimental design was decided upon by the candidate (100%).
Experimental work:
All experimental work except $CHAP_K$ production/ purification and vancomycin SEM was conducted by the candidate (90%).
Presentation of data in journal format:
Manuscript was written and prepared by the candidate with an additional insert into the materials and methods regarding $CHAP_K$ production and isolation (90%).</td></tr>
<tr><td>Statement from Candidate</td><td colspan="9">This paper reports on original research I conducted during the period of my Higher Degree by Research candidature.</td></tr>
<tr><td>Signed</td><td colspan="5">  </td><td>Date</td><td colspan="3">29.09.17</td></tr>
</table>

5.3.2 Copyright Agreement

5.3.3 Data Access Statement

All data created during this research is openly available from the University of Bath data archive at http://doi.org/10.15125/BATH-00247.

5.3.4 Published Article

Thermally Triggered Release of the Bacteriophage Endolysin $CHAP_K$ and the Bacteriocin Lysostaphin for the Control of Methicillin Resistant *Staphylococcus aureus* (MRSA)

Hollie Hathaway[1], Jude Ajuebor[2], Liam Stephens[1], Aidan Coffey[2], Ursula Potter[3], J. Mark Sutton[4], A. Toby A. Jenkins[1]*

1. Department of Chemistry, University of Bath, UK, BA2 7AY
2. Department of Biological Sciences, Cork Institute of Technology, Ireland, T12 P928
3. Microscopy and Analysis Suite, University of Bath, UK, BA2 7AY
4. Technology Development Group, Public Health England, Porton Down, UK, SP4 0JG

*Corresponding Author: Email: a.t.a.jenkins@bath.ac.uk, Tel: +44 (0) 1225 386118

Abstract

Staphylococcus aureus infections of the skin and soft tissue pose a major concern to public health, largely owing to the steadily increasing prevalence of drug resistant isolates. As an alternative mode of treatment both bacteriophage endolysins and bacteriocins have been shown to possess antimicrobial efficacy against multiple species of bacteria including otherwise drug resistant strains. Despite this, the administration and exposure of such antimicrobials should be restricted until required in order to discourage the continued evolution of bacterial resistance, whilst maintaining the activity and stability of such proteinaceous structures. Utilising the increase in skin temperature during infection, the truncated bacteriophage endolysin $CHAP_K$ and the staphylococcal bacteriocin lysostaphin have been co-administered in a thermally triggered manner from Poly(N-isopropylacrylamide) (PNIPAM) nanoparticles. The thermoresponsive nature of the PNIPAM polymer has been employed in order to achieve the controlled expulsion of a synergistic enzybiotic cocktail consisting of $CHAP_K$ and lysostaphin. The point at which this occurs is modifiable, in this case corresponding to the threshold temperature associated with an infected wound. Consequently, bacterial lysis was observed at 37 °C, whilst growth was maintained at the uninfected skin temperature of 32 °C.

Keywords: PNIPAM, Bacteriophage Endolysin, Bacteriocin, Thermal Release

Introduction

Staphylococcus aureus (*S.aureus*) is a frequent inhabitant of the human skin flora colonizing up to 30% of individuals at any given time, primarily through nasal carriage [15]. Requiring a suitable portal of entry into the body, the skin normally provides such a barrier to progressive infection. However a breach in the skin, often as a result of a scratch, cut or burn provides a suitable infection point for the opportunistic bacteria. *S.aureus* is the leading cause of skin and soft tissue infections (SSTI) across all continents, thus resulting in both delayed wound healing and further systemic infections, such as sepsis, osteomyelitis and endocarditis [16]. With the discovery of staphylococcal drug resistance and the subsequent global epidemic that methicillin resistant *S. aureus* (MRSA) has become, the need to source alternative treatment has become paramount. Hospital acquired MRSA (HA-MRSA) has a mortality rate twice that of its methicillin susceptible counterpart, and is more than twice as expensive to treat [17]. Furthermore, the isolation of these 'super-bugs' is not confined to the hospital setting. Indeed, community acquired MRSA (CA-MRSA) is proving an equal challenge to clinicians worldwide [18].

Bacteriophage (phage), (the naturally occurring parasitic viruses of bacteria, able to infect and destroy bacterial cells) were first utilised as a treatment to infection in the 1930s within the former Soviet Union. Despite the continued development of phage products throughout the Cold War, bacteriophage therapy was largely disregarded in the West from under the relative comfort of the antibiotic blanket. However, the alarming rise in multi-drug resistance (MDR) in recent times has regenerated interest in phage therapy [19]. One of the main disadvantages associated with the use of whole phage to treat infection is the viral nature of the phage itself. Containing a vast amount of genetic material, temperate phage have been known to increase the virulence of certain species of bacteria through transduction, an example of which includes the bacterial acquisition of the gene encoding the Panton Valentine Leucocidin toxin, causing 'scalded skin syndrome' [20]. Whilst this is selected against when sourcing phage for treatment, the regulation and control of suitable virulent phage for clinical use is often timely and uncertain.

Bacteriophage-encoded endolysins (peptidoglycan hydrolases synthesised by phage infected bacterial cells) are utilised in the end stages of phage infection. Lysins are capable of destroying the bacterial cell wall through digestion of the peptidoglycan polymer, resulting in cell death through osmolysis [21]. The isolation of these hydrolases has the potential to overcome many issues surrounding the use of whole phage. As hydrolytic enzymes, they

retain specificity without affecting commensal flora, are capable of rapid bacterial lysis, are unlikely to encounter resistance owed to the essential bacterial binding sites and they do not contain transducible genetic information [22]. The specific mechanism of action of these endolysins is discussed elsewhere [23]. Endolysins demonstrating activity towards both Gram-positive and Gram-negative bacteria have been isolated and characterised, including lysins active against *Acinetobacter baumanni*, *Bacillus anthracis*, *Streptococcus pyogenes* and in some cases active against both Gram-positive and –negative bacteria simultaneously [24-26]. The phage endolysin designated LysK isolated from the staphylococcal bacteriophage K has been shown to have potent antimicrobial activity against a range of staphylococci including MRSA [1]. LysK has been truncated to its single catalytic domain, a cysteine, histidine-dependent aminohydrolase/peptidase ($CHAP_K$). This single domain, 18.6 kDa antimicrobial enzyme has been fully characterised and has demonstrated retention of lytic activity *in vitro*, *in vivo* and against staphylococcal biofilms [3,27,28].

Another class of potential alternative antimicrobials are bacteriocins. Lysostaphin, a 26.8 kDa metalloendopeptidase is produced naturally by *Staphylococcus simulans* [29]. Consisting of a single lytic domain (glycyl-glycine M23 endopeptidase), lysostaphin demonstrates potent antistaphylococcal activity through cleavage of the pentaglycine cross-bridges within the peptidoglycan of the bacterial cell wall. Active against a multitude of antibiotic susceptible, intermediate and resistant strains of bacteria, lysostaphin exhibits synergistic behaviour with multitude of antibiotics, phage lysins and antimicrobial peptides [30-32]. Successful application of lysostaphin has been demonstrated in cases of ocular infection, osteitis and endocarditis [33-35].

Despite the discovery and development of new potential antimicrobial candidates, the mode of delivery of any such pharmacologically active substance remains equally as important as the discovery itself. Ensuring activity, stability and dosage conditions are correct (especially when considering biological material), is crucial to successful administration in order to maximise the therapeutic benefit and to reduce any potential side effects. The triggered release of a therapeutic agent (small molecule, protein or virus) may rely on a variety of external stimuli in order to release the active cargo, including pH, temperature, ultrasound, magnetism or biomarker signals [36,37]. Utilising the difference between the healthy and the diseased state may provide certain conditions whereby treatment can be administered in a controlled fashion. Consequently, high local concentrations are achieved only in the specific location required. When considering treatment of bacterial infection, preventing the

administration of unnecessary or sub-lethal concentrations of an antibiotic or antimicrobial agent is crucial in preventing the continued development of antibiotic resistance [38].

Poly(*N*-isopropylacrylamide) (PNIPAM) has been widely investigated as a triggered drug release vehicle [39]. As a thermoresponsive polymer, PNIPAM undergoes a reversible, entropically driven phase transition at a lower critical solution temperature (LCST), resulting in the expulsion of water and a subsequent change in polymer volume. The LCST of PNIPAM and its associated structures (nanoparticles, micelles, nanogels etc.) can be manipulated through control of polymer concentration, copolymers and surfactants. Through adjusting the LCST to that of a clinically relevant temperature, PNIPAM has been extensively investigated in a wide range of biomedical applications including cancer therapy, wound healing, bioscaffolding and cell cultivation [40-43].

In previous studies, PNIPAM nanoparticles were formulated with allylamine for the controlled release of Bacteriophage K, which demonstrated potent antistaphyloccal activity through the thermally controlled collapse of the nanoparticles [44]. However in this study, phage virions were replaced with a synergisitic enzybiotic cocktail. Allylamine was used in order to adjust the LCST to a biologically relevant temperature of 34 °C, which is indicative of an infected wound. A bacterial infection of a wound as been shown to present as an elevation in skin temperature of around 3.6 °C (demonstrated in infected leg ulcers), in comparision to the surface temperature of approximately 32 °C seen in healthy skin [45]. PNIPAM nanoparticles were anchored to non-woven polypropylene to simulate a wound dressing using plasma deposited maleic anhydride and free amine groups from allylamine. Plasma based deposition strategies for surface activation have been well documented elsewhere [46-48]. As a representative bacterial isolate, MRSA252 was chosen, which is a HA-MRSA bacterium belonging to the clinically relevant epidemic MRSA-16 clone (EMRSA-16), and considered endemic in the majority of UK hospitals [49].

Materials and Methods

Materials

N-isopropylacrylamide, allylamine, ethylene-glycol diacrylate, sodium persulfate, sodium dodecylsulfate (SDS), phosphate buffered saline (PBS) tablets (pH 7.4), vancomycin hydrochloride from *Streptomyces orientalis* and maleic anhydride were all purchased from Sigma-Aldrich (Poole, Dorset, UK).

Lysostaphin from *Staphylococcus simulans*, Tryptic Soy Broth (TSB) and Tryptic Soy Agar (TSA) were purchased from Sigma-Aldrich (Poole, Dorset, UK). Coomassie (Bradford) Protein Assay Kit was purchased from Pierce Scientific. MRSA 252 was sourced from a bacterial strain collection belonging to the Biophysical Chemistry Research Group housed at the University of Bath.

Material Preparation

PNIPAM Nanoparticle Synthesis, Plasma Deposition and Surface Grafting

Particles were synthesised via precipitation polymerisation and anchored onto of non-woven polypropylene (2 x 2 cm) squares via plasma deposited maleic anhydride as previously described [44], the only modification being an increase in the surface grafting duration from 1 to 24 h. Following surface attachment, samples were washed in deionised (DI) water, air dried and kept under aseptic conditions prior to enzyme addition.

Electron Microscopy

Samples were prepared as above, freeze dried, sputter coated with gold and imaged via a Scanning Electron Microscope (SEM) (JEOL JSM6480LV operated at 10 KV).

Microbiology

Bacteria and Growth Conditions

MRSA 252 was taken from freezer stock (stored as a 15% (v/v) glycerol at -80 °C), streaked across a TSA culture plate with a loop spreader and incubated at 37 °C overnight in order to obtain single colonies. Bacterial cultures were prepared by inoculating 10 ml TSB with a single colony and incubating at 37 °C with agitation overnight.

$CHAP_K$ Production

$CHAP_K$ production was performed as previously described [28]. Briefly, the truncated lysin $CHAP_K$ was previously cloned and expressed using a pQE60 vector (Qiagen) in *Escherichia coli* (*E. coli*) XL1-Blue [50]. This recombinant *E. coli* was grown at 37 °C with shaking. Protein expression was achieved by inducing the cells with Isopropyl β-D-1-thiogalactopyranoside

(IPTG). After which, the cells were lysed and active $CHAP_K$ was purified to >90% homogeneity by cation exchange chromatography and quantified via the Bradford assay [51].

Minimum Inhibitory Concentration (MIC)

MICs for both $CHAP_K$ and lysostaphin were determined by the classical microdilution broth method, conducted according to the Clinical and Laboratory Standards Institute (CLSI) guidelines [52,53]. Briefly, MRSA 252 cells at 7 x10^5 colony forming units per millilitre (CFU/ml) were added to wells containing varying concentrations of $CHAP_K$ (64 – 1 μg/ml) and lysostaphin (0.25 - 0.004 μg/ml) in a microtitre plate. The plate was then incubated for 18 h with shaking in a micro-plate reader (SPECTROstar Omega, BMG LABTECH) and bacterial growth monitored as a function of optical density (OD) at 600 nm. Experiments were conducted in triplicate both at 37 °C and 32 °C. DI water was used to make enzyme stock solutions and for control experiments.

Turbidity Reduction Assays

The *in vitro* activity of both $CHAP_K$ and lysostaphin was assessed according to the rate of bacterial cell lysis. MRSA 252 cells at 7 x10^5 CFU/ml were grown to an OD of 0.5, centrifuged at 4000 rpm for 20 min at 4 °C, washed twice and resuspended in PBS to reattain an OD of 0.5. A range of $CHAP_K$ and lysostaphin solutions were prepared in DI water with concentrations relative to their MIC (0-16%) in order to assess enzyme activity in the presence of excess substrate: 100 μl of enzyme solution was added to 100 μl of bacterial solution in a microtitre plate in triplicate, the plate was shaken for 5 s to ensure sufficient mixing and the reduction in OD at 600 nm over 5 min was monitored using a micro-plate reader at either 37 °C and 32 °C. Control experiments were undertaken using DI water in place of either $CHAP_K$ or lysostaphin.

Synergy

Synergy was assessed according to the checkerboard assay [54]. Briefly, 100 μl of 7 x10^5 CFU/ml MRSA 252 was added to each well of an 8 x 8 section of a 96 well microtitre plate containing varying ratios of $CHAP_K$: lysostaphin, ranging from 64 – 1 μg/ml $CHAP_K$ and 0.25 - 0.004 μg/ml lysostaphin. The plate was incubated at 37 °C for 24 h without shaking and bacterial growth assessed visually. Synergy was confirmed by observation of wells with no

visible bacterial growth at enzyme concentrations lower than the MICs of the individual antimicrobials.

Electron Microscopy

Bacterial samples were grown on Melinex® film overnight in 5 ml TSB at 37 °C with minimal agitation (70 rpm). The volume of growth media was adjusted to 2 ml and exposed to either 64 μg/ml $CHAP_K$, 0.125 μg/ml lysostaphin, a combination of 8 μg/ml + 0.031 μg/ml lysostaphin or DI water (control) for 10 min at 37 °C. Samples were then fixed with 2.5% glutaraldehyde in 0.1 M sodium cacodylate buffer, postfixed in aqueous 1% osmium tetroxide, dehydrated in an acetone series (50 - 100%) and chemically dried in hexamethyldisilazane (HMDS). Samples were sputter coated with a thin layer of chromium and imaged using a Field Emission Scanning Electron Microscope (FESEM) (JEOL JSM6301F operating at 5 KV).

Controlled Release Experiments

Addition of $CHAP_K$ and Lysostaphin to Anchored Nanoparticles

A cocktail consisting of 80 μg/ml $CHAP_K$ and 0.31 μg/ml lysostaphin (10 times the concentration shown to generate synergistic inhibition) was incorporated into the anchored gel matrix via soaking the dried gel modified polypropylene fabric in 500 μl of enzyme solution for 2 h at room temperature (20 °C). The fabric was washed in DI water and air dried. Control experiments were undertaken using DI water in place of enzyme solution. In order to estimate protein loading of the nanoparticles, the Bradford assay was used to quantify total protein concentration both in the soaking solution (as confirmation of synergy concentration) and in the solution in which the fabric swatches were washed post soaking. All experiments were performed in triplicate and corrected against control swatches (soaked in DI water) in order to eliminate any non-protein associated solution absorbance. An average blank reading was used to baseline correct all absorbance readings, using DI water only. The residual protein concentration post washing was subtracted from the initial soaking concentration in order to estimate loading efficiency (LE) according to the following equation:

$$\text{LE } (\%) = \frac{(\text{total protein added - protein in washings})}{\text{total protein added}} \times 100$$

Thermal Release of $CHAP_K$/Lysostaphin Cocktail from Grafted PNIPAM Nanoparticles

Polypropylene-nanoparticle swatches incorporating the enzybiotics were soaked individually in 250 µl of MRSA 252 of fixed concentration (1.2 x10^8 CFU/ml in PBS) at either 32 °C or 37 °C for 30 min. Each square of fabric was then removed from solution and placed into 24.75 ml DI water (diluting the original solution volume 100-fold) alongside any residual liquid that had not been soaked up by the fabric. The 25 ml culture tube containing the fabric swatch was vortexed to remove any bacteria attached to the fabric and the solution from each tube was diluted and plated (in triplicate) on TSA plates and incubated at 37 °C overnight. Plates were assessed the following day for growth and any colonies counted. Control experiments were undertaken using the swatches without enzyme and each individual experiment was repeated 6 times.

Results and Discussion

Material Analysis

PNIPAM Nanoparticle Characterisation and Surface Grafting

The PNIPAM nanoparticles have been characterised by dynamic light scattering (DLS) and according to zeta potential analysis as reported in a previous study [44]. The LCST of the nanoparticles was shown to be transitional but clearly definitive at 34 °C, manifesting as a change in the hydrodynamic radius from 400 nm ± 50 nm in the expanded state (< 33 °C), to 170 nm ± 30 nm in the collapsed state (> 35 °C). Therefore the collapse of the nanoparticles and subsequent release of the enzybiotic cargo is targeted to occur only at a higher temperature associated with bacterial wound infection (around 36 °C), whilst remaining intact and preventing the release of the antimicrobial payload at temperatures indicative of an uninfected wound (around 32 °C). Successful deposition of maleic anhydride onto the non-woven polypropylene as anchor points for the nanoparticles was confirmed by Fourier Transform Infrared Spectroscopy (FT-IR) (Figure 1, Supplementary Information) as previously described.

Electron Microscopy

SEM images indicated the incorporation of the PNIPAM nanoparticle solution to non-woven polypropylene following surface activation with plasma deposited maleic anhydride and

wash steps, as shown in Figures 4A and 4B. The large polymer webs (Figure 4B) seen throughout the fibre matrix, appear to consist of individual nanoparticles held together by the polymeric sheets (Figure 4C). The nanoparticles are of varying sizes encompassing both the swollen and the collapsed state, possibly as a result of the freeze drying during the sample preparation. Figure 4D shows the surface attachment of individual nanospheres.

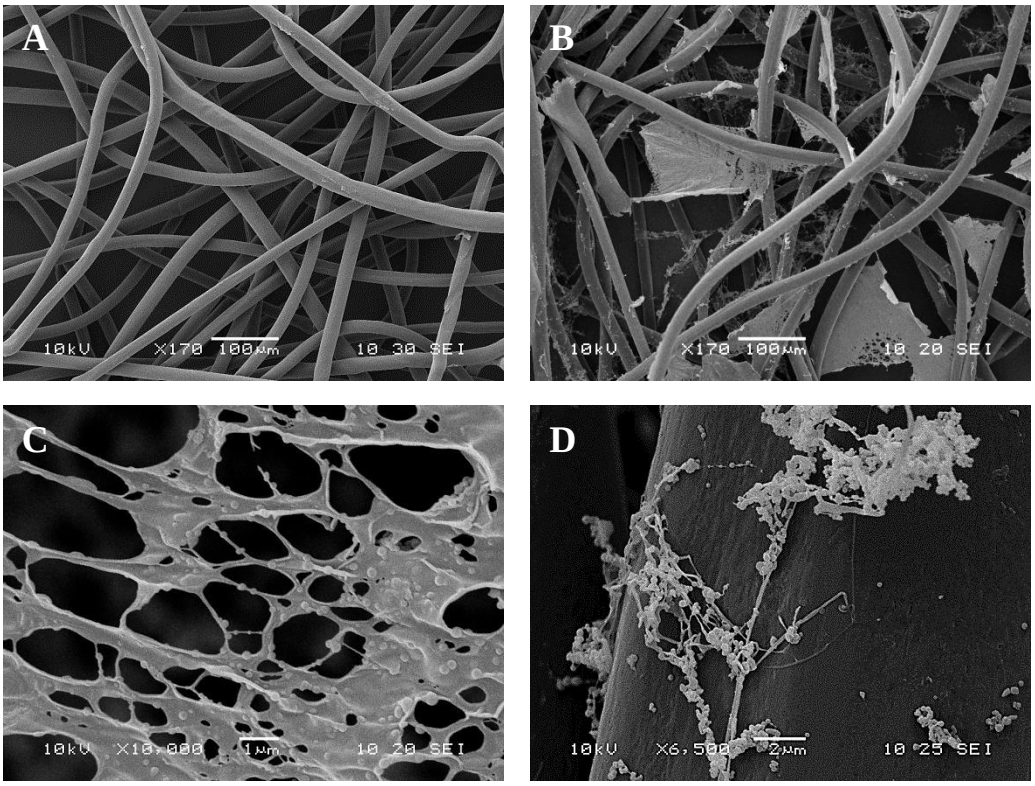

Figure 4 SEM images of non-woven polypropylene fabric **(A)** Untreated **(B)** Following PNIPAM nanoparticle attachment **(C)** Polymeric matrix seen dispersed within the fibre network **(D)** Nanoparticles attached to the surface of a polypropylene fibre.

Microbiological Analysis

Minimum Inhibitory Concentration (MIC)

The MIC was determined at both 32 °C and 37 °C as 64 µg/ml and 0.125 µg/ml, for $CHAP_K$ and lysostaphin, respectively, illustrating no change in the ability of either enzyme to prevent bacterial growth within this temperature range.

Turbidity Reduction and Rate of Cell Lysis

The rate at which both $CHAP_K$ and lysostaphin catalyse cell lysis was determined by assessing the reduction in turbidity (OD) of a bacterial suspension over the course of 60 s, defined as the initial rate of reaction (Figure 2 - Supplementary Information). This was investigated at 32 °C (below the LCST of the nanospheres) and at 37 °C (above the LCST), and at low concentrations of enzyme in order to prevent substrate concentration from becoming a limiting factor. Initial rates were calculated by means of tangents and plotted as a function of enzyme concentration relative to the MIC (Figure 5A and B).

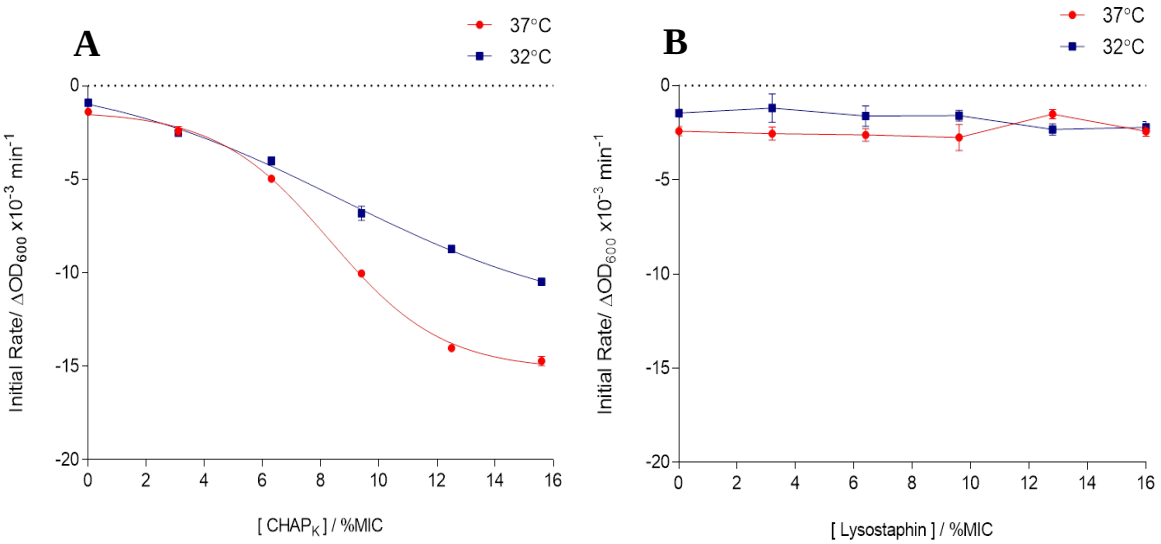

Figure 5 Comparison of the initial rate of bacterial cell lysis by: **(A)** $CHAP_K$ **(B)** lysostaphin.

From these results it can be seen that $CHAP_K$ is capable of eliciting a rapid reduction in turbidity (associated with bacterial cell lysis) which follows a standard dose response at both temperatures, whilst slightly more linear at 32 °C. There is a small difference in the initial rate of reaction at the two temperatures, more noticeably at higher concentrations of $CHAP_K$ but not to such an extent that indicates enzyme activity is substantially hindered at the lower temperature. However it appears that lysostaphin is unable to initiate a substantial degree of cell lysis (even at the highest concentrations) in such a short timeframe despite having a very low overall MIC, with values being similar to that of the control and demonstrating little temperature associated effect. This is in keeping with previous studies whereby $CHAP_K$

exhibited a greater reduction in turbidity over a 5 min period when compared to lysostaphin of the same absolute concentration (independent of MIC) [3].

Assessment of Synergistic Behaviour

Synergy was assessed both visually (non-growth of bacteria in well plate) and via calculation of fractional inhibitory concentration (FIC), taking the value of the MIC of the enzymes in combination, divided by the MIC of the individual enzyme. To achieve strong synergy the sum of the two FICs ($\Sigma FIC = FIC_A + FIC_B$) must be less than 0.5 [55]. As shown in Figure 6, synergy is indicated across the microtitre plate, at a range of different concentrations and confirmed in a total of 11 wells with FICs ranging from 0.144 (well G5) to 0.378 (well C5). A combination of 8 µg/ml $CHAP_K$ and 0.031 µg/ml lysostaphin was chosen as a concentration which demonstrates a strong synergistic combination (corresponding to a three-fold reduction in the MIC of lysostaphin and a four-fold reduction in the MIC of $CHAP_K$), in order to utilise the ability of lysostaphin to inhibit bacterial growth at low concentration, together with an increased rate of cell lysis exhibited by $CHAP_K$.

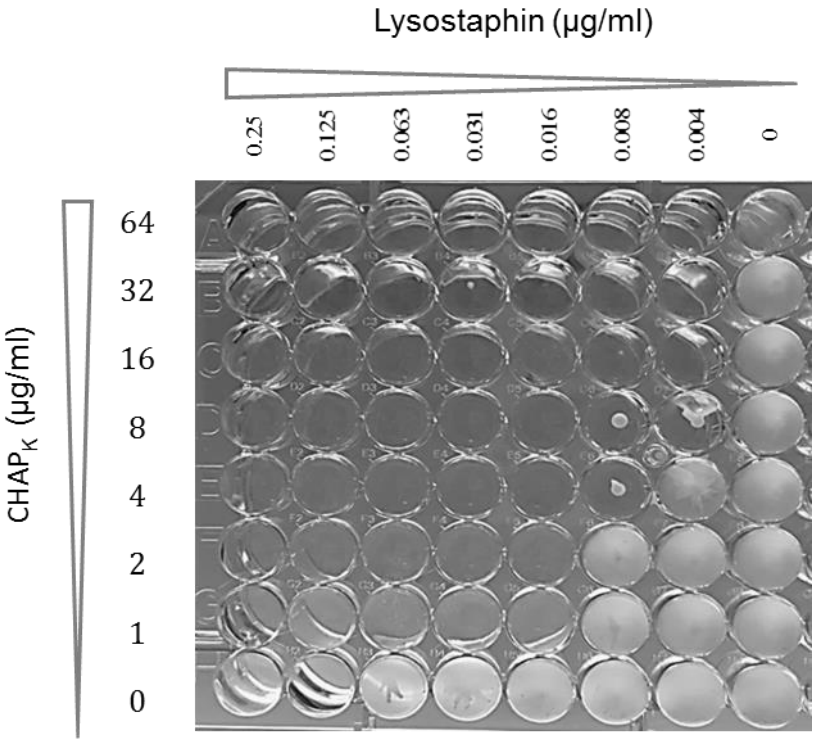

Figure 6 Synergy analysis of $CHAP_K$ (MIC = 64 µg/ml) (ordinate) and lysostaphin (MIC = 0.125 µg/ml) (abscissa).

Electron Microscopy

Untreated MRSA cells exhibited uniformity in the presentation of their cell morphology as shown in Figure 7A, active cell division was also observed. Cells treated with vancomycin at twice the MIC (12.5 μg/ml) for 10 min as shown in Figure 7B, did not present any change in their surface morphology or exhibit any visible membrane damage.

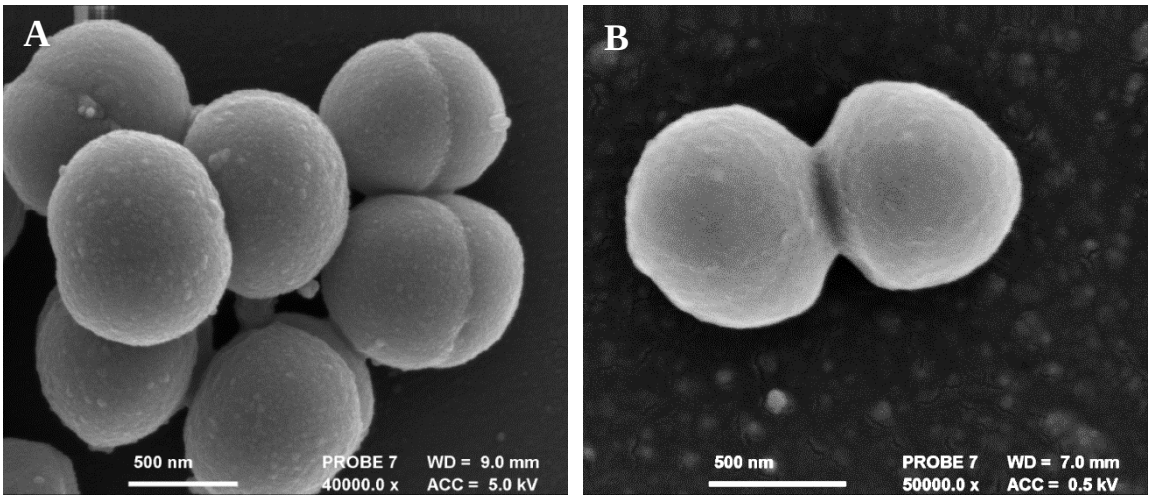

Figure 7 SEM images of untreated and antibiotic treated *S. aureus* MRSA 252 cells **(A)** cells exposed to DI water (control) **(B)** cells exposed to 2 x MIC (12.5 μg/ml) vancomycin. 10 min incubation time. Cell division observed in both cases.

Cells treated with $CHAP_K$ (at the MIC) (Figure 8A) show some surface damage and slightly more extracellular debris when compared to the control (Figure 7A); however the majority of the cells appear unaffected. When evaluating cells exposed to lysostaphin at the MIC (Figure 8B), they are comparable in appearance to those in the control group. This is in keeping with the established rate of lysis observed in solution, with $CHAP_K$ being much faster in eliciting a response. The synergistic effect of the cocktail of the two enzymes can be clearly observed in Figure 8C: blebbing (protrusion of the plasma membrane) was seen (red arrow) and a high degree of debris. Figure 8D also shows clear evidence of cell lysis by the enzybiotic cocktail.

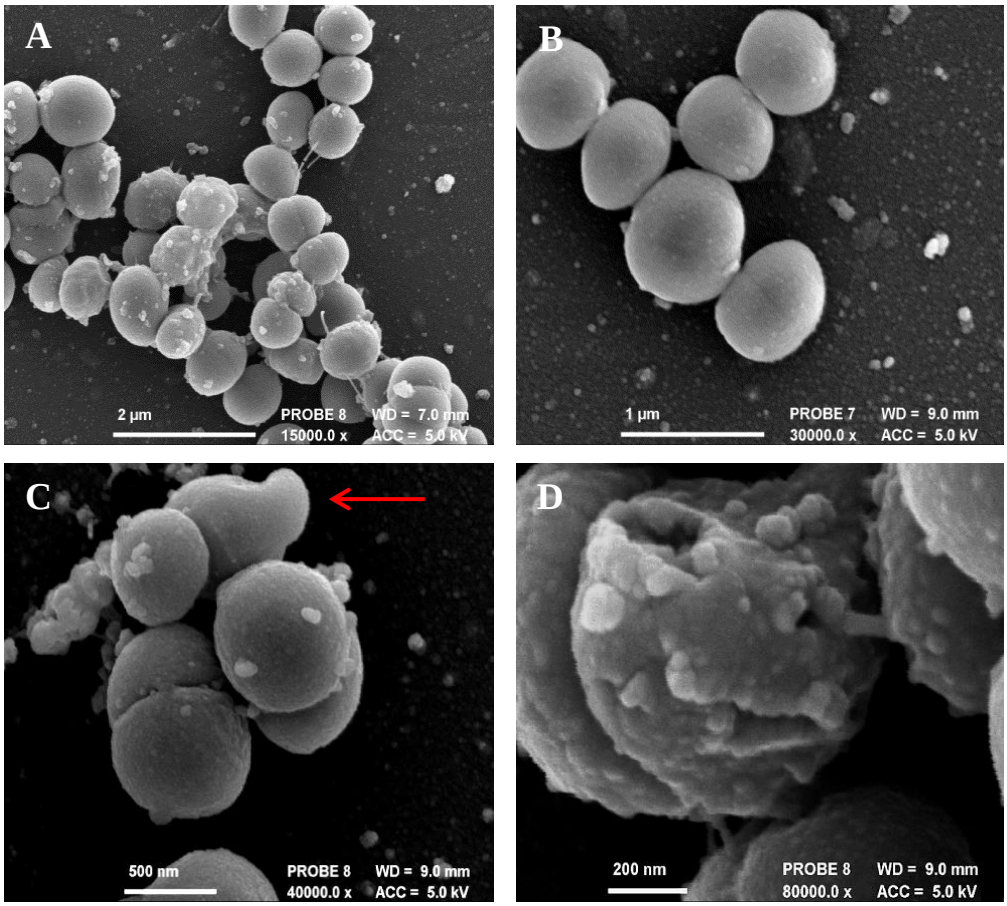

Figure 8 SEM images of *S. aureus* MRSA 252 cells treated with antimicrobial enzymes **(A)** at MIC: 64 µg/ml $CHAP_K$ **(B)** at MIC 0.125 µg/ml lysostaphin **(C +D)** sub-individual MIC 8 µg/ml $CHAP_K$ + 0.031 µg/ml lysostaphin. 10 min incubation time.

Controlled Release

Fabric swatches with surface anchored PNIPAM nanoparticle gel were soaked in an enzyme solution consisting of 80 µg/ml $CHAP_K$ and 0.31 µg/ml lysostaphin (10 times the synergy MIC), this was confirmed using the Bradford assay. The unencapsulated, residual protein concentration in solution post soaking and washing was calculated (Table 1), thus giving an estimated loading concentration of 49.7 ± 23.4 µg/ml or approximately 56%. As the effective synergistic combination of the bactericidal enzymes equates to approximately 8 µg/ml, even at the lower limit of this estimate, this is over three times the concentration of the cocktail required to inhibit bacterial growth.

Table 1 Concentration of protein added to modified fabric, residual non-adsorbed protein and hence encapsulated protein concentration.

Protein added μg / ml	Residual non-absorbed protein μg / ml	Encapsulated protein μg / ml
88.0 +/- 9.2	38.3 +/- 21.5	49.7 +/- 23.4

PNIPAM nanoparticles are able to deliver an enzymatic formulation in a temperature controlled manner as shown by evaluating the difference in cell count post incubation at temperatures both above and below the LCST. Samples plated after incubation at 32 °C demonstrate very little difference in the number of colonies between the controls (nanoparticles without enzybiotic cocktail) (Figure 9A) and the samples containing the enzybiotic cocktail (Figure 9B). The control experiments also confirm that the nanoparticles alone do not affect the bacteria. Whereas samples tested at 37 °C indicate a drastic decrease in the number of viable cells post treatment (Figure 9D). Figure 9C confirms that the collapse of the nanoparticles above the LCST does not affect the survival of the bacteria, being comparable to the controls undertaken at 32 °C.

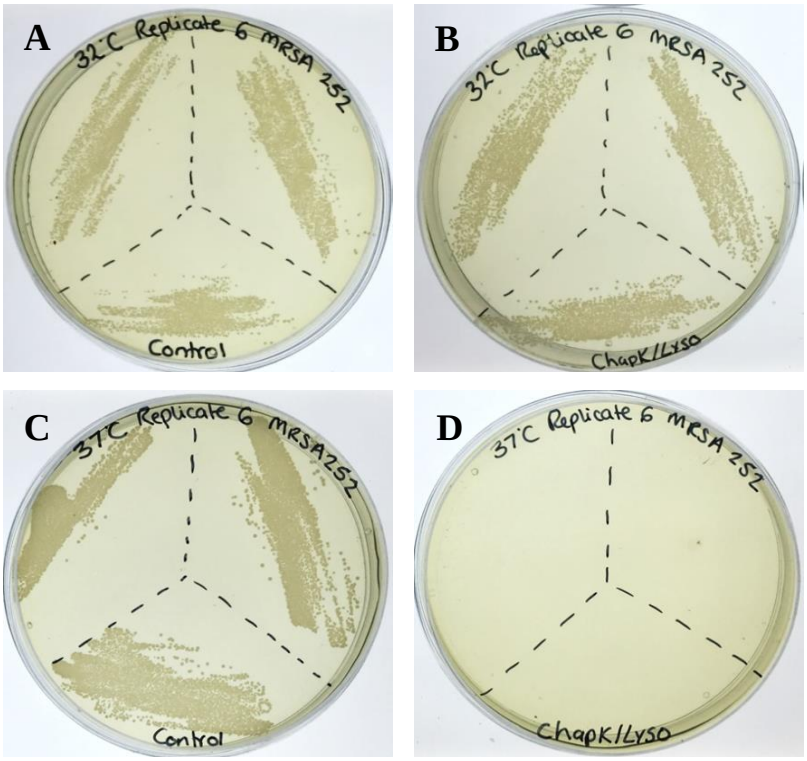

Figure 9 Plate analysis of *S. aureus* MRSA 252 survival and growth
(A) PNIPAM control at 32 °C **(B)** PNIPAM/$CHAP_K$/lysostaphin at 32 °C **(C)** PNIPAM control at 37 °C **(D)** PNIPAM/$CHAP_K$/lysostaphin at 37 °C.

Quantitative analysis (colony counting) showed a significant difference in the number of viable cells at the two temperatures ($p \leq 0.0001$, Student's *t*-test). Whilst there is a relatively small change in the number of CFU/ml between the control and the experimental sample at 32 °C, this is not unreasonable when taking into account possible passive diffusion or leaching of the enzymes from the particles. Nonetheless, when compared to samples incubated at 37 °C there is a clear difference in survival, manifesting as a >4 log reduction in CFU/ml compared to <1 log difference at 32 °C (Figure 10).

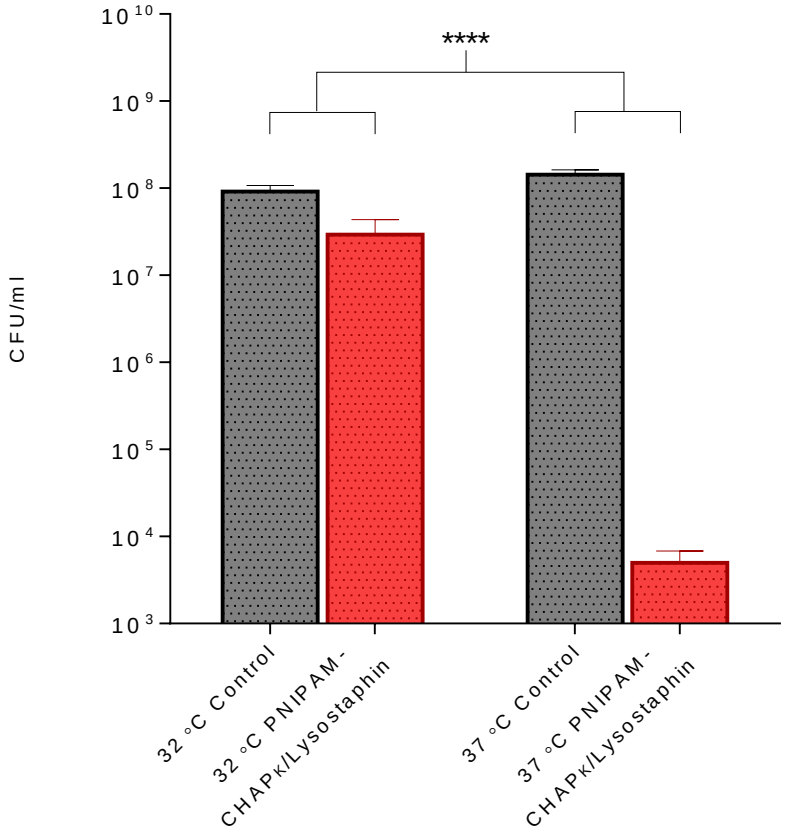

Figure 10 Comparison of bacterial survival at 32 °C and 37 °C for PNIPAM nanoparticle entrapped $CHAP_K$/ lysostaphin cocktail, relative to PNIPAM nanoparticles without enzymatic cocktail (control) **** $p < 0.0001$.

Conclusion

In summary this study demonstrates a new and previously unreported application of a novel enzybiotic cocktail for the thermally triggered control of *Staphylococcus aureus*. As potentially viable alternatives to antibiotic therapy, the use of enzybiotics may indicate a possible future treatment for drug resistant bacterial infection. Through exploitation of the ability of

lysostaphin to inhibit bacterial growth at very low concentration, and the fast acting nature of the bacteriophage-encoded endolysin $CHAP_K$, the two antimicrobial enzymes have been shown to work synergistically in the inhibition and subsequent lysis of bacterial cells, demonstrating a faster response time when compared to the current antibiotic of choice for the treatment of MRSA. Moreover, restricting the administration of such antimicrobials by means of an external trigger (in this case an increase in skin temperature associated with infection), limits the possibility of the development of resistance through prevention of any sub-lethal selection pressure. Through exploitation of the thermoresponsive behaviour of PNIPAM, nanoparticles were employed as a drug delivery system capable of releasing their antimicrobial cargo at a biologically relevant temperature indicative of infection. Which, when compared to the same system containing whole phage, the use of an enzybiotic cocktail which is not self-replicating but relies solely on successful diffusion from the polymer matrix and full retention of stability, the results are a promising step forward in the controlled release of an alternative antimicrobial formulation, whilst avoiding any issues associated with the administration of whole phage [44]. Although the clinical indication of our delivery system would be chronic wound infection via utilisation of a dressing/bandage concept, the technology presented here offers the possibility of infection control through use of enzybiotics for a range of conditions owing to the proven stability and retention of activity of the proteins.

Acknowledgements

The authors wish to acknowledge the Biotechnology and Biological Sciences Research Council (BBSRC) (BB/K011995/1) and Public Health England for funding this work. Special thanks to Diana Lednitzky for her help with the SEM and Charlotte Hind for her help with microbiology. All data created during this research is openly available from the University of Bath data archive at http://doi.org/10.15125/BATH-00247.

Supplementary Information

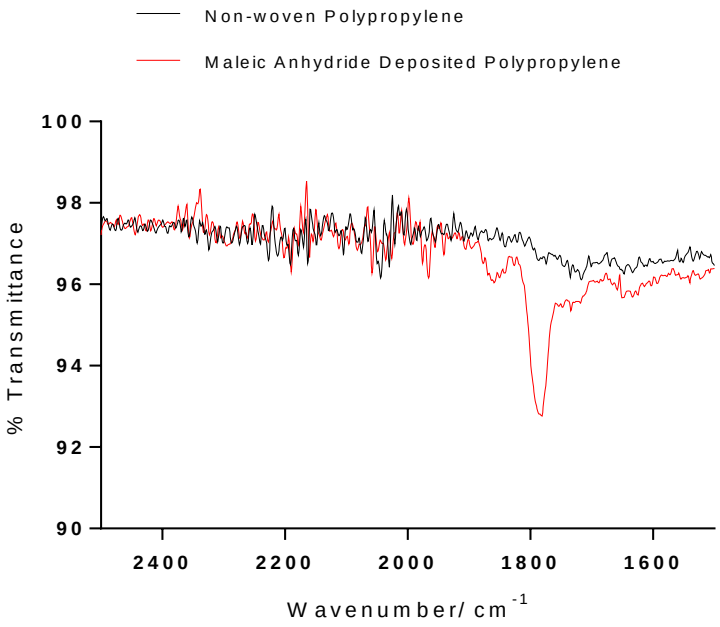

Supplementary Figure 1 FT-IR confirming addition of carbonyl functionality (peak at 1782 cm^{-1}) to non-woven polypropylene via plasma deposition of maleic anhydride.

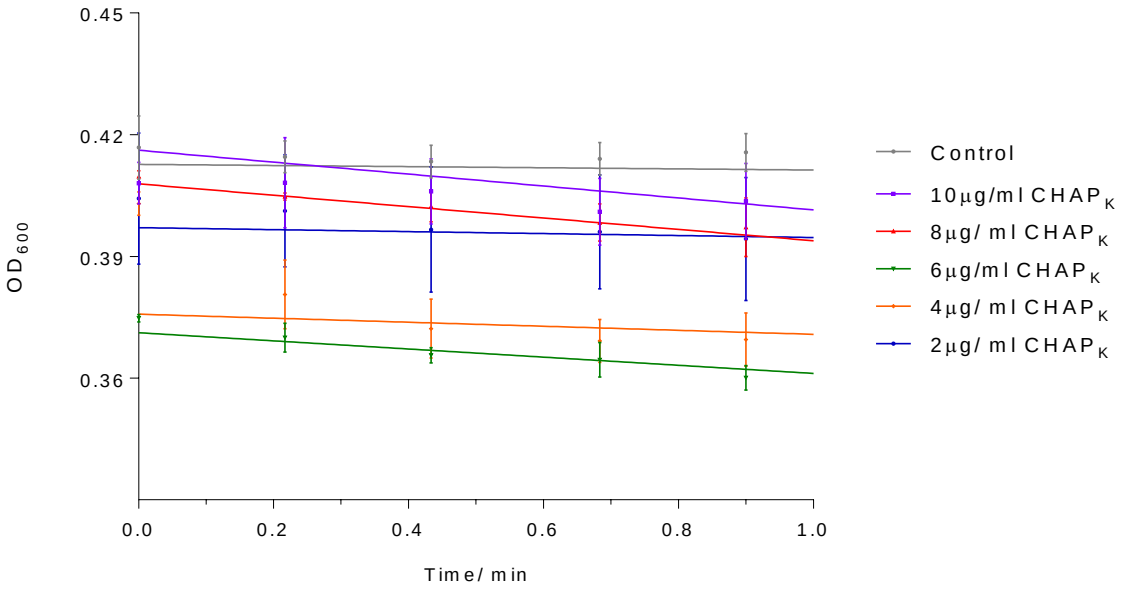

Supplementary Figure 2 Reduction in turbidity of planktonic MRSA 252 cells (measured as change in OD at 600 nm) over a 1 minute period as a function of $CHAP_K$ concentration. Tangents fitted in order to calculate initial rate of reaction. Each data point corresponds to the mean of three individual experiments and error bars represent the standard deviation.

5.4 Additional Results

5.4.1 Lytic Spectrum of $CHAP_K$

In order to assess the lytic spectrum of $CHAP_K$, numerous staphylococcal strains were screened and classified according to their susceptibility to the endolysin. Cultures were grown over an 18 hour period with the addition of 64 μg/ml of $CHAP_K$ (according to the methodology detailed in Section in 5.3.4). Of the 15 staphylococcal strains tested, 6 strains were classed as resistant (defined as the ability to sustain bacterial growth within 12 hours). The growth curves of the resistant isolates are shown in Figure 11, alongside growth media only (TSB) as the negative control.

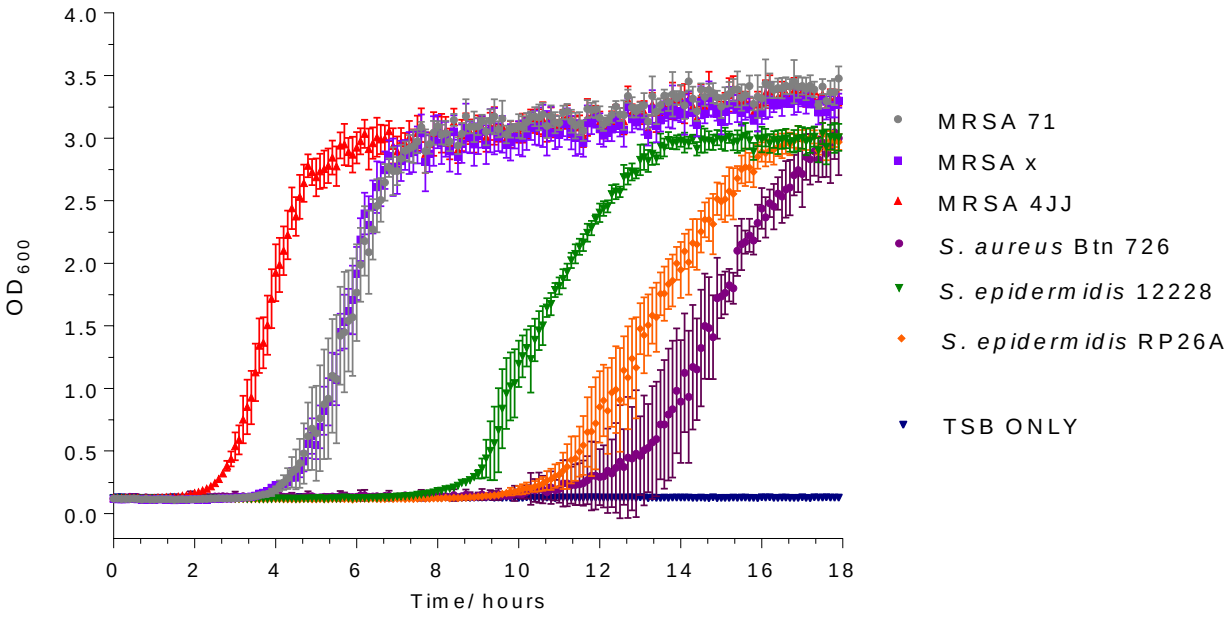

Figure 11 Growth of various resistant staphylococcal strains over 18 hours with the addition of 64 μg/ml of $CHAP_K$. Each data point represents the mean of three individual biological replicates and the error bars represent the standard deviation.

Additionally, five bacterial strains were classified as intermediate, indicating their ability to grow in the presence of $CHAP_K$ post 12 hour incubation (meaning growth is severely delayed rather than suppressed). A further four isolates were susceptible to $CHAP_K$, illustrated by the complete suppression of bacterial growth over the full 18 hours. The growth curves of the intermediate and susceptible strains are shown in Figure 12 and the susceptibility of all strains tested is summarised in Table 2.

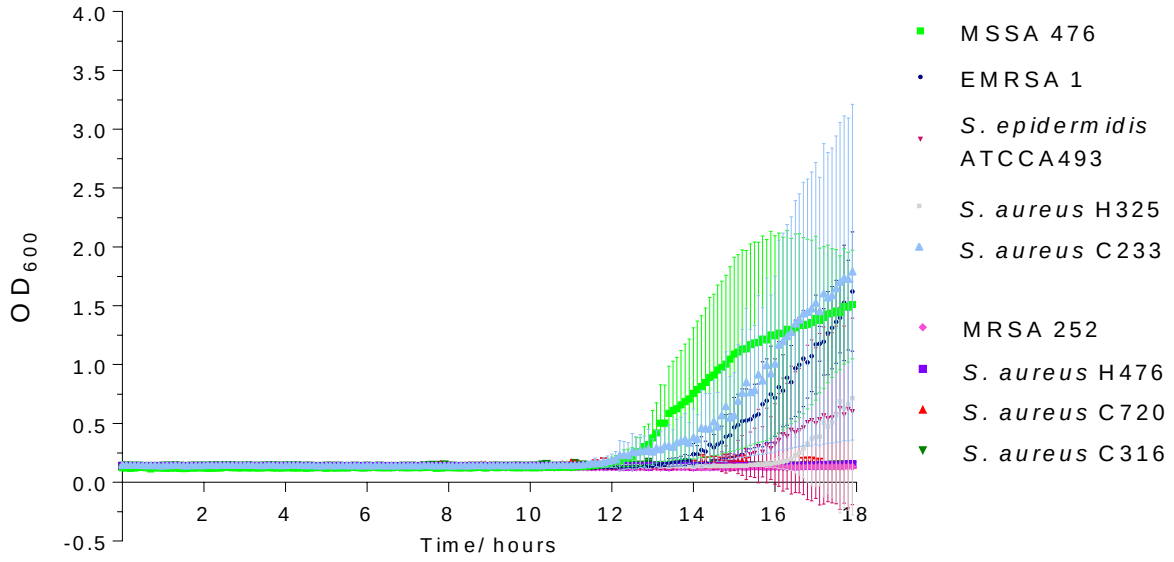

Figure 12 Growth of various intermediate and susceptible staphylococcal strains over 18 hours with the addition of 64 µg/ml of $CHAP_K$. Each data point represents the mean of three individual biological replicates and the error bars represent the standard deviation.

Table 2 Summary of the susceptibility of various staphylococcal strains to 64 µg/ml $CHAP_K$ following 18 hour incubation. Resistant (R) = Sustained bacterial growth within 12 hours. Intermediate (I) = Delayed bacterial growth, initiated after 12 hours. Susceptible (S) = Complete suppression of bacterial growth over 18 hours.

Staphylococcal Strain	**Susceptibility to $CHAP_K$**
MRSA 71	R
MRSA x	R
MRSA 4JJ	R
EMRSA 1	I
MRSA 252	S
MSSA 476	I
S. epidermidis ATCCA493	I

S. epidermidis RP26A	R
S. epidermidis 12228	R
S. aureus Btn 726	R
S. aureus H325	I
S. aureus H476	S
S. aureus C720	S
S. aureus C316	S
S. aureus C233	I

Of the four susceptible strains, MRSA 252 was chosen to take forward for further experiments, owing to its clinical relevance and drug-resistance profile.

5.4.2 Effect of Temperature on Enzybiotic Activity

The MIC of both $CHAP_K$ and lysostaphin was then determined for MRSA 252 at 32 °C and 37 °C (as detailed in the publication), with the intention of assessing the lytic ability of the endolysins at a reduced temperature. This was an important parameter to establish in order to confirm that any observable effect on bacterial growth (when considering the thermoresponsive release of the enzybiotics), is indeed a function of controlled release as oppose to reduced enzymatic activity. The results for lysostaphin and $CHAP_K$ are shown in Figures 13 and 14 respectively. The variation in OD values between the left and right axes is purely a function of the spectrophotometer used. Whilst the absolute values differ, the increase in OD (or lack thereof) remains representative of the effect of the endolysins.

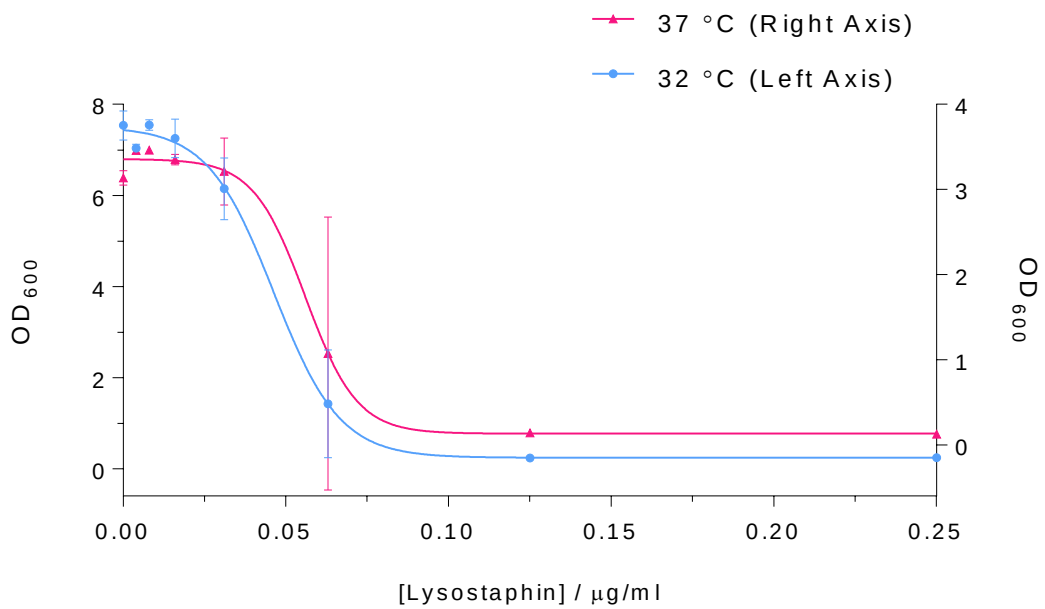

Figure 13 Endpoint OD measurements of MRSA 252 as a result of the addition of varying concentrations of lysostaphin at 37 °C (pink - right axis) and 32 °C (blue - left axis). Each data point represents the mean of three independent replicates and error bars represent the standard deviation. The data is fitted to a standard sigmoidal dose-reponse curve.

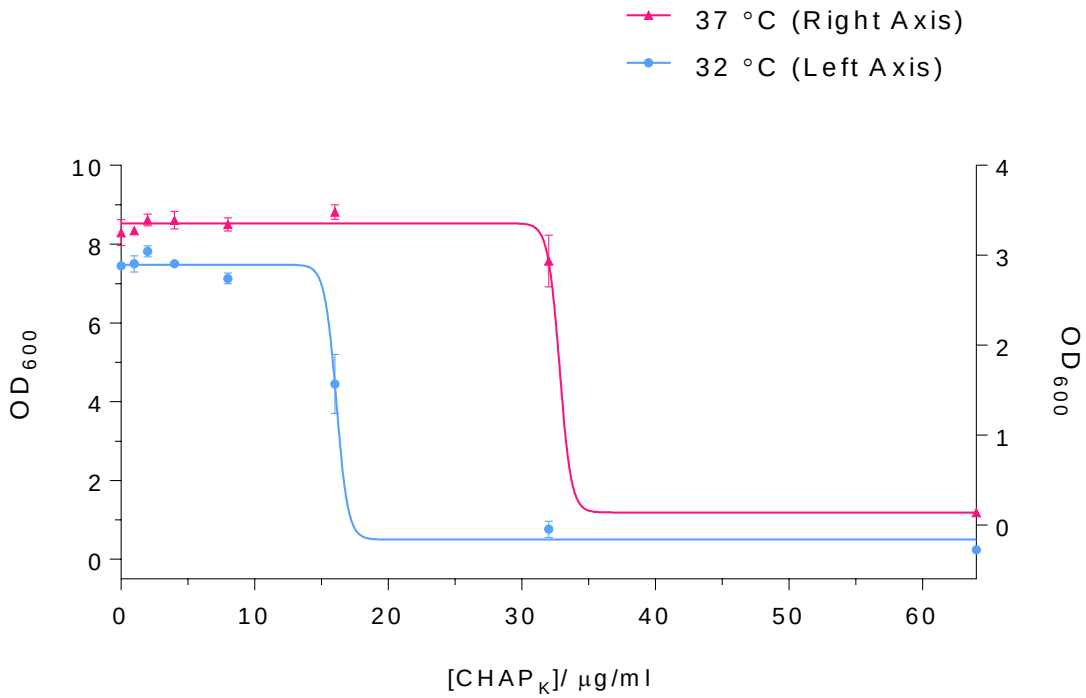

Figure 14 Endpoint OD measurements of MRSA 252 as a result of the addition of varying concentrations of $CHAP_K$ at 37 °C (pink - right axis) and 32 °C (blue - left axis). Each data point represents the mean of three independent replicates and error bars represent the standard deviation. The data is fitted to a standard sigmoidal dose-reponse curve.

These data demonstrate no change in the MIC of lysostaphin at 32 °C, inhibition of bacterial growth occurs at 0.125 μg/ml of lysostaphin in both cases. For $CHAP_K$, the degree of bacterial growth is reduced at 32 °C, at sub-MIC concentrations (i.e. 32 μg/ml); however, the MIC remains at 64 μg/ml as shown by complete inhibition of bacterial growth. The purpose of this study was to ensure that the endolysins are able to elicit bacterial lysis at a reduced temperature, which has been proven in both cases. In fact, the apparent increase in bacteriostatic activity of $CHAP_K$ at 32 °C may provide a more challenging evaluation of the thermoresponsive system employed, owing to the fact that a smaller proportion of $CHAP_K$ released from the nanoparticles at the lower temperature, compared to 37 °C, would potentially manifest as a reduction in bacterial cell count, thus reducing the observed thermoresponsive behaviour of the system.

5.5 Conclusions and Future Work

The research published in the preceding article describes the development of a novel enzybiotic cocktail, which has been employed in a stimuli-responsive, polymeric carrier matrix. To date, this is the first example (to the best of the author's knowledge) of the incorporation of a phage-encoded endolysin into a triggered release system. The study builds on the research presented in Chapter 4 via the acquisition of quantitative data, demonstrating statistically significant bacterial lysis of MRSA from thermally responsive PNIPAM nanoparticles. Owing to time constraints it has not been possible to deduce the exact mechanism of enzyme immobilisation/ encapsulation. However, similar studies aimed at encapsulation of various drug molecules within PNIPAM polymer networks (including particles), have also demonstrated effective diffusion-mediated entrapment. PNIPAM nanoparticles copolymerised with allylamine and acrylamide have been successfully loaded with doxorubicin by means of physical entrapment over a 3 day period via continuous stirring in buffer solution [56]. A possible explanation for the apparent immobilisation of both drugs and proteins within PNIPAM particles may involve electrostatic interactions between the drug/protein and the polymer chains [57]. Proteins (in this case antimicrobial enzymes), consist of multiple amino acids which, depending on pH, may contain charged side chains. At physiological pH certain amino acids are protonated (such as lysine and histidine) and others are deprotonated (glutamate and aspartate). Whilst it is challenging to predict the overall charge on the surface of a protein from amino acid sequence alone (as pKa values of isolated amino acids differ to those in a folded protein), the variation in amino acid structure (resulting in the presence of both cationic and anionic groups), often results in areas of localised charge which can interact with the external environment. The synthesised PNIPAM

nanoparticles (designed to house the antimicrobial enzymes), are likely to contain protonated amine groups at pH 7 (as a result of copolymerisation with allylamine), which are able to facilitate electrostatic interactions with the anionic amino acid side chains located within the structure of the enzybiotics. Additionally, the use of a radical initiator during the precipitation polymerisation may result in the incorporation of carboxyl and sulphate groups within the polymer chains, providing small areas of localised negative charge [58]. This may promote additional polymer-protein interactions, resulting in electrostatic retention of the immobilised proteins following diffusion into the carrier matrix. The collapse of the polymer chains above the LCST initiates in a change in polymer structure from a random coil to a hydrophobic globule. The contraction of the polymer chains then forces the expulsion of the hydrophilic proteins from within the polymeric matrix into the surrounding environment.

Alongside deducing the mechanism of entrapment, the long term stability of the immobilised enzymes should be established in order to assess the clinical potential of the system, both in terms of longevity and storage requirements. Many of the factors associated with the development of this technology are in keeping with those discussed in Chapter 4, with some additional considerations.

5.5.1 Bacterial Resistance

As discussed in Chapter 3, there are currently no identified examples of resistance mechanisms towards phage-encoded endolysins. However, there is some concern surrounding the therapeutic use of lysostaphin. Lysostaphin-resistant *S. aureus* isolates have occasionally been reported *in vitro* and *in vivo*, potentially limiting the suitability of this particular peptidase for therapeutic treatment [59]. Resistance towards lysostaphin is reported to occur as a result of mutations in the *femA* gene, which is responsible for the addition of the second and third glycine residues in the pentaglycine bridge of staphylococcal peptidoglycan, resulting in monoglycine cross bridges (thus removing the target site of lysostaphin). Interestingly, numerous studies documenting the occurrence of lysostaphin resistance also demonstrate restoration of methicillin susceptibility [60,61]. Additionally, lysostaphin resistance is accompanied by a significant reduction in the fitness of the host, including decreased virulence and decreased growth rate. In one study this resulted in the resistant variants being outcompeted in cocultures by their wild-type parental strain [62]. Therefore, it has been argued that the emergence of resistant isolates during lysostaphin therapy would result in less virulent infections which are easily treatable with β-lactam antibiotics (removing the necessity to administer valuable, last-resort antibiotics in the first instance). Nonetheless, any

potential for the development of resistance (regardless of the mode of treatment: topical, systemic etc.), should be fully evaluated. The use of an enzybiotic cocktail may alleviate some of the concerns surrounding the development of resistance to lysostaphin; however this should be tested and quantified.

5.5.2 Immunogenic Response

In addition to any immune/cytotoxic response arising as a result of the surface anchored polymer particles (Chapter 4), any immunogenic effects of the enzybiotic cocktail should be established. There is limited experimental data surrounding the immunogenicity of phage-encoded endolysins, however some studies have indicated that lysin administration can result in the formation of antibodies, yet the production of such immune complexes has thus far exhibited minimal effect on the efficacy of lysin treatment [63,64]. A recent phase I clinical trial of the phage-encoded endolysin SAL-200 (based on a recombinant form of the phage-encoded endolysin SAL-1, derived from the staphylococcal phage SAP-1), analysed anti-SAL antibody levels following intravenous administration. The results illustrated the presence of serum antibodies in 37% of the participants, however no serious adverse effects were observed and the endolysin retained clinical efficacy [65].

In contrast, the immunogenic profile of lysostaphin as a potential therapeutic agent for the treatment of staphylococcal infection in animals and humans has been widely investigated. Consequently, there is a mounting body of evidence to suggest that lysostaphin elicits a potent immune response in animal models (small animal and non-human primates) and in humans [66]. The formation of lysostaphin-antibody immune complexes *in vivo* (as a result of T cell activation and immunoglobulin G antibody production), has thus far hindered the therapeutic development of lysostaphin. However, recent efforts focused on mutagenic deletion of immunogenic T cell epitopes (responsible for antibody recognition), have demonstrated promising results in the production of deimmunised lysostaphin variants, exhibiting enhanced antimicrobial activity whilst evading immune surveillance [67,68]. This may prove a promising strategy in the engineering of antimicrobial proteins with reduced immunogenic properties.

5.5.3 Increasing the Therapeutic Window

The reported increase in skin temperature as a result of infection (and the corresponding polymeric release of antimicrobial enzymes), exists as a transitional process across a temperature gradient of approximately 4 °C. This relatively small therapeutic window may limit the use of such a system, owing to certain environmental factors which may contribute to an increase in skin temperature. Furthermore, the transitional collapse of the polymeric nanoparticles could potentially facilitate partial release of the therapeutic cargo at temperatures not associated with infection. A potential solution may involve raising the temperature at which the nanoparticles collapse, to a point which is irrespective of either healthy or infected skin temperature, but may be manually induced. For example, PNIPAM-*co*-acrylamide-*co*-allylamine nanoparticles have been synthesised (of varying sizes depending on surfactant concentration), which exhibit a sharp phase transition at 40 °C [56]. Subject to the positive diagnosis of infection (an indication of which could be achieved via co-incorporation of a diagnostic platform, as demonstrated by Thet *et al* [69]), external application of a heating element such as a heat pad, would raise the external temperature of the dressing, forcing the nanoparticles to collapse, thereby releasing the antimicrobial cargo contained within.

5.5.4 Increasing the Lytic Spectrum

The enzybiotic cocktail presented in this research utilises two peptidoglycan hydrolase enzymes, both of which are ineffective against Gram-negative bacteria. The specificity of $CHAP_K$ and lysostaphin limit their application in polymicrobial infections. Predominantly effective against staphylococcal species, the utilisation of such an antimicrobial cocktail would rely on successful identification of the pathogens responsible for infection. However, as discussed in Chapter 3, protein engineering has provided a means of extending the antimicrobial spectrum of endolysins to include Gram-negative species [70]. Utilisation of lysins active against both Gram-positive and –negative bacterial species would greatly enhance the versatility of this system, especially when considering chronic wound infections which may harbour a range of genetically diverse pathogens.

5.6 References

1 O'Flaherty, S., Coffey, A., Meaney, W., Fitzgerald, G. F. & Ross, R. P. The Recombinant Phage Lysin LysK Has a Broad Spectrum of Lytic Activity against Clinically Relevant Staphylococci, Including Methicillin-Resistant Staphylococcus aureus. *Journal of Bacteriology* **187**, 7161-7164 (2005).

2 Sanz-Gaitero, M., Keary, R., Garcia-Doval, C., Coffey, A. & van Raaij, M. J. Crystal structure of the lytic CHAP(K) domain of the endolysin LysK from Staphylococcus aureus bacteriophage K. *Virology Journal* **11**, 133 (2014).

3 Fenton, M., Ross, R. P., McAuliffe, O., O'Mahony, J. & Coffey, A. Characterization of the staphylococcal bacteriophage lysin CHAP(K). *Journal of Applied Microbiology* **111**, 1025-1035 (2011).

4 Yang, S.-C., Lin, C.-H., Sung, C. T. & Fang, J.-Y. Antibacterial activities of bacteriocins: application in foods and pharmaceuticals. *Frontiers in Microbiology* **5**, 241 (2014).

5 Cotter, P. D., Hill, C. & Ross, R. P. Bacteriocins: developing innate immunity for food. *Nauture Reviews Microbiology* **3**, 777-788 (2005).

6 Behrens, H. M., Six, A., Walker, D. & Kleanthous, C. The therapeutic potential of bacteriocins as protein antibiotics. *Emerging Topics in Life Sciences* **1**, 65-74 (2017).

7 Ramu, R., Shirahatti, P. S., Devi, A. T., Prasad, A., Kumuda, J., Lochana, M. S., Zameer, F., Dhananjaya, B. L. & Nagendra Prasad, M. N. Bacteriocins and Their Applications in Food Preservation. *Critical Reviews in Food Science and Nutrition*, (2015).

8 Kumar, J. K. Lysostaphin: an antistaphylococcal agent. *Applied Microbiology and Biotechnology* **80**, 555-561 (2008).

9 Yang, X. Y., Li, C. R., Lou, R. H., Wang, Y. M., Zhang, W. X., Chen, H. Z., Huang, Q. S., Han, Y. X., Jiang, J. D. & You, X. F. In vitro activity of recombinant lysostaphin against Staphylococcus aureus isolates from hospitals in Beijing, China. *Journal of Medical Microbiology* **56**, 71-76 (2007).

10 Kiri, N., Archer, G. & Climo, M. W. Combinations of Lysostaphin with β-Lactams Are Synergistic against Oxacillin-Resistant Staphylococcus epidermidis. *Antimicrobial Agents and Chemotherapy* **46**, 2017-2020 (2002).

11 Cui, F., Li, G., Huang, J., Zhang, J., Lu, M., Lu, W., Huan, J. & Huang, Q. Development of chitosan-collagen hydrogel incorporated with lysostaphin (CCHL) burn dressing with anti-methicillin-resistant Staphylococcus aureus and promotion wound healing properties. *Drug Delivery* **18**, 173-180 (2011).

12 Bastos, M. d. C. d. F., Coutinho, B. G. & Coelho, M. L. V. Lysostaphin: A Staphylococcal Bacteriolysin with Potential Clinical Applications. *Pharmaceuticals* **3**, 1139 (2010).

13 Sabala, I., Jagielska, E., Bardelang, P. T., Czapinska, H., Dahms, S. O., Sharpe, J. A., James, R., Than, M. E., Thomas, N. R. & Bochtler, M. Crystal structure of the antimicrobial peptidase lysostaphin from Staphylococcus simulans. *Febs Journal* **281**, 4112-4122 (2014).

14 Raulinaitis, V., Tossavainen, H., Aitio, O., Juuti, J. T., Hiramatsu, K., Kontinen, V. & Permi, P. Identification and structural characterization of LytU, a unique peptidoglycan endopeptidase from the lysostaphin family. *Scientific Reports* **7**, 6020 (2017).

15 Wertheim, H. F. L., Melles, D. C., Vos, M. C., van Leeuwen, W., van Belkum, A., Verbrugh, H. A. & Nouwen, J. L. The role of nasal carriage in Staphylococcus aureus infections. *Lancet Infectious Diseases* **5**, 751-762 (2005).

16 Dryden, M. S. Complicated skin and soft tissue infection. *Journal of Antimicrobial Chemotherapy* **65**, iii35-iii44 (2010).

17 Filice, G. A., Nyman, J. A., Lexau, C., Lees, C. H., Bockstedt, L. A., Como-Sabetti, K., Lesher, L. J. & Lynfield, R. Excess Costs and Utilization Associated with Methicillin Resistance for Patients with Staphylococcus aureus Infection. *Infection Control and Hospital Epidemiology* **31**, 365-373 (2010).

18 Glaser, P., Martins-Simoes, P., Villain, A., Barbier, M., Tristan, A., Bouchier, C., Ma, L., Bes, M., Laurent, F., Guillemot, D., Wirth, T. & Vandenesch, F. Demography and Intercontinental Spread of the USA300 Community-Acquired Methicillin-Resistant Staphylococcus aureus Lineage. *Mbio* **7** (2016).

19 Nobrega, F. L., Costa, A. R., Kluskens, L. D. & Azeredo, J. Revisiting phage therapy: new applications for old resources. *Trends in Microbiology* **23**, 185-191 (2015).

20 Chi, C.-Y., Wang, S.-M., Lin, H.-C. & Liu, C.-C. A Clinical and Microbiological Comparison of Staphylococcus aureus Toxic Shock and Scalded Skin Syndromes in Children. *Clinical Infectious Diseases* **42**, 181-185 (2006).

21 Becker, S. C., Roach, D. R., Chauhan, V. S., Shen, Y., Foster-Frey, J., Powell, A. M., Bauchan, G., Lease, R. A., Mohammadi, H., Harty, W. J., Simmons, C., Schmelcher, M., Camp, M., Dong, S., Baker, J. R., Sheen, T. R., Doran, K. S., Pritchard, D. G., Almeida, R. A., Nelson, D. C., Marriott, I., Lee, J. C. & Donovan, D. M. Triple-acting Lytic Enzyme Treatment of Drug-Resistant and Intracellular Staphylococcus aureus. *Scientific Reports* **6** (2016).

22 Fischetti, V. A., Nelson, D. & Schuch, R. Reinventing phage therapy: are the parts greater than the sum? *Nature Biotechnology* **24**, 1508-1511 (2006).

23 Pastagia, M., Schuch, R., Fischetti, V. A. & Huang, D. B. Lysins: the arrival of pathogen-directed anti-infectives. *Journal of Medical Microbiology* **62**, 1506-1516 (2013).

24 Schuch, R., Nelson, D. & Fischetti, V. A. A bacteriolytic agent that detects and kills Bacillus anthracis. *Nature* **418**, 884-889 (2002).

25 Shen, Y., Koeller, T., Kreikemeyer, B. & Nelson, D. C. Rapid degradation of Streptococcus pyogenes biofilms by PlyC, a bacteriophage-encoded endolysin. *Journal of Antimicrobial Chemotherapy* **68**, 1818-1824 (2013).

26 Lai, M.-J., Lin, N.-T., Hu, A., Soo, P.-C., Chen, L.-K., Chen, L.-H. & Chang, K.-C. Antibacterial activity of Acinetobacter baumannii phage Phi AB2 endolysin (LysAB2) against both Gram-positive and Gram-negative bacteria. *Applied Microbiology and Biotechnology* **90**, 529-539 (2011).

27 Fenton, M., Casey, P. G., Hill, C., Gahan, C. G. M., Ross, R. P., McAuliffe, O., O'Mahony, J., Maher, F. & Coffey, A. The truncated phage lysin CHAP(k) eliminates Staphylococcus aureus in the nares of mice. *Bioengineered Bugs* **1**, 404-407 (2010).

28 Fenton, M., Keary, R., McAuliffe, O., Ross, R. P., O'Mahony, J. & Coffey, A. Bacteriophage-Derived Peptidase CHAP(K) Eliminates and Prevents Staphylococcal Biofilms. *International Journal of Microbiology* **2013**, 625341 (2013).

29 Schindler, C. A. & Schuhardt, V. T. Lysostaphin: A New Bacteriolytic Agent for the Staphylococcus. *Proceedings of the National Academy of Sciences of the United States of America* **51**, 414-421 (1964).

30 Aguinaga, A., Francés, M. L., Del Pozo, J. L., Alonso, M., Serrera, A., Lasa, I. & Leiva, J. Lysostaphin and clarithromycin: a promising combination for the eradication of Staphylococcus aureus biofilms. *International Journal of Antimicrobial Agents* **37**, 585-587 (2011).

31 Becker, S. C., Foster-Frey, J. & Donovan, D. M. The phage K lytic enzyme LysK and lysostaphin act synergistically to kill MRSA. *Fems Microbiology Letters* **287**, 185-191 (2008).

32 Desbois, A. P., Sattar, A., Graham, S., Warn, P. A. & Coote, P. J. MRSA decolonization of cotton rat nares by a combination treatment comprising lysostaphin and the antimicrobial peptide ranalexin. *Journal of Antimicrobial Chemotherapy* **68**, 2569-2575 (2013).

33 Dajcs, J. J., Thibodeaux, B. A., Girgis, D. O., Shaffer, M. D., Delvisco, S. M. & O'Callaghan, R. J. Immunity to lysostaphin and its therapeutic value for ocular MRSA infections in the rabbit. *Investigative Ophthalmology & Visual Science* **43**, 3712-3716 (2002).

34 Windolf, C. D., Lögters, T., Scholz, M., Windolf, J. & Flohé, S. Lysostaphin-Coated Titan-Implants Preventing Localized Osteitis by Staphylococcus aureus in a Mouse Model. *Plos One* **9**, e115940 (2014).

35 Patron, R. L., Climo, M. W., Goldstein, B. P. & Archer, G. L. Lysostaphin treatment of experimental aortic valve endocarditis caused by a Staphylococcus aureus isolate with reduced susceptibility to vancomycin. *Antimicrobial Agents and Chemotherapy* **43**, 1754-1755 (1999).

36 Bean, J. E., Alves, D. R., Laabei, M., Esteban, P. P., Thet, N. T., Enright, M. C. & Jenkins, A. T. A. Triggered Release of Bacteriophage K from Agarose/Hyaluronan Hydrogel Matrixes by Staphylococcus aureus Virulence Factors. *Chemistry of Materials* **26**, 7201-7208 (2014).

37 Mura, S., Nicolas, J. & Couvreur, P. Stimuli-responsive nanocarriers for drug delivery. *Nature Materials* **12**, 991-1003 (2013).

38 Andersson, D. I. & Hughes, D. Evolution of antibiotic resistance at non-lethal drug concentrations. *Drug Resistance Updates* **15**, 162-172 (2012).

39 Ashraf, S., Park, H.-K., Park, H. & Lee, S.-H. Snapshot of phase transition in thermoresponsive hydrogel PNIPAM: Role in drug delivery and tissue engineering. *Macromolecular Research* **24**, 297-304 (2016).

40 Nash, M. E., Carroll, W. M., Velasco, D., Gomez, J., Gorelov, A. V., Elezov, D., Gallardo, A., Rochev, Y. A. & Elvira, C. Synthesis and characterization of a novel thermoresponsive copolymer series

and their application in cell and cell sheet regeneration. *Journal of Biomaterials Science Polymer Edition* **24**, 253-268 (2013).

41 Zhou, M. Y., Liu, S. H., Jiang, Y. Q., Ma, H. R., Shi, M., Wang, Q. S., Zhong, W., Liao, W. J. & Xing, M. M. Q. Doxorubicin-Loaded Single Wall Nanotube Thermo-Sensitive Hydrogel for Gastric Cancer Chemo-Photothermal Therapy. *Advanced Functional Materials* **25**, 4730-4739 (2015).

42 Pawar, M. D., Rathna, G. V. N., Agrawal, S. & Kuchekar, B. S. Bioactive thermoresponsive polyblend nanofiber formulations for wound healing. *Materials Science and Engineering: C* **48**, 126-137 (2015).

43 Deptula, T., Warowicka, A., Wozniak, A., Grzeszkowiak, M., Jarzebski, M., Bednarowicz, M., Patkowski, A. & Slomski, R. Cytotoxicity of thermo-responsive polymeric nanoparticles based on N-isopropylacrylamide for potential application as a bioscaffold. *Acta Biochimica Polonica* **62**, 311-316 (2015).

44 Hathaway, H., Alves, D. R., Bean, J., Esteban, P. P., Ouadi, K., Mark Sutton, J. & Jenkins, A. T. Poly(N-isopropylacrylamide-co-allylamine) (PNIPAM-co-ALA) nanospheres for the thermally triggered release of Bacteriophage K. *European Journal of Pharmaceutics and Biopharmaceutics* **96**, 437-441 (2015).

45 Fierheller, M. & Sibbald, G. A Clinical Investigation into the Relationship between Increased Periwound Skin Temperature and Local Wound Infection in Patients with Chronic Leg Ulcers. *Advances in Skin & Wound Care* **23**, 369-378 (2010).

46 Foerch, R., Chifen, A. N., Bousquet, A., Khor, H. L., Jungblut, M., Chu, L.-Q., Zhang, Z., Osey-Mensah, I., Sinner, E.-K. & Knoll, W. Recent and expected roles of plasma-polymerized films for biomedical applications. *Chemical Vapor Deposition* **13**, 280-294 (2007).

47 Jenkins, A. T. A., Hu, J., Wang, Y. Z., Schiller, S., Foerch, R. & Knoll, W. Pulsed plasma deposited maleic anhydride thin films as supports for lipid bilayers. *Langmuir* **16**, 6381-6384 (2000).

48 Mishra, G. & McArthur, S. L. Plasma Polymerization of Maleic Anhydride: Just What Are the Right Deposition Conditions? *Langmuir* **26**, 9645-9658 (2010).

49 Johnson, A. P., Aucken, H. M., Cavendish, S., Ganner, M., Wale, M. C. J., Warner, M., Livermore, D. M., Cookson, B. D. & Uk Earss participants, t. Dominance of EMRSA-15 and -16 among MRSA causing nosocomial bacteraemia in the UK: analysis of isolates from the European Antimicrobial Resistance Surveillance System (EARSS). *Journal of Antimicrobial Chemotherapy* **48**, 143-144 (2001).

50 Horgan, M., O'Flynn, G., Garry, J., Cooney, J., Coffey, A., Fitzgerald, G. F., Ross, R. P. & McAuliffe, O. Phage lysin LysK can be truncated to its CHAP domain and retain lytic activity against live antibiotic-resistant staphylococci. *Applied Environmental Microbiology* **75**, 872-874 (2009).

51 Bradford, M. M. A rapid and sensitive method for the quantitation of microgram quantities of protein utilizing the principle of protein-dye binding. *Analytical Biochemistry* **72**, 248-254 (1976).

52 Clinical and Laboratory Standards Institute (CLSI). Methods for Dilution Antimicrobial Susceptibility Tests for Bacteria That Grow Aerobically; Approved Standard- Ninth Edition *CLSI document M07-A9* (2012).

53 Wiegand, I., Hilpert, K. & Hancock, R. E. Agar and broth dilution methods to determine the minimal inhibitory concentration (MIC) of antimicrobial substances. *Nature Protocols* **3**, 163-175 (2008).

54 Lorian, V. *Antibiotics in Laboratory Medicine*. 367-373 (Lippincott Williams & Wilkins, 2005).

55 Hall, M. J., Middleton, R. F. & Westmacott, D. The fractional inhibitory concentration (FIC) index as a measure of synergy. *Journal of Antimicrobial Chemotherapy* **11**, 427-433 (1983).

56 Rahimi, M., Kilaru, S., Sleiman, G. E. H., Saleh, A., Rudkevich, D. & Nguyen, K. Synthesis and Characterization of Thermo-Sensitive Nanoparticles for Drug Delivery Applications. *Journal of biomedical nanotechnology* **4**, 482-490 (2008).

57 Town, A. R., Giardiello, M., Gurjar, R., Siccardi, M., Briggs, M. E., Akhtar, R. & McDonald, T. O. Dual-stimuli responsive injectable microgel/solid drug nanoparticle nanocomposites for release of poorly soluble drugs. *Nanoscale* **9**, 6302-6314 (2017).

58 McPhee, W., Tam, K. C. & Pelton, R. Poly (N-isopropylacrylamide) latices prepared with sodium dodecyl sulfate. *Journal of colloid and interface science* **156**, 24-30 (1993).

59 Kusuma, C., Jadanova, A., Chanturiya, T. & Kokai-Kun, J. F. Lysostaphin-resistant variants of Staphylococcus aureus demonstrate reduced fitness in vitro and in vivo. *Antimicrobial Agents and Chemotherapy* **51**, 475-482 (2007).

60 Climo, M. W., Ehlert, K. & Archer, G. L. Mechanism and suppression of lysostaphin resistance in oxacillin-resistant Staphylococcus aureus. *Antimicrobial Agents and Chemotherapy* **45**, 1431-1437 (2001).

61 Rohrer, S. & Berger-Bachi, B. FemABX peptidyl transferases: a link between branched-chain cell wall peptide formation and beta-lactam resistance in gram-positive cocci. *Antimicrobial Agents and Chemotherapy* **47**, 837-846 (2003).

62 Stranden, A. M., Ehlert, K., Labischinski, H. & Berger-Bachi, B. Cell wall monoglycine cross-bridges and methicillin hypersusceptibility in a femAB null mutant of methicillin-resistant Staphylococcus aureus. *Journal of Bacteriology* **179**, 9-16 (1997).

63 Loeffler, J. M., Djurkovic, S. & Fischetti, V. A. Phage Lytic Enzyme Cpl-1 as a Novel Antimicrobial for Pneumococcal Bacteremia. *Infection and Immunity* **71**, 6199-6204 (2003).

64 Loeffler, J. M., Nelson, D. & Fischetti, V. A. Rapid killing of Streptococcus pneumoniae with a bacteriophage cell wall hydrolase. *Science* **294**, 2170-2172 (2001).

65 Jun, S. Y., Jang, I. J., Yoon, S., Jang, K., Yu, K. S., Cho, J. Y., Seong, M. W., Jung, G. M., Yoon, S. J. & Kang, S. H. Pharmacokinetics and Tolerance of the Phage Endolysin-Based Candidate Drug SAL200 after a Single Intravenous Administration among Healthy Volunteers. *Antimicrobial Agents and Chemotherapy* **61** (2017).

66 Kokai-Kun, J. F. Lysostaphin: a Silver Bullet for Staph. *Antimicrobial Drug Discovery: Emerging Strategies*, 147-165 (2012).

67 Zhao, H., Verma, D., Li, W., Choi, Y., Ndong, C., Fiering, Steven N., Bailey-Kellogg, C. & Griswold, Karl E. Depletion of T Cell Epitopes in Lysostaphin Mitigates Anti-Drug Antibody Response and Enhances Antibacterial Efficacy In Vivo. *Chemistry & Biology* **22**, 629-639 (2015).

68 Blazanovic, K., Zhao, H., Choi, Y., Li, W., Salvat, R. S., Osipovitch, D. C., Fields, J., Moise, L., Berwin, B. L., Fiering, S. N., Bailey-Kellogg, C. & Griswold, K. E. Structure-based redesign of lysostaphin yields potent antistaphylococcal enzymes that evade immune cell surveillance. *Molecular Therapy - Methods & Clinical Development* **2**, 15021 (2015).

69 Thet, N. T., Alves, D. R., Bean, J. E., Booth, S., Nzakizwanayo, J., Young, A. E., Jones, B. V. & Jenkins, A. T. Prototype Development of the Intelligent Hydrogel Wound Dressing and Its Efficacy in the Detection of Model Pathogenic Wound Biofilms. *ACS Applied Materials and Interfaces* **8**, 14909-14919 (2016).

70 Criscuolo, E., Spadini, S., Lamanna, J., Ferro, M. & Burioni, R. Bacteriophages and Their Immunological Applications against Infectious Threats. *Journal of Immunology Research* **2017**, 3780697 (2017).

Part C: Future Perspective

"A conclusion is the place where you got tired thinking".

Martin H. Fischer – Physician, renowned for his teachings in the art and practice of medicine.

The Role of Biotechnology in the Prevention and Treatment of Infection

The timely detection and effective treatment of hospital-associated infection will be of paramount importance in the future prevention of infectious disease. In the USA alone, 1 in 25 hospitalised patients will develop an infection directly related to their medical care at any given time, resulting in over 1 million infections annually, costing over $30 billion [1]. In Europe, over 4 million people acquire a healthcare-associated infection each year, ~37,000 of which result in death. As such, there has been a substantial increase in the number of global incentives aimed at combating such (arguably) avoidable infections. The significant investment and dissemination of global epidemiology surveillance data in recent years has, to some extent, alleviated certain aspects related to hospital-associated infections. For example, from 2011 – 2014 the number of HA-MRSA bacteraemia infections in the USA decreased by 13% [2], and from 2009 – 2012 the number of death certificates citing MRSA as the underlying cause of death in England and Wales decreased by 32% [3]. However, a recent report published by the WHO (September 2017), highlights a significant lack of novel antibiotics under development, especially for infections posing the greatest threat to health [4]. Furthermore, of the 51 antibiotics and 11 biologics in clinical trials, it is estimated that only 10 will be granted approval over the next 5 years, suggesting a distinct void in the developmental pipeline for treatment of priority resistant organisms.

There can be little doubt that efficient monitoring of potentially pathogenic microorganisms will play a crucial role in retaining the efficacy of current treatment options. The successful clinical detection of infectious agents (prior to the onset of various disease states), will not only reduce the ever-increasing burden on healthcare services worldwide, but will also prevent the unnecessary administration of increasingly valuable 'last-line' treatment strategies, thus controlling the spread of both infection and microbial resistance. The specificity of biological entities (such as enzymes or antibodies) has facilitated their development as efficient biosensors for proteinaceous contamination (including both viral and microbial). For example, there are currently a number of clinical biosensors for the detection of the causative agents responsible for a range of infectious diseases, including influenza, HIV, malaria, tuberculosis, various *E. coli* and Group A and B streptococcal infections and of course, residual surface contaminants responsible for a range of spongiform encephalopathies [5]. The development of biosensor technology is an encouraging prospect in the prevention of infection, especially in the healthcare setting where time is of the essence

and conventional diagnostics (i.e. PCR) are often time consuming, expensive and require specialist equipment and skills beyond those of the primary care clinician.

The implementation of biological therapeutics for the treatment of infection has undergone significant development in recent years. Advances in genetic and protein engineering have paved the way for enhancing the activity, stability, and clinical application of various biologically-inspired antimicrobials. Indeed, of the new antimicrobial candidates currently undergoing clinical trials, all of the biologics are considered innovative, owing to their unique MOA, which is in direct contrast to the meretricious antibiotics also undergoing clinical assessment. Amongst the developmental biotherapeutics (predominantly consisting of monoclonal antibodies), two phage endolysins; CF-301 (discussed in Chapter 3) and SAL-200 (discussed in Chapter 5), are in currently in phase II trials, both of which have demonstrated potent activity against priority pathogens (as defined by the WHO). The utilisation of biological therapeutics in order to expand the seemingly limited arsenal of effective antimicrobial treatment options (especially those effective against MDR infections), is a promising strategy, albeit still very much in its infancy. However, the utilisation of nature's own evolutionary-defined antimicrobials (potentially exhibiting some modifications, courtesy of modern synthetic biology), alongside conventional antibiotics as an adjunctive therapy, may hold the key for the future of antimicrobial therapy.

Whilst it cannot be denied that new and novel treatment options are desperately required for future infection control; the translation of such technology from bench to bedside will undoubtedly rely on global collaboration in order to meet the current clinical standards required. Such collaboration, not only from scientists, but also from regulatory/ approval bodies, clinicians and governments worldwide will be of the utmost importance in the successful implementation of viable and effective alternative treatment options. The potential advancement of biological therapeutics will depend heavily on securing investment for the often lengthy clinical approval process. Nonetheless, this is an exciting time for the development of antimicrobial biotechnology which, in light of the relentless increase in antibiotic resistance, may be the difference between progression into the future of infection control, or a return to the pre-antibiotic era whereby infection is no longer treatable.

References

1 Centers for Disease Control and Prevention (CDC). Healthcare-associated Infections (2017). https://www.cdc.gov/winnablebattles/healthcareassociatedinfections/index.html

2 Centers for Disease Control and Prevention (CDC). National and State Healthcare Associated Infections Progress Report (2016). https://www.cdc.gov/HAI/pdfs/progress-report/hai-progress-report.pdf

3 Office for National Statistics. Deaths involving MRSA: 2008 to 2012 (August 2013). https://www.ons.gov.uk/peoplepopulationandcommunity/birthsdeathsandmarriages/deaths/bulletins/deathsinvolvingmrsa/2013-08-22

4 Centers for Disease Control and Prevention (CDC). Antibacterial Agents in Clinical Development - An analysis of the antibacterial clinical development pipeline, including tuberculosis. (Sepetember 2017). http://www.who.int/medicines/areas/rational_use/antibacterial_agents_clinical_development/en/

5 Bahadır, E. B. & Sezgintürk, M. K. Applications of commercial biosensors in clinical, food, environmental, and biothreat/biowarfare analyses. *Analytical Biochemistry* **478**, 107-120 (2015).